(NASA-TM-72858) EFFECT OF SAMPLING RATE AND RECORD LENGTH ON THE DETERMINATION OF STABILITY AND CONTROL DERIVATIVES (NASA) 140 p HC A07/MF A01 CSCL 01C

N79-12096

Unclas
G3/08 38901

NASA Technical Memorandum 72858

EFFECT OF SAMPLING RATE AND RECORD LENGTH ON THE DETERMINATION OF STABILITY AND CONTROL DERIVATIVES

Martin J. Brenner, Kenneth W. Iliff, and Robert K. Whitman

December 1978

NASA

NASA Technical Memorandum 72858

EFFECT OF SAMPLING RATE AND RECORD LENGTH ON THE DETERMINATION OF STABILITY AND CONTROL DERIVATIVES

Martin J. Brenner, Kenneth W. Iliff, and Robert K. Whitman

Dryden Flight Research Center
Edwards, California

National Aeronautics and
Space Administration

1978

EFFECT OF SAMPLING RATE AND RECORD LENGTH ON THE DETERMINATION OF STABILITY AND CONTROL DERIVATIVES

Martin J. Brenner, Kenneth W. Iliff,
and Robert K. Whitman

NASA Hugh L. Dryden Flight Research Center

INTRODUCTION

Stability and control derivatives extracted from flight data have been used for many years to provide final verification of the predicted full-scale aircraft aerodynamic characteristics and for the verification of prediction techniques. The flight-determined derivatives can be compared with calculated derivatives and wind-tunnel predictions, and this comparison can be used to update prediction methods for the improvement of future aircraft designs. Many areas need to be studied to assess the reliability of the flight-measured stability and control derivatives. Among these areas is the effect of sampling rate and record length. The desire to minimize the amount of data processing required for any given flight program creates a need for more economical data handling techniques. A reduction in sampling rate and/or record length would significantly economize on computer utilization for processing flight data in such an analysis. Little effort has been devoted to this subject in aircraft parameter estimation.

The computation time required to perform a derivative estimation is directly proportional to the number of data points. The number of data points is determined by the sampling rate and the record length. The lowest sampling rates possible for derivative analysis are examined in this report, although the sampling rate required for filtering in the data acquisition system is usually higher than that necessary to obtain stability and control derivatives. This report presents the results of determining stability and control derivatives from flight data using the maximum likelihood estimation technique (ref. 1). Several lateral-directional and longitudinal maneuvers were analyzed at different sampling rates and record lenghts to assess the effect of sampling rate and/or record length. Time shifting effects (ref. 2), which also influence the quality of the estimates, are not investigated in this report.

SYMBOLS

a_n	normal acceleration, g
a_y	lateral acceleration, g
C_ℓ	nondimensional rolling-moment coefficient
C_m	nondimensional pitching-moment coefficient
C_n	nondimensional yawing-moment coefficient
C_Y	nondimensional side-force coefficient
C_Z	nondimensional normal-force coefficient
p	roll rate, deg/sec or rad/sec
$\dot{p}$	rolling angular acceleration, deg/sec^2
q	pitch rate, deg/sec or rad/sec
$\bar{q}$	dynamic pressure, kN/m^2 (lb/ft^2)
r	yaw rate, deg/sec or rad/sec
$\dot{r}$	yawing angular acceleration, deg/sec^2
V	velocity, m/sec (ft/sec)
α	angle of attack, deg or rad
β	angle of sideslip, deg or rad
δ_a	aileron deflection, deg or rad
δ_{c_1}	differential tail deflection, deg or rad
δ_{c_2}	blended combination of spoiler and differential tail deflections, deg or rad
δ_e	elevator deflection, deg or rad
δ_r	rudder deflection, deg or rad
θ	pitch angle, deg or rad
ϕ	roll angle, deg or rad

Subscripts:

p, q, r, α, β partial derivative with respect to the

δ_a, δ_{c_1}, δ_{c_2} subscripted variables

δ_e, δ_r

METHOD OF ANALYSIS

A maximum likelihood estimation (MLE) method of analysis, described in reference 1, was used to determine a complete set of linear stability and control derivatives from the maneuvers performed in flight. The method is a digital computational technique that determines the best set of coefficients (stability and control derivatives) of the linearized equations of motion. This technique minimizes a weighted integral squared error between flight-measured and estimated time histories.

The result is that the estimated time history tends to match the flight time history. Examples of matches of lateral-directional data for each of the five aircraft investigated are shown in figure 1, and the matches for the longitudinal data are shown in figure 2. The solid line is the measured data and the dashed line is the MLE estimated data. The elements of the weighting matrices for each vehicle (discussed in general in reference 3) are given in reference 2.

The Cramer-Rao bound (refs. 3 and 4) provides an estimate of the degree of confidence that should be placed in the derivatives extracted from flight data. This bound, also called the uncertainty level, provides an estimate of the lower bound of the covariance of the parameters estimated from a given set of flight data.

TEST AIRCRAFT AND DATA SYSTEM

Flight test data from several types of aircraft were analyzed to obtain results that were independent of the aircraft configuration. The choice of aircraft was based largely on the availability of the proper dynamic response data for determining stability and control derivatives. The data are from flight test programs conducted at the NASA Dryden Flight Research Center. These aircraft represent a wide variety of aircraft configurations.

Data from five aircraft, referred to as aircraft A, B, C, D, and E, were used. Aircraft A was a PA-30 aircraft, a light, twin-engine general aviation airplane described in reference 5. An unpowered remotely piloted 3/8-scale model of the F-15 airplane (ref. 6) was aircraft B. The JetStar airplane, a

low-winged executive jet transport, was aircraft C (ref. 7). Aircraft D was an F-111A airplane (ref. 8), a fighter with a variable sweep wing. The HL-10 lifting body research vehicle (ref. 9) was aircraft E.

Table 1 lists the flight conditions for which the data from the five aircraft were acquired. Each individual case represents a single maneuver. All of the tests were performed at a nominal load factor of 1g with stability augmentation systems off. The sense of the rudder direction for aircraft C and the sense of lateral control for aircraft D are opposite to the sense of these controls for the other aircraft.

The test aircraft were instrumented to measure three-axis linear accelerations and angular rates, Euler angles, angle of sideslip, angle of attack, control surface deflections, velocity, and altitude. The data were recorded on a nine-bit pulse code modulation (PCM) magnetic tape system. The basic sampling rates of the PCM system were 200 samples per second per channel for aircraft A, B, and C; 20 samples per second per channel for aircraft D; and 50 samples per second per channel for aircraft E. Data from aircraft A, B, and C were thinned to 50 samples per second for processing. The tabulated values in table 1 for the sampling rates are referred to as the baseline sampling rates.

Before being encoded and recorded by the PCM system, the data were filtered with a first-order, low-pass anti-aliasing filter. The 200 samples per second data for aircraft B were also digitally filtered to remove high frequency structural resonance before thinning.

RESULTS AND DISCUSSION

The high quality data from aircraft A were selected for more extensive analysis than the data from the other four aircraft. Once conclusions had been drawn from the aircraft A data, the results from the other aircraft were used to generalize these conclusions. Consequently, treatment of aircraft A will be more thorough than that of the other aircraft, and comparisons will be cited where applicable. Aircraft B, C, D, and E represent a broad class of aircraft for a wide variety of flight conditions (Mach number, angle of attack, etc.). The acceptable data from these four aircraft showed greater nonlinearities (indicated by poorer matches between computed and actual flight data) than did the data from aircraft A. Lateral-directional and longitudinal maneuvers for each aircraft (except aircraft E, where a longitudinal maneuver was not used) were analyzed. The type of input for each maneuver is listed in table 1. The values of the elements of the weighting matrices used in the maximum likelihood estimator are shown in table 2. The values of the derivative estimates computed from the baseline sampling rates (table 1) are designated as baseline derivative values. These values are presented in table 3.

Experience has shown that data obtained at 50 samples per second for record lengths at least twice the characteristic time of the aircraft have provided satisfactory stability and control derivative estimates. Therefore, it was not necessary to study sampling rates higher than 50 samples per second.

The aircraft A data base contained lateral-directional and longitudinal maneuvers with control inputs of two different amplitudes. Five small amplitude maneuvers with nearly identical control inputs and four large amplitude maneuvers with nearly identical control inputs were used for the lateral-directional analysis; and similiarly, two groups of four longitudinal maneuvers were analyzed. The nearly identical control inputs were obtained by uplinking (ref. 10) the computer-generated control commands. The ratio between the large and small amplitude similarly-shaped control inputs is a factor of 1.4 for the longitudinal maneuvers, and a factor of 2.0 for the lateral-directional maneuvers. A comparison of the resulting stability and control derivatives from the large and small amplitude maneuvers reveals information about the consistency of the estimated derivative trends as sampling rate and/or record length are reduced. No study was done on the other aircraft to show the effect of record length or control input amplitude.

EFFECT OF SAMPLING RATE AND RECORD LENGTH ON TIME HISTORY MATCHES

As expected, the matches between flight and estimated time histories, when data with very low sampling rates were used in the analysis, were less satisfactory than the matches obtained with baseline data. This is due to limited definition of the measured signals. For example, figures 1(a) and 2(a) show the matches that resulted with the baseline data at 50 samples per second for a lateral-directional and a longitudinal maneuver from aircraft A, and the matches for the same maneuvers are represented at a reduced sampling rate of five samples per second in figures 3(a) and 3(b). The degradation of the matches between estimated and actual data, as a result of thinning the data, is evident. It was also observed that as the sampling rate was reduced, the number of iterations required for convergence increased. The computation time still decreased at lower sampling rates, but because of the increased number of iterations the decrease was not proportionate to the reduction in number of data points. Divergence occurred when the sampling rate approached 5 samples per second. In most cases, the maximum likelihood estimation program converged to a reasonable answer even if the sampling rate was severely reduced.

Reducing record length did not show any significant effect on the quality of the time history matches. The lateral-directional and longitudinal maneuvers of figures 1(a) and 2(a) are shown again at the same sampling rate in figures 4(a) and 4(b), but this time with half record length, and in figures 5(a) and 5(b) with fourth record length. The deviation from the original maneuvers is very slight in a few of the parameters or not noticeable at all. The weighted error sums derived from the maximum likelihood estimator are a measure of the quality of the match. The error sums did not change appreciably as record length decreased. The number of iterations required for convergence was nearly the same as for the full record length despite any change in record length.

EFFECT OF SAMPLING RATE AND RECORD LENGTH ON DERIVATIVE ESTIMATES

The sampling rates for both lateral-directional and longitudinal maneuvers for each aircraft were reduced (by thinning the data) from their baseline rates to as low as 2.5 samples per second, or until the maximum likelihood estimation computer algorithm failed to uniformly converge to an answer. First, the baseline values of the derivatives were estimated for each aircraft (table 3). To assess the effect of reduced sampling rate, the rate was lowered and a new set of derivatives was obtained for each maneuver. The difference in the derivatives was attributed to the decreased number of data points analyzed per unit of time. Since the number of data points used is a function of both the sampling rate and the record length, the combined effect of sampling rate and record length was also investigated. To evaluate this combined effect, only the high quality data from aircraft A were used.

The first step in measuring the combined effect of sampling rate and record length on the derivative estimates was to shorten each aircraft A maneuver to one-half and then one-fourth of its baseline record length. Next the sampling rate was lowered using each new record length to acquire a different set of derivatives for every maneuver. The portion of each maneuver where the control input occurred was always included in the data. At a fixed sampling rate, a comparison between the estimated derivatives determined using full record lengths with the estimates found at each reduced record length shows the effect of record length on the estimates. It should be noted, for example, that the same number of data points are used for the analysis of the entire record length at 25 samples per second as are used for the half record length at 50 samples per second. Based on the derivatives computed at 50 samples per second and full record length, the percentages of change of the estimates determined at 25 samples per second were compared to those found with half record length at 50 samples per second. Similarly, the derivatives obtained at 12.5 samples per second were compared to those determined with quarter record length at 50 samples per second. The results are shown in tables 4(a) (lateral-directional maneuvers) and 4(b) (longitudinal maneuvers). Comparing these differences demonstrates the desirability of lessening sampling rate as opposed to reducing record length as a method of reducing the total computer time required in a stability and control analysis.

The stability and control derivatives for each set of maneuvers from aircraft A are presented as functions of sampling rate in figures 6, 7, 8, and 9 for full record length (top), half record length (middle), and quarter record length (bottom). The maneuvers are grouped according to type (lateral-directional and longitudinal) and amplitude of control input. All the lateral-directional maneuvers from aircraft A have only aileron inputs since aircraft A is known to have a rudder input response which is inadequate for determining a complete set of stability and control derivatives. Since the rudder maneuvers do not lend themselves to yielding high quality stability and control derivatives for the maximum sampling rate, it was felt that it would not be valid to evaluate the effect of sampling rate and record length on these data.

Figure 6 shows the plots of the lateral-directional stability and control derivatives versus sampling rate for the five smaller ($|\delta_a| < 10$ degrees) control input lateral-directional maneuvers from aircraft A. A point is plotted on the right that represents the root mean square average of those derivatives computed at 50 samples per second, and the vertical bar associated with this symbol is the average of the corresponding uncertainty levels. These uncertainty levels show the amount of scatter that might be expected at the highest sampling rate. Similar plots of the four larger ($|\delta_a| < 20$ degrees) input lateral-directional maneuvers are shown in figure 7. Figures 10, 11, 12, and 13 show the lateral-directional derivatives versus sampling rate for aircraft B, C, D, and E, respectively. The longitudinal stability and control derivatives versus sampling rate obtained from the four smaller ($|\delta_e| < 1.1$ degrees) control input longitudinal maneuvers from aircraft A are shown in figure 8. Figure 9 represents similar results for the four larger ($|\delta_e| < 1.5$ degrees) input longitudinal maneuvers . The longitudinal derivatives as a function of sampling rate for aircraft B, C, and D are plotted in figures 14, 15, and 16, respectively.

Lateral-Directional Derivatives

Effect of sampling rate. - The lateral-directional results for aircraft A summarized in table 4(a) indicate that, except for $C_{Y_{\delta_a}}$ and $C_{n_{\delta_a}}$ the change due to sampling rate reductions from 50 to 12.5 samples per second is not greater than two percent. The percentages of change in $C_{Y_{\delta_a}}$ and $C_{n_{\delta_a}}$ are large because the baseline values are close to zero. A study of the plots in figures 6 and 7 reveals the following significant observations of the effect of sampling rate on the aircraft A derivatives.

1. The change in the non-control static derivatives is insignificant to as low as five samples per second. They show very consistent trends with respect to sampling rate reduction.

2. The rotary derivatives and the coefficient of the partial derivatives of side force and yawing moment with respect to the control input ($C_{Y_{\delta_a}}$ and $C_{n_{\delta_a}}$) are not predicted as well when sampling rate is reduced for the cases with smaller amplitude inputs. Usually, the trends of these estimates, are constant, but more scatter about the trend was evident in some cases.

3. Rates as low as 5 to 10 samples per second are acceptable to compute derivative estimates for aircraft A.

The lateral-directional plots in figures 10, 11, 12, and 13 demonstrate good agreement between aircraft A and the aircraft B, C, D, and E findings. Static derivatives show consistent trends, yet the rotary derivatives and the

coefficient of the partial derivative of side force with respect to the control motion ($C_{Y_{\delta_a}}$, $C_{Y_{\delta_r}}$, $C_{Y_{\delta_{c_1}}}$, and $C_{Y_{\delta_{c_2}}}$), occasionally show increased fluctuations as sampling rate is reduced. Nevertheless, 10 samples per second are sufficient to compute derivative estimates with little variation from the baseline values, and 5 samples per second are acceptable for most estimates.

Effect of record length. - Table 4(a) shows that the effect of reducing the record lengths of the aircraft A maneuver is much more pronounced, with up to nearly 100 percent change in the estimates of C_{ℓ_r}. Changes in $C_{Y_{\delta_a}}$ and $C_{n_{\delta_a}}$ are again large partly because of their very small baseline values. Figures 6 and 7 show that the trends of the estimates with respect to sampling rate and record length for the smaller and larger amplitude maneuvers are similar. The greater scatter in the small amplitude cases is characteristic of each record length. For full record lengths (top plots), the estimates in general do not change significantly until a sampling rate of about five samples per second is used, the exceptions being $C_{Y_{\delta_a}}$ and $C_{n_{\delta_a}}$. At one-half record length, the trends are still obvious and very similar to full record length trends, but with slightly more scatter present. The quarter record length plots do not indicate well defined trends in the derivatives, especially in C_{n_r}, C_{ℓ_r}, C_{n_β}, and C_{ℓ_β} for the smaller inputs. The control derivatives do not get worse when record length is decreased as the entire pulse was retained when the length of the maneuver was shortened, thus increasing the relative information of these derivatives.

No study was done on the effect of record length on the maneuvers for other aircraft.

Longitudinal Derivatives

Effect of sampling rate. - The longitudinal results for aircraft A depicted in table 4(b) indicate that, except for C_{m_α} and $C_{Z_{\delta_e}}$, the change due to sampling rate reduction from 50 to 12.5 samples per second is not more than three percent. The C_{m_α} and $C_{Z_{\delta_e}}$ changes are large because the 50 samples per second values are small. (C_{m_α} is small due to the aft center of gravity location.) Derivative estimate trends in figures 8 and 9 are very similar to each other, yet greater scatter in the smaller amplitude control input maneuvers exists, as was noted for the lateral-directional maneuvers discussed earlier.

C_{m_α} and $C_{Z_{\delta_e}}$ are exceptions to the otherwise very consistent trends in the derivatives as sampling rate is reduced for full record lengths. These trends are consistent when sampling rate is reduced to 10 samples per second. Five samples per second is tolerable for most estimates.

The important observations of the effect of sampling rate on the estimated longitudinal derivatives, based only on the data analyzed, are summarized below:

1. $C_{Z_{\delta_e}}$ shows the least consistent trend of the estimates as sampling rate is reduced. The other longitudinal derivatives are very consistent.

2. Ten samples per second are more than adequate to estimate derivatives.

Figures 14, 15, and 16 show good comparison between results for aircraft B, C, and D, and the aircraft A results. $C_{Z_{\delta_e}}$ fluctuates in most cases as sampling rate is reduced, while the other derivatives are steady. Ten samples per second is satisfactory for derivative extraction for all aircraft.

Effect of record length. - Table 4(b) shows that the effect of reducing record length is much greater than lessening sampling rate. Furthermore, figures 8 and 9 show that the derivative values obtained at quarter record length are very similar to those derived at half record length. C_{m_α} and $C_{Z_{\delta_e}}$ changes are large for the same reason mentioned in the previous section. Observations of the effect of record length on the longitudinal derivatives correspond very well with the effects on the lateral-directional estimates discussed earlier.

EFFECT OF CONTROL INPUT SHAPE

The effects of time duration and rapidity of the control inputs on the derivative estimate trends with reduced sampling rate and record length were studied for lateral-directional and longitudinal maneuvers from aircraft A. The maneuvers were performed with slowly-varying control inputs and had the same input energy as the standard pulses previously discussed. The time duration and rapidity of the control inputs had no substantial effect on the trends of the derivatives. The more slowly-varying control inputs, however, demonstrated much more scatter with reduced record length and/or sampling rate, as would be expected since the entire pulse may not be represented in a shortened maneuver. As a result, the effects of sampling rate and record length reductions were not as obvious with a longer, slower-varying control input. Hence, the maneuvers with sharp, larger pulses were

presented in this report to demonstrate the effects of sampling rate and/or record length on the derivatives.

In summary, it has been determined from the data for the lateral-directional and longitudinal derivatives that if it is desirable to obtain accurate estimates of the control derivatives (especially $C_{Y_{\delta_a}}$, $C_{n_{\delta_a}}$, and $C_{Z_{\delta_e}}$) and to a lesser degree the rotary derivatives (C_{n_r}, C_{ℓ_p}, C_{n_p}, and C_{m_q}), sampling rates of 10 samples per second or higher should be used in the analysis. The derivatives that have the greatest effect on the aircraft response, like C_{n_β}, were not affected until very low rates and short record lengths were reached. An important aspect of all the derivative trends from both types of aircraft A maneuvers is the increased scatter in the estimates as the amplitude of the control inputs is decreased.

The lowest tolerable sampling rate for extracting reasonably accurate stability and control derivatives is nearly identical (5 to 10 samples per second) for all these aircraft. Any vehicle being tested should be studied to determine the lowest acceptable sampling rate with the requirements of individual testing and computation facilities. Since the sampling rate required for digital data filtering is usually higher than that necessary to obtain stability and control derivatives, the data must be filtered before it is thinned. The effect of sampling rate needs to be checked regularly to verify that the estimation process yields sufficiently good estimates.

EFFECT OF SAMPLING RATE AND RECORD LENGTH ON UNCERTAINTY LEVELS

The vertical lines through the data points at the baseline sampling rates in figures 6 through 16 indicate uncertainty levels. The uncertainty levels at the highest sampling rate represent the inherent error in the baseline estimates. These levels are bounds that a particular derivative for a particular maneuver should remain within to be considered satisfactory as sampling rate is reduced. For the aircraft A maneuvers (figures 6, 7, 8, and 9), the trends of the uncertainty levels are consistent with the theoretical definition of uncertainty level. The uncertainty levels are the smallest for maximum record length, and as the error due to reduced record length (less information of the aircraft response) increases, the size of the uncertainty level increases. The uncertainty levels are also larger for the smaller amplitude control input cases (figures 6 and 8) as compared to the larger amplitude maneuvers (figures 7 and 9). A major determining factor in any stability and control analysis is the accurate definition of control motion. The resolutions of the signals used for processing will affect the estimated aircraft response to the control input to a greater degree for a small input

than for a larger one. Consequently, less information is present in the data and more error is introduced into the estimated derivatives.

As an example of the influence on the uncertainty levels due to reductions in the sampling rate, figure 17 shows derivative plots, with confidence levels, of the lateral-directional aircraft A maneuver of figure 1(a). The levels are fairly constant with reduced sampling rate. The disagreement at 2.5 samples per second was found to be a result of missing the initiation of control motion. Therefore, the vehicle appeared to start responding at a different initial time point than the control motion. Consequently, the control time history resulted in unacceptable predictions of motion, degrading the estimated derivatives.

The uncertainty levels get larger when greater scatter exists in the derivatives at the lower sampling rates and shorter record lengths. The confidence level trends are as expected when less information is given in the data. Trends in the confidence levels from the maneuvers of the other aircraft and aircraft A were in good agreement.

CONCLUDING REMARKS

The effects of sampling rate and record length on flight determined stability and control derivatives were determined by reducing the sampling rate and record length from their baseline values. The derivatives for the data were extracted by using the maximum likelihood estimation method and analyzed as a function of sampling rate. The combined effect of sampling rate and record length was also investigated.

Several types of aircraft were studied to determine the effects of sampling rate and record length on the derivatives. A wide variety of aircraft configurations and flight conditions were used to distinquish between the results dependent upon the class of aircraft and the quality of the data, and those effects that were independent of these variables. The effects of sampling rate derived from the high quality PA-30 (aircraft A) data were verified with some lower quality (but still acceptable) data from various other aircraft in different flight conditions. Confirmation of the results by these other aircraft was convincing. Generalizations for all aircraft should not be made because the data base was small, but the following conclusions about the effects of reductions in sampling rate and record length of the maneuvers used in this study may be drawn.

1. Excluding digital filtering and data time-shifting considerations, a sampling rate of 5 to 10 samples per second has been found to be adequate to obtain reasonably accurate stability and control derivatives by using the maximum likelihood estimation method.

2. Reducing the sampling rate is more desirable than reducing the record length as a method of lessening the total computation time required

for estimation without greatly degrading the quality of the estimates. If the record length and sampling rate are reduced simultaneously, the magnitude of the tolerable reductions is smaller.

3. Reducing sampling rate and record length degraded the accuracy of the derivative estimates. The determining factor is the accurate definition of control motion. The small amplitude inputs demonstrate greater degradation than the larger amplitude control inputs. The less significant control derivatives and the lateral-directional rotary derivatives were affected more than the other derivatives by the reduction of sampling rate and/or record length.

Dryden Flight Research Center
National Aeronautics and Space Administration
Edwards, California, October 31, 1978

REFERENCES

1. Iliff, Kenneth W.; and Taylor, Lawrence W., Jr.: Determination of Stability Derivatives From Flight Data Using a Newton-Raphson Minimization Technique. NASA TN D-6579, 1972.

2. Steers, Sandra Thornberry; and Iliff, Kenneth W.: Effects of Time-Shifted Data on Flight-Determined Stability and Control Derivatives. NASA TN D-7830, 1975.

3. Maine, Richard E.; and Iliff, Kenneth W.: A FORTRAN Program for Determining Aircraft Stability and Control Derivatives From Flight Data. NASA TN D-7831, 1975.

4. Iliff, Kenneth W.; and Maine, Richard E.: Further Observations on Maximum Likelihood Estimates of Stability and Control Characteristics Obtained From Flight Data. AIAA 77-1133, Aug. 1977.

5. Fink, Marvin P.; and Freeman, Delma C., Jr.: Full-Scale Wind-Tunnel Investigation of Static Longitudinal and Lateral Characteristics of a Light Twin-Engine Airplane. NASA TN D-4983, 1969.

6. Holleman, Euclid C.: Summary of Flight Tests To Determine the Spin and Controllability Characteristics of a Remotely Piloted, Large-Scale (3/8) Fighter Airplane Model. NASA TN D-8052, 1976.

7. Clark, Daniel C.; and Kroll, John: General Purpose Airborne Simulator-Conceptual Design Report. NASA CR-544, 1966.

8. Sisk, Thomas R.; Matheny, Neil W.; Kier, David A.; and Manke, John A.: A preliminary Flying-Qualities Evaluation of a Variable-Sweep Fighter-Type Aircraft. NASA TM X-1583, 1968.

9. Pyle, Jon S.: Lift and Drag Characteristics of the HL-10 Lifting Body During Subsonic Gliding Flight. NASA TN D-6263, 1971.

10. Edwards, John W.; and Deets, Dwain A.: Development of a Remote Digital Augmentation System and Application to a Remotely Piloted Research Vehicle. NASA TN D-7941, 1975.

TABLE 1. TEST CONDITIONS

(A) AIRCRAFT A

CASE (MANEUVER)	α, DEG	V, M/SEC (FT/SEC)	$\bar{q}$, KN/M^2 (LB/FT^2)	INPUT	BASELINE SAMPLING RATE, SAMPLES/SECOND
LATERAL-DIRECTIONAL MANEUVERS					
26A/(3)	8.58	42.8(140.3)	0.89(18.6)	δ_a	50
26B/(1)	8.64	43.1(141.3)	0.90(18.8)	δ_a	50
27 /(2)	8.10	43.3(142.1)	0.91(19.0)	δ_a	50
28 /(4)	8.76	42.4(139.1)	0.87(18.2)	δ_a	50
29 /(5)	9.08	42.1(138.2)	0.86(18.0)	δ_a	50
30 /(3)	8.97	42.7(140.2)	0.89(18.5)	δ_a	50
31 /(1)	9.06	42.4(139.2)	0.88(18.4)	δ_a	50
32 /(2)	9.33	42.2(138.6)	0.87(18.1)	δ_a	50
33 /(4)	9.24	42.2(138.3)	0.86(18.0)	δ_a	50
LONGITUDINAL MANEUVERS					
9 /(3)	8.06	43.3(142.1)	0.90(18.9)	δ_e	50
10 /(1)	8.70	42.9(140.9)	0.89(18.6)	δ_e	50
11 /(2)	9.46	41.8(137.3)	0.85(17.7)	δ_e	50
12 /(4)	8.94	42.7(140.0)	0.88(18.4)	δ_e	50
13 /(3)	8.86	42.3(138.7)	0.86(18.0)	δ_e	50
14 /(1)	9.03	42.4(139.2)	0.87(18.2)	δ_e	50
15 /(2)	9.04	42.4(139.0)	0.87(18.1)	δ_e	50
16 /(4)	9.52	41.7(136.9)	0.84(17.6)	δ_e	50

TABLE 1. - TEST CONDITIONS

(CONTINUED)

(B) AIRCRAFT B, C, D, AND E

LATERAL-DIRECTIONAL MANEUVERS

CASE	MACH NUMBER	α, DEG	V, M/SEC (FT/SEC)	$\bar{q}$, KN/M^2 (LB/FT^2)	INPUT	BASELINE SAMPLING RATE, SAMPLES/SECOND
AIRCRAFT B						
1:2	0.44	5.13	129.7(425.4)	2.00(41.7)	δ_r	50
1:3	0.60	4.74	175.5(575.8)	4.40(92.0)	δ_{c_1}	50
1:10B	0.32	13.94	95.7(314.1)	1.55(32.4)	δ_{c_1}	50
1:13	0.24	17.25	74.2(243.3)	1.28(26.7)	δ_a	50
1:14B	0.24	17.52	74.1(243.2)	1.32(27.6)	δ_{c_1}	50
AIRCRAFT C						
182:29	0.40	9.70	126.4(414.8)	3.60(75.2)	δ_a, δ_r	50
AIRCRAFT D						
7:5	0.80	7.00	239.0(784.0)	11.30(236.0)	δ_{c_2}	20
7:6	0.81	6.50	245.1(804.0)	11.87(248.0)	δ_r	20
7:9	0.90	11.50	264.3(867.0)	10.25(214.0)	δ_r	20
7:17	1.24	5.50	367.9(1207.0)	20.49(428.0)	δ_r	20
8:4	0.78	5.00	248.1(814.0)	14.65(306.0)	δ_{c_2}	20
AIRCRAFT E						
19:2	1.22	16.60	361.8(1187.0)	7.09(148.0)	δ_a, δ_r	50

TABLE 1. - TEST CONDITIONS

(CONTINUED)

(c) AIRCRAFT B, C, AND D

LONGITUDINAL MANEUVERS

CASE	MACH NUMBER	α, DEG	V, M/SEC (FT/SEC)	$\bar{q}$ KN/M^2 (LB/FT^2)	INPUT	BASELINE SAMPLING RATE, SAMPLES/SECOND
AIRCRAFT B						
2:1	0.70	3.20	206.6(677.7)	5.49(114.7)	δ_e	50
2:2	0.41	11.19	120.0(393.8)	1.79(37.3)	δ_e	50
2:4	0.35	14.85	101.7(333.5)	1.54(32.2)	δ_e	50
5:1A	0.53	7.86	126.6(415.2)	1.87(39.0)	δ_e	50
AIRCRAFT C						
1:4A:27	0.32	9.10	105.2(345.0)	5.03(105.0)	δ_e	50
AIRCRAFT D						
1:4	0.87	5.50	289.3(949.2)	16.40(342.5)	δ_e	20
6:12	1.20	2.20	386.2(1267.0)	53.6(1119.0)	δ_e	20
7:18	1.[illegible]	5.25	422.1(1385.0)	26.62(556.0)	δ_e	20
8:3	0.80	4.40	243.8(800.0)	14.20(296.5)	δ_e	20

TABLE 2

ELEMENTS OF WEIGHTING MATRICES USED IN THE ERROR MINIMIZATION FOR AIRCRAFT A, B, C, D, AND E

WEIGHTING MATRICES	SIGNAL	AIRCRAFT				
		A	B	C	D	E
Lateral-Directional	$\dot{r}$	0	0	0	0	0
	$\dot{p}$	0	0	0	0	0
	A_y	35,000	19,100	100,000	66,500	31,430
	ϕ	55,000	86,100	31,500	13,000	30,050
	r	200,000	1,410,000	480,000	383,000	122,600
	p	35,000	66,300	11,500	2,610	4,293
	β	100,000	450,000	250,000	74,300	577,300
Longitudinal	a_n	4,890	6,300	3,500	10,000	-------
	θ	41,500	2,000,000	1,100,000	400,000	-------
	q	115,000	364,000	130,000	70,000	-------
	α	225,000	571,000	1,000,000	100,000	-------

TABLE 3. - BASELINE DERIVATIVES

(A) AIRCRAFT A

CASE (MANEU-VER)	C_{Y_β}	C_{ℓ_β}	C_{ℓ_p}	C_{ℓ_r}	C_{n_β}	C_{n_p}	C_{n_r}	$C_{Y_{\delta_a}}$	$C_{\ell_{\delta_a}}$	$C_{n_{\delta_a}}$
26A/(3)	-.004482	-.000730	-.466699	.160378	.000920	-.131333	-.083484	.000052	.001482	.000043
26B/(1)	-.007345	-.000850	-.445315	.153288	.000955	-.140828	-.116617	-.000874	.001375	.000042
27/(2)	-.007724	-.000623	-.486669	.145719	.001014	-.112246	-.087739	-.000388	.001457	.000050
28/(4)	-.001685	-.000760	-.490028	.168551	.000993	-.131206	-.116014	.000163	.001383	.000047
29/(5)	-.004655	-.000704	-.514497	.151878	.001038	-.127660	-.115218	.000239	.001594	000043
30/(3)	-.006892	-.000814	-.488391	.152899	.000955	-.135685	-.106806	-.000435	.001425	.000054
31/(1)	-.005920	-.000704	-.486051	.164788	.001011	-.145416	-.119596	-.000320	.001432	.000072
32/(2)	.007133	-.000782	-.457303	.174060	.000928	-.141000	-.106620	-.000122	.001403	.000087
33/(4)	-.006588	-.000690	-.466667	.155463	.000942	-.144986	-.106462	-.000338	.001377	.000076

CASE	C_{Z_α}	C_{m_α}	C_{m_q}	$C_{Z_{\delta_e}}$	$C_{m_{\delta_e}}$
9/(3)	-.091901	-.000673	-14.425	.014825	-.052204
10/(1)	-.074408	-.002204	-12.977	-.001034	-.053938
11/(2)	-.084847	-.001271	-16.567	.019184	-.059901
12/(4)	-.071606	-.000694	-18.405	-.025075	-.052921
13/(3)	-.086552	-.000533	-14.392	.006852	-.045673
14/(1)	-.077679	-.001356	-12.805	-.020775	-.042113
15/(2)	-.077002	-.00092	-14.437	-.017026	-.045039
16/(4)	-.096072	-.002169	-13.470	.023548	-.045871

TABLE 3. - BASELINE DERIVATIVES
(CONTINUED)

(B) AIRCRAFT B, C, D, AND E
LATERAL-DIRECTIONAL MANEUVERS

AIRCRAFT	CASE	C_{Y_β}	C_{ℓ_β}	C_{ℓ_p}	C_{ℓ_r}	C_{n_β}	C_{n_p}	C_{n_r}	$C_{Y_{control}}$	$C_{\ell_{control}}$	$C_{n_{control}}$
B	1:2	-.012184	-.002547	-.317871	-.047294	.002755	.036209	-.408326	.003176	.000172	-.001717
	1:3	-.015325	-.002643	-.318136	.042319	.003203	-.071563	-.420688	-.001122	.000755	.000581
	1:10B	-.011936	-.002513	-.172917	.374353	.002012	.005954	-.482112	-.001267	.000904	.000478
	1:13	-.012818	-.002639	.009039	2.12605	.001435	-.162535	-.142619	.002711	-.000308	-.001301
	1:14B	-.012152	-.002413	-.122280	-.070561	.001008	-.108303	-.303001	-.000728	.000581	.000610
C	182:29	-.010415	-.002038	-.431599	.125808	.001637	-.153677	-.310910	-.000461	.000859	.000110
									.004715	.000947	.000274
D	7:5	-.005803	-.002509	-.309363	.844474	.000992	-.020386	-.551064	.001064	-.001588	-.000251
	7:6	-.010871	-.000824	-.298147	.240379	.000986	-.279433	-.734938	.00129	.000265	-.001466
	7:9	-.00893	-.002221	-.16676	-.156507	.000610	-.027255	-.333556	.001034	.000308	-.001270
	7:17	-.01056	-.002030	-.181933	.094089	.001546	-.007562	-.265229	.000060	.000151	-.001095
	8:4	-.009935	-.002507	-.407971	.862307	.000852	-.050581	-.270586	.00183	-.002069	-.000281
E	19:2	-.017656	-.003964	-.082154	1.19239	.003022	.294935	-1.15735	.000858	.000431	-.001261
									.000856	.000883	.000540

TABLE 3. - BASELINE DERIVATIVES
(CONTINUED)

(c) AIRCRAFT B, C, AND D

LONGITUDINAL MANEUVER

AIRCRAFT	CASE	C_{Z_α}	C_{m_α}	C_{m_q}	$C_{Z_{\delta_e}}$	$C_{m_{\delta_e}}$
B F-15 RPRV	2:1	-.065409	-.006057	-6.2785	-.002019	-.010208
	2:2	-.048862	-.004474	-6.5334	-.006970	-.009925
	2:4	-.042239	-.008746	-3.3774	-.008296	-.009850
	5:1A	-.079106	-.005367	-6.53377	-.008547	-.010398
C JETSTAR	184A:27	-.094349	-.014897	-15.177	-.00728	-.016588
D F-111A	5:4	-.095696	-.027798	-43.5252	-.002445	-.04019
	6:12	-.045465	-.047253	-23.3456	-.005089	-.029245
	7:18	-.049059	-.050011	-25.5086	-.001827	-.02690
	8:3	-.103698	-.020826	-36.72383	.006117	-.032379

TABLE 4. - PERCENT DIFFERENCE IN DERIVATIVES FOR AIRCRAFT A
(ALL NUMBERS IN PERCENT)

(A) LONGITUDINAL MANEUVERS

FROM TO	50 SPS 25 SPS	FULL RECORD LENGTH (25 SPS) 1/2 RECORD LENGTH (50 SPS)	50 SPS 12.5 SPS	FULL RECORD LENGTH (12.5 SPS) 1/4 RECORD LENGTH (50 SPS)
C_{Y_β}	1.7	11.6	1.7	54.9* (34.9)
C_{ℓ_β}	1.2	10.1	1.6	44.1
C_{ℓ_p}	.7	11.3	2.0	10.9
C_{ℓ_r}	.7	55.9	1.1	95.0
C_{n_β}	.3	4.7	.6	14.1
C_{n_p}	.7	21.4	1.8	18.1
C_{n_r}	.7	30.4	1.1	59.7
$C_{Y_{\delta_a}}$	14.0	119.2* (40.8)	65.0	193.7* (127.0)
$C_{\ell_{\delta_a}}$	.6	5.0	1.5	3.0
$C_{n_{\delta_a}}$	6.5	18.7	19.6	61.2

* ASTERISK DESIGNATES AVERAGE COMPUTED WITH EXTREME VALUES. AVERAGES TAKEN EXCLUDING THESE VALUES ARE IN PARENTHESES.

TABLE 4. - PERCENT DIFFERENCE IN
DERIVATIVES FOR AIRCRAFT A
(ALL NUMBERS IN PERCENT)

(B) LATERAL-DIRECTIONAL MANEUVERS

FROM TO	50 SPS 25 SPS	FULL RECORD LENGTH (25 SPS) 1/2 RECORD LENGTH (50 SPS)	50 SPS 12.5 SPS	FULL RECORD LENGTH (12.5 SPS) 1/4 RECORD LENGTH (50SPS)
C_{Z_α}	0.5	11.5	1.0	7.3
C_{m_α}	4.1	61.7	17.7	68.7
C_{m_q}	1.8	5.9	2.7	5.7
$C_{Z_{\delta_e}}$	21.3* (7.7)	257.3* (78.8)	48.7* (16.4)	319.4* (131.3)
$C_{m_{\delta_e}}$	1.4	4.4	2.0	4.4

* ASTERISK DESIGNATES AVERAGE COMPUTED WITH EXTREME VALUES. AVERAGES TAKEN EXCLUDING THESE VALUES ARE IN PARENTHESES.

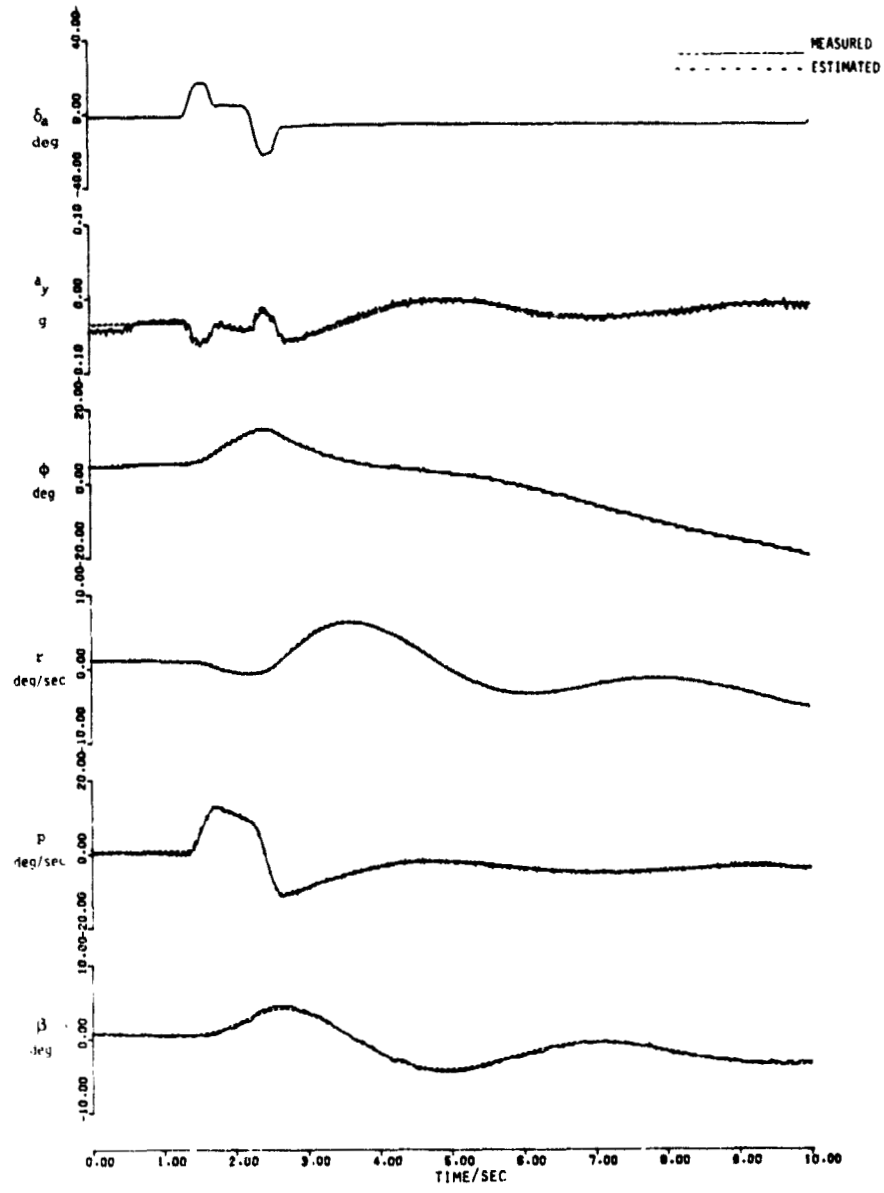

(a) Aircraft A; δa pulse.

Figure 1. Typical match between estimated and measured flight time histories for a lateral-directional maneuver at the baseline sampling rate and full record length.

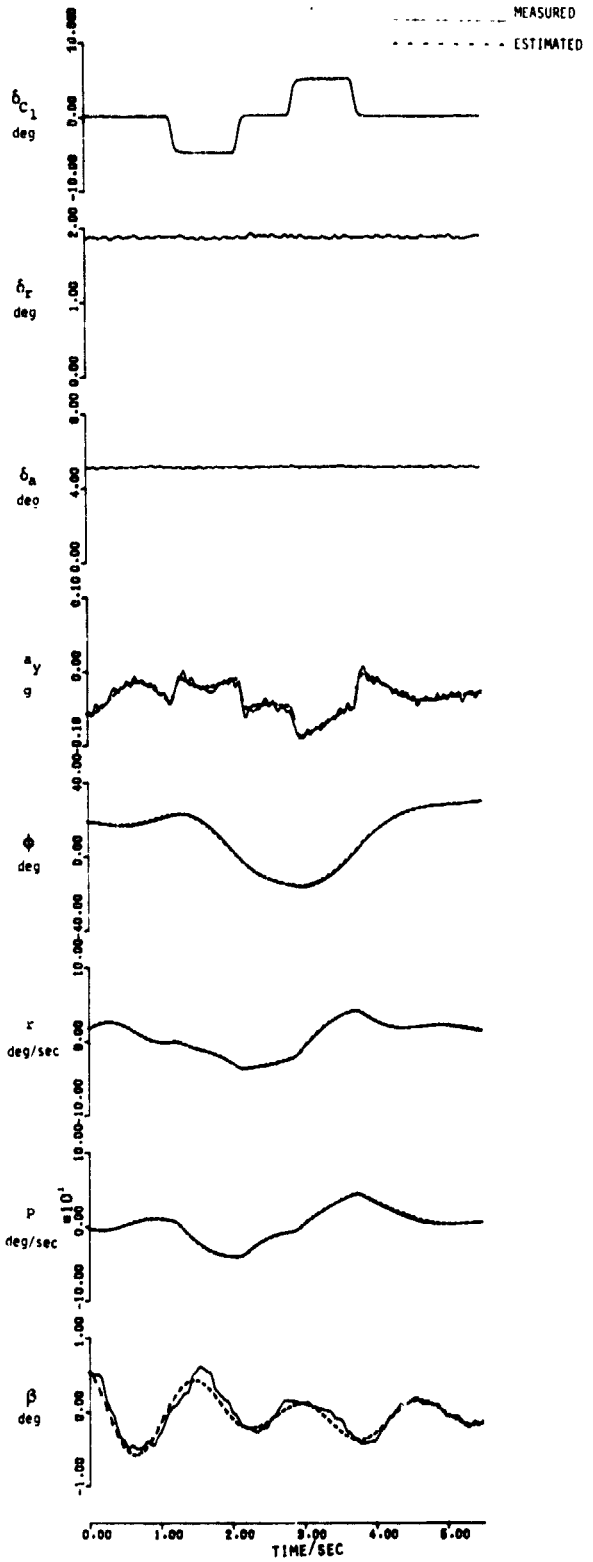

(b) Aircraft B; δ_{C_1} pulse.

Figure 1. Continued

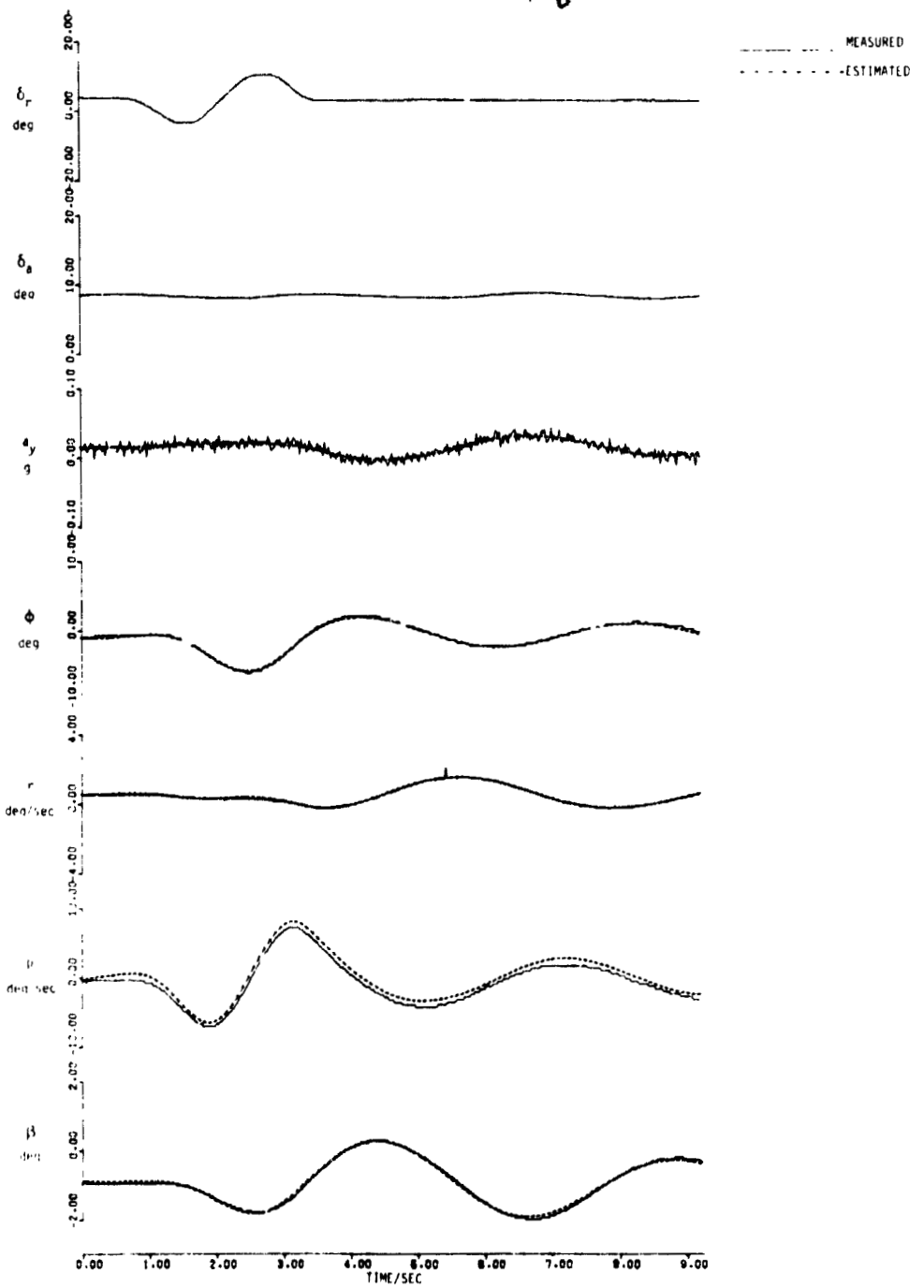

(c) Aircraft C: δ_r pulse.

Figure 1. Continued.

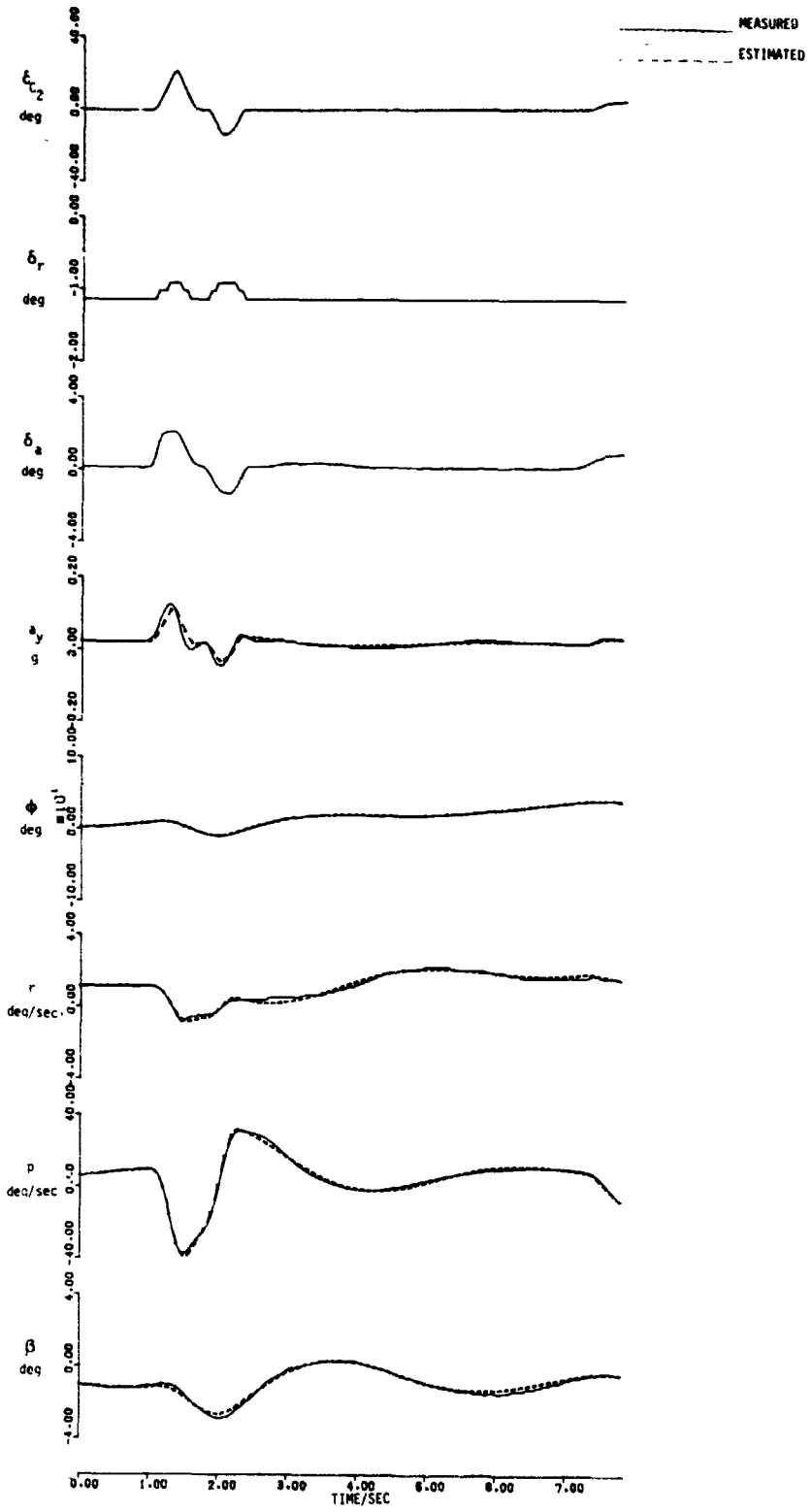

(d) Aircraft D; δ_{c_2} pulse.

Figure . Continued.

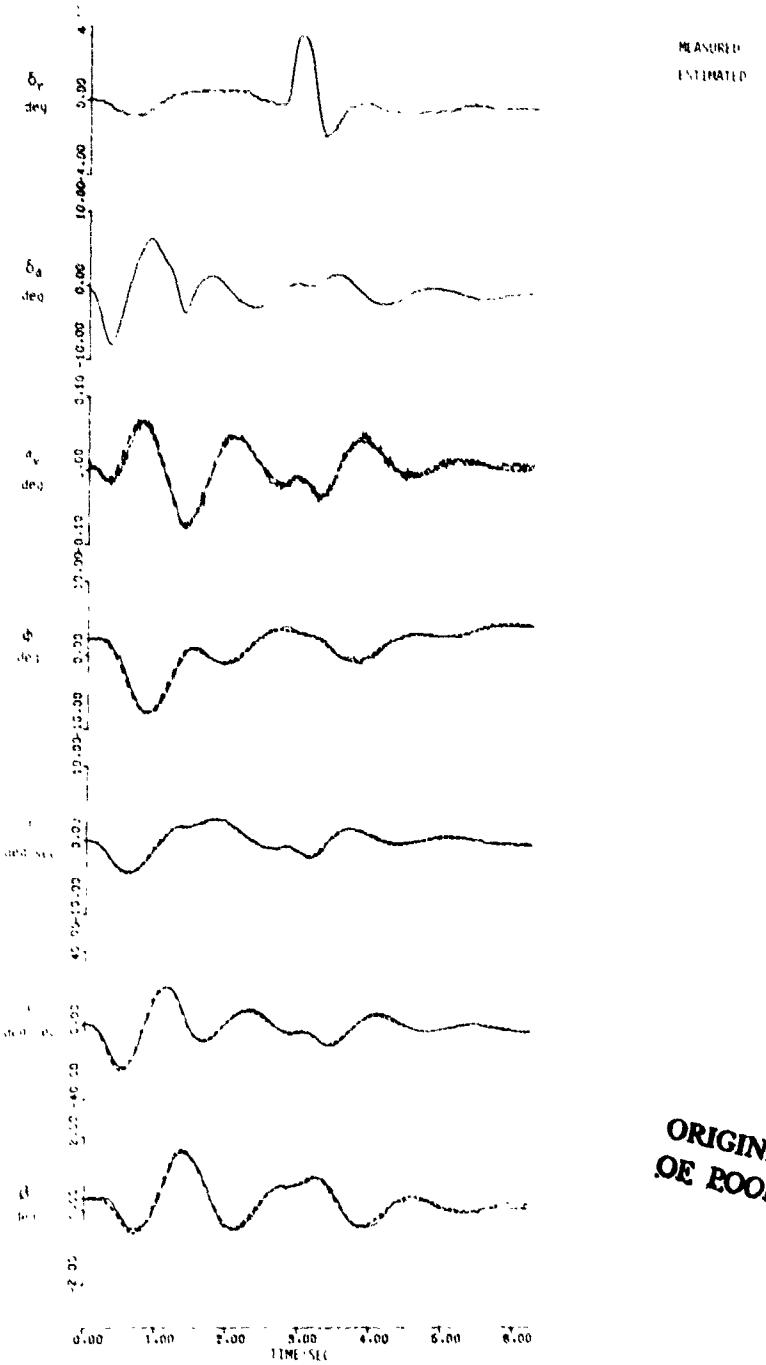

(e) Aircraft E: δ_a, δ_r pulses.

Figure 1. Concluded

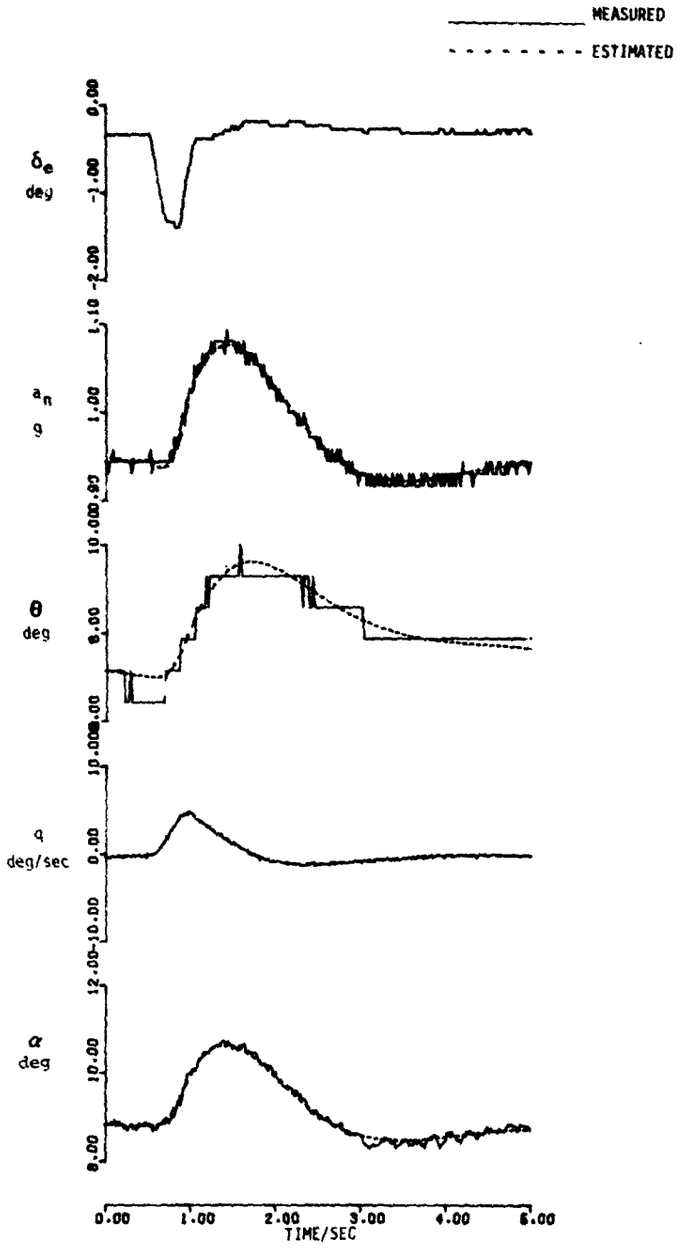

(a) Aircraft A.

Figure 2. Typical match between estimated and measured time histories for a longitudinal maneuver at the baseline sampling rate and full record length.

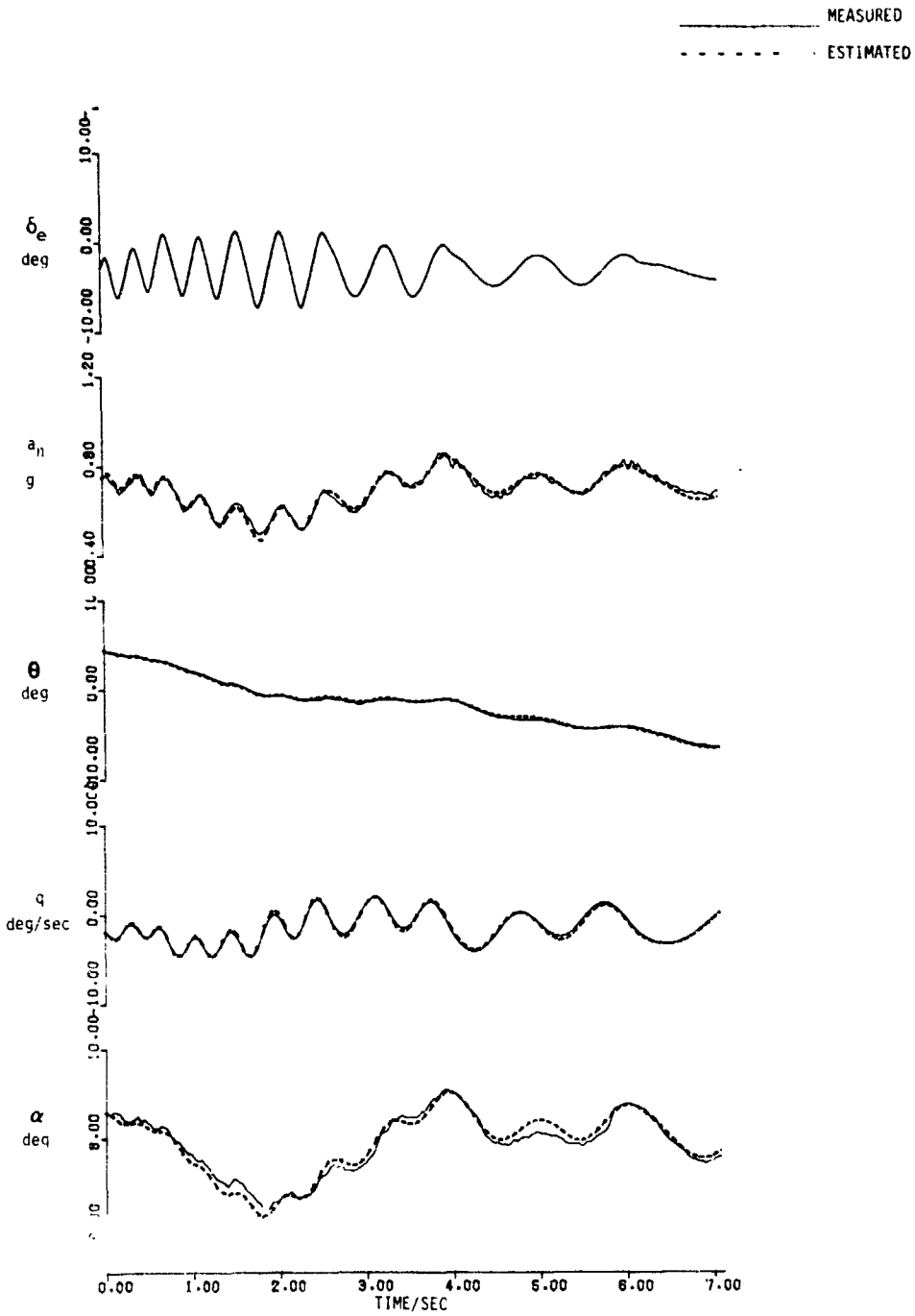

(b) Aircraft B.

Figure 2. Continued

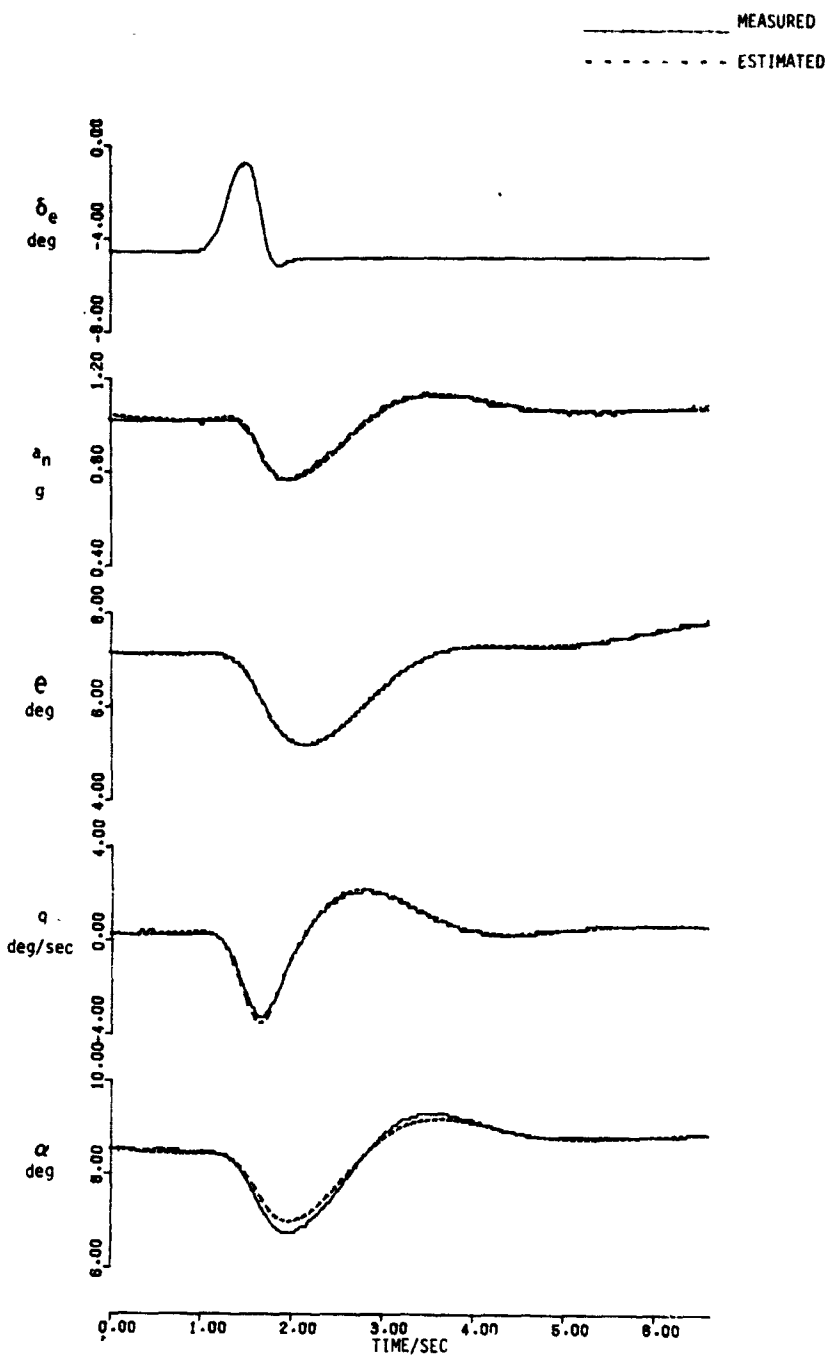

(c) Aircraft C.

Figure 2. Continued.

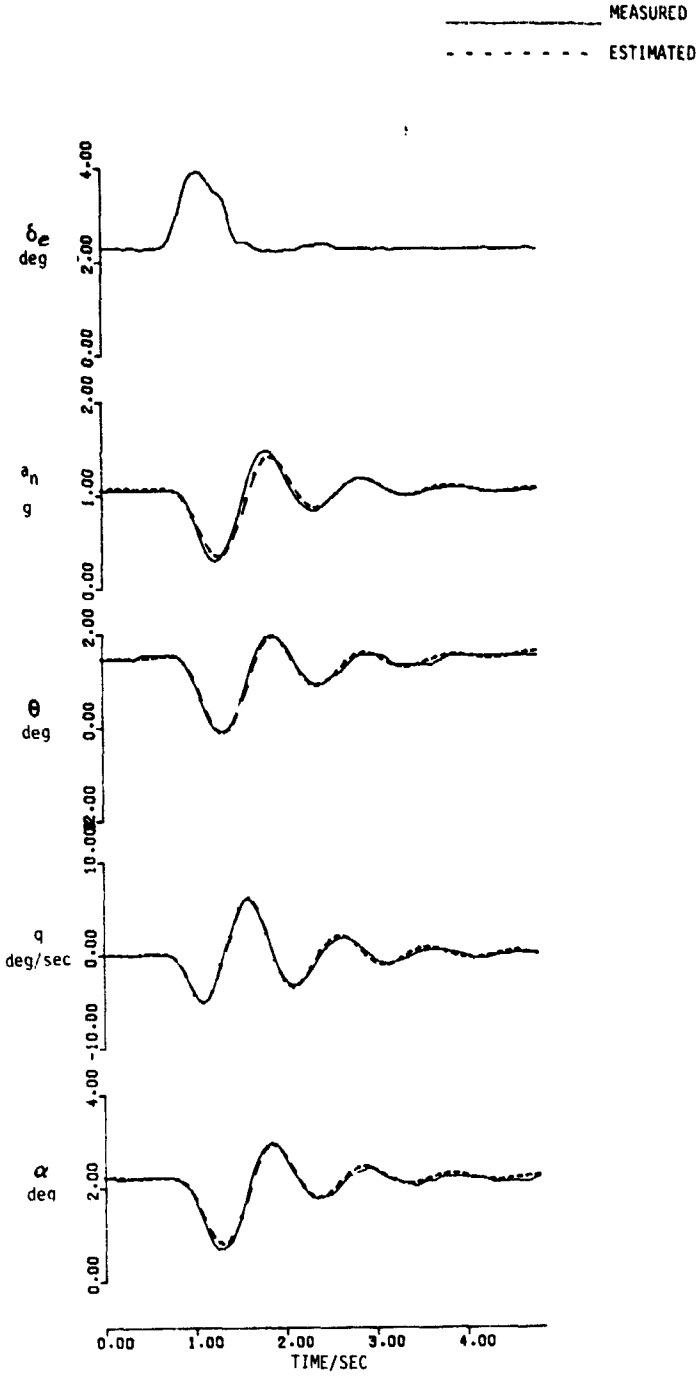

(d) Aircraft D.

Figure 2. Concluded.

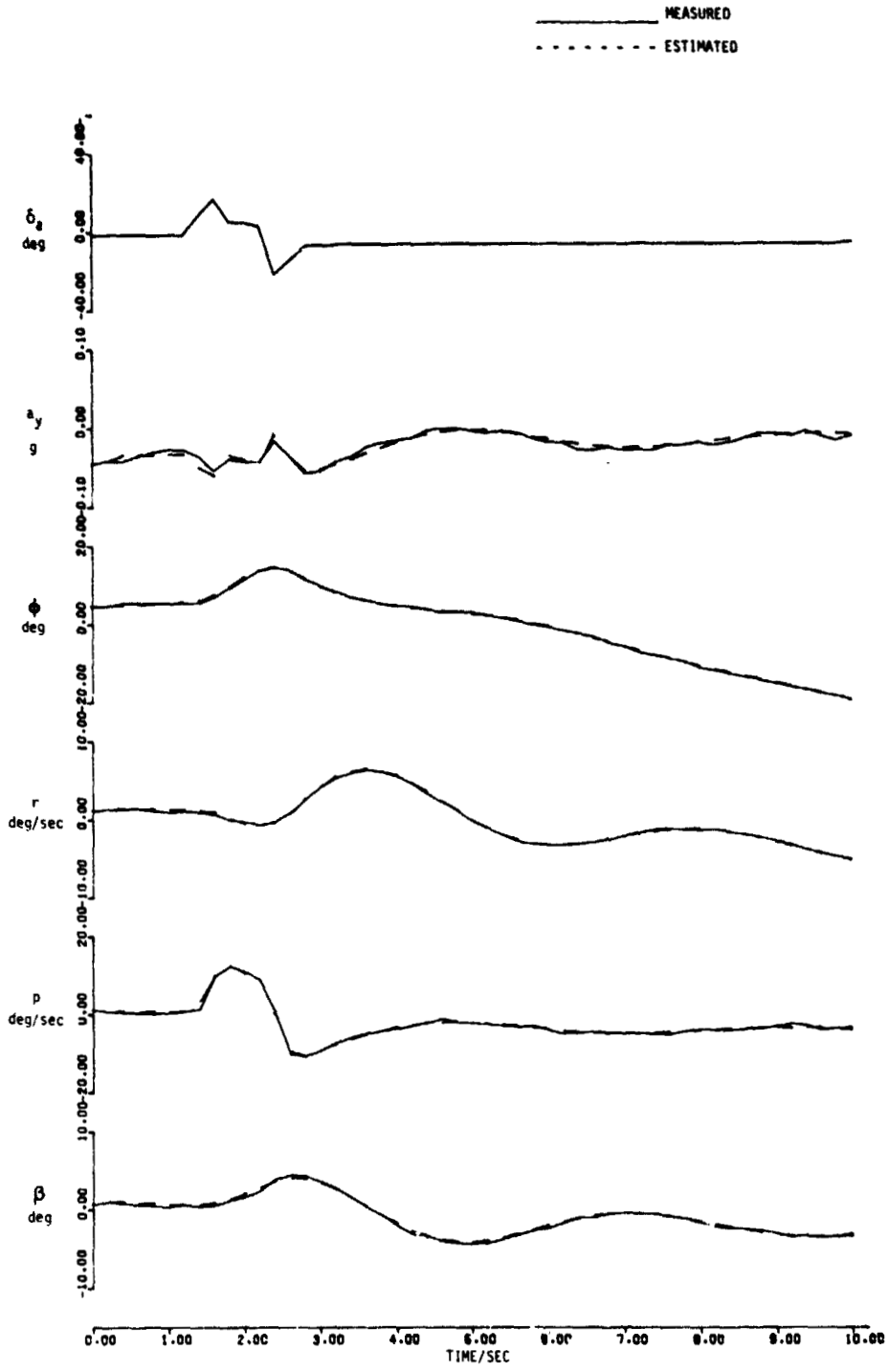

(a) Lateral-directional.

Figure 3. Matches between estimated and measured flight time histories for Aircraft A maneuver with sampling rate reduced to five samples per second.

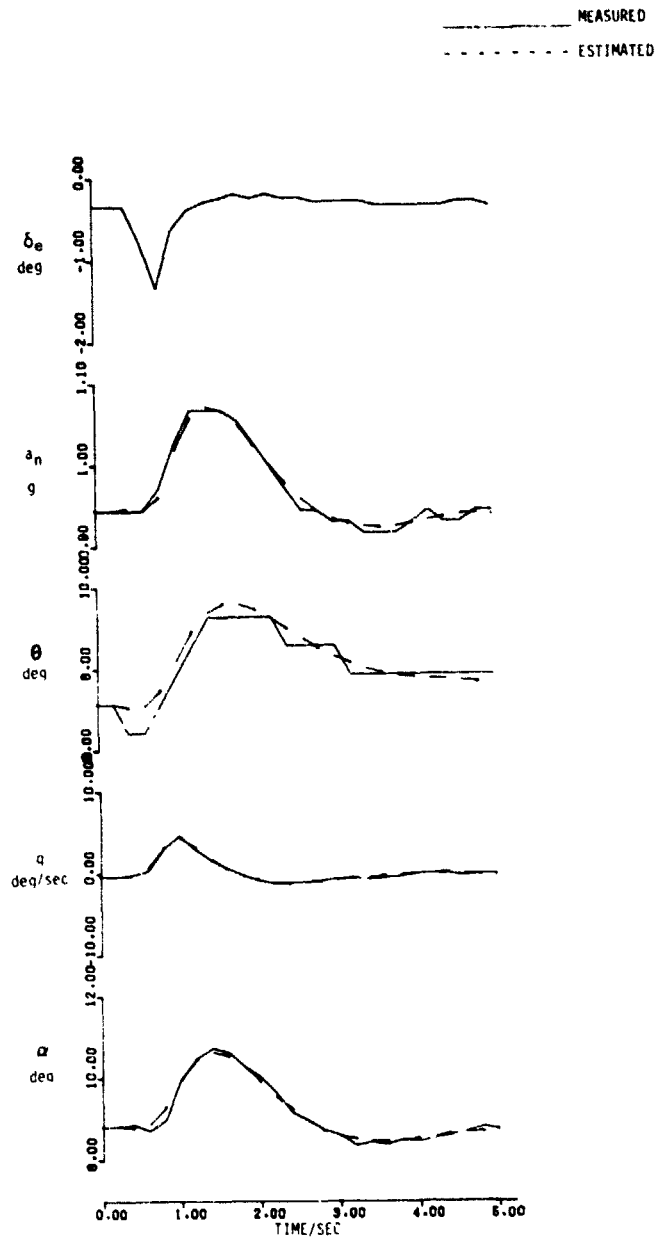

(b) Longitudinal.

Figure 3. Concluded.

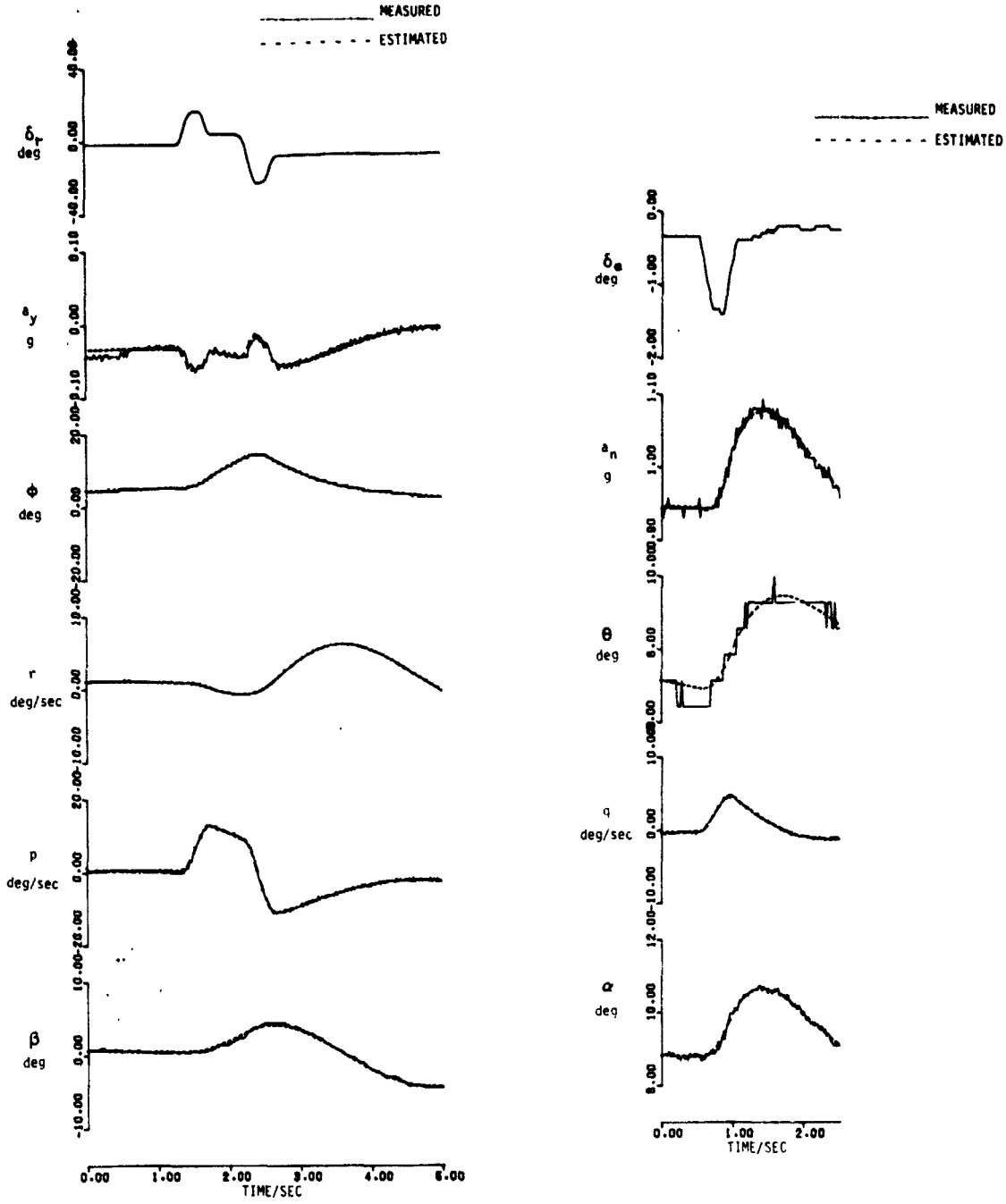

(a) Lateral-directional.

(b) Longitudinal.

Figure 4. Matches between estimated and measured flight time histories for Aircraft A maneuver with record length reduced to one-half.

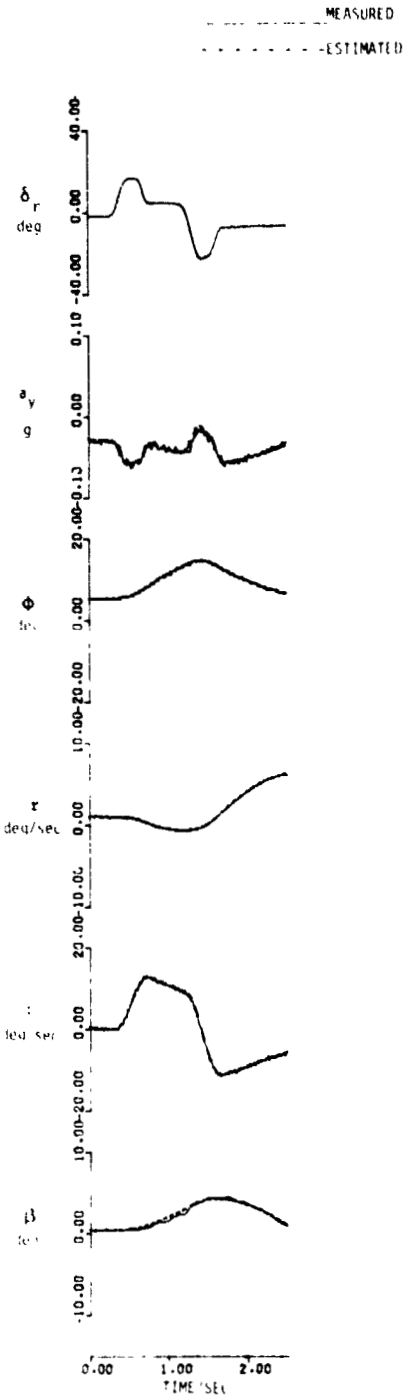

(a) Lateral-directional

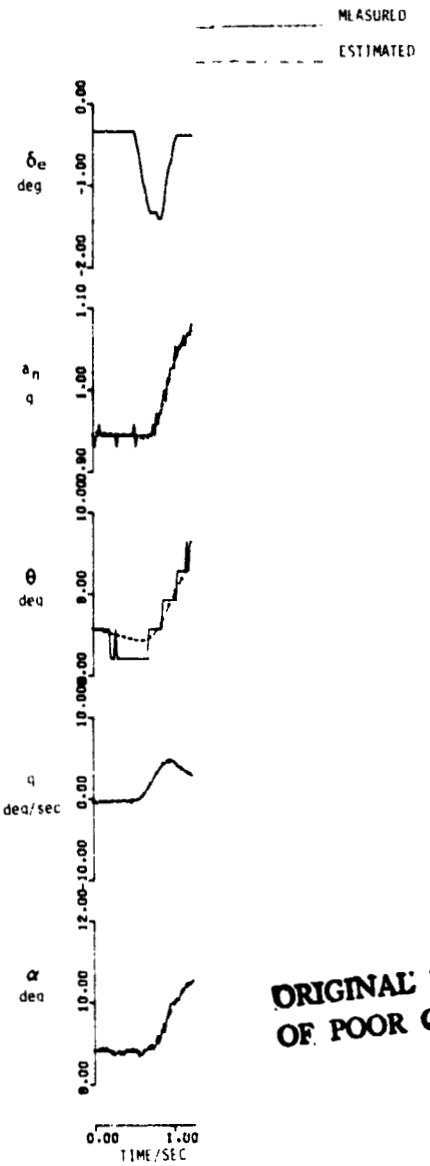

(b) Longitudinal

Figure 5. Matches between estimated and measured flight time histories for Aircraft A maneuver with record length reduced one-quarter.

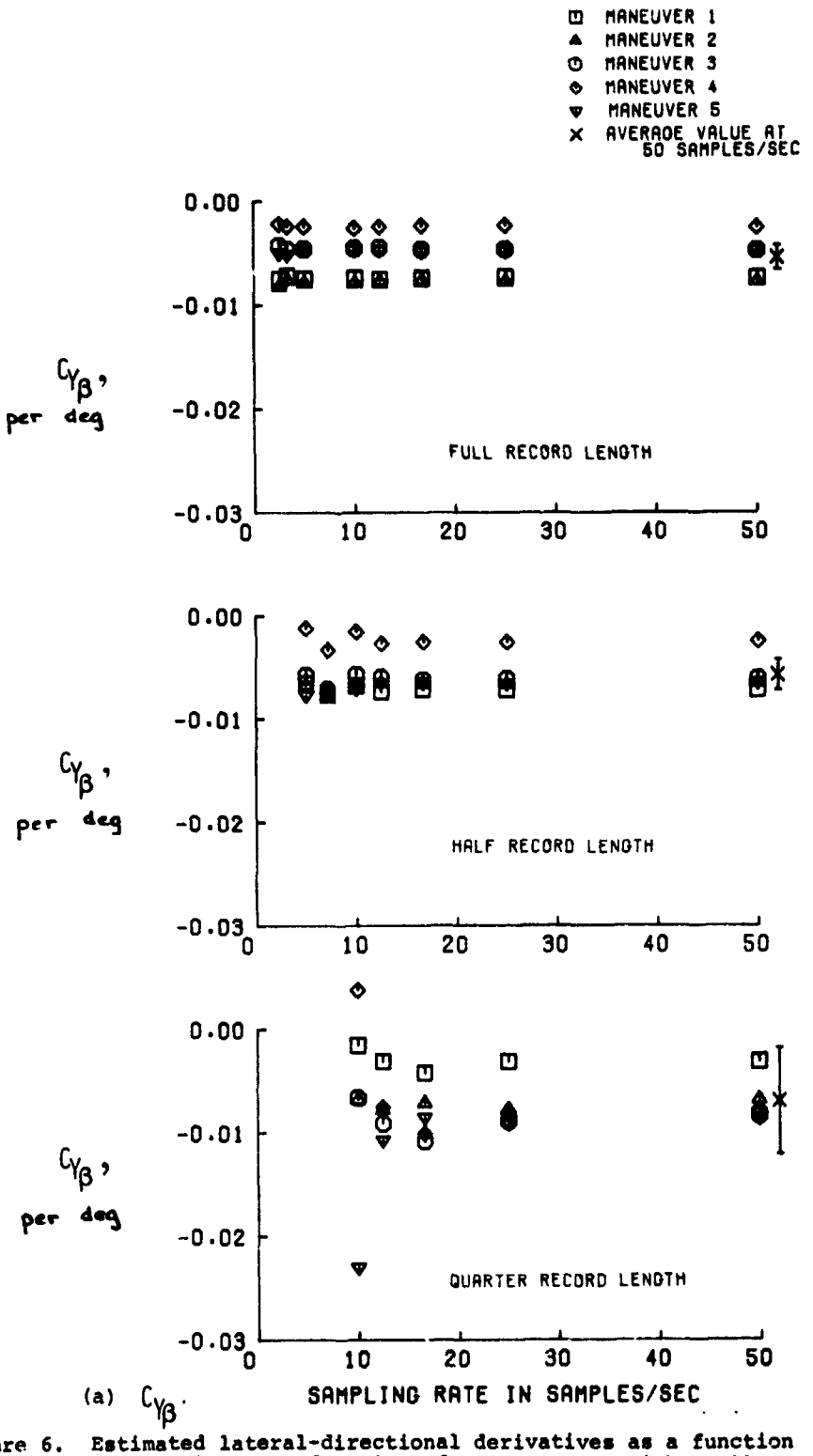

(a) C_{Y_β}.

Figure 6. Estimated lateral-directional derivatives as a function of sampling rate for Aircraft A maneuvers with small amplitude control inputs.

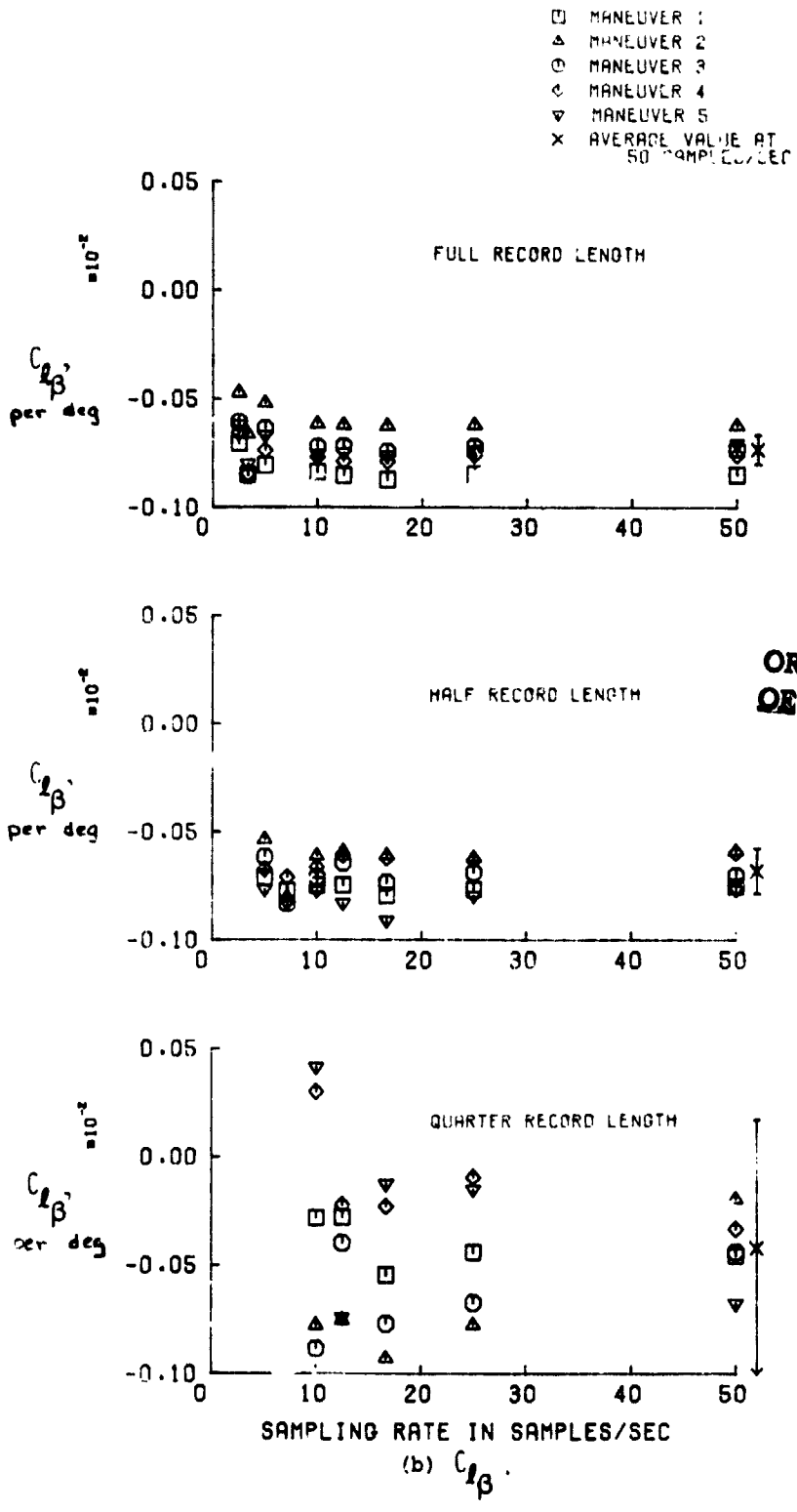

(b) C_{ℓ_β}.

Figure 6. Continued

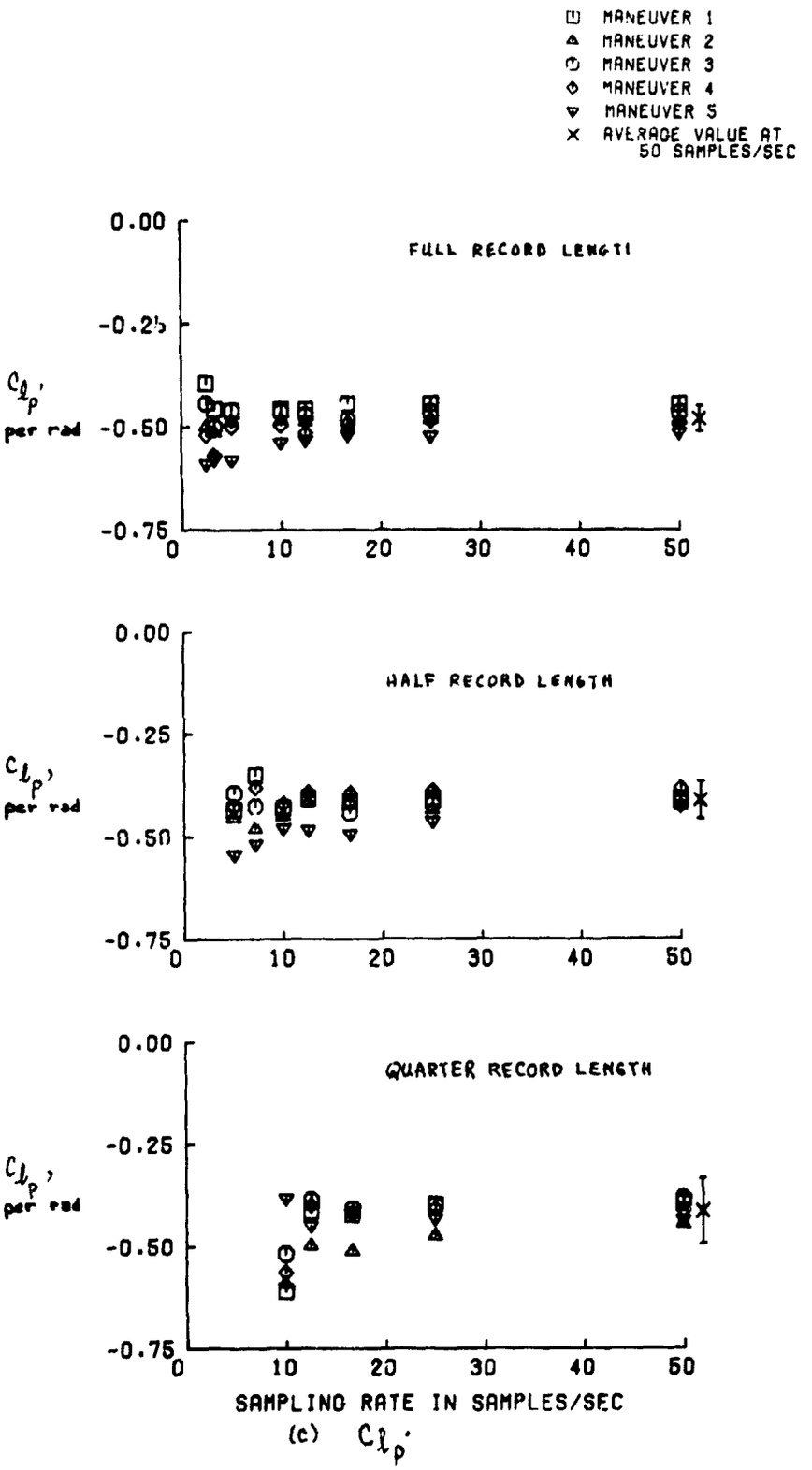

(c) C_{l_p}

Figure 6. Continued.

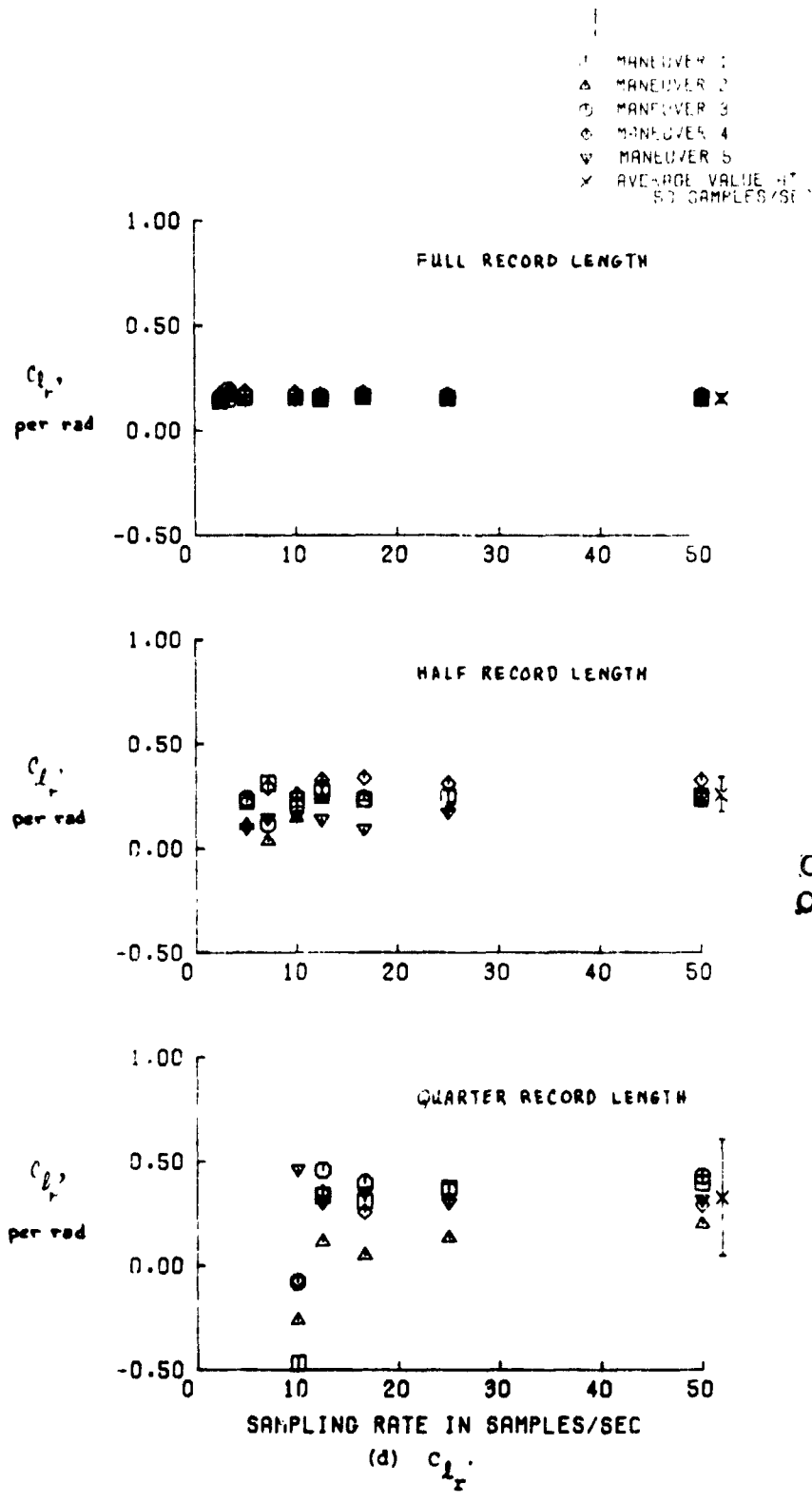

(d) C_{l_r}

Figure 6. Continued.

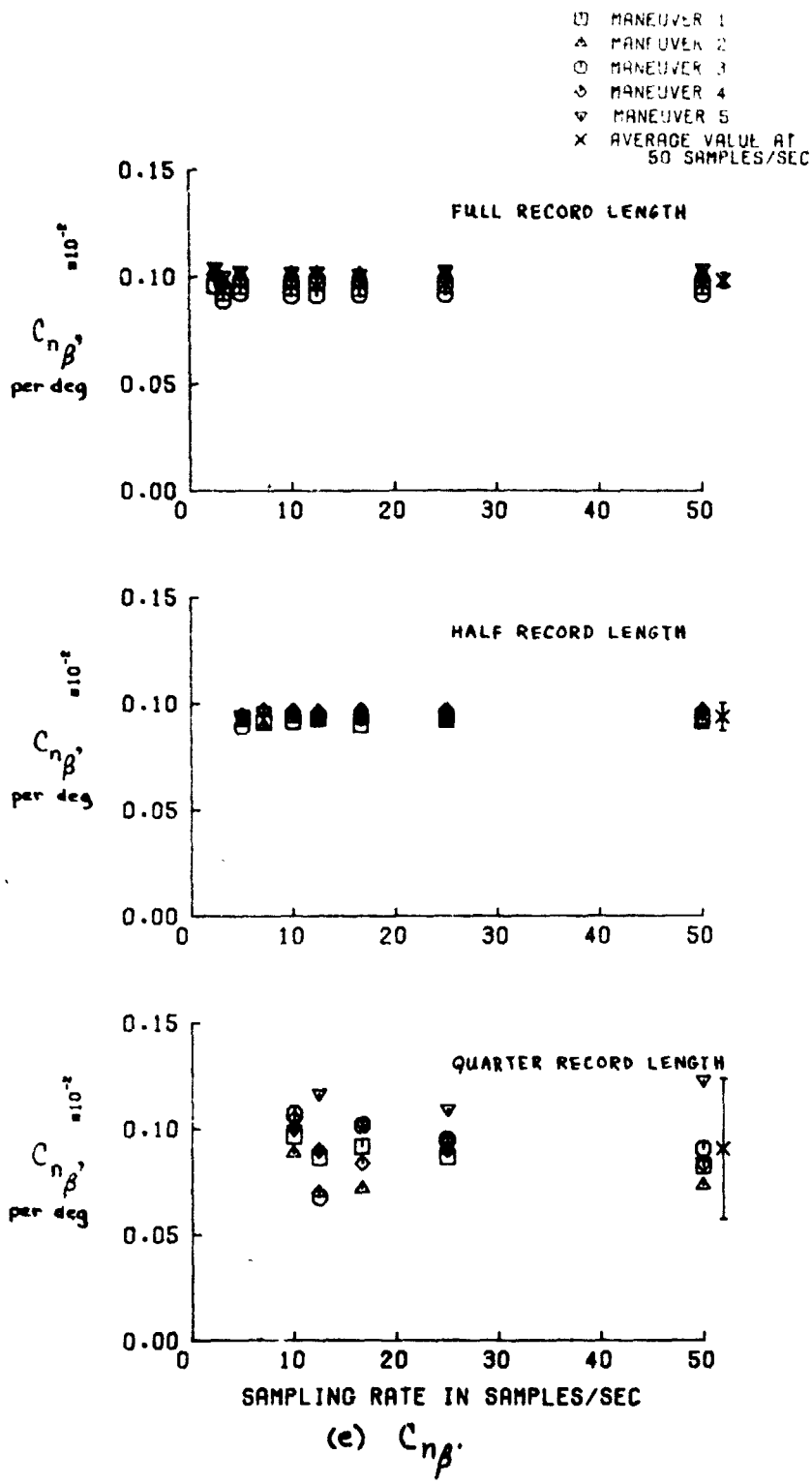

(e) C_{n_β}.

Figure 6. Continued.

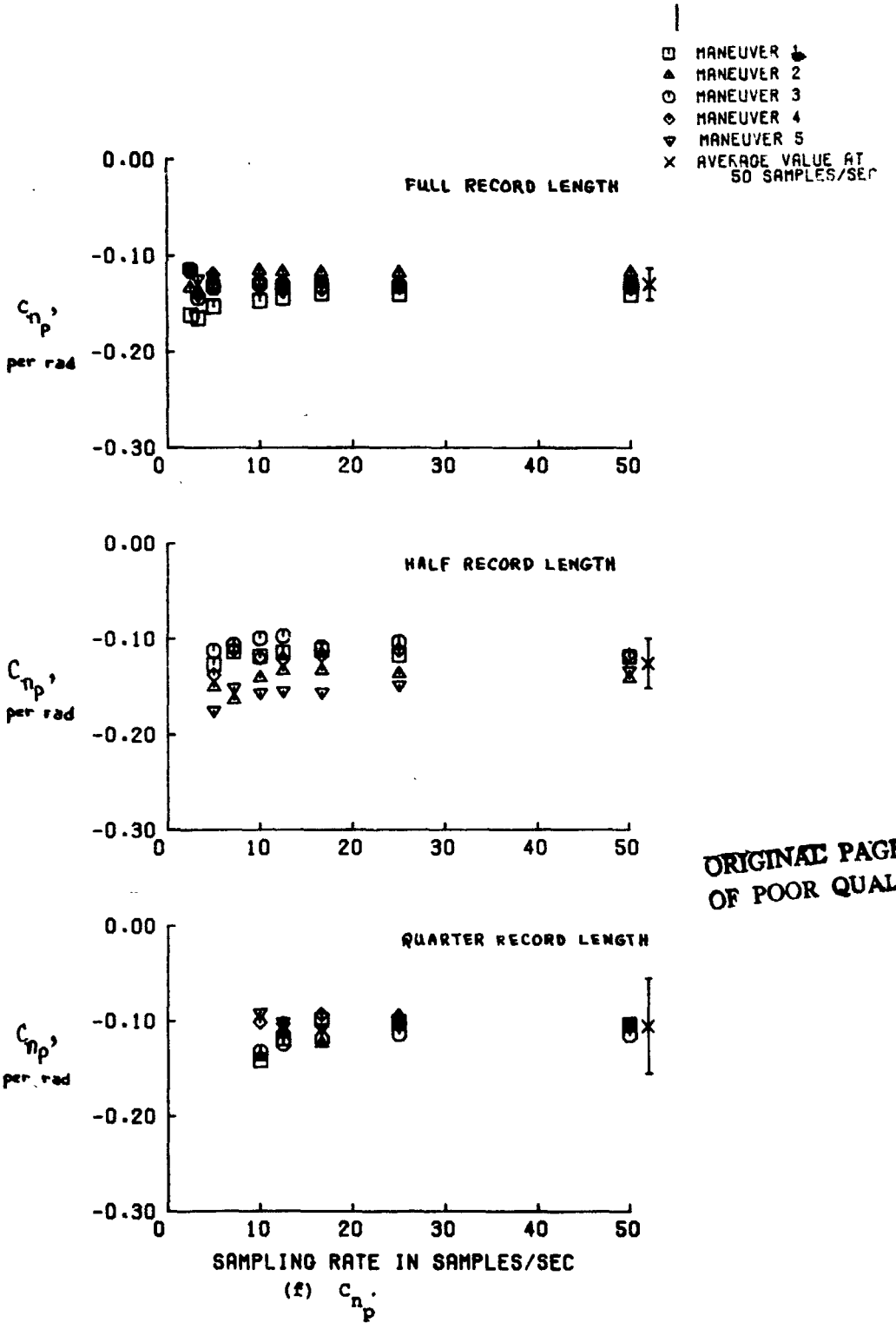

(f) C_{n_p}.

Figure 6. Continued.

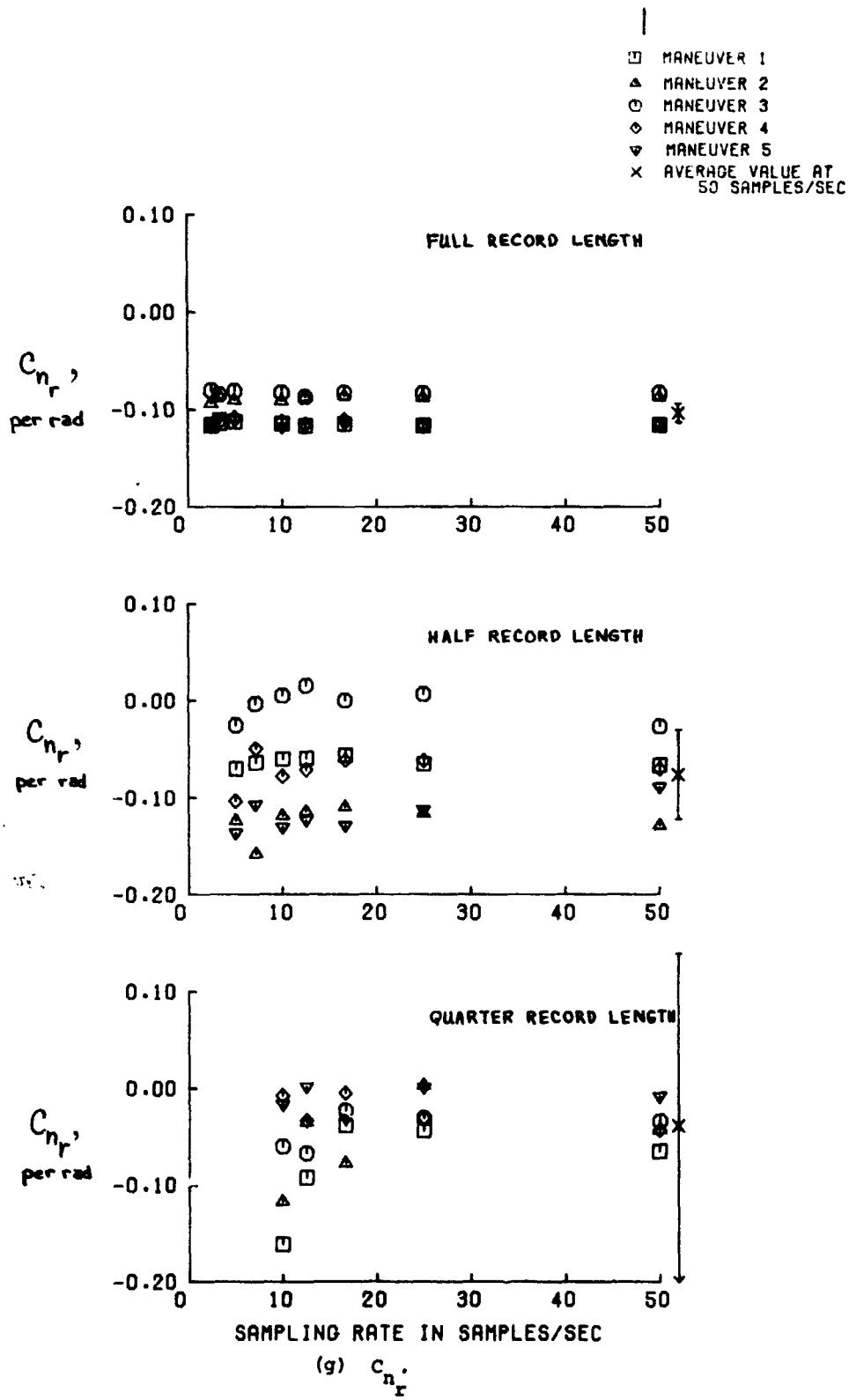

(g) C_{n_r}.

Figure 6. Continued.

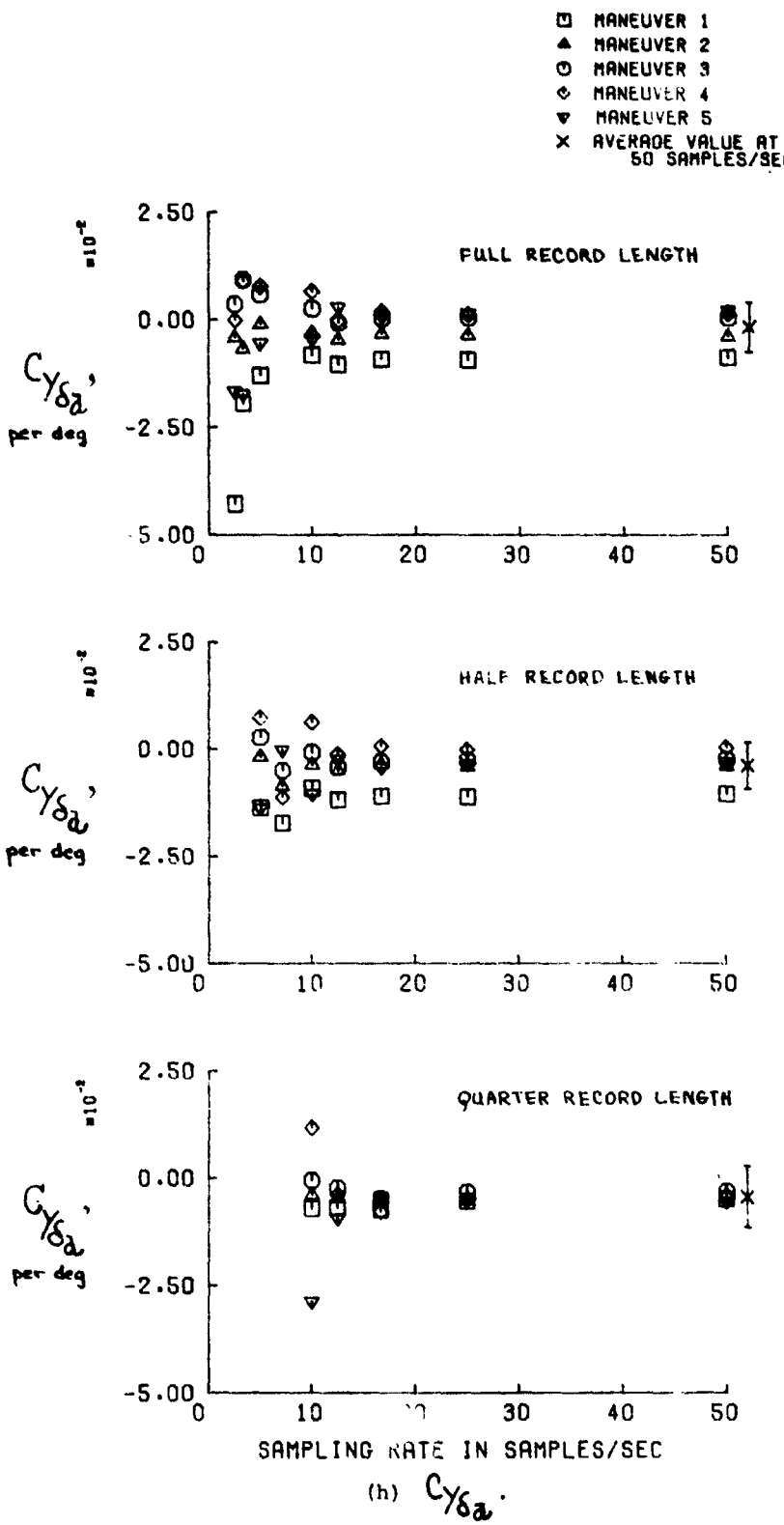

(h) $C_{Y_{\delta_a}}$.

Figure 6. Continued.

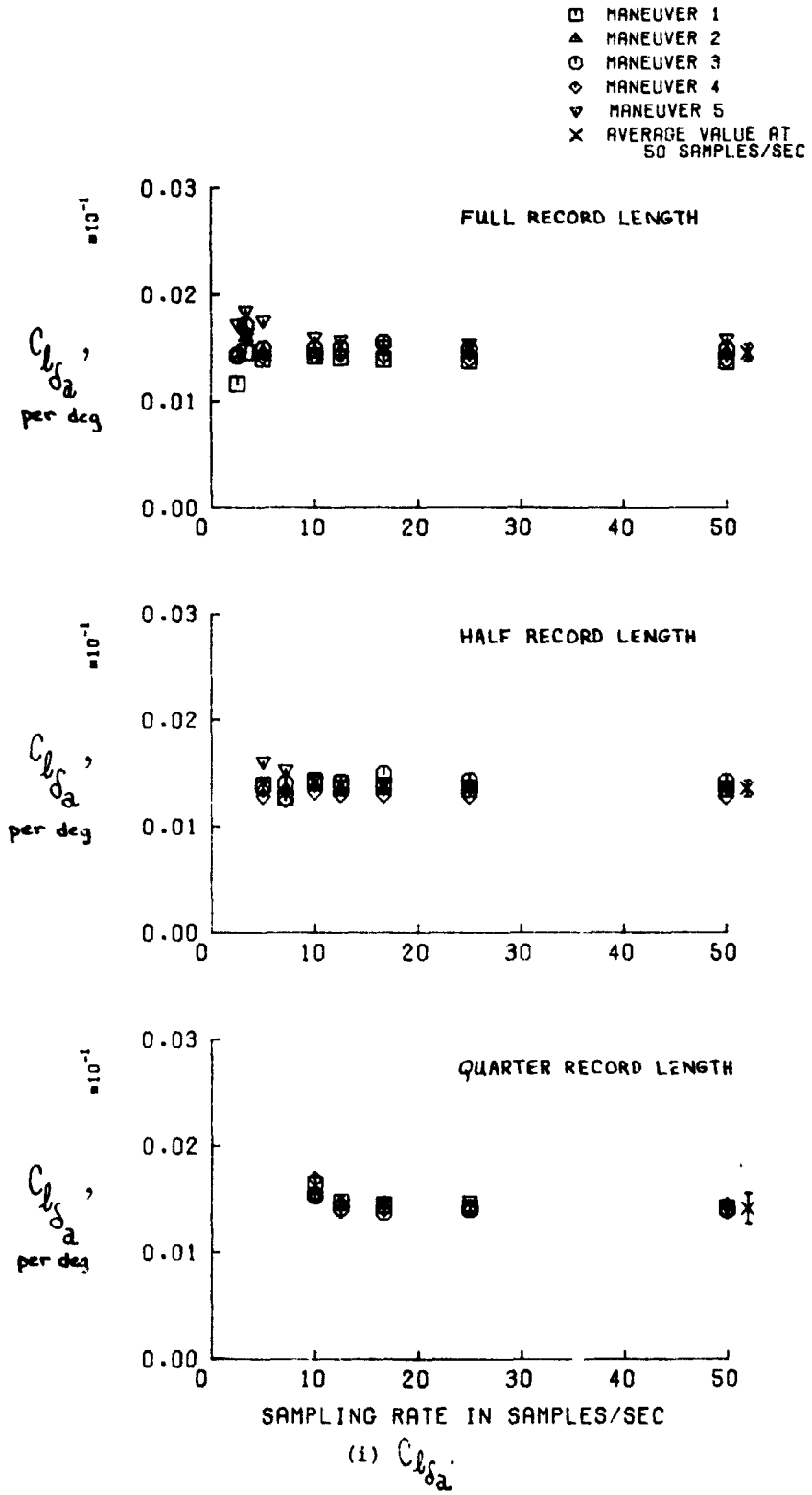

(i) $C_{l_{\delta_a}}$.

Figure 6. Continued.

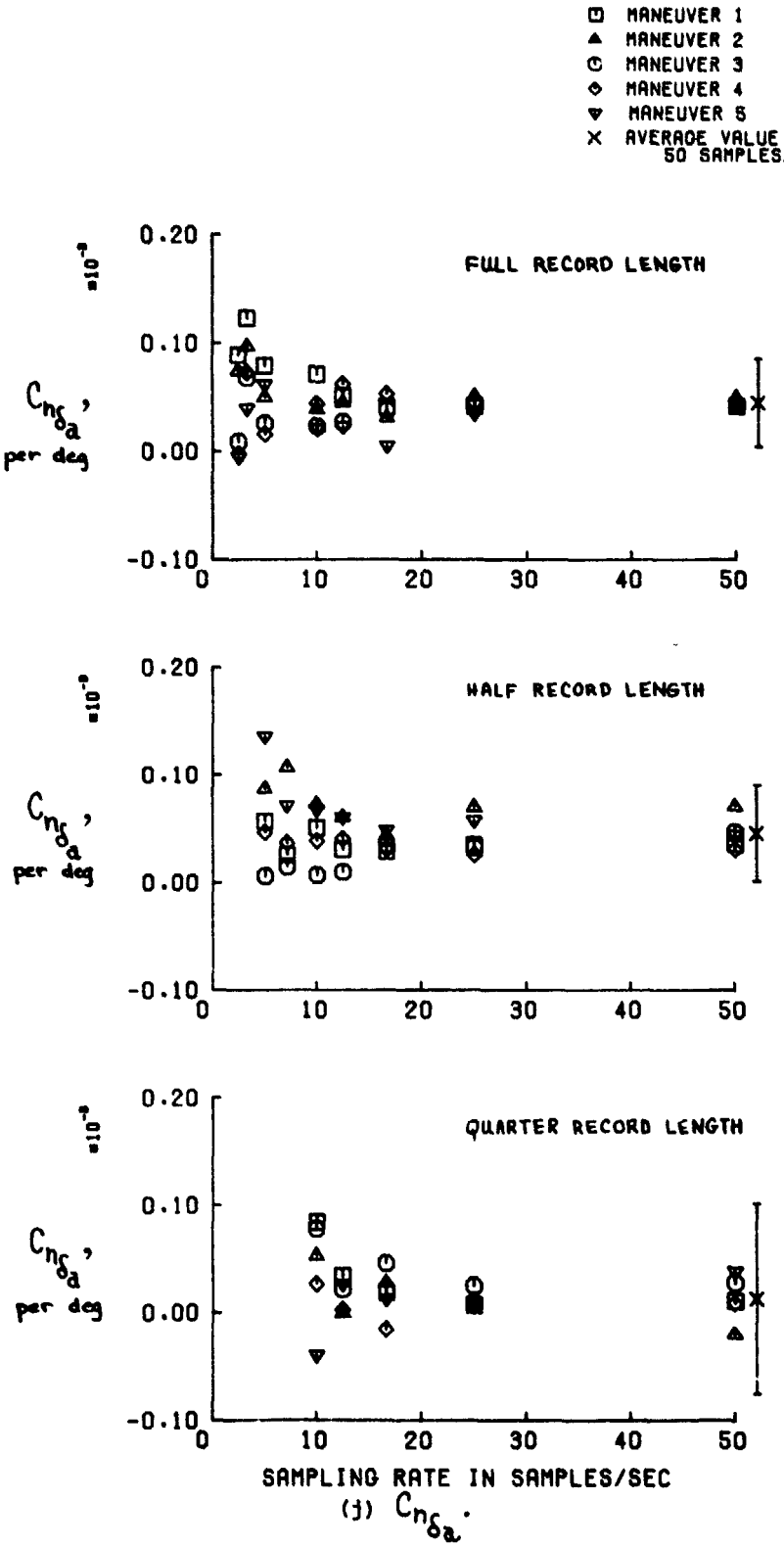

(j) $C_{n_{\delta_a}}$.

Figure 6. Concluded.

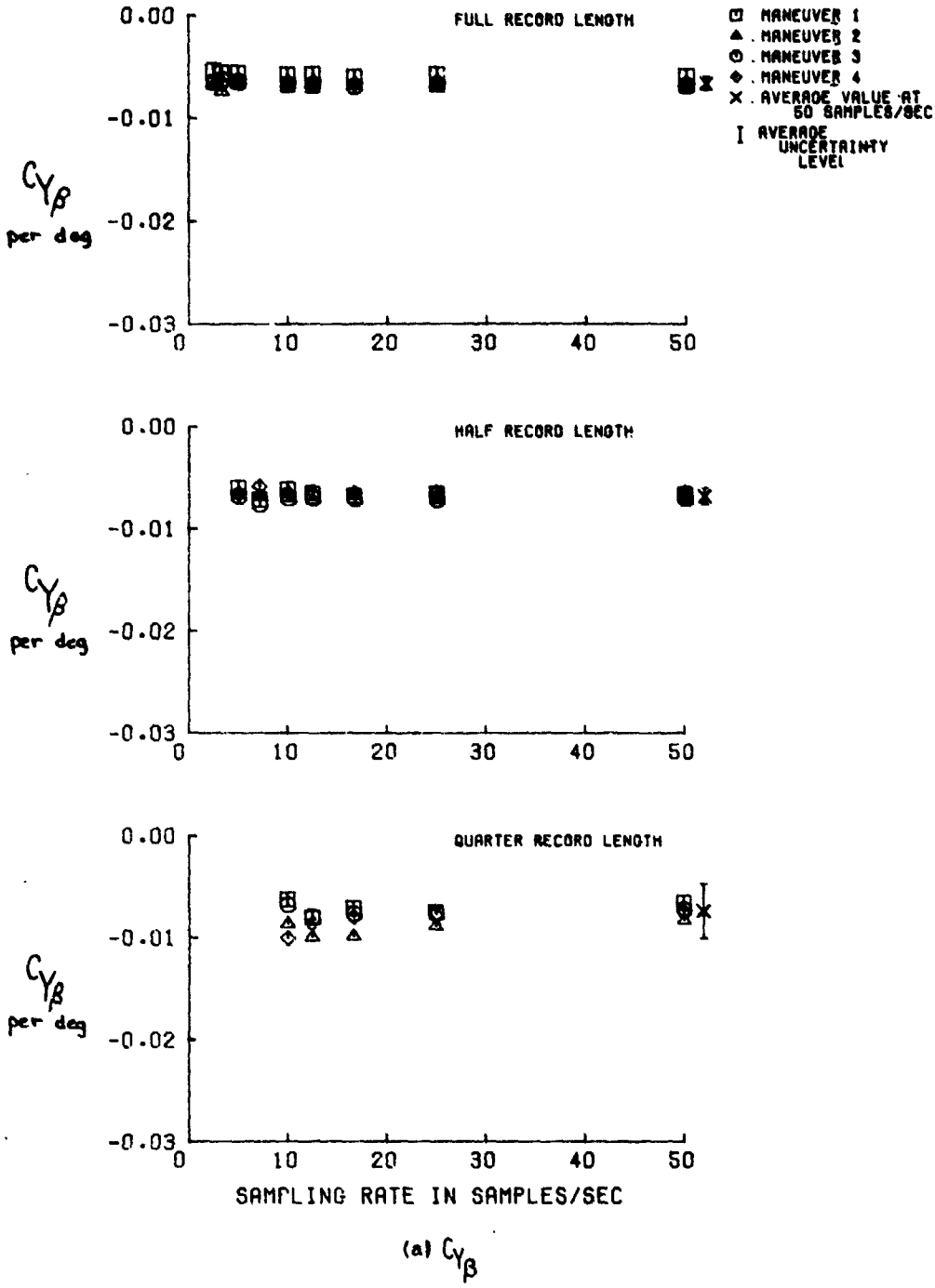

Figure 7. Estimated lateral-directional derivatives as a function of sampling rate for Aircraft A maneuvers with large amplitude control inputs.

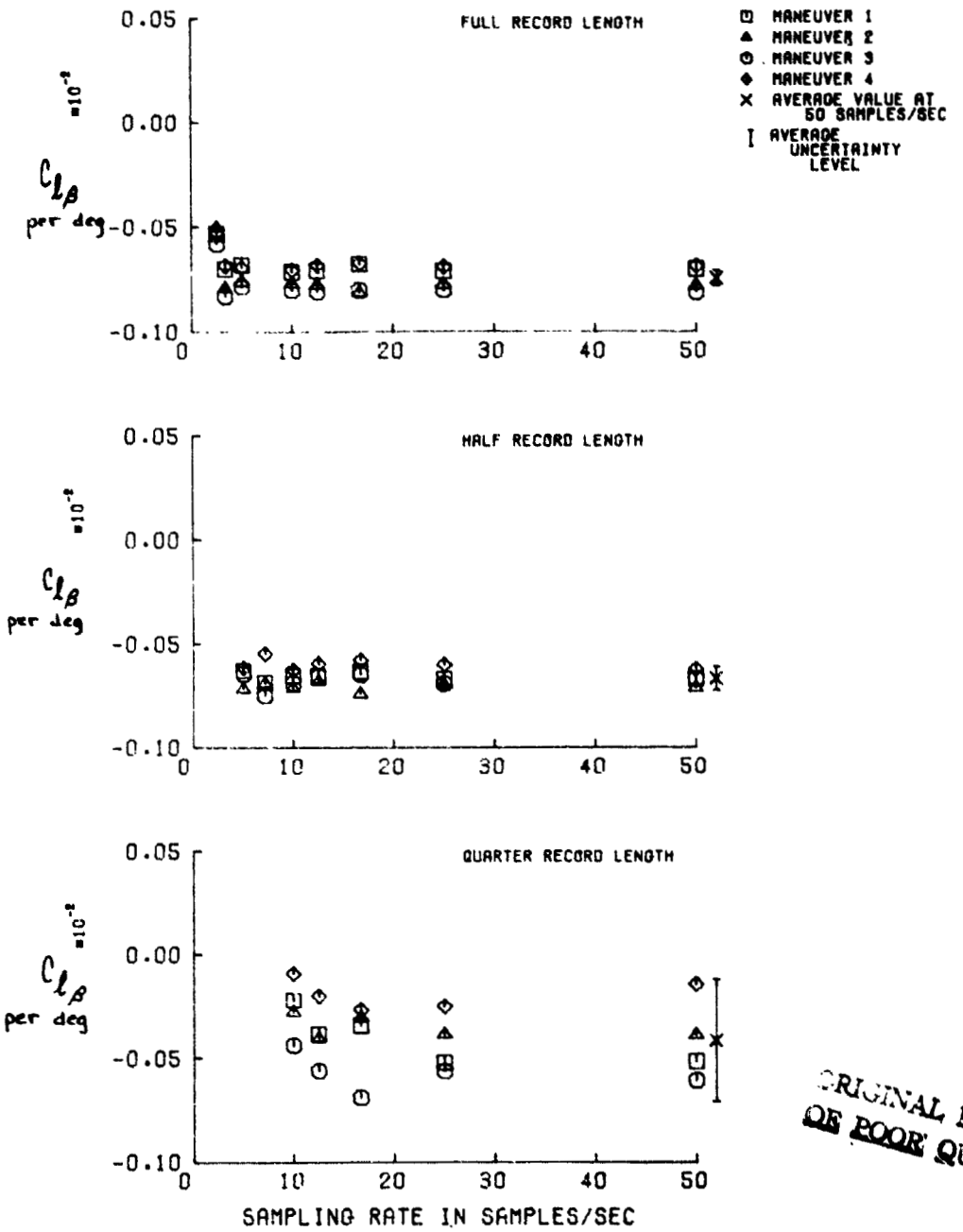

(b) C_{l_β}

Figure 7. Continued.

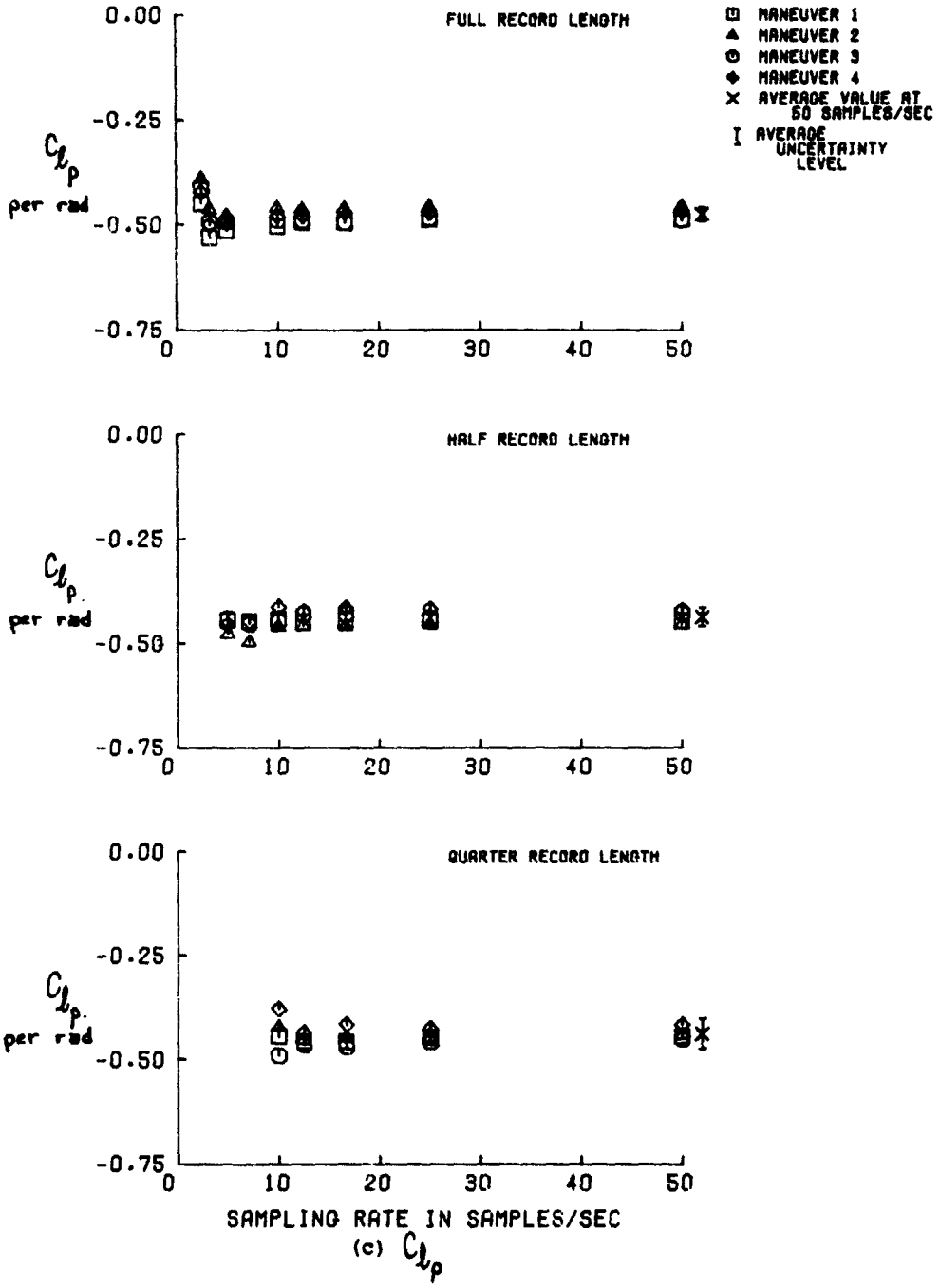

(c) C_{l_p}

Figure 7. Continued

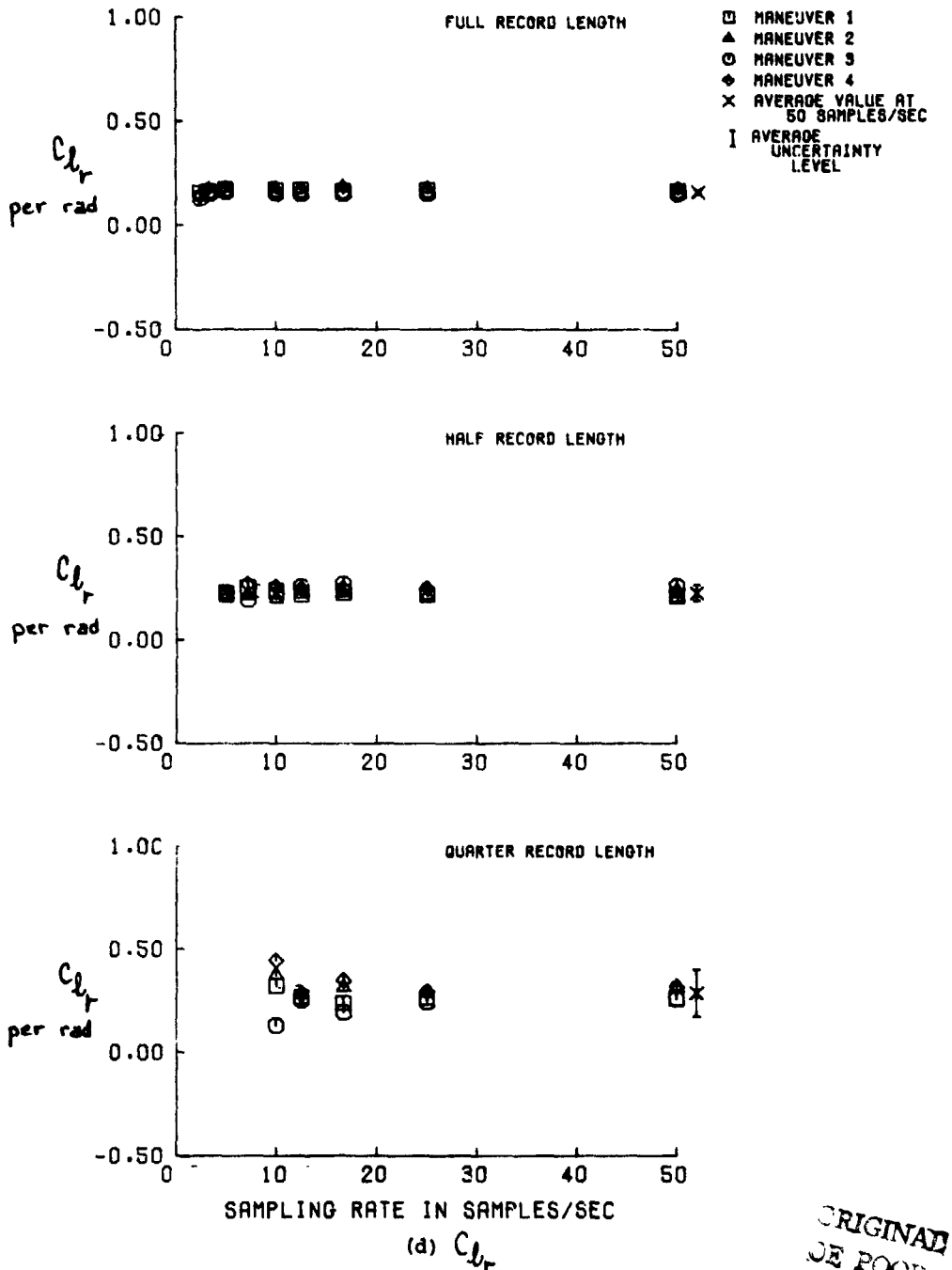

(d) C_{l_r}

Figure 7. Continued.

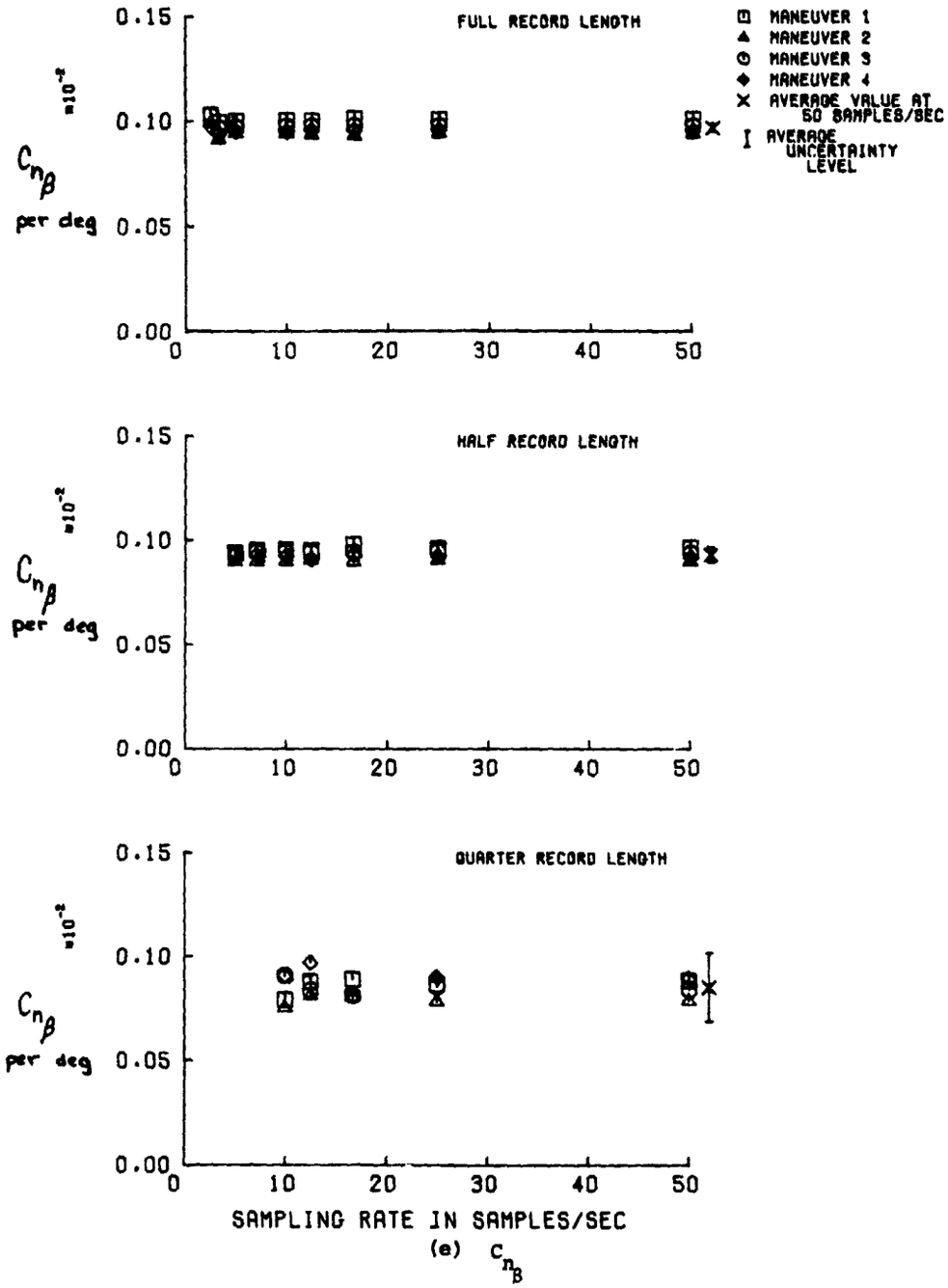

(e) C_{n_β}

Figure 7. Continued.

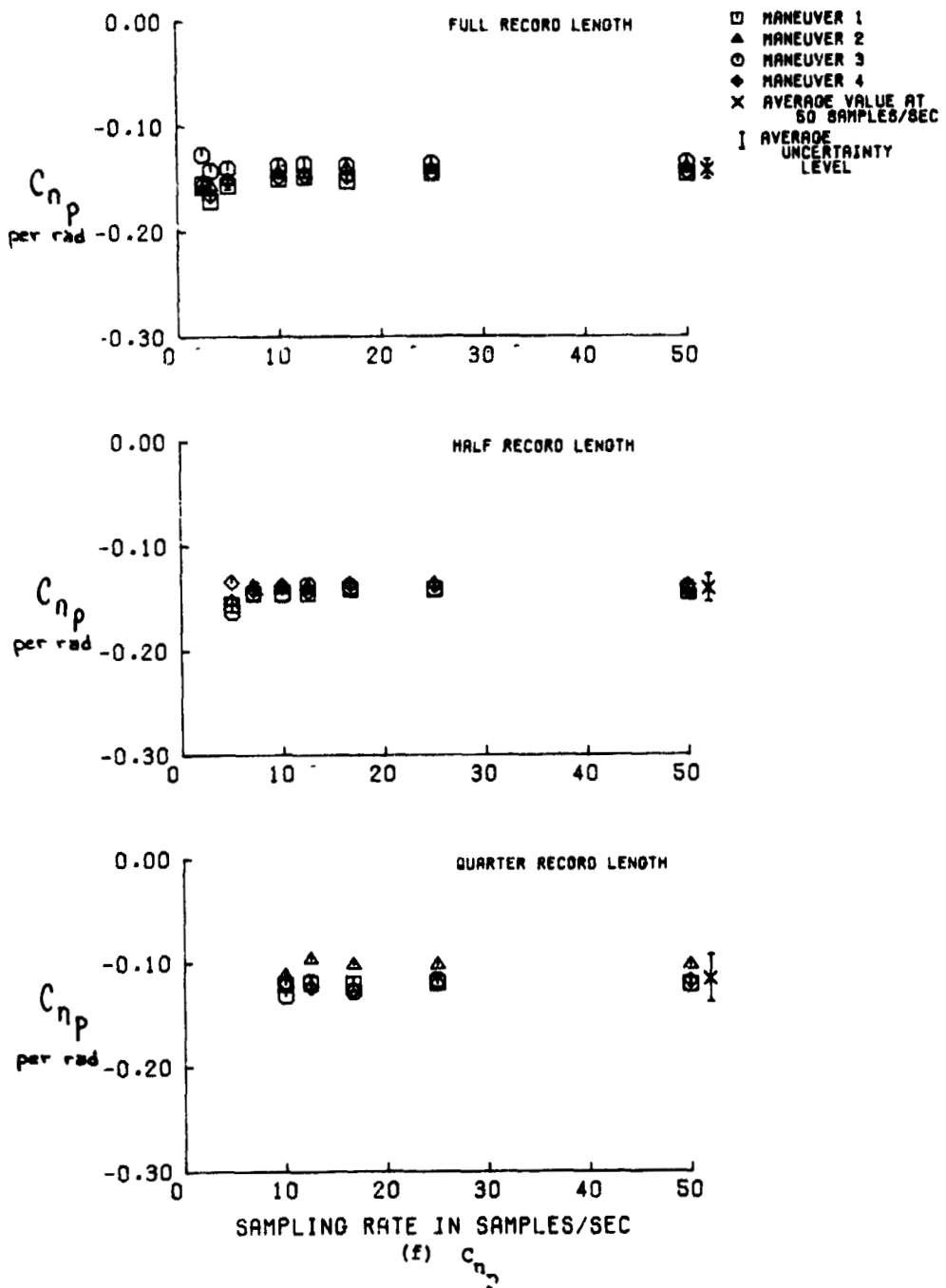

(f) C_{n_p}

Figure 7. Continued.

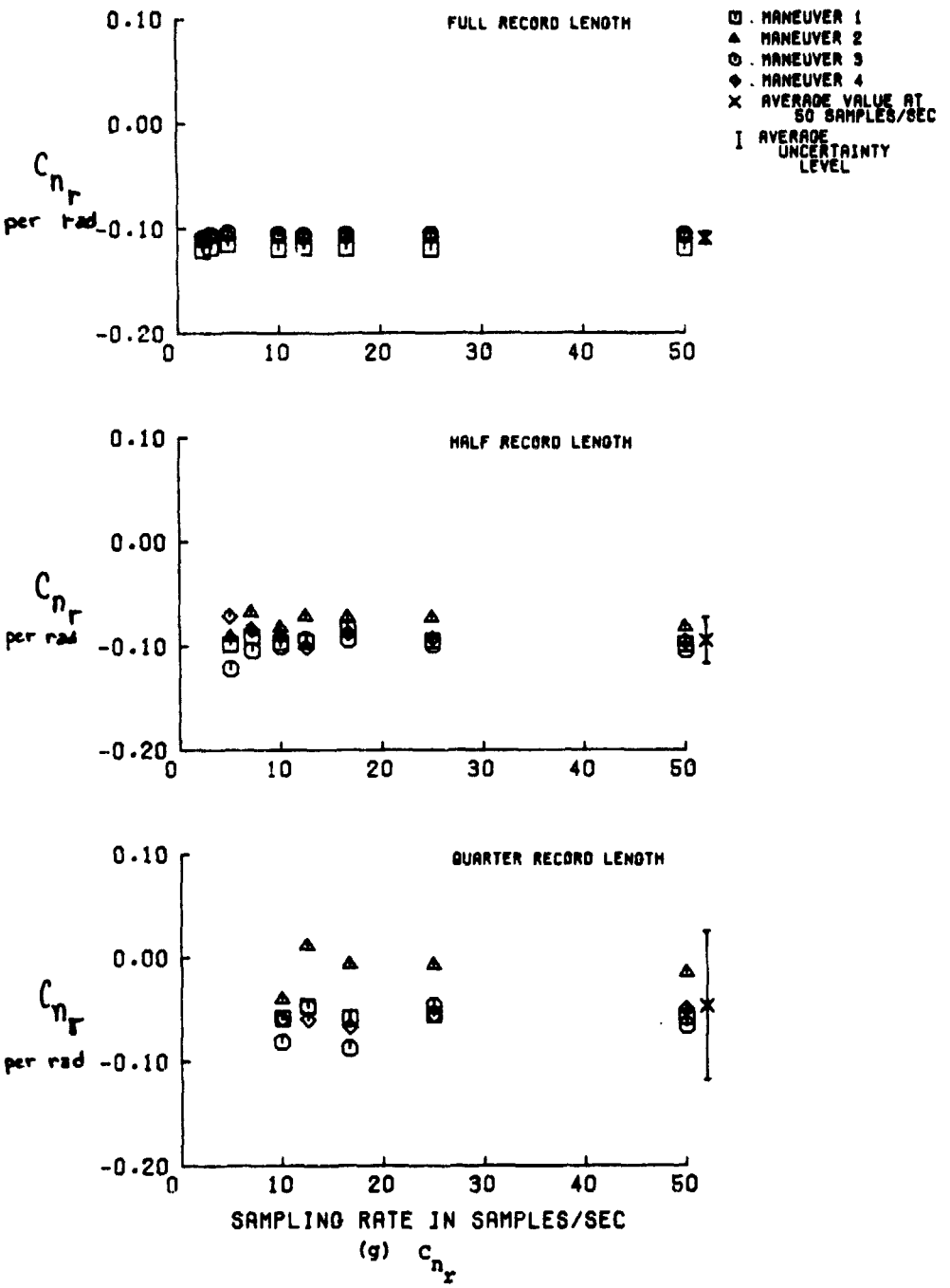

(g) C_{n_r}

Figure 7. Continued.

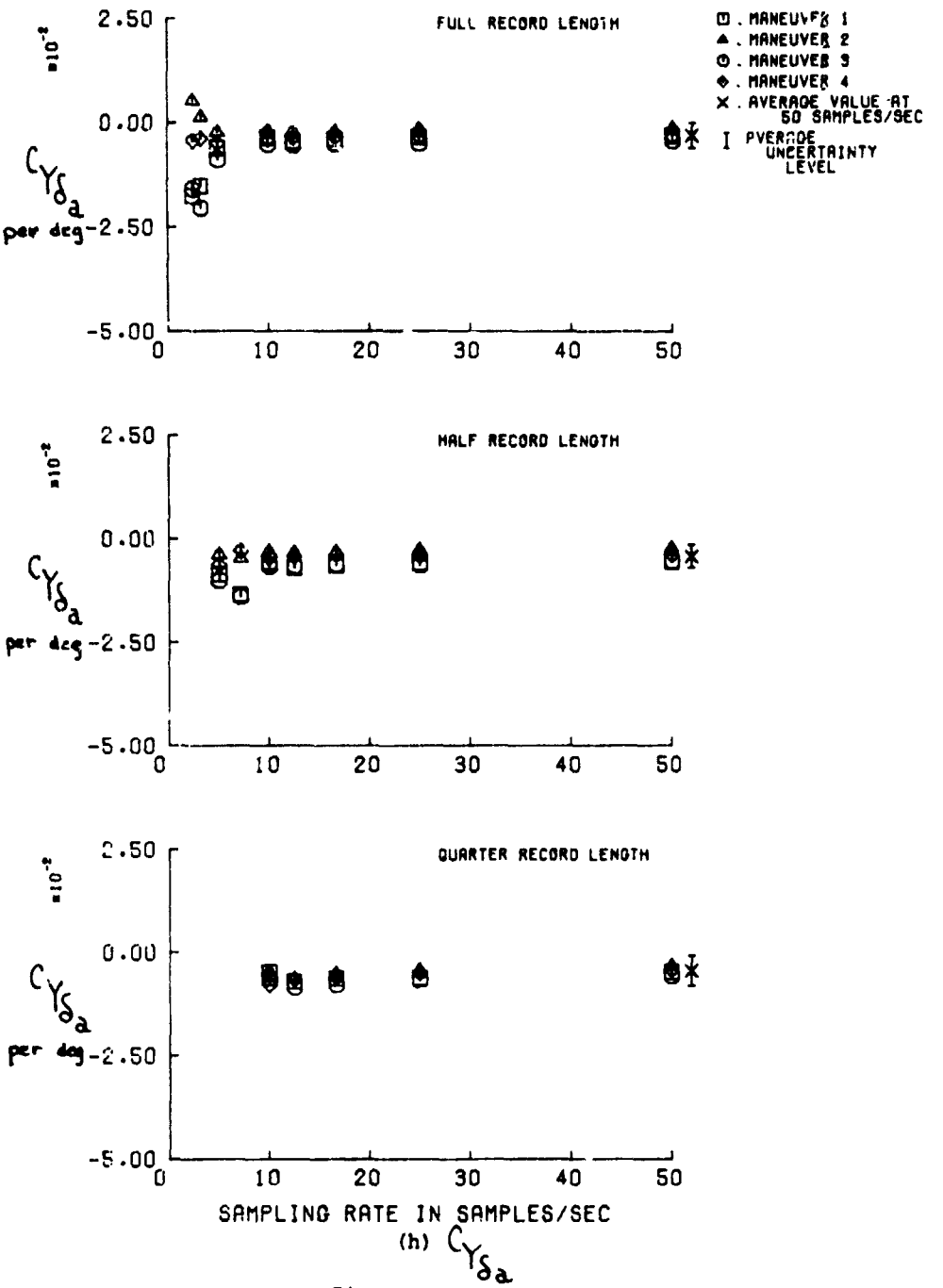

(h) $C_{Y_{\delta_a}}$

Figure 7. Continued.

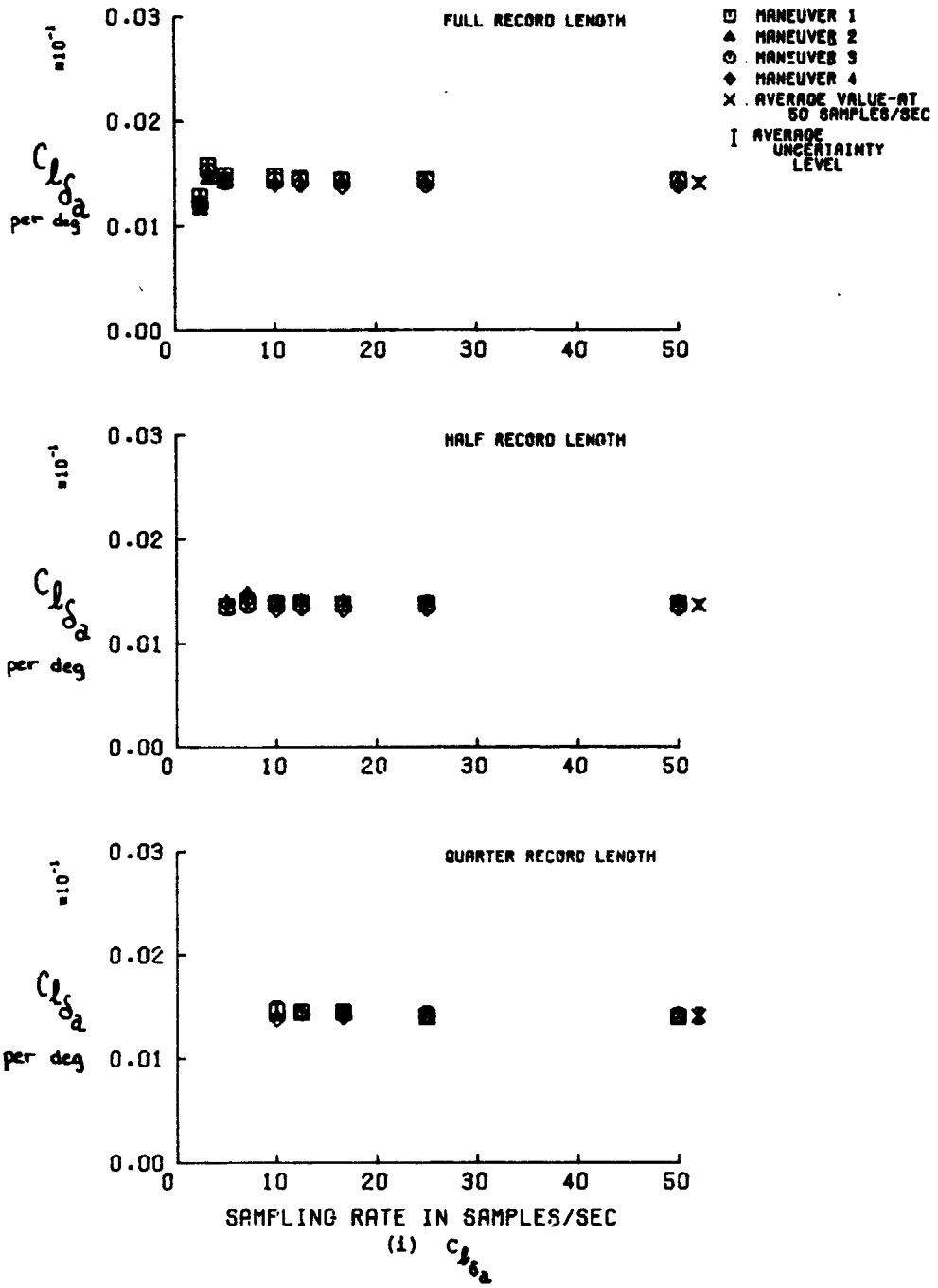

(i) $C_{l_{\delta_a}}$

Figure 7. Continued.

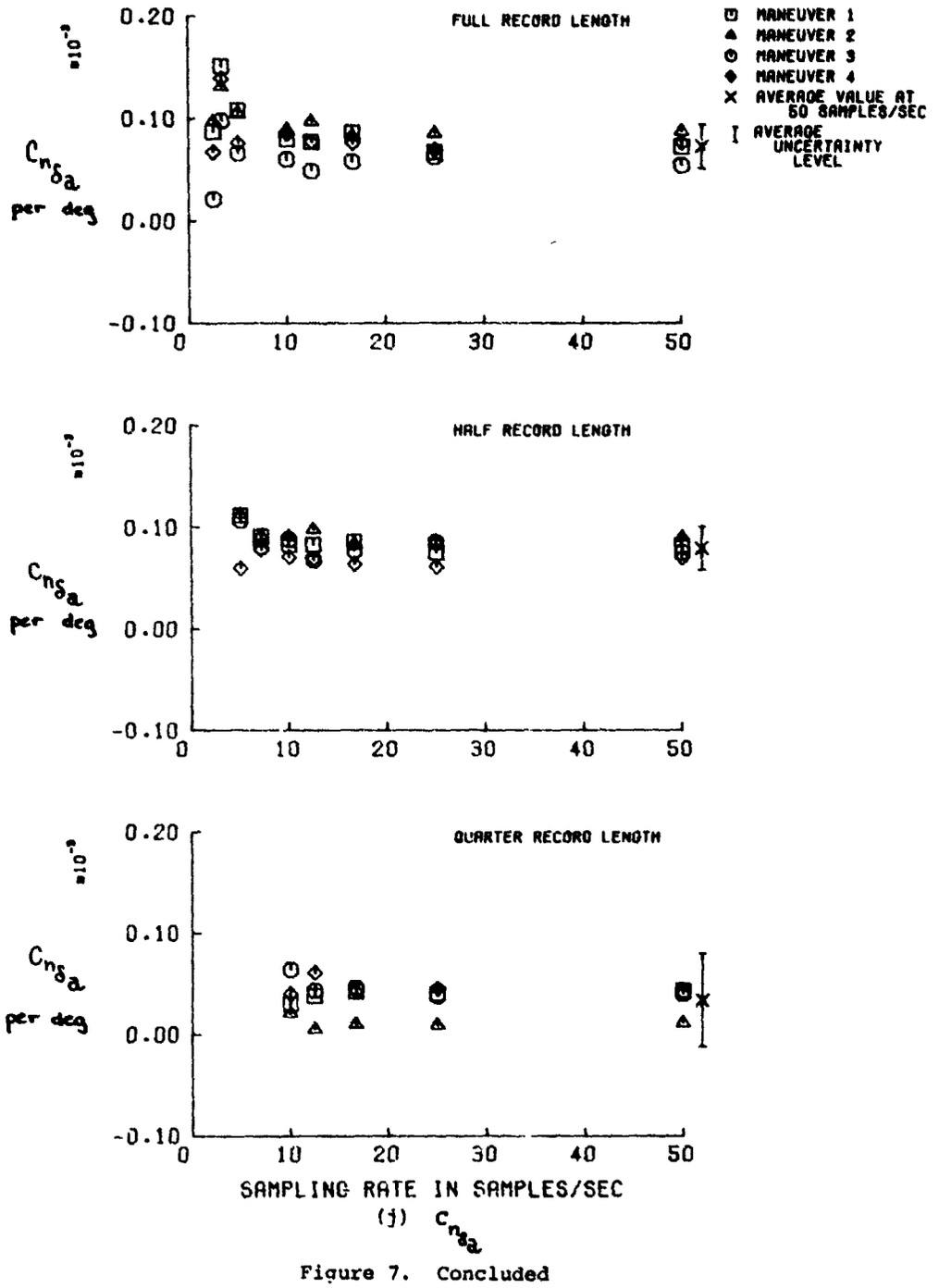

(j) $C_{n_{\delta_a}}$

Figure 7. Concluded

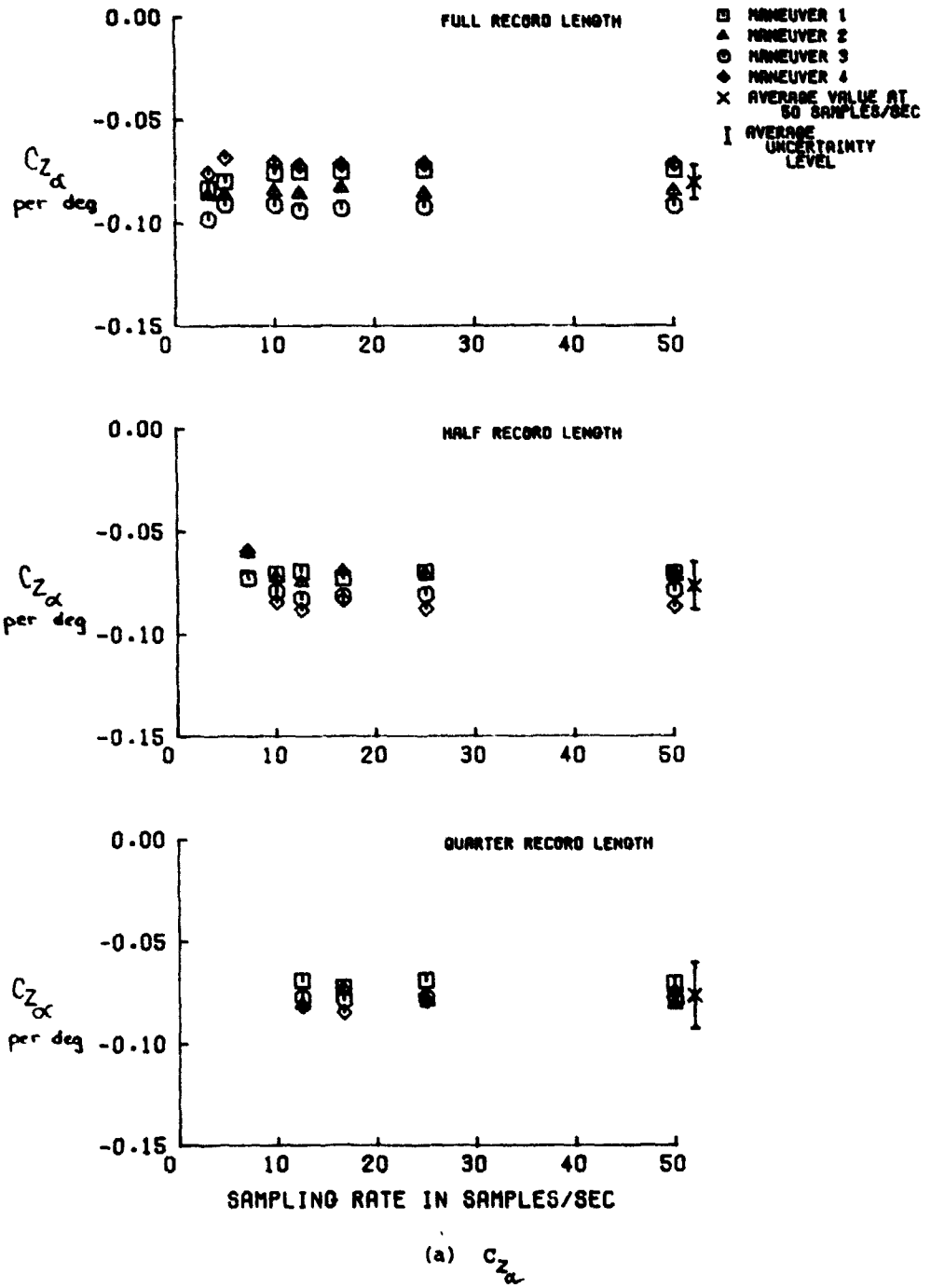

(a) C_{Z_α}

Figure 8. Estimated longitudinal derivatives as a function of sampling rate for Aircraft A maneuvers with small amplitude control inputs.

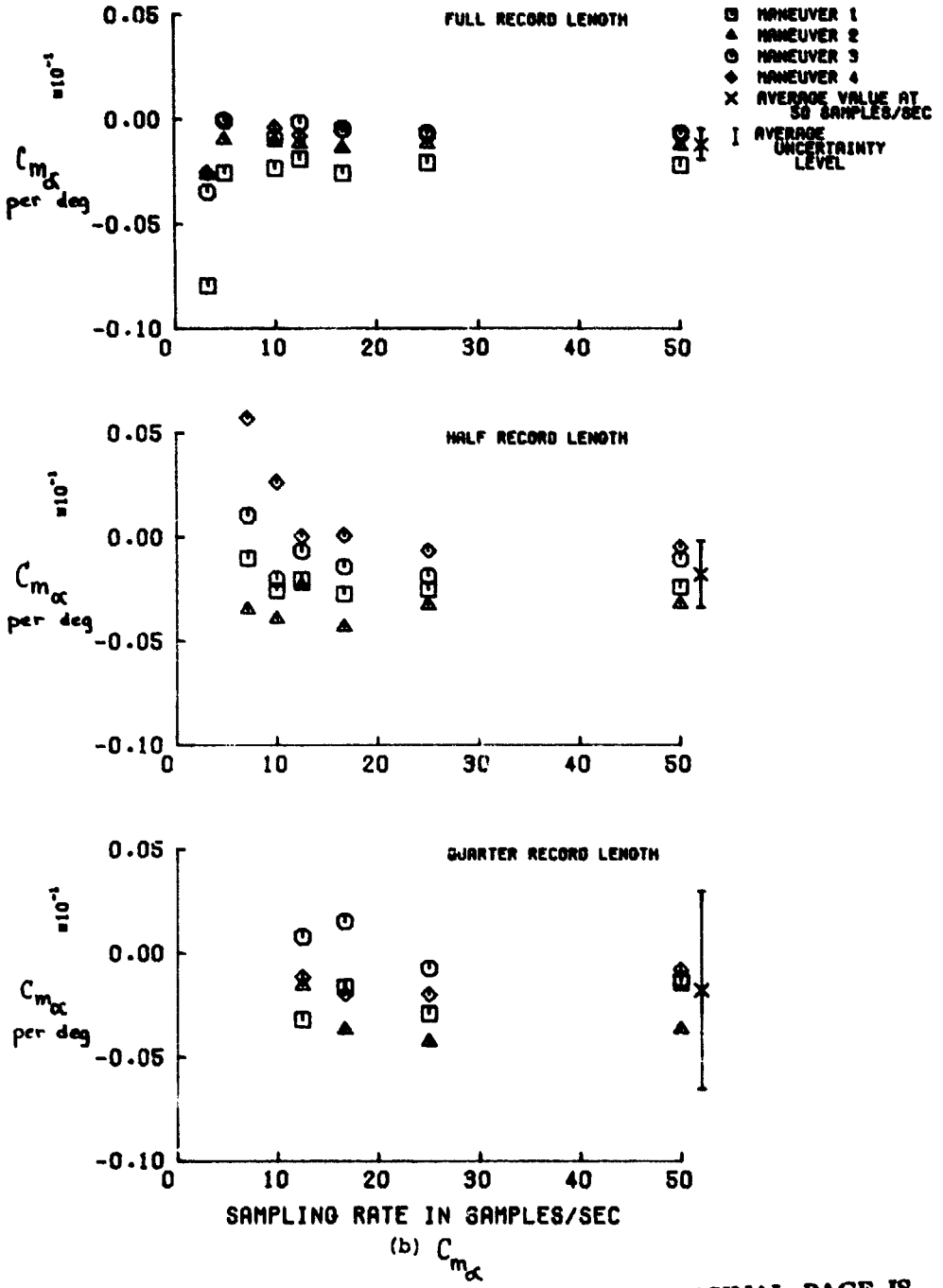

(b) C_{m_α}

Figure 8. Continued.

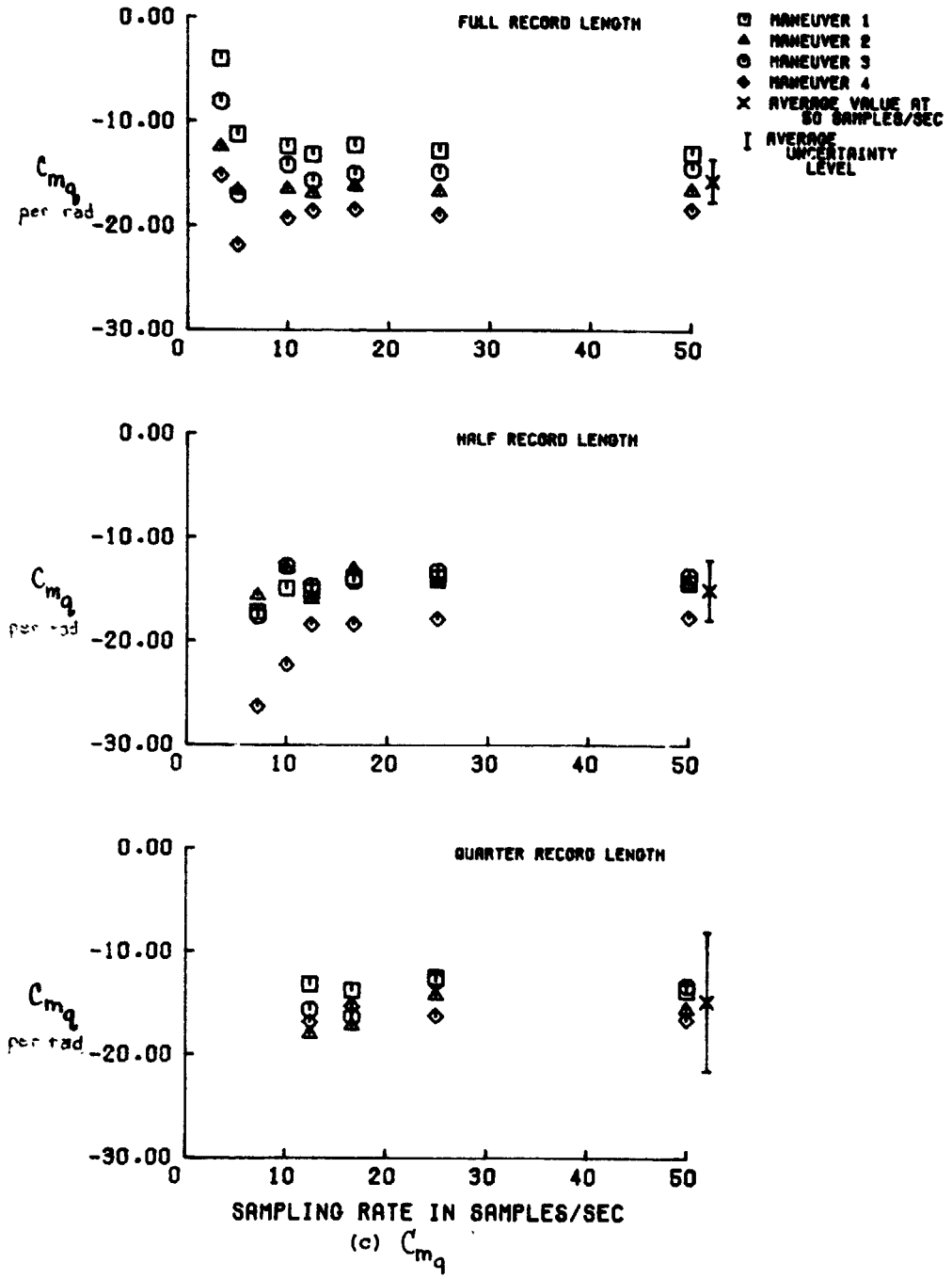

(c) C_{m_q}

Figure 8. Continued.

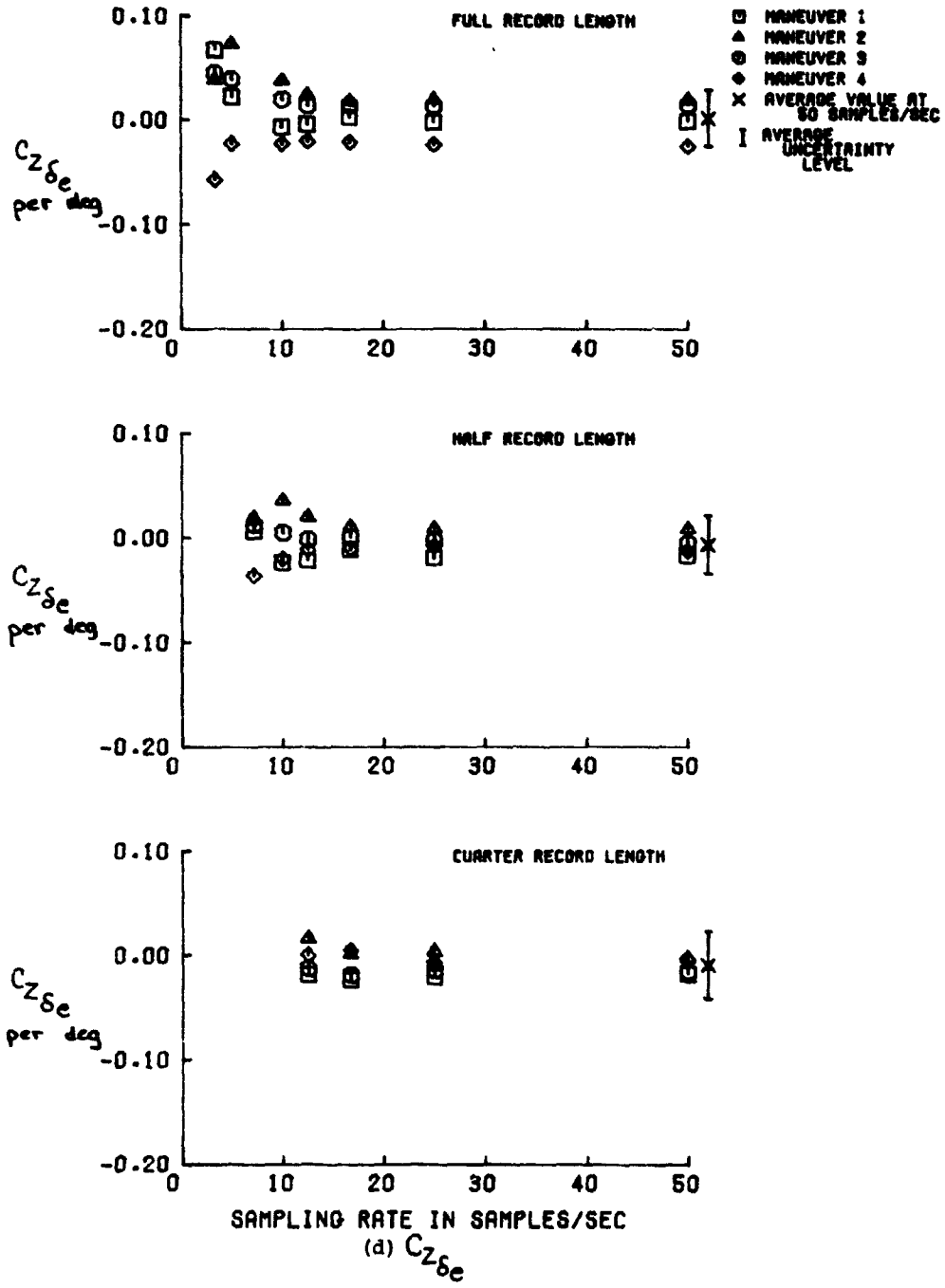

(d) $C_{Z_{\delta_e}}$

Figure 8. Continued

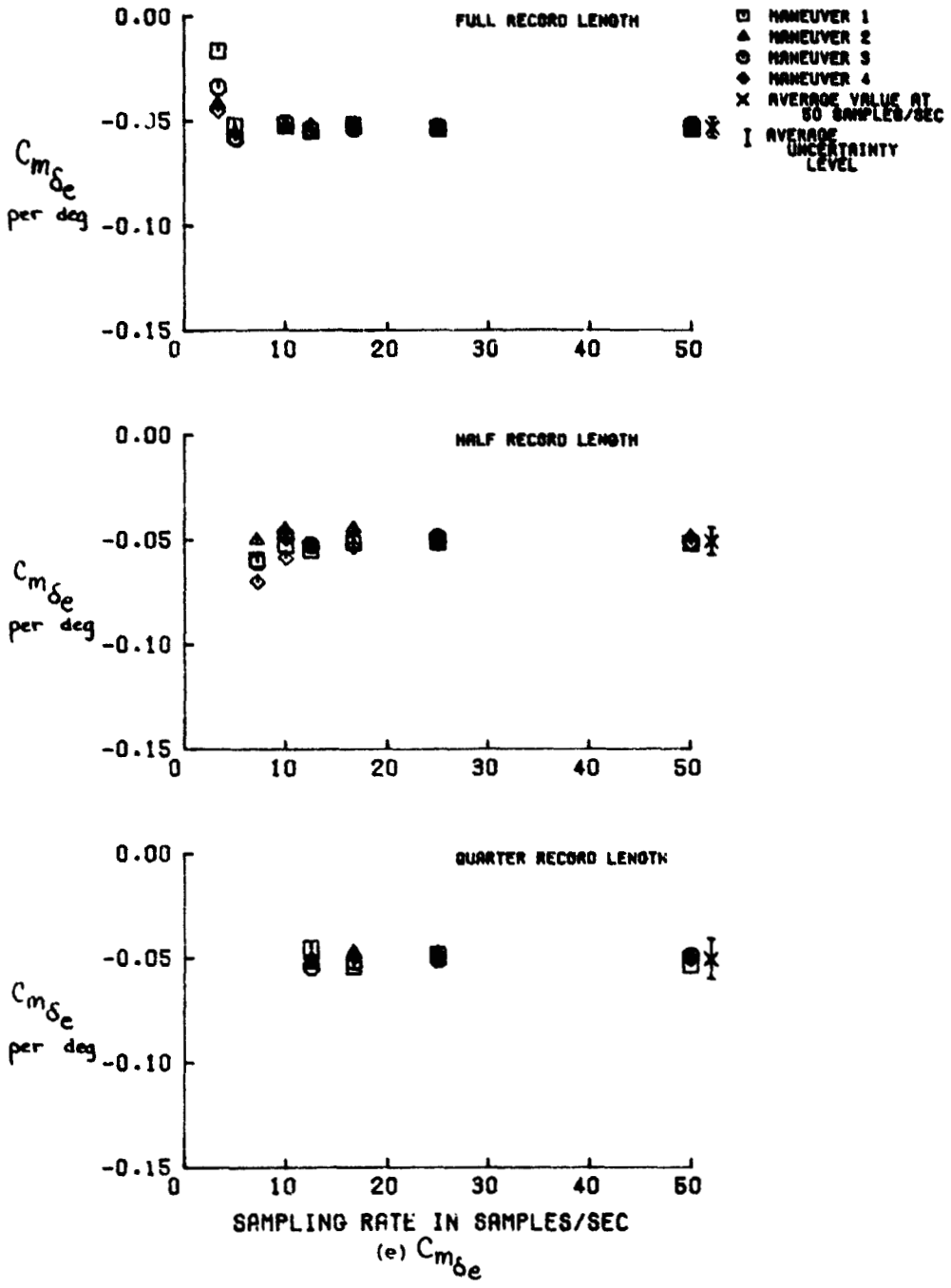

(e) $C_{m_{\delta_e}}$

Figure 8. Concluded

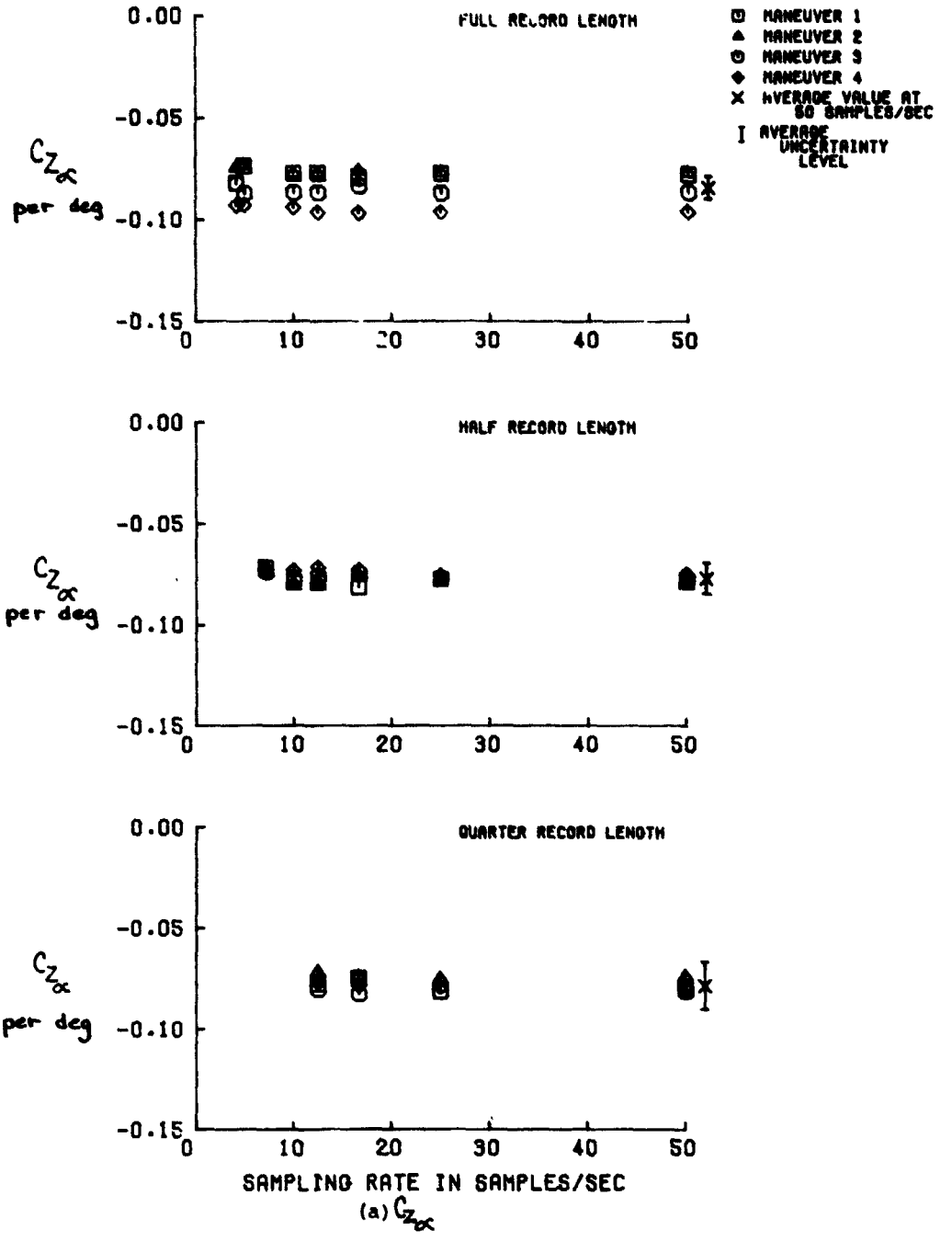

Figure 9. Estimated longitudinal derivatives as a function of sampling rate for Aircraft A maneuvers with large amplitude control inputs.

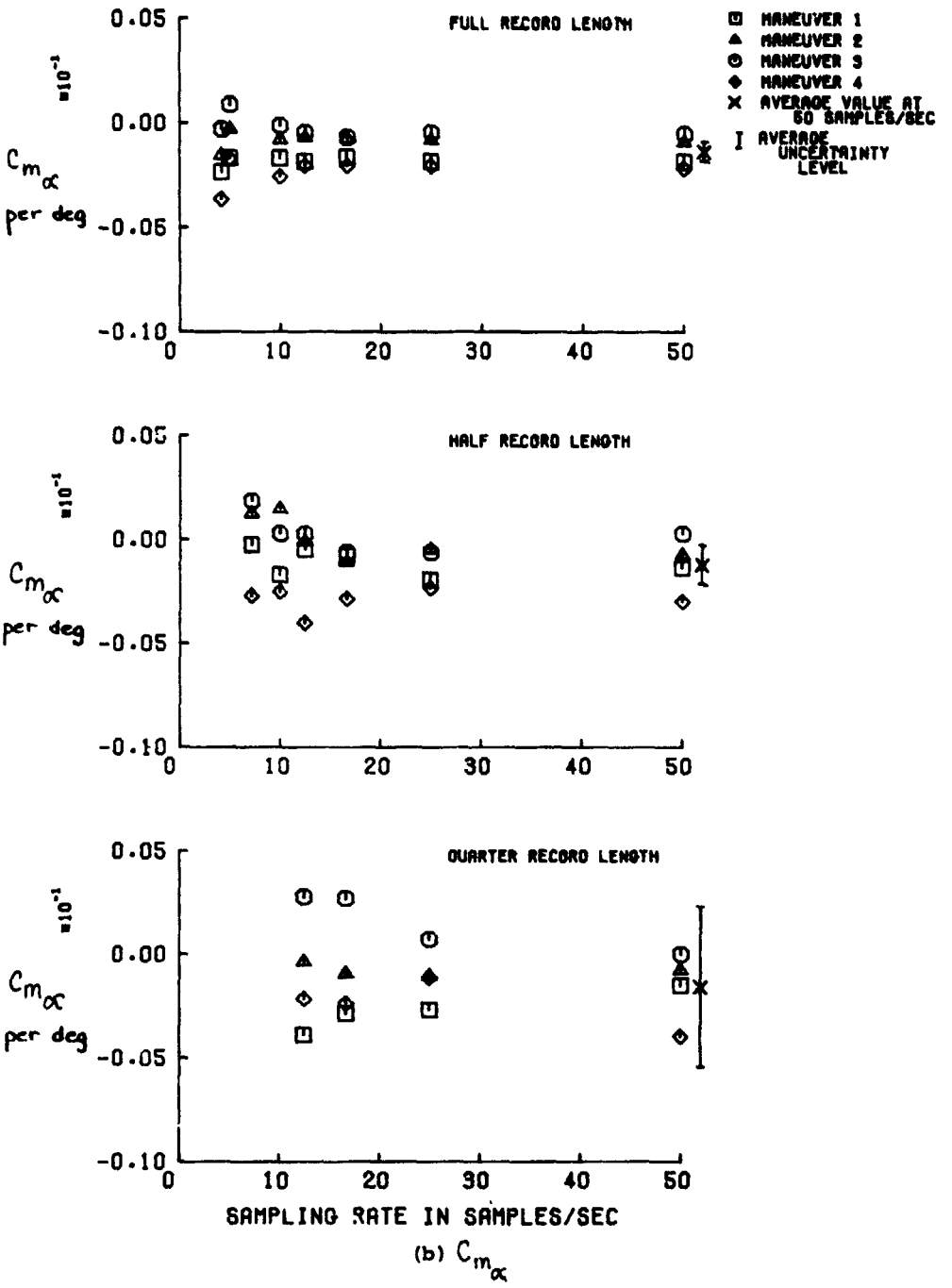

(b) C_{m_α}

Figure 9. Continued.

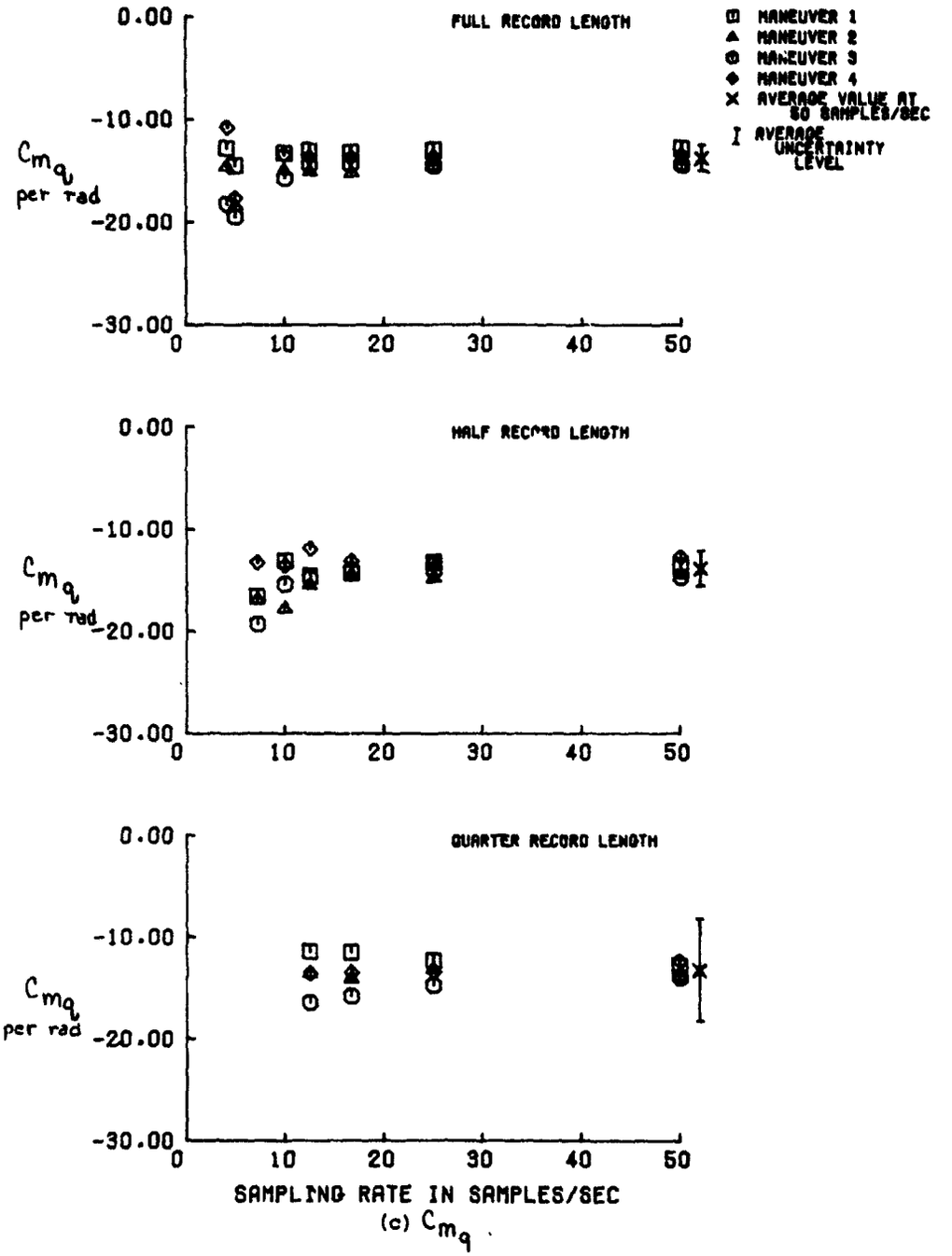

(c) C_{m_q}.

Figure 9. Continued

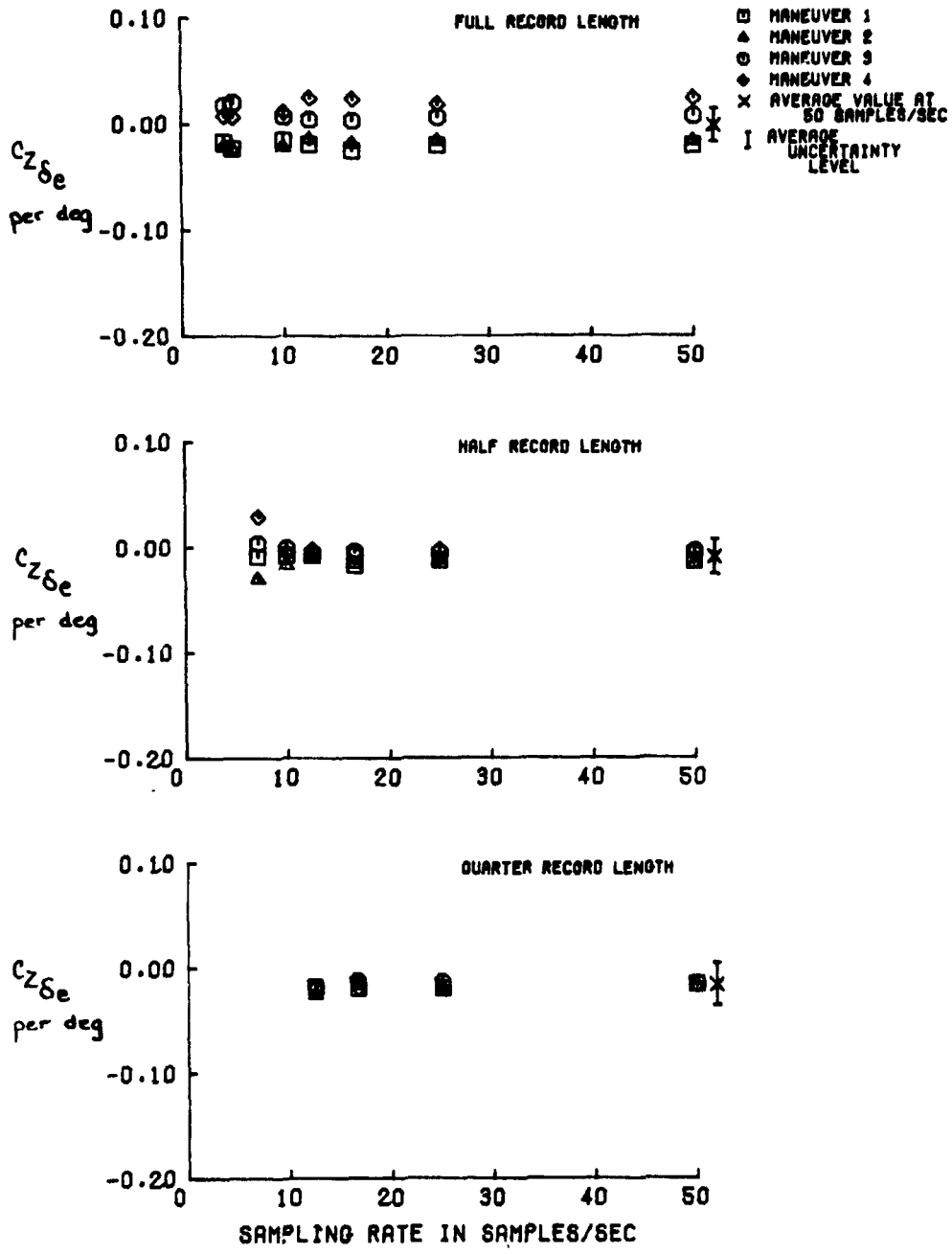

(d) $C_{Z_{\delta_e}}$

Figure 9 Continued

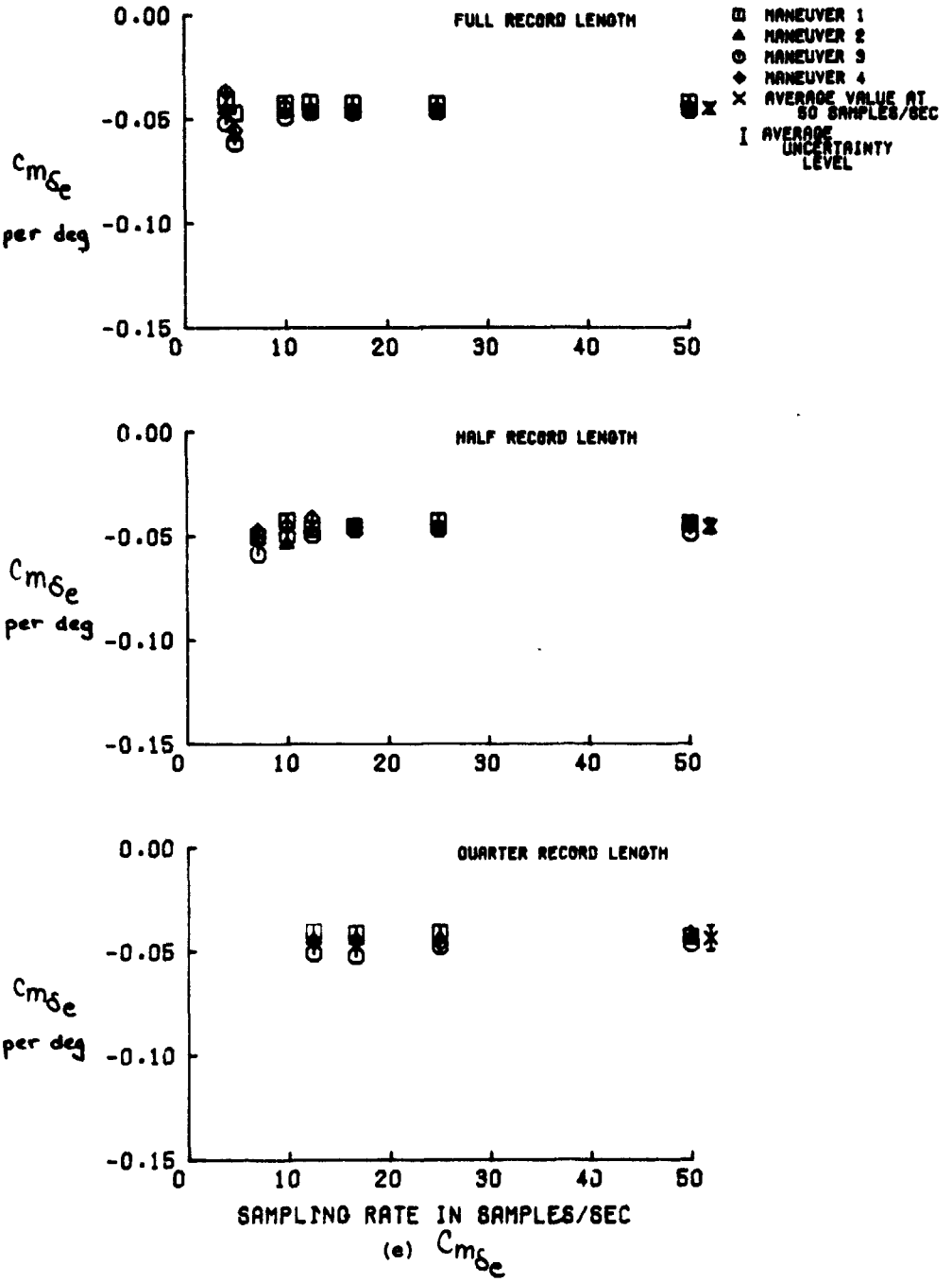

(e) $C_{m_{\delta_e}}$

Figure 9. Concluded

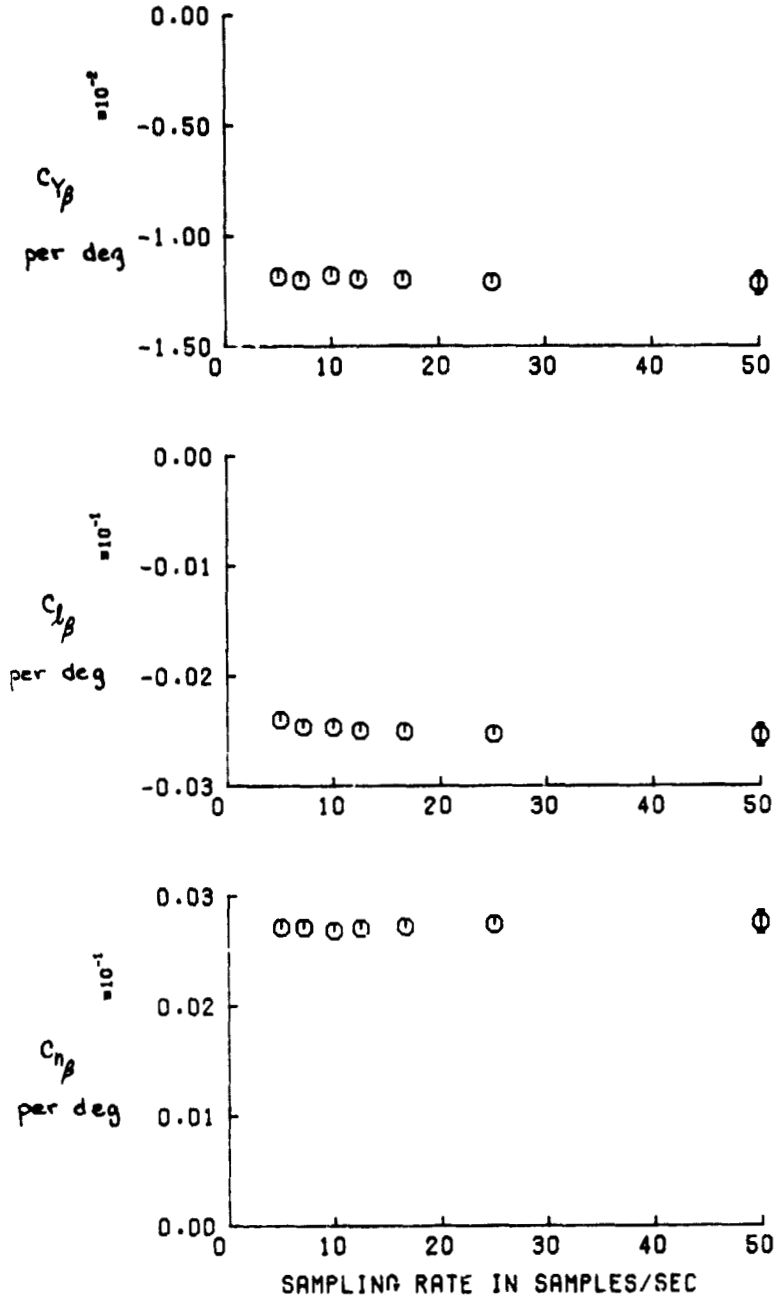

(a) C_{Y_β}, C_{l_β}, C_{n_β} for case 1:2.

Figure 10. Estimated lateral-directional derivatives for five cases as functions of sampling rate. Aircraft B.

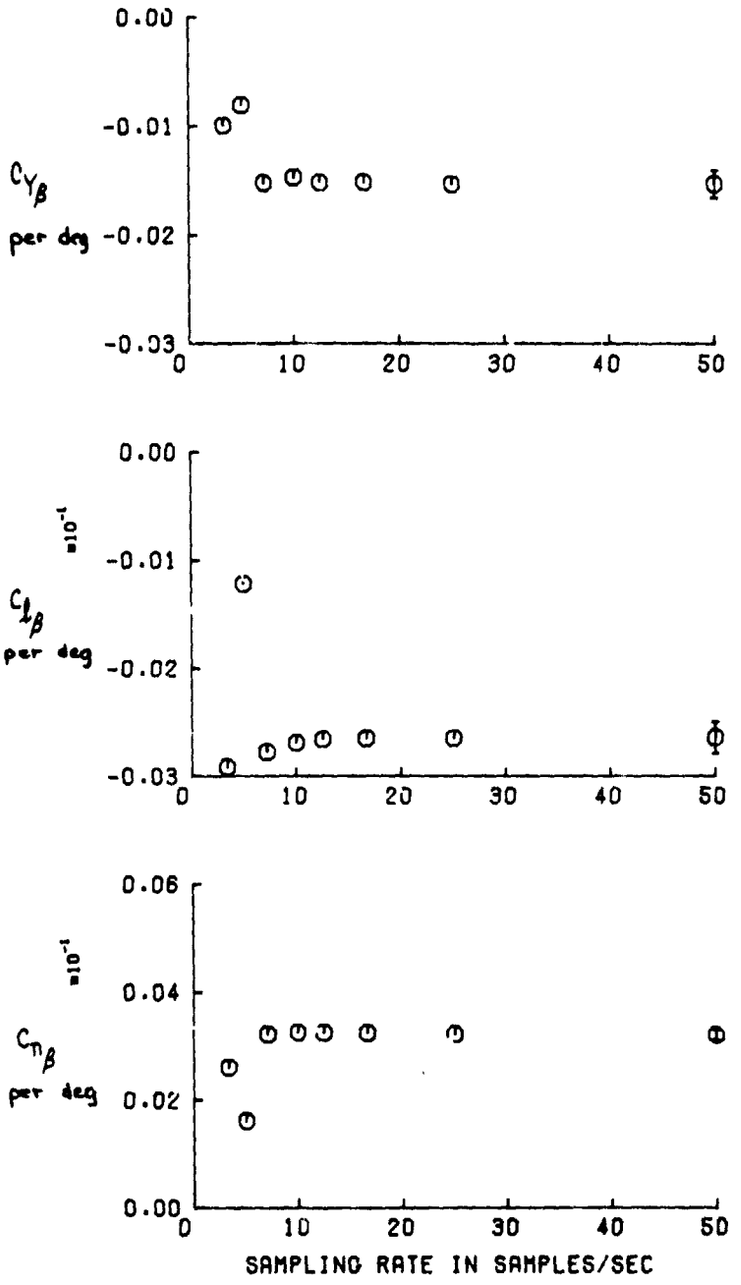

(b) C_{Y_β}, C_{l_β}, C_{n_β} for case 1:3.

Figure 10. Continued.

ORIGINAL PAGE IS
OF POOR QUALITY.

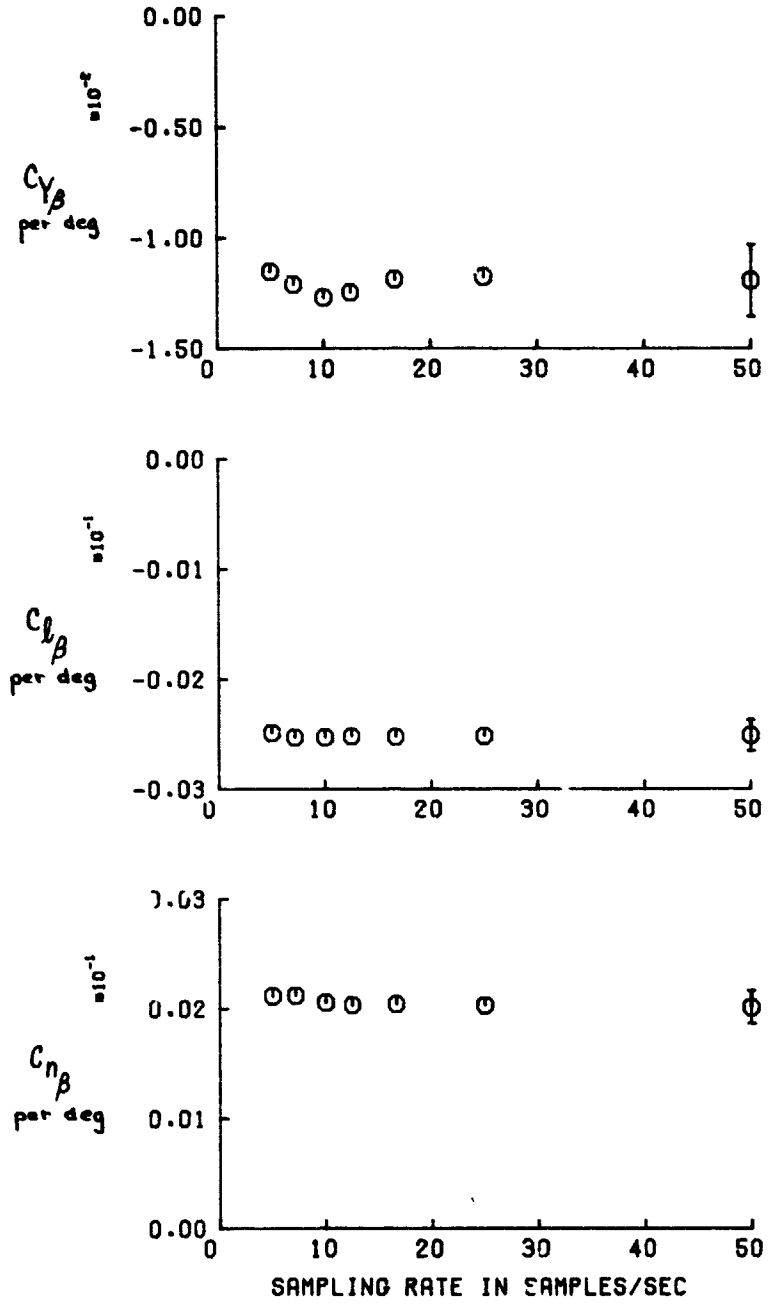

(c) C_{Y_β}, C_{ℓ_β}, C_{n_β} for case 1:10B

Figure 10. Continued.

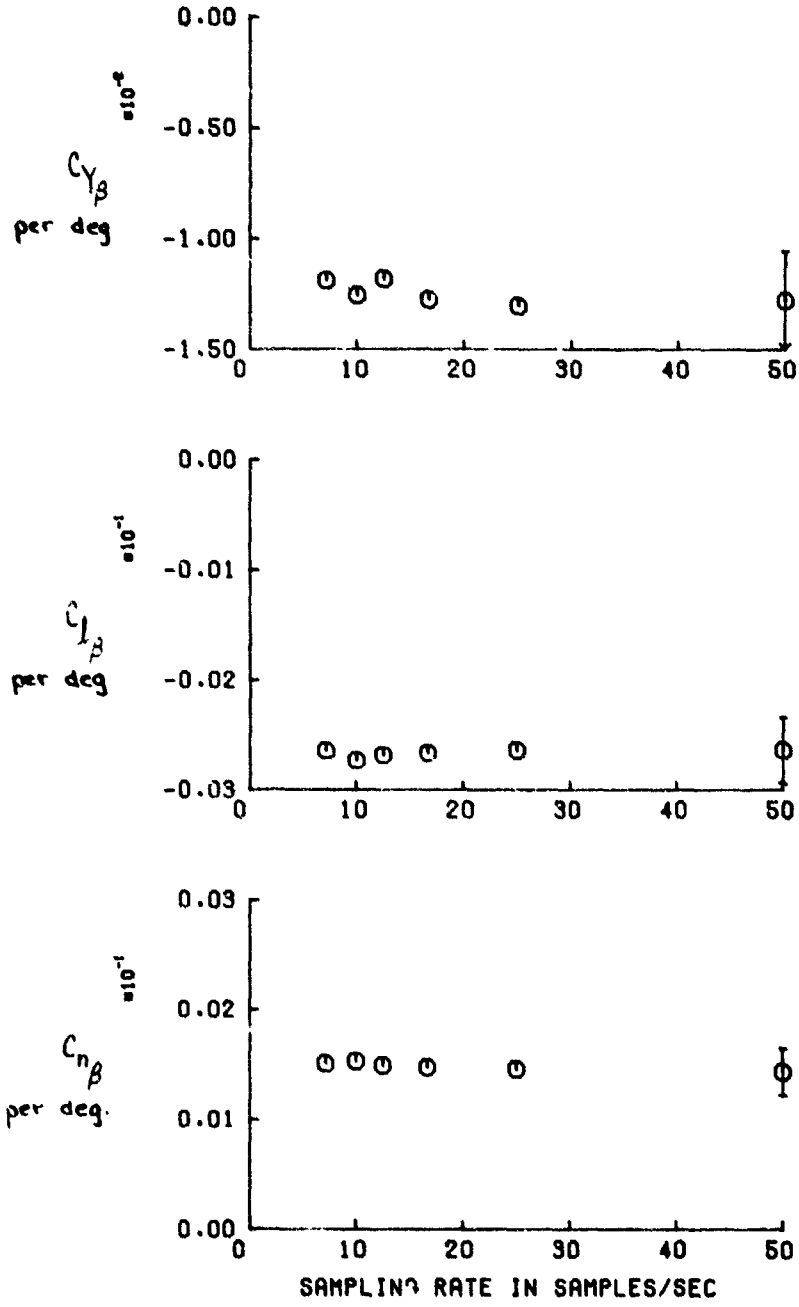

(d) C_{Y_β}, C_{l_β}, C_{n_β} for case 1:13.

Figure 10. Continued.

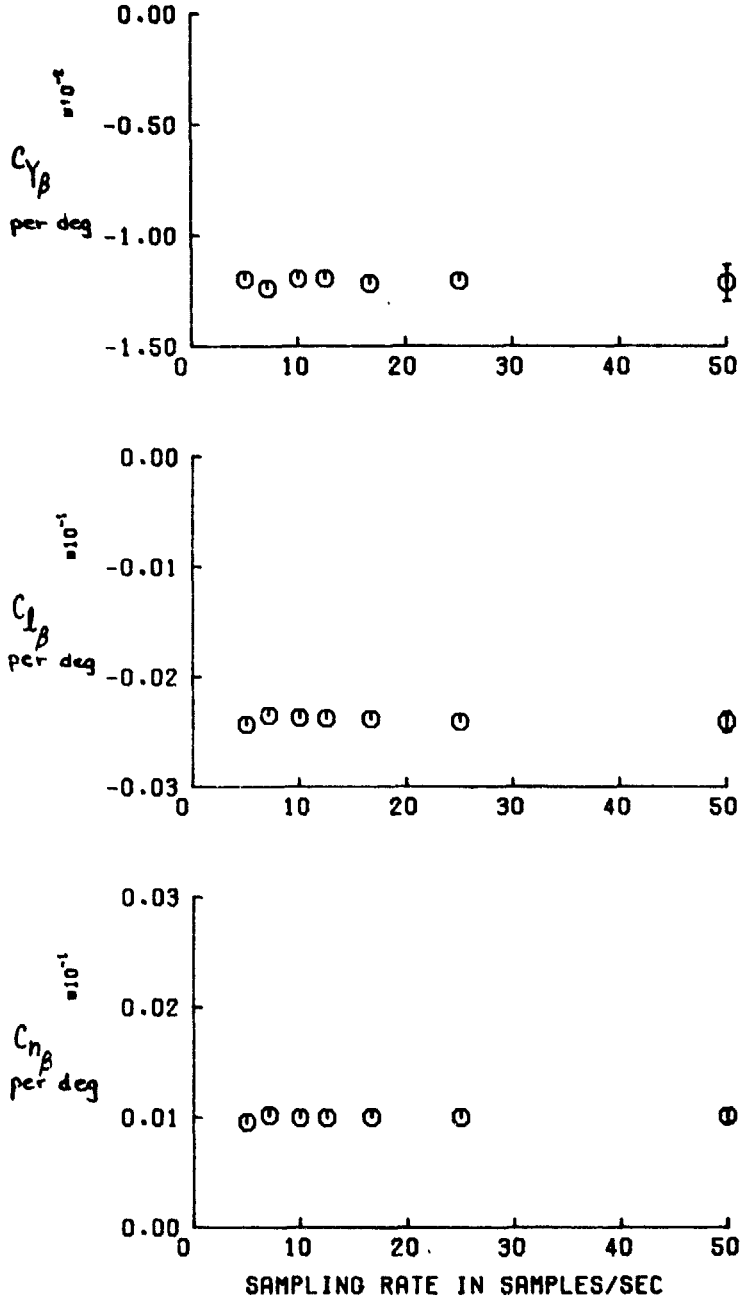

(e) C_{Y_β}, C_{l_β}, C_{n_β} for case 1:14B.

Figure 10. Continued.

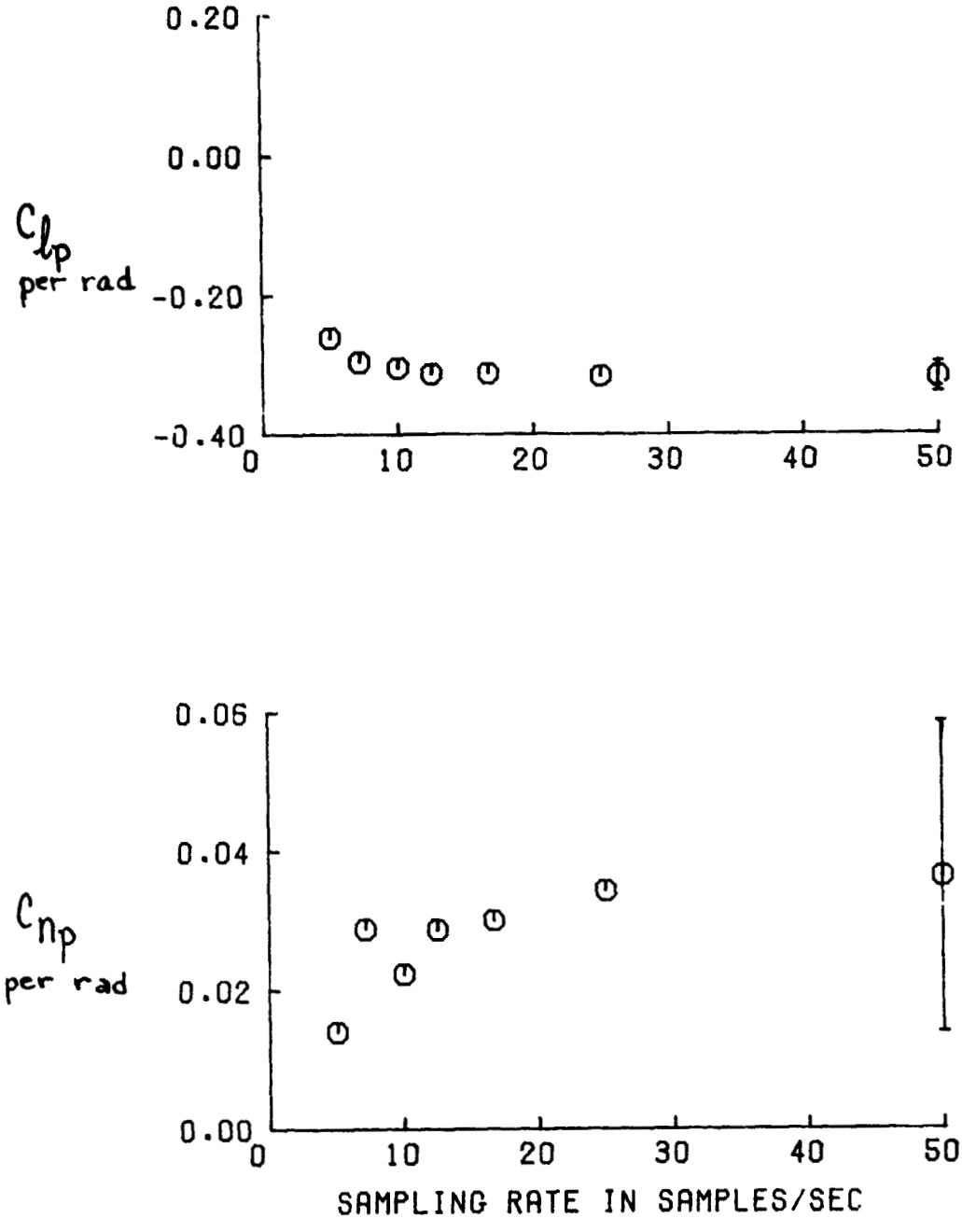

(f) C_{l_p}, C_{n_p} for case 1:2

Figure 10. Continued.

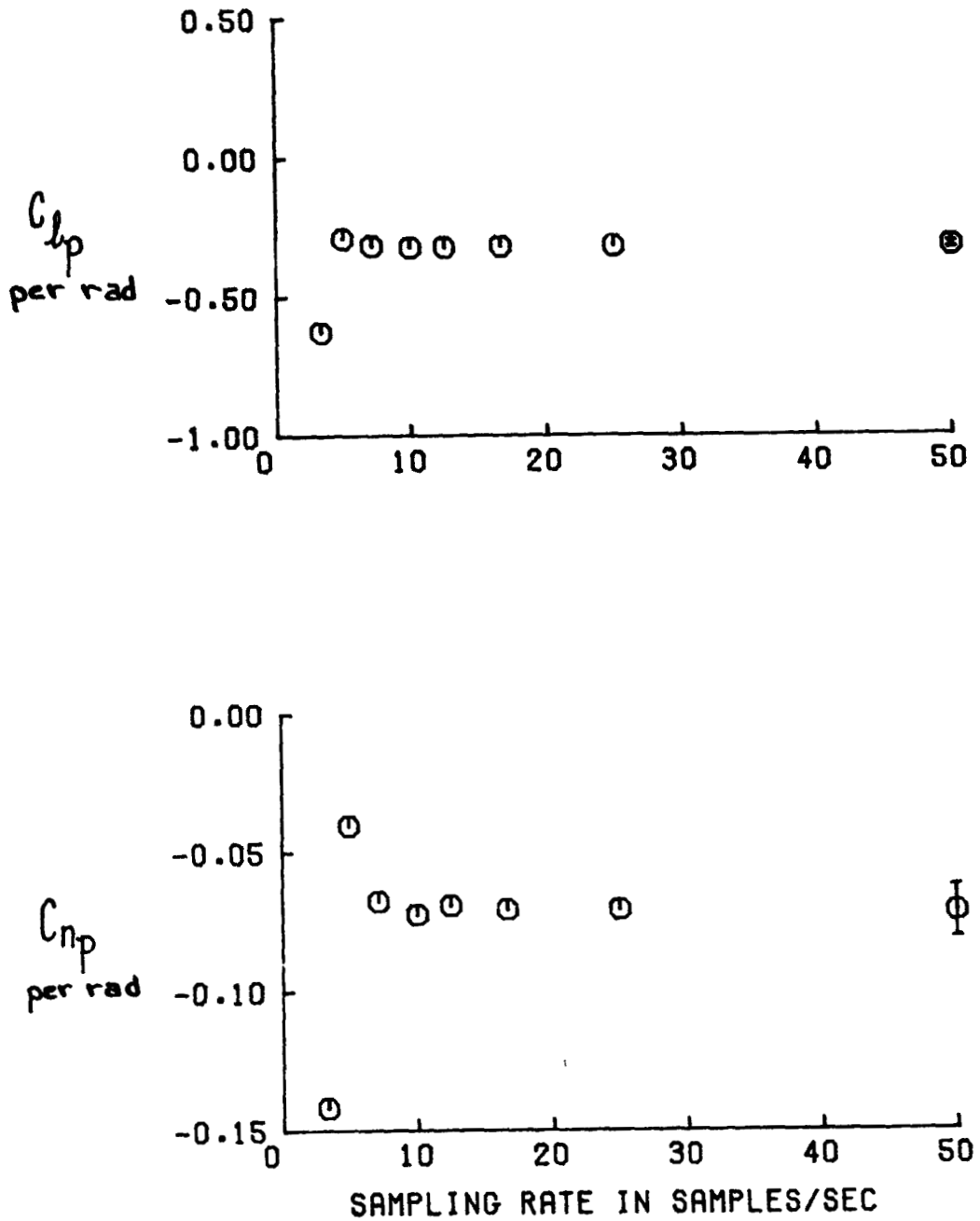

(g) C_{l_p}, C_{n_p} for case 1:3.

Figure 10. Continued.

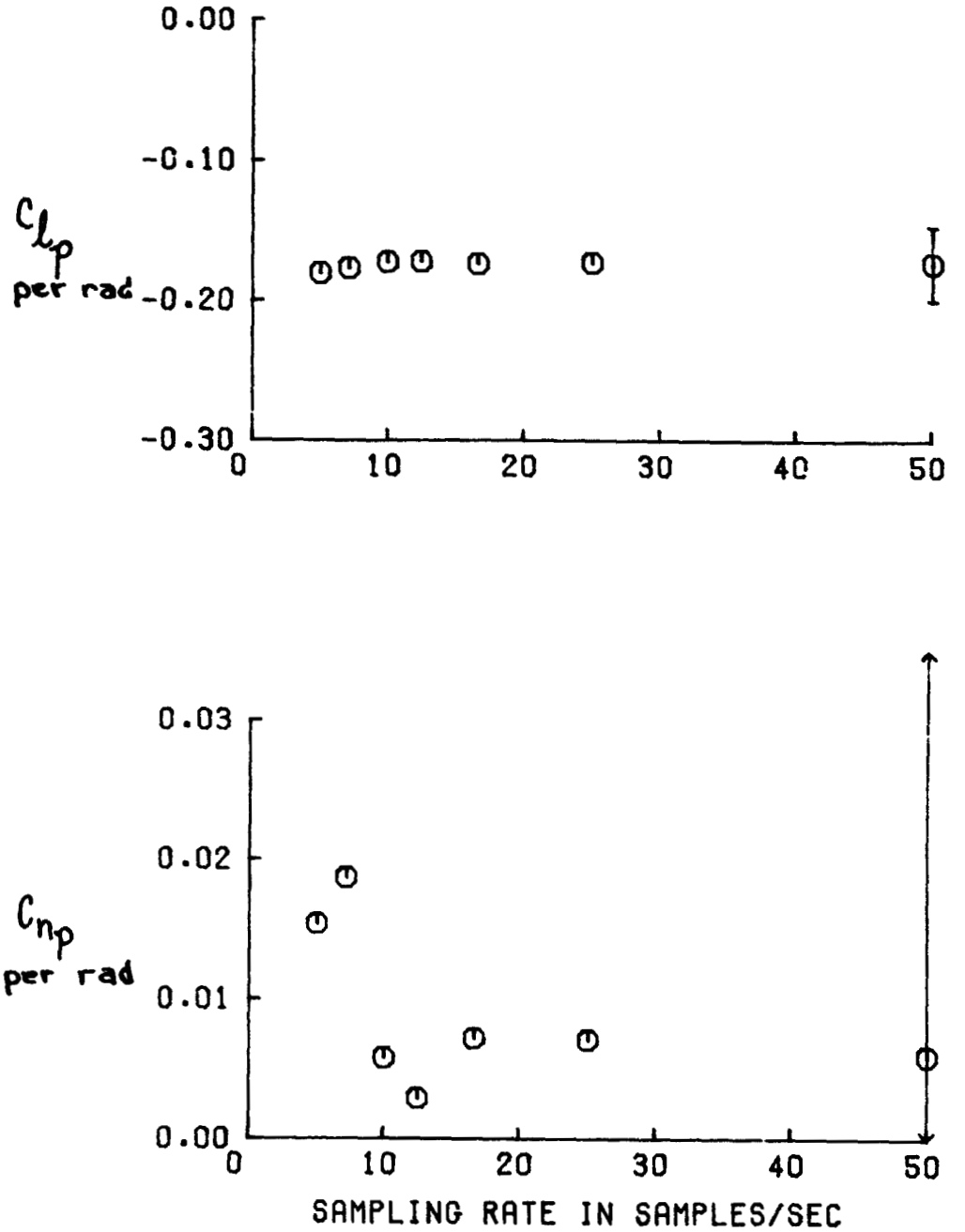

(h) C_{l_p}, C_{n_p} for case 1:103.

Figure 10. Continued.

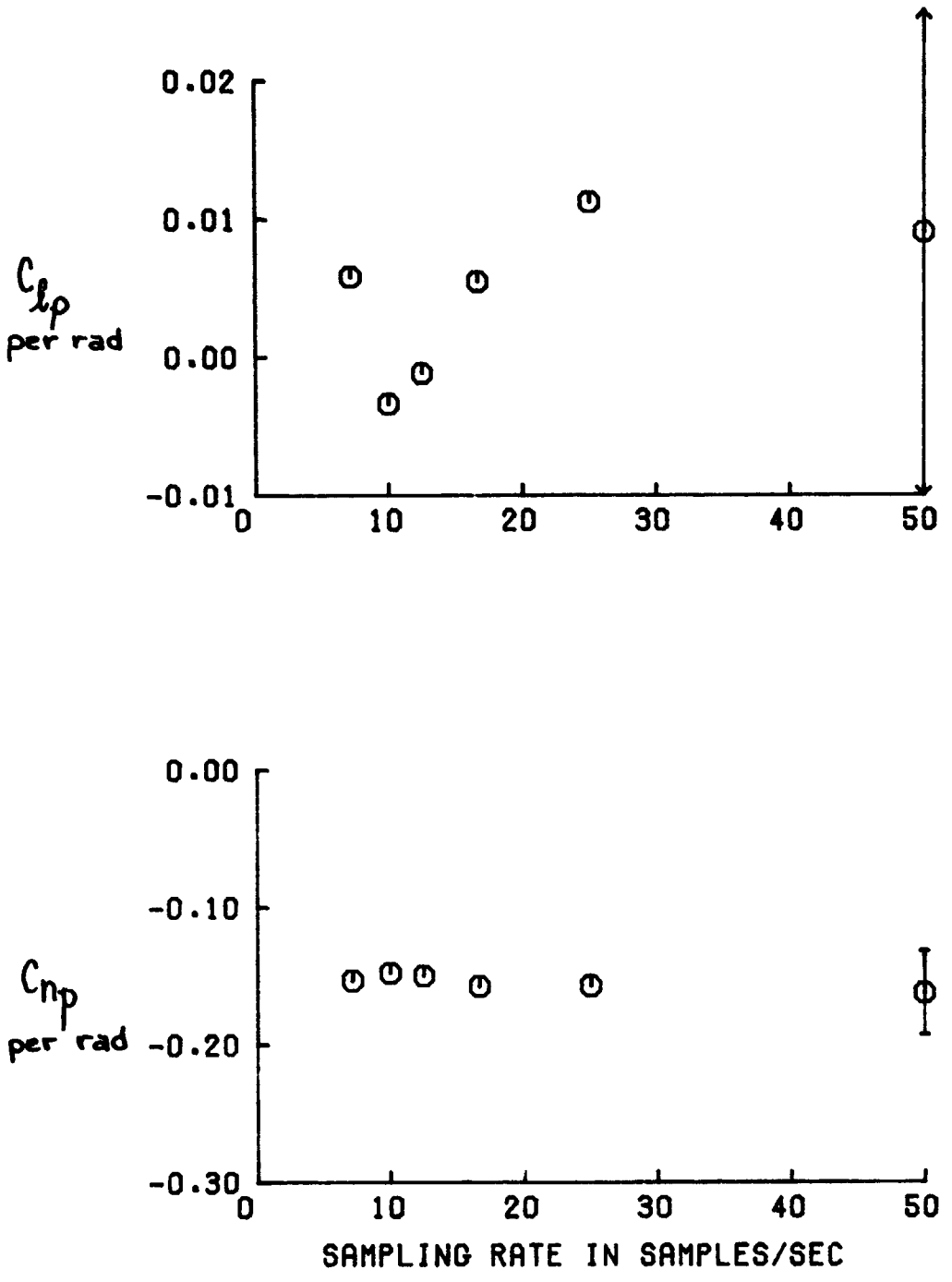

(i) C_{l_p}, C_{n_p} for case 1:13.

Figure 10. Continued.

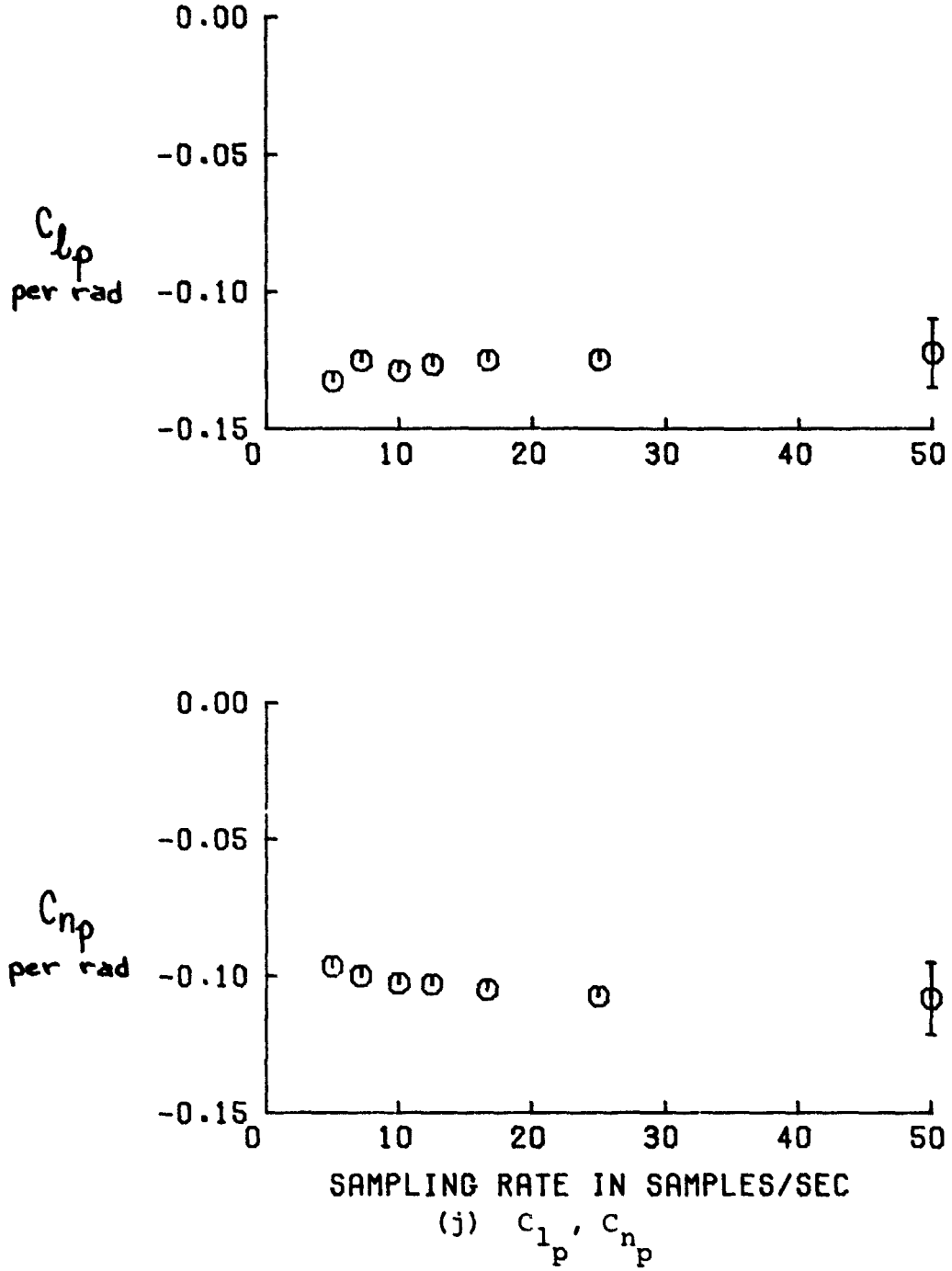

(j) C_{l_p}, C_{n_p}

for case 1:14B.

Figure 10. Continued.

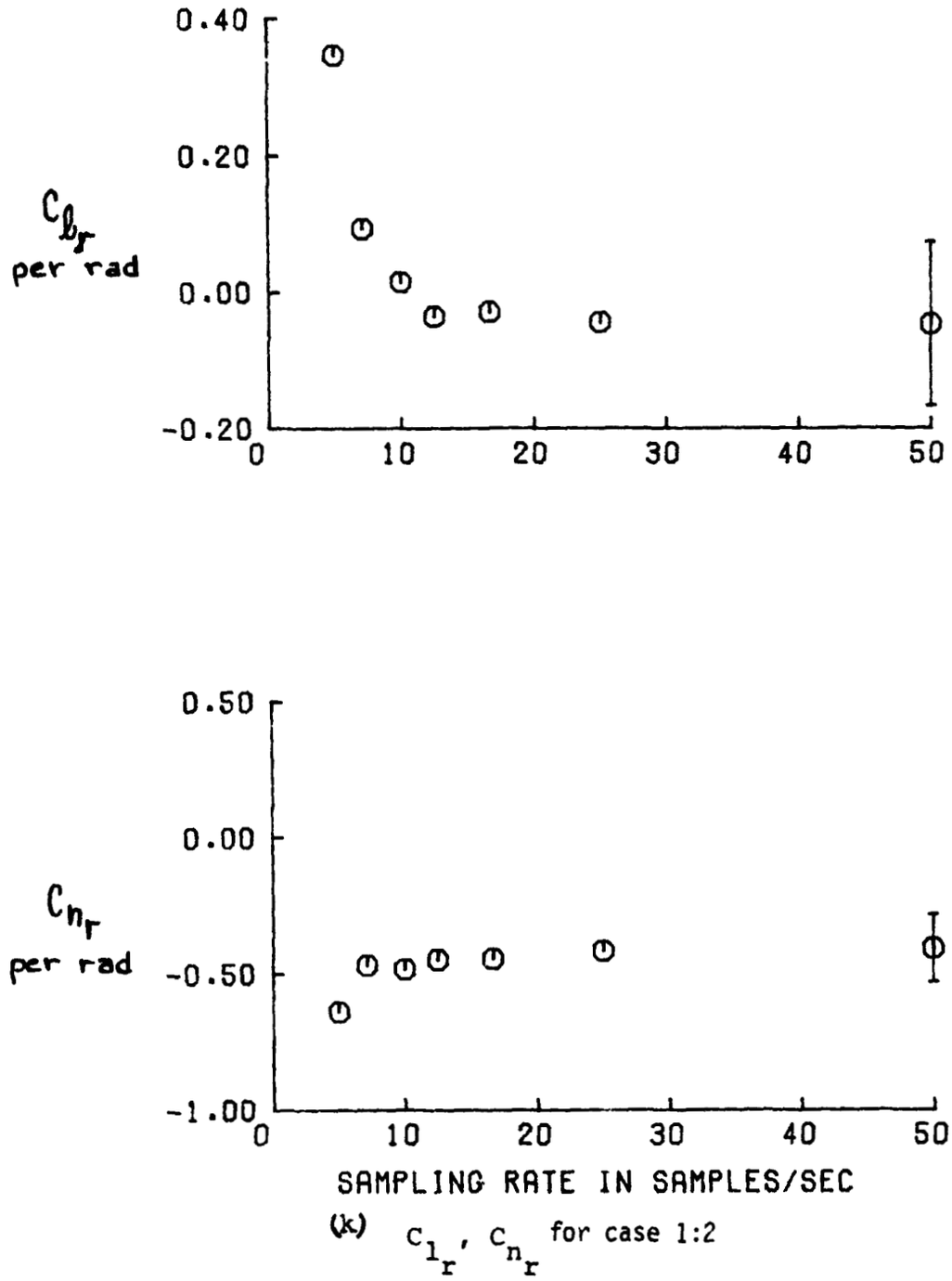

(k) C_{l_r}, C_{n_r} for case 1:2

Figure 10. Continued

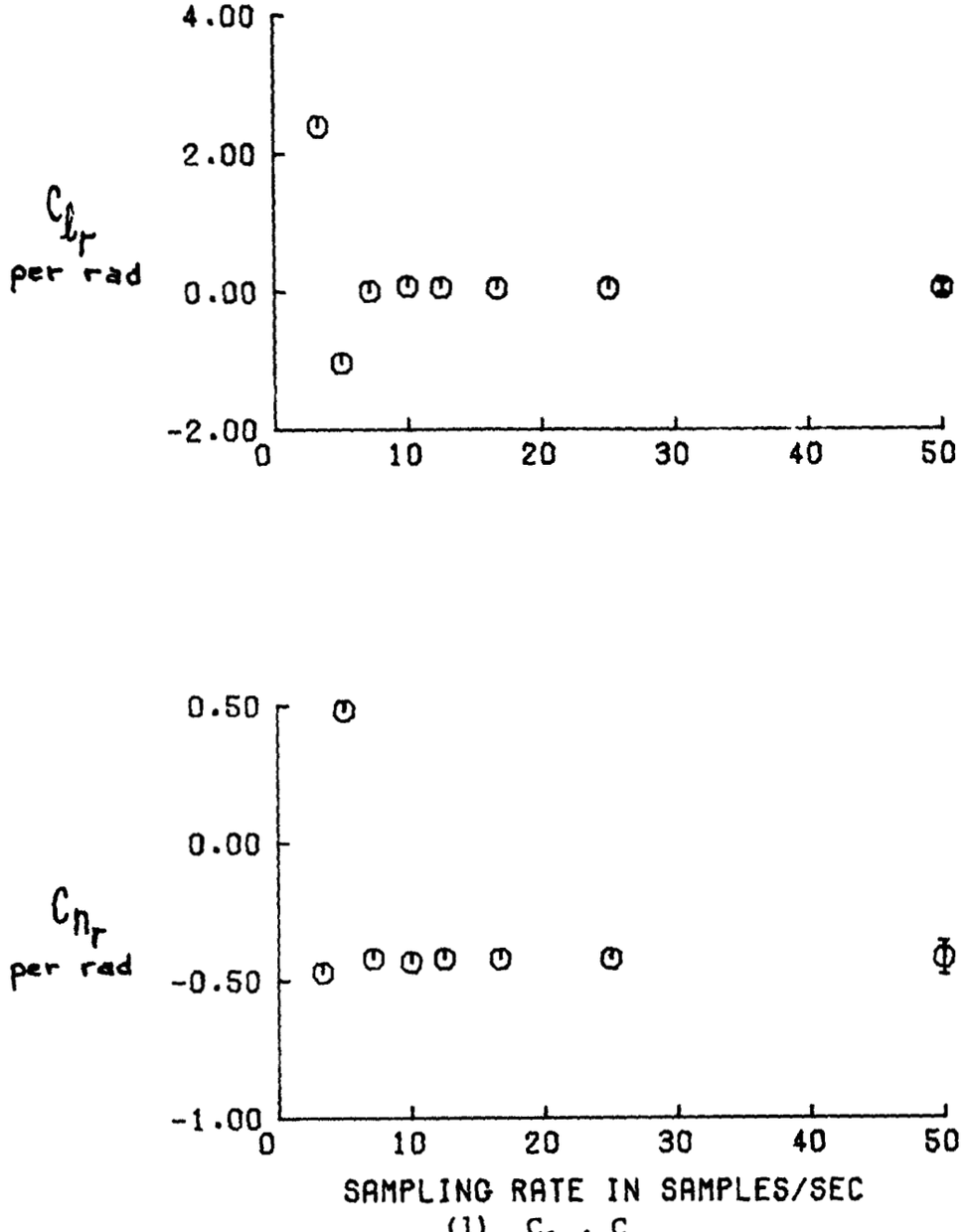

(1) C_{l_r}, C_{n_r} for case 1:3.

Figure 10. Continued.

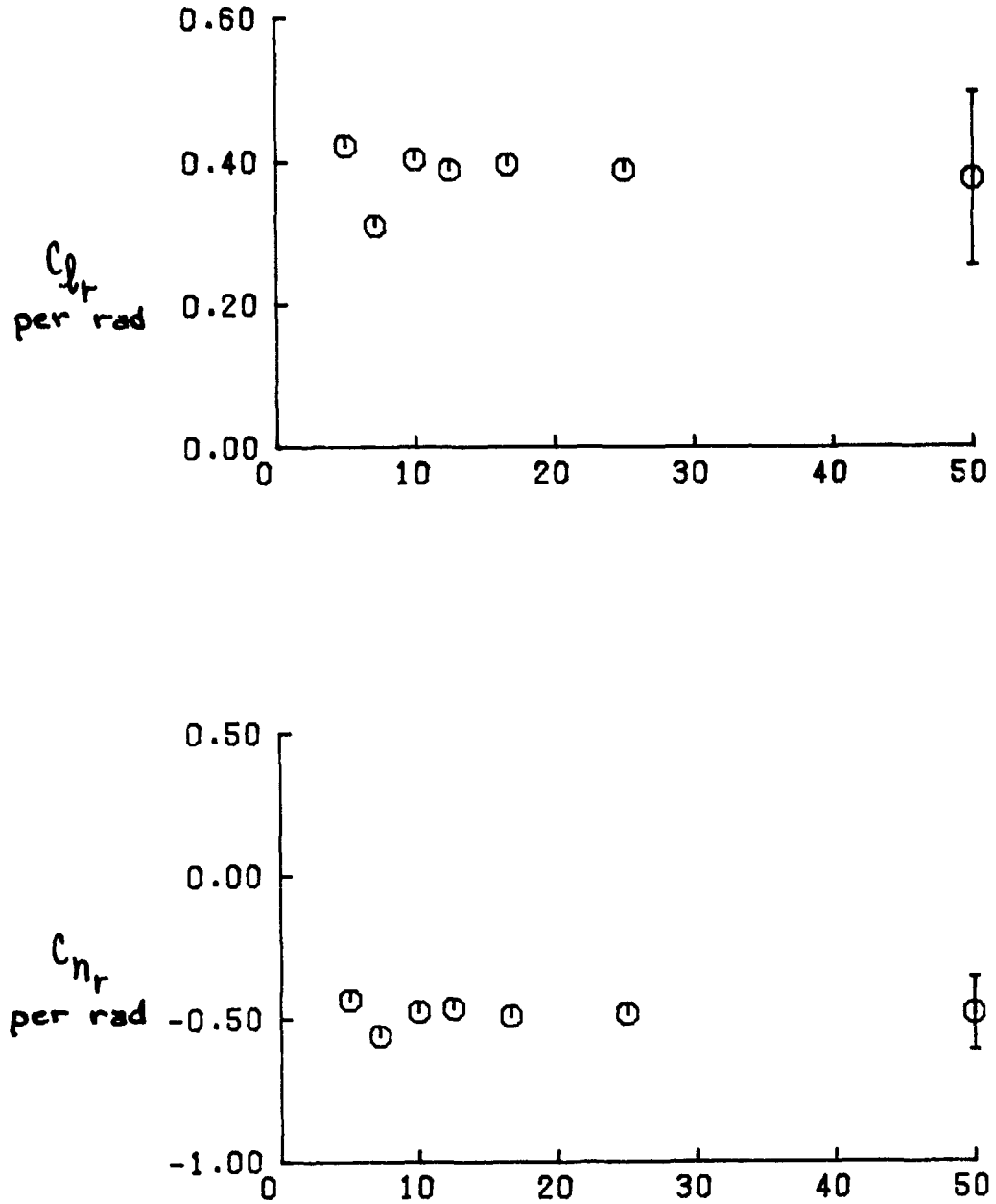

(m) C_{l_r}, C_{n_r} for case 1:10B.

Figure 10. Continued.

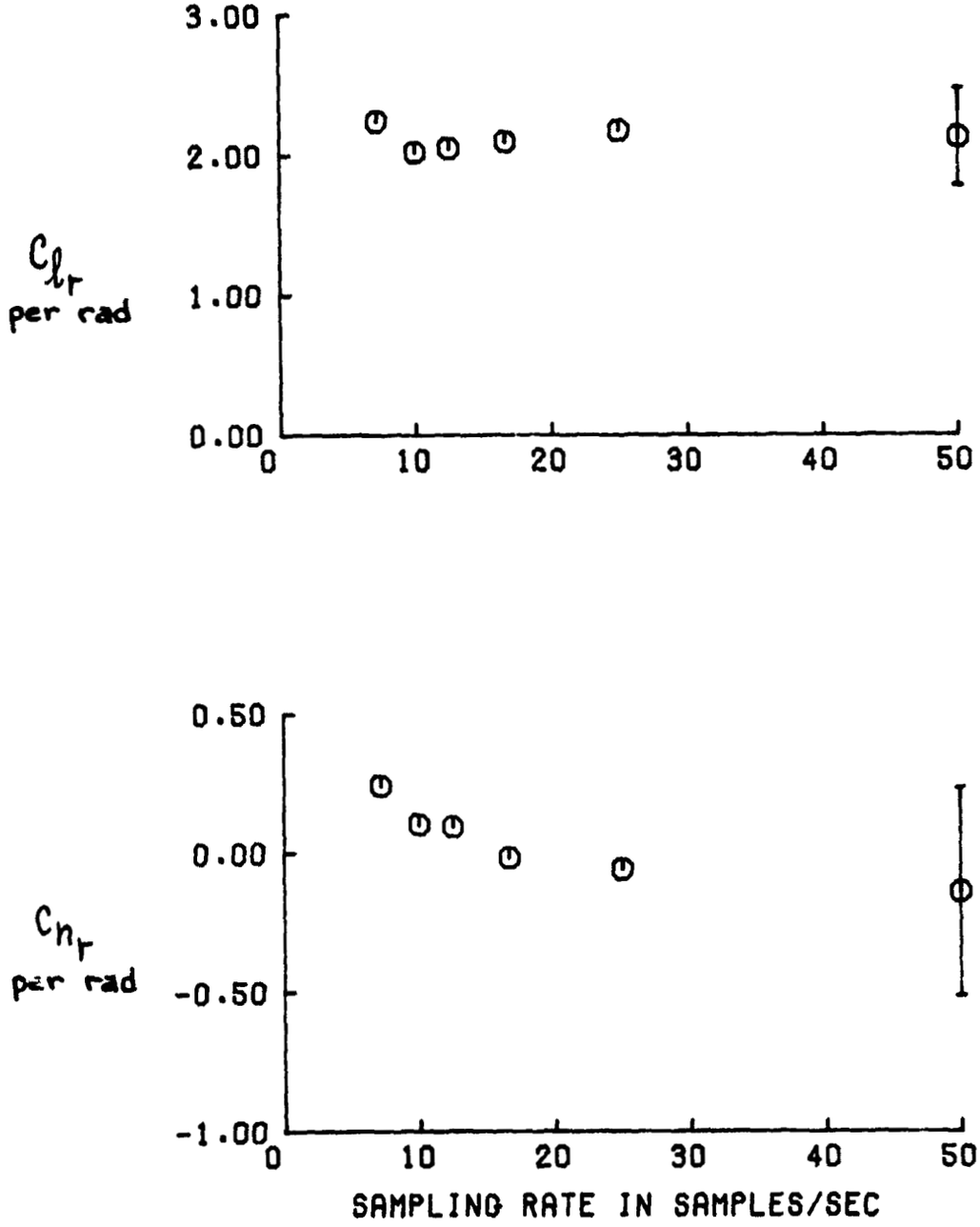

(n) C_{l_r}, C_{n_r} for case 1:13.

Figure 10. Continued.

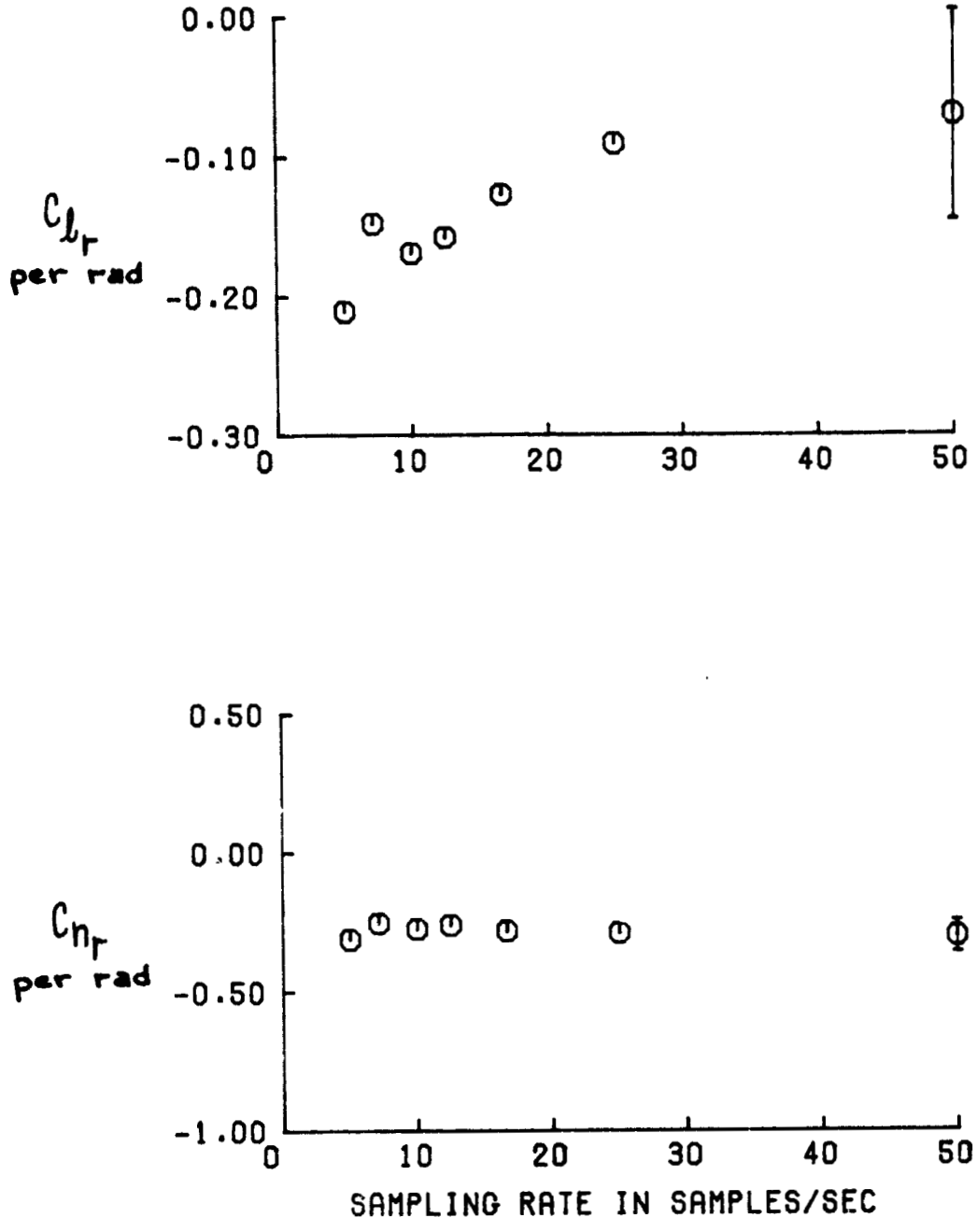

(b) C_{l_r}, C_{n_r} for case 1:14B.

Figure 10. Continued.

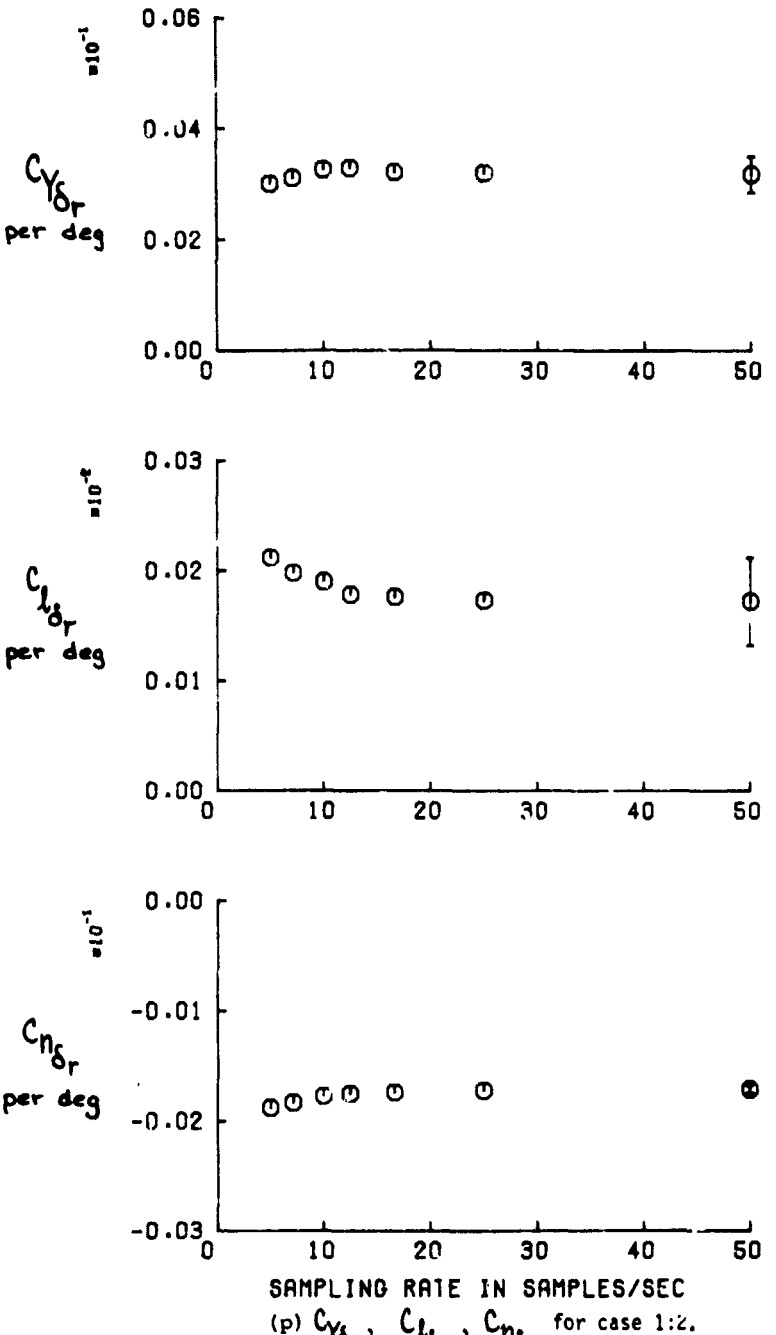

(p) $C_{Y_{\delta_r}}$, $C_{l_{\delta_r}}$, $C_{n_{\delta_r}}$ for case 1:2.

Figure 10. Continued.

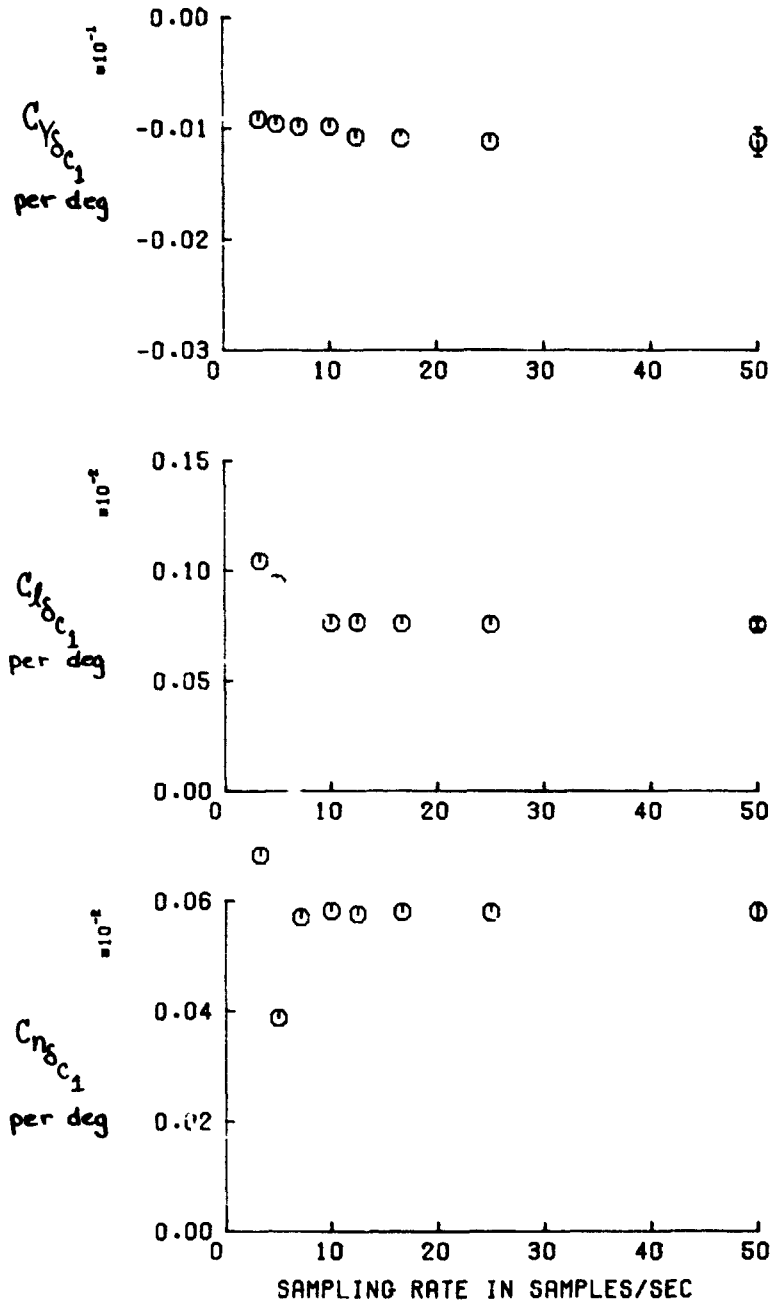

(q) $C_{Y_{\delta_{c_1}}}$, $C_{l_{\delta_{c_1}}}$, $C_{n_{\delta_{c_1}}}$ for case 1:3.

Figure 10. Continued.

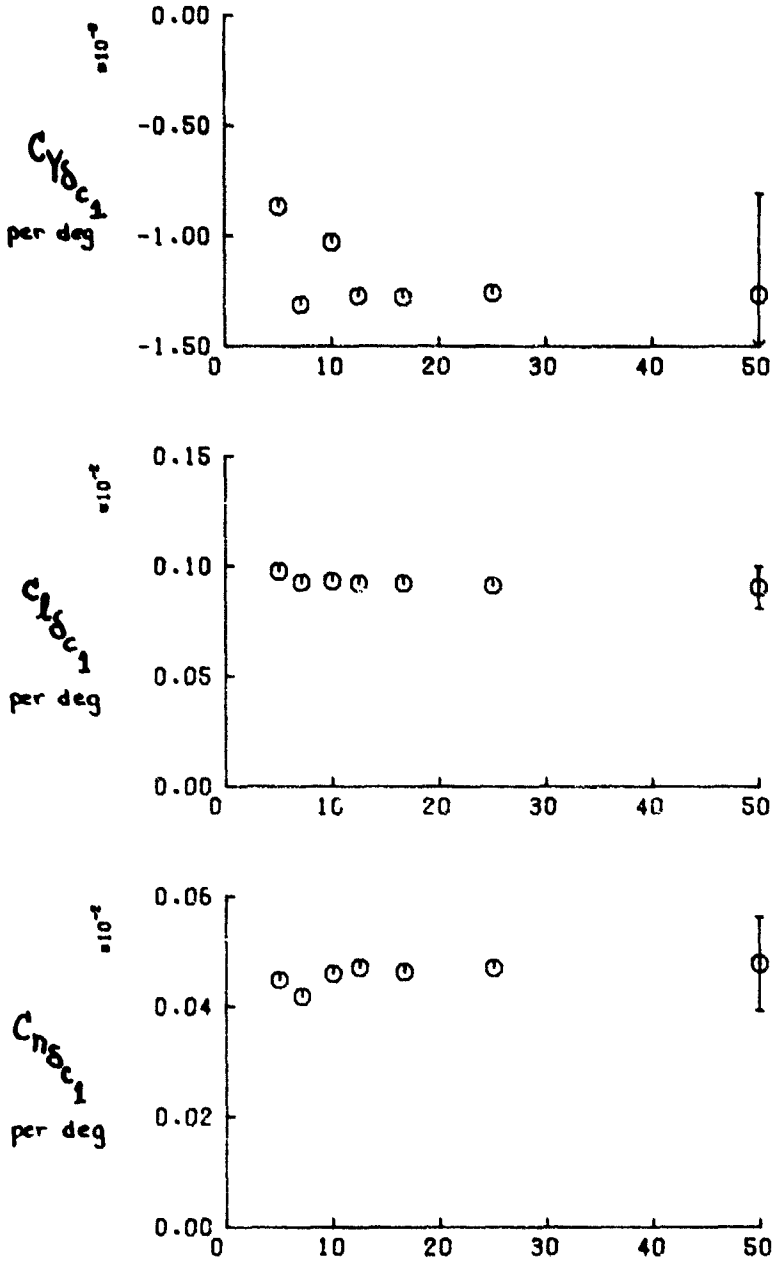

(r) $C_{Y_{\delta c_1}}$, $C_{l_{\delta c_1}}$, $C_{n_{\delta c_1}}$ for case 1: 16 B.

Figure 10. Continued.

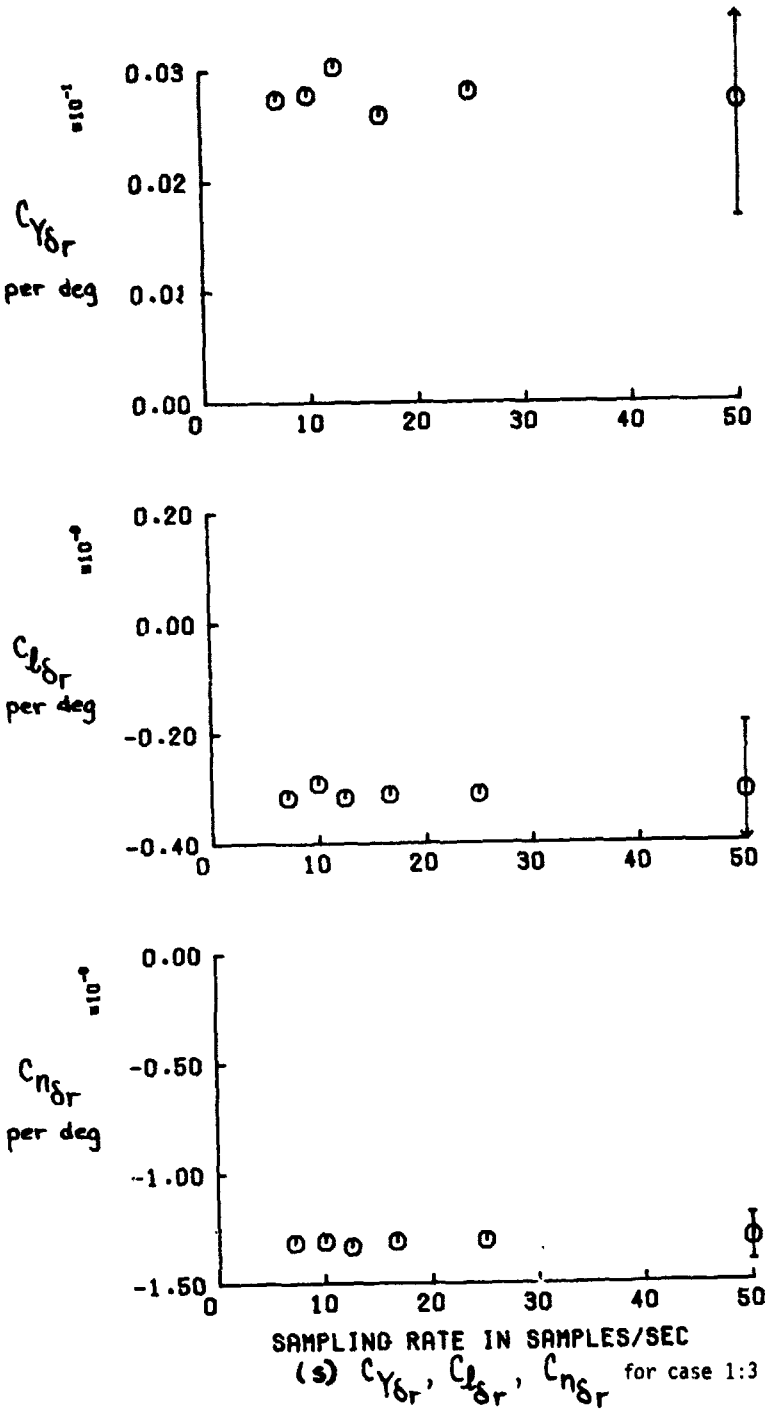

(s) $C_{Y_{\delta r}}$, $C_{\ell_{\delta r}}$, $C_{n_{\delta r}}$ for case 1:3

Figure 10. Continued.

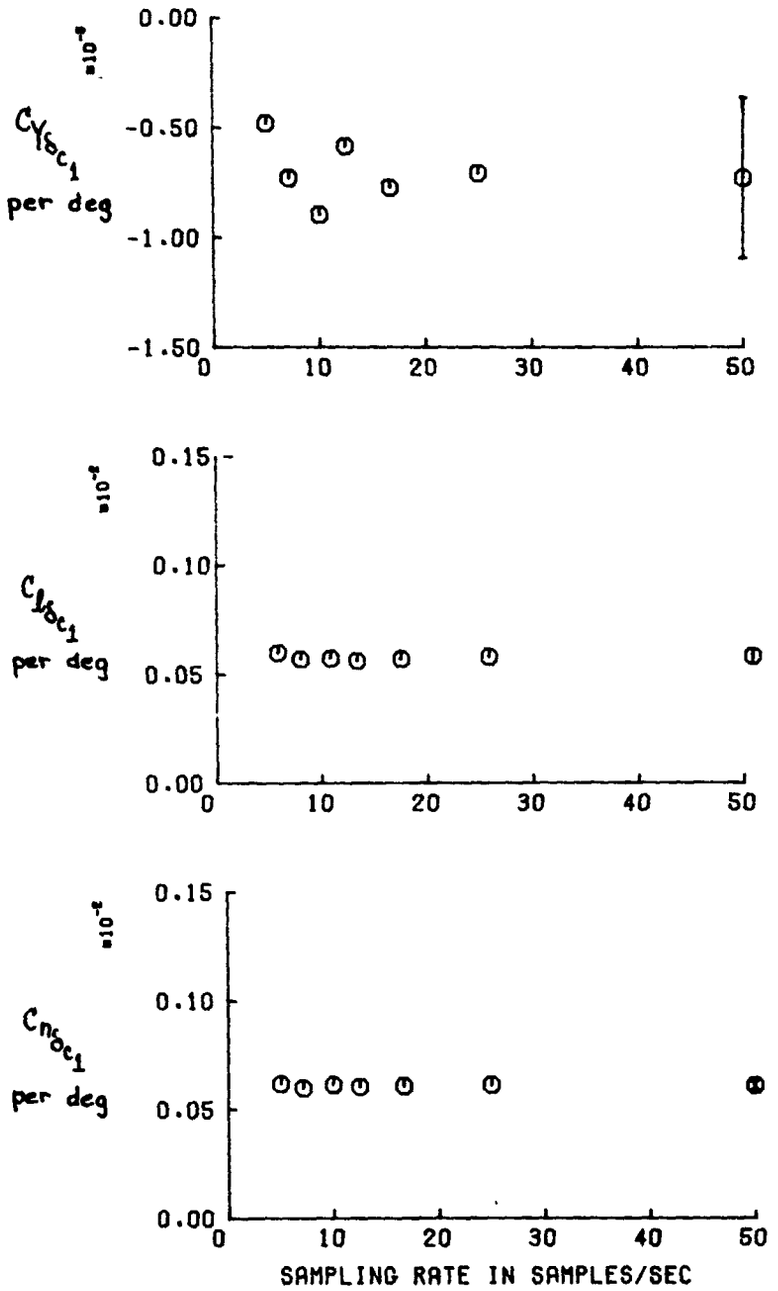

(t) $C_{Y_{\delta_{c_1}}}$, $C_{l_{\delta_{c_1}}}$, $C_{n_{\delta_{c_1}}}$ for case 1:14B

Figure 10. Concluded.

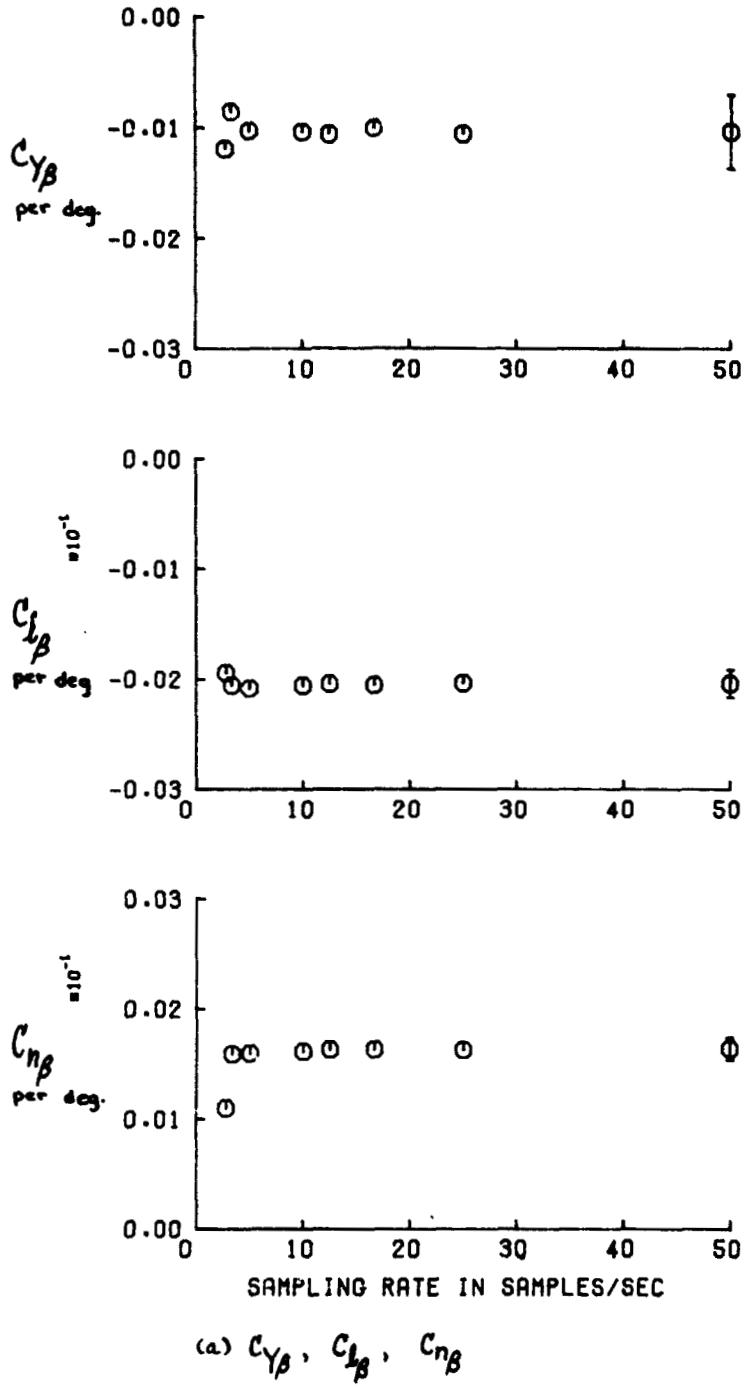

(a) C_{Y_β}, C_{l_β}, C_{n_β}

Figure 11. Estimated lateral-directional derivatives as a function of sampling rate, Aircraft C.

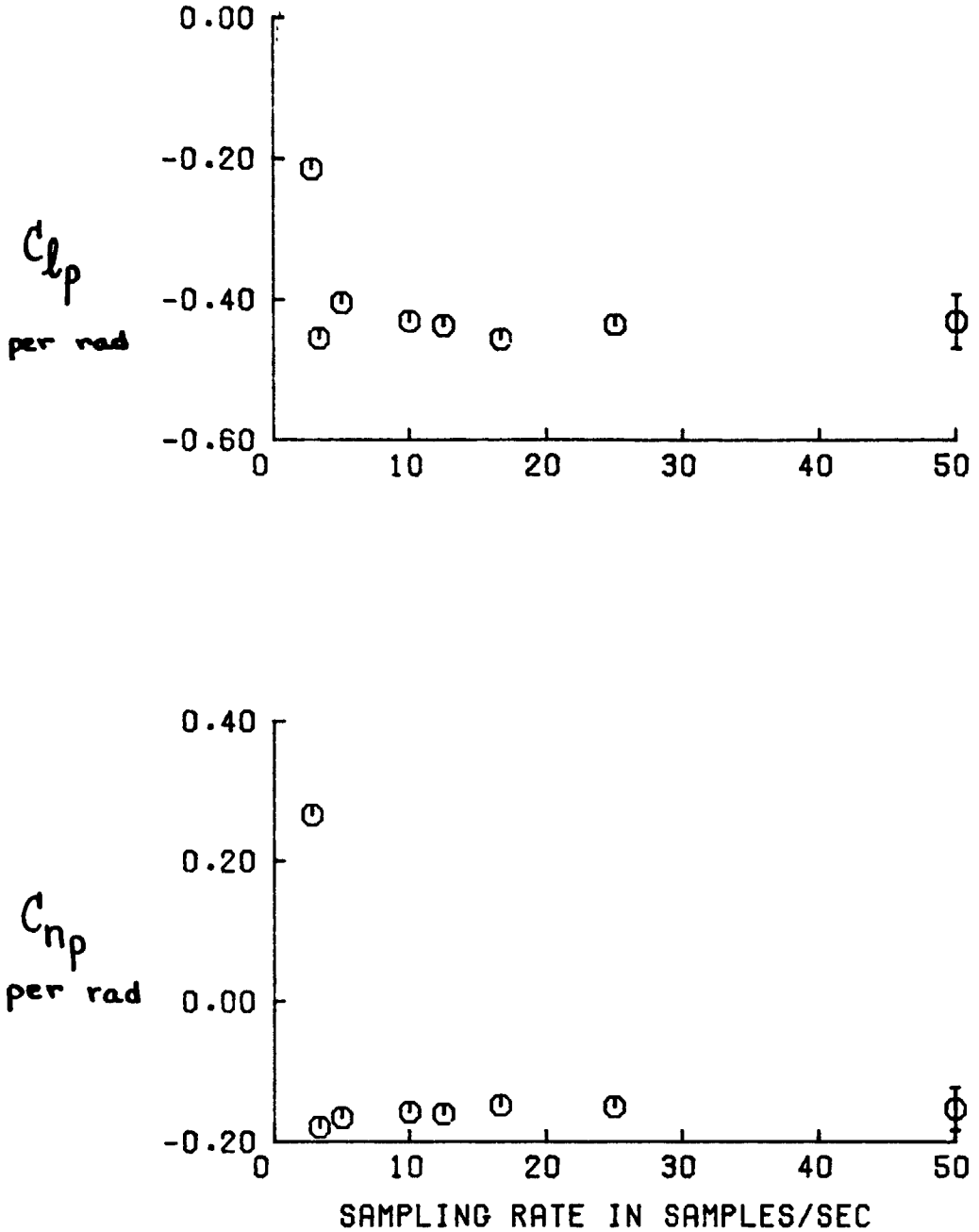

(b) C_{l_p}, C_{n_p}

FIGURE 11. CONTINUED.

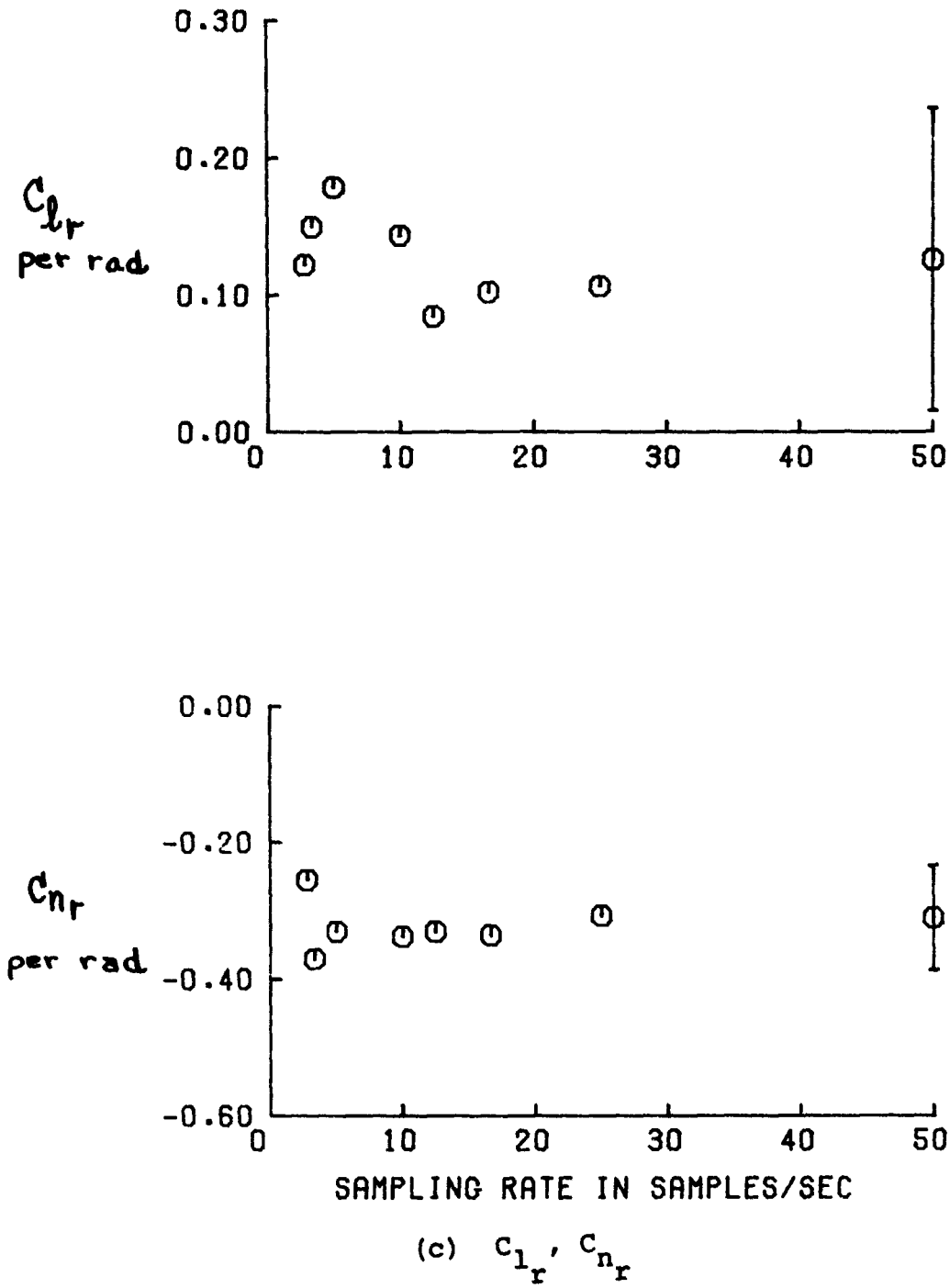

(c) C_{l_r}, C_{n_r}

FIGURE 11. CONTINUED.

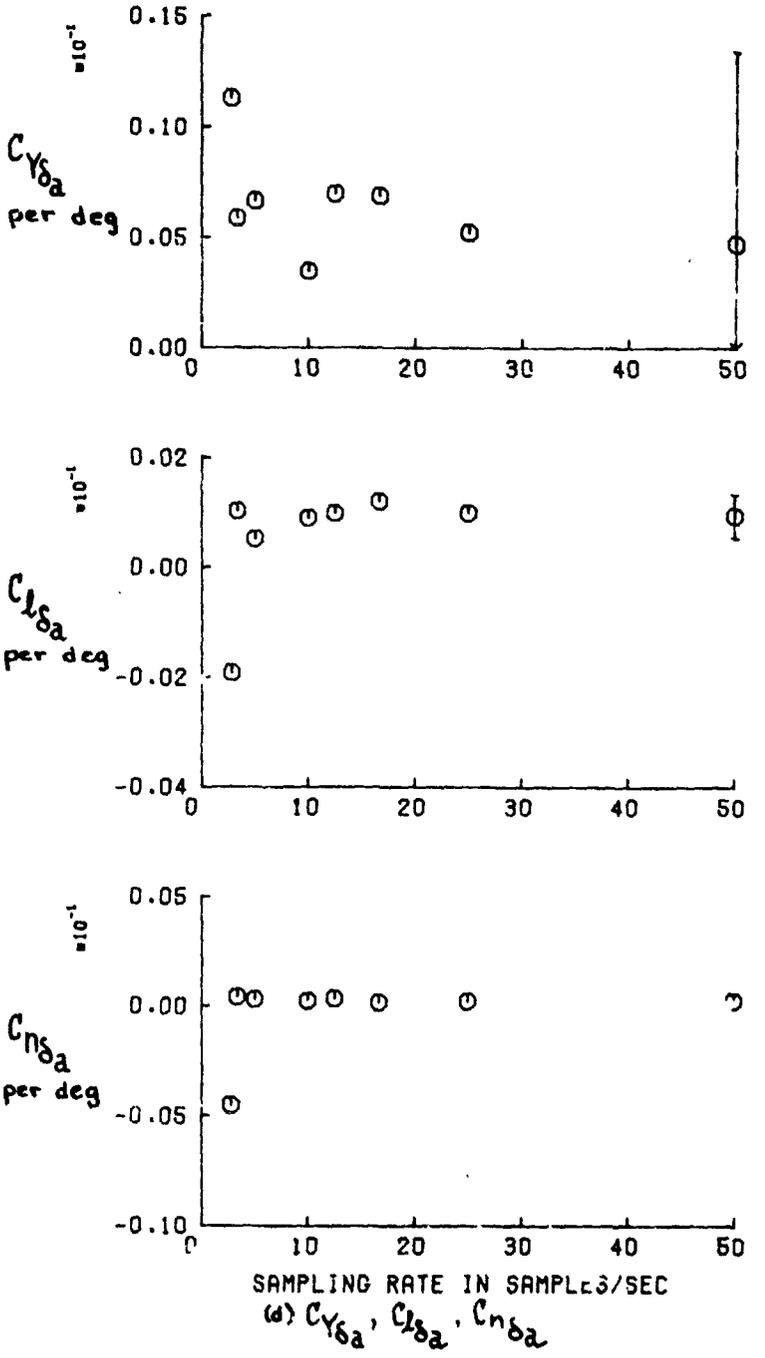

(d) $C_{Y_{\delta a}}$, $C_{l_{\delta a}}$, $C_{n_{\delta a}}$

FIGURE 11. CONTINUED.

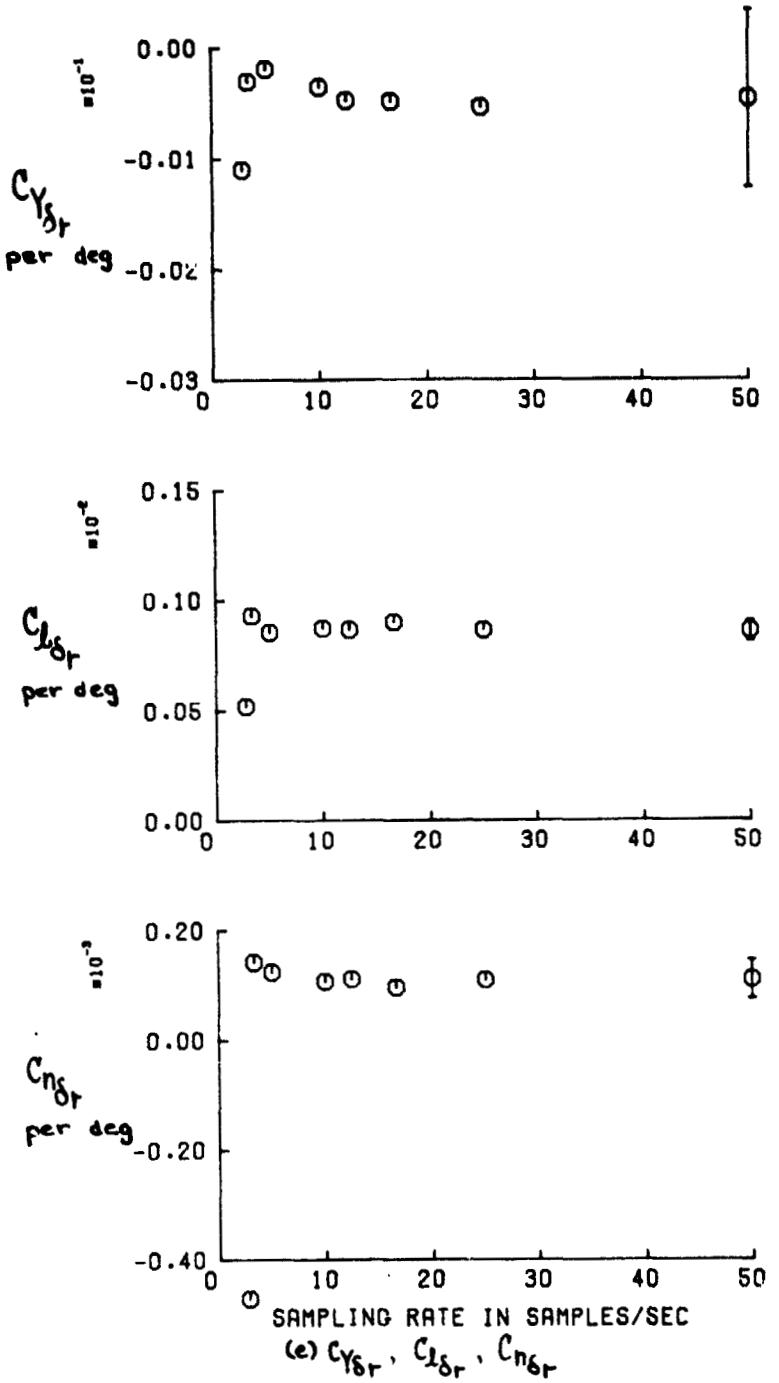

(e) $C_{Y_{\delta r}}$, $C_{l_{\delta r}}$, $C_{n_{\delta r}}$

FIGURE 11. CONCLUDED.

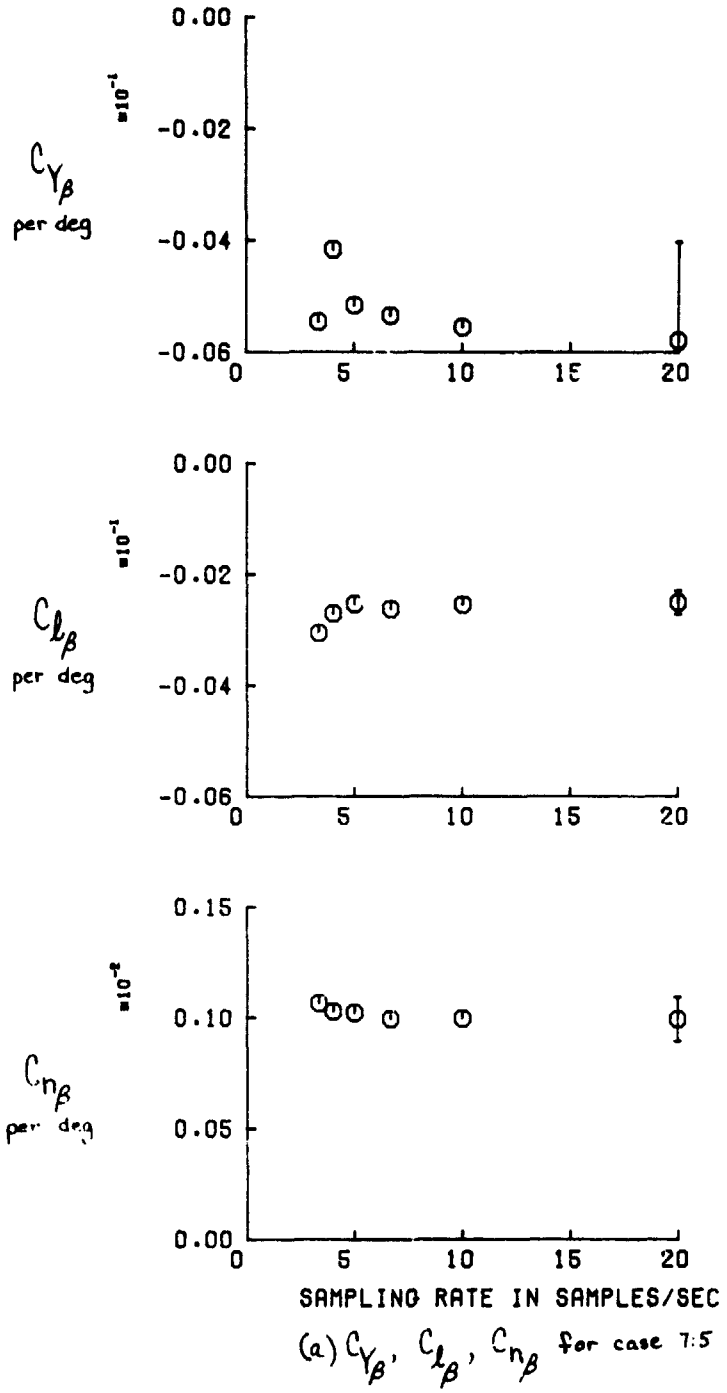

Figure 12. Estimated lateral-directional derivatives obtained from five cases as a function of sampling rate. Aircraft D.

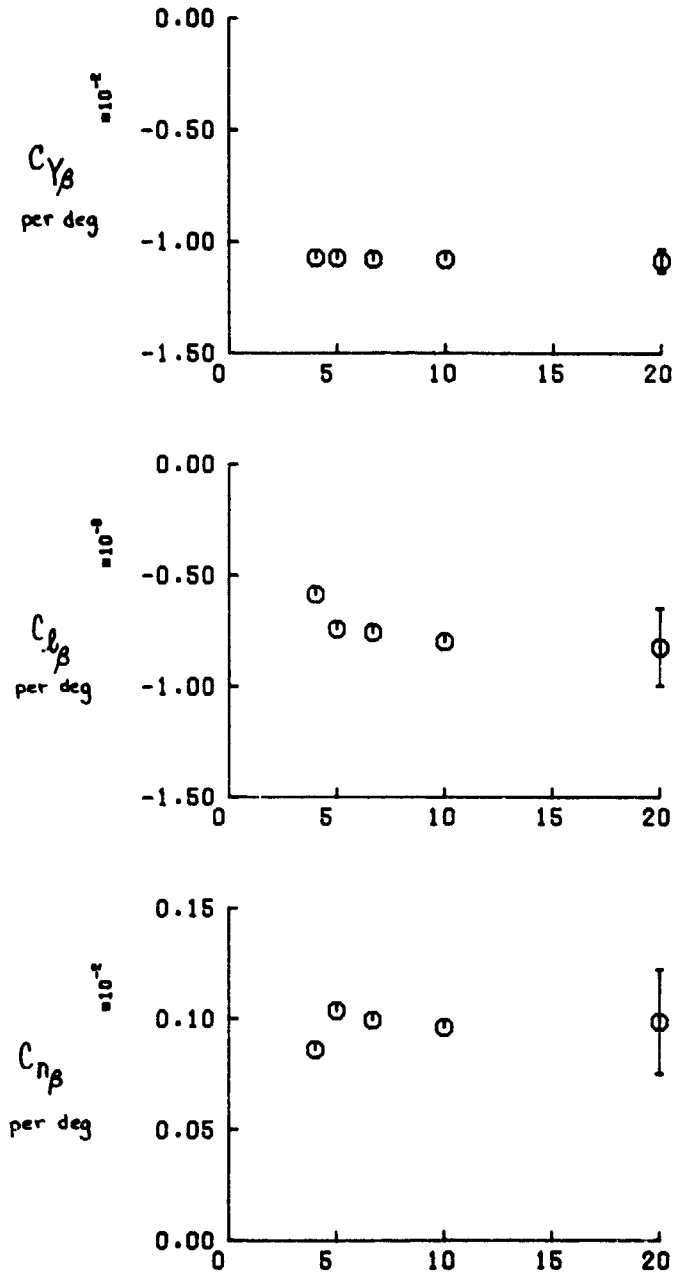

(b) C_{Y_β}, C_{ℓ_β}, C_{n_β} FOR CASE 7:6.

Figure 12. Continued

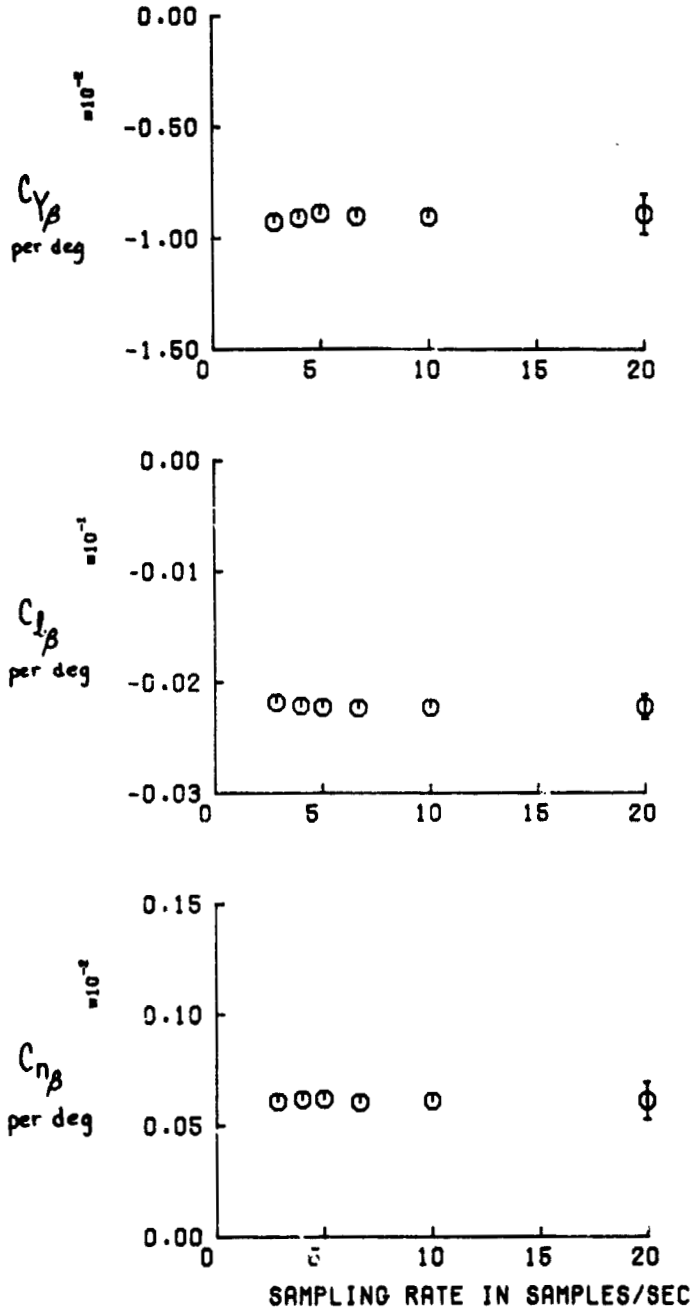

(c) C_{Y_β}, C_{l_β}, C_{n_β} FOR CASE 7:9

Figure 12. Continued.

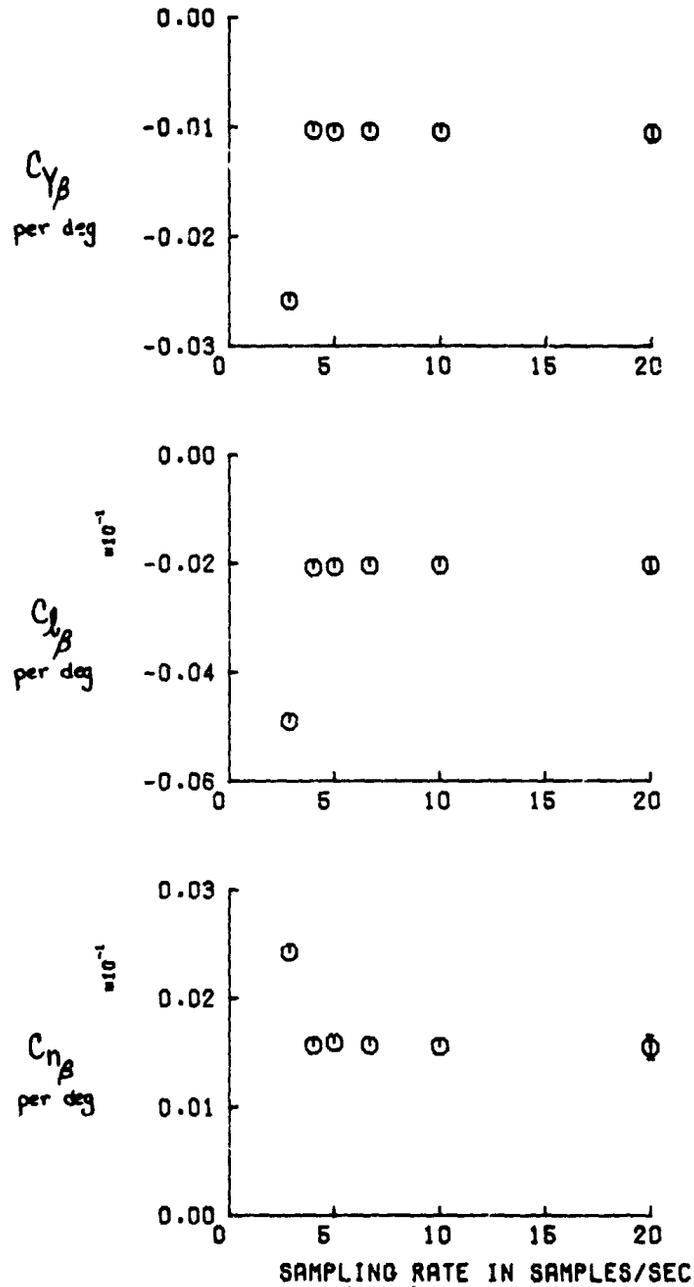

(d) C_{Y_β}, C_{l_β}, C_{n_β} FOR CASE 7:17

Figure 12. Continued.

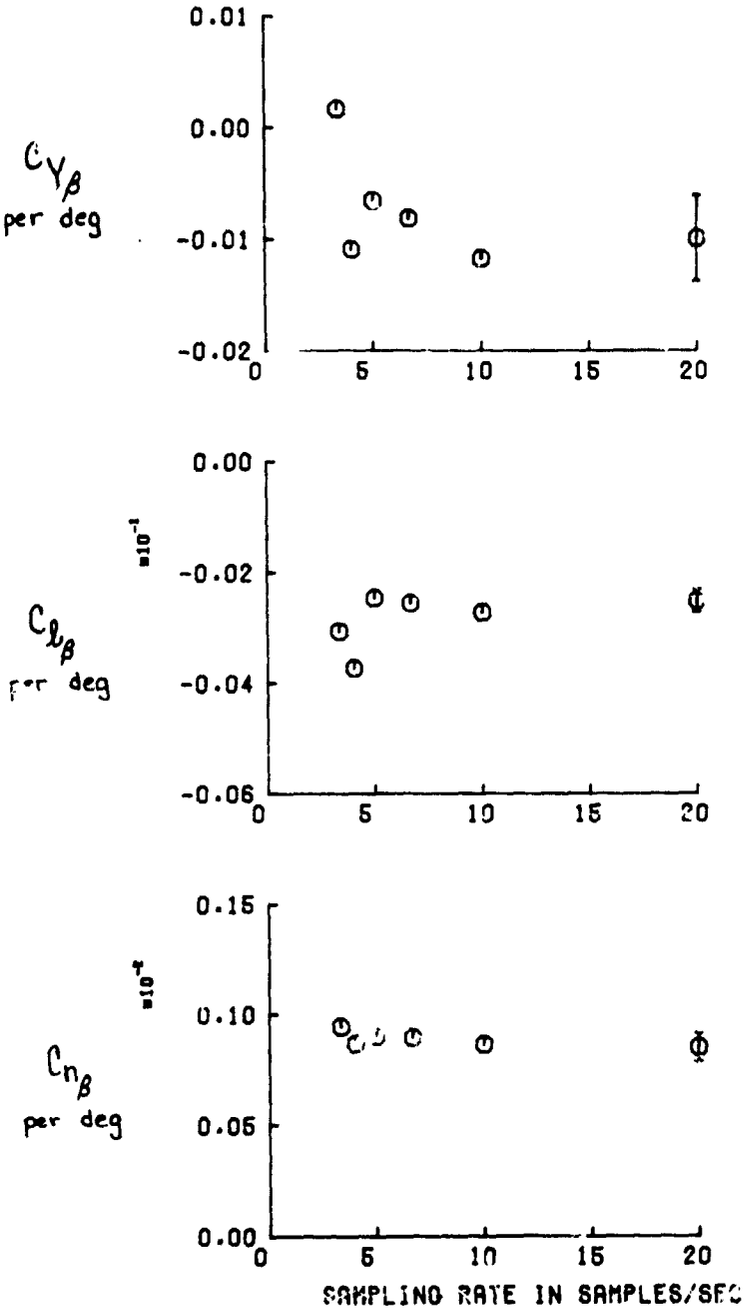

(e) C_{Y_β}, C_{l_β}, C_{n_β} FOR CASE 814.

Figure 12. Continued.

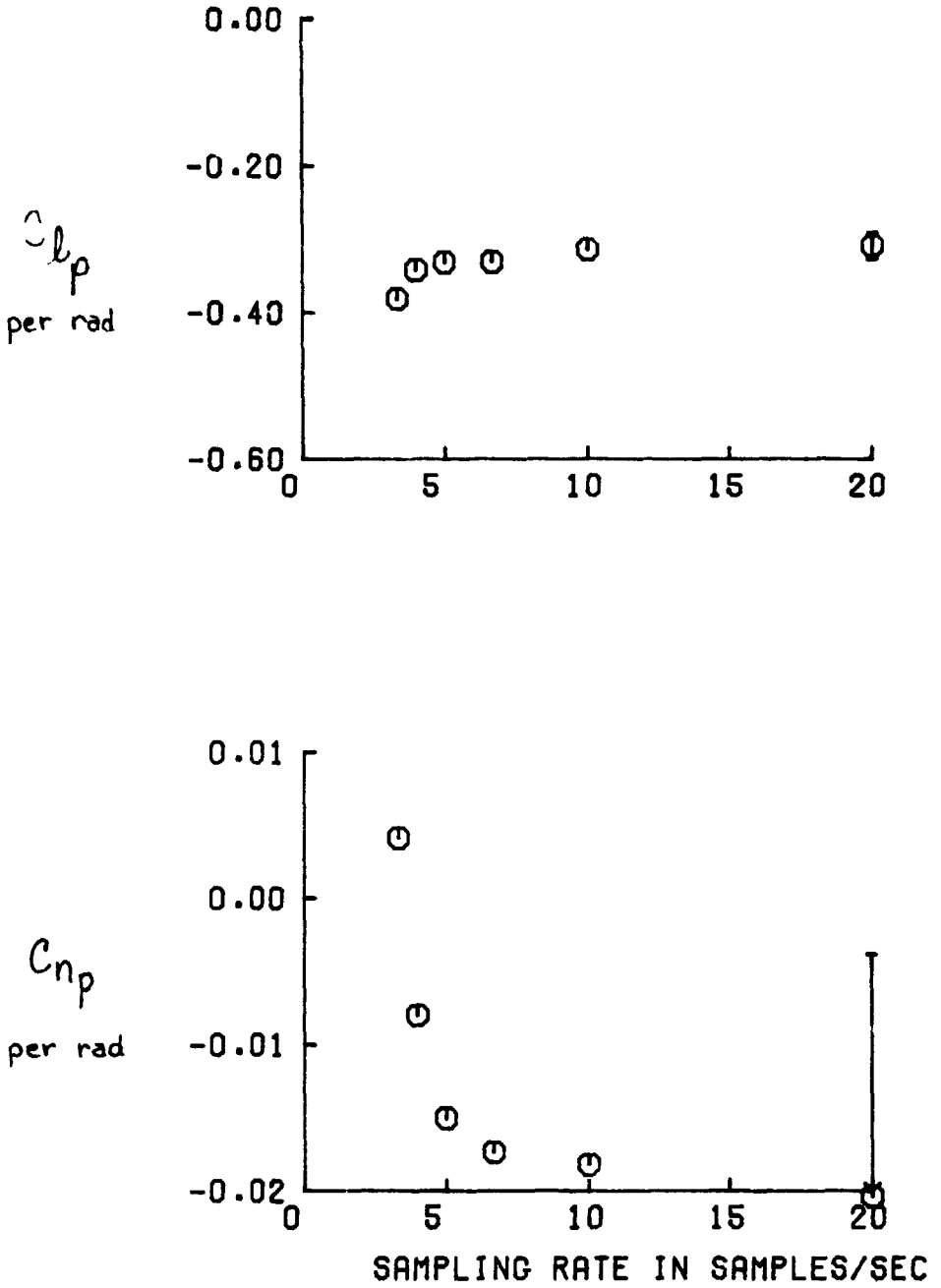

(f) C_{l_p}, C_{n_p} FOR CASE 7:5

Figure 12. Continued.

C-2

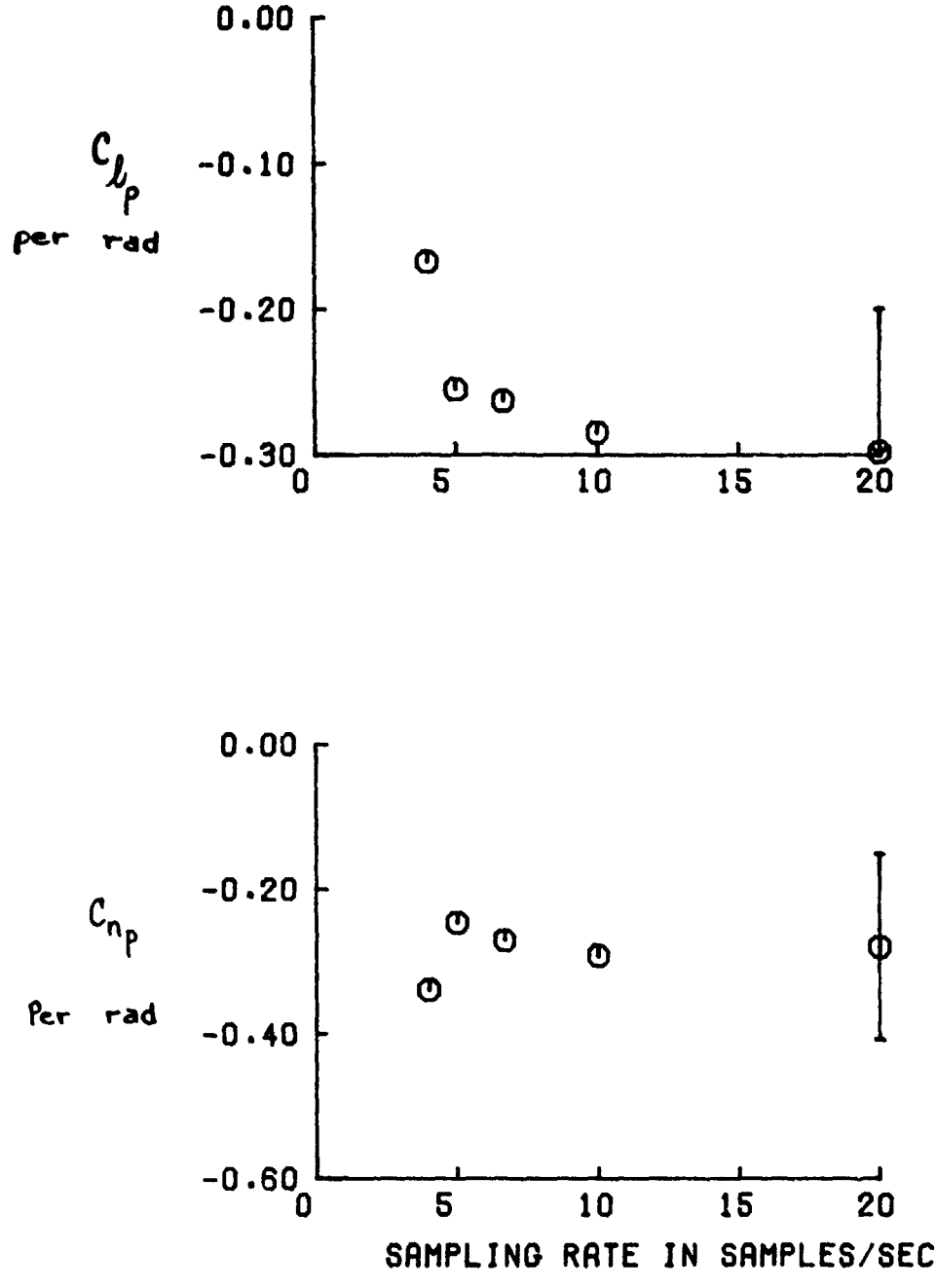

(g) C_{l_p}, C_{n_p} FOR CASE 7:6.

Figure 12. Continued.

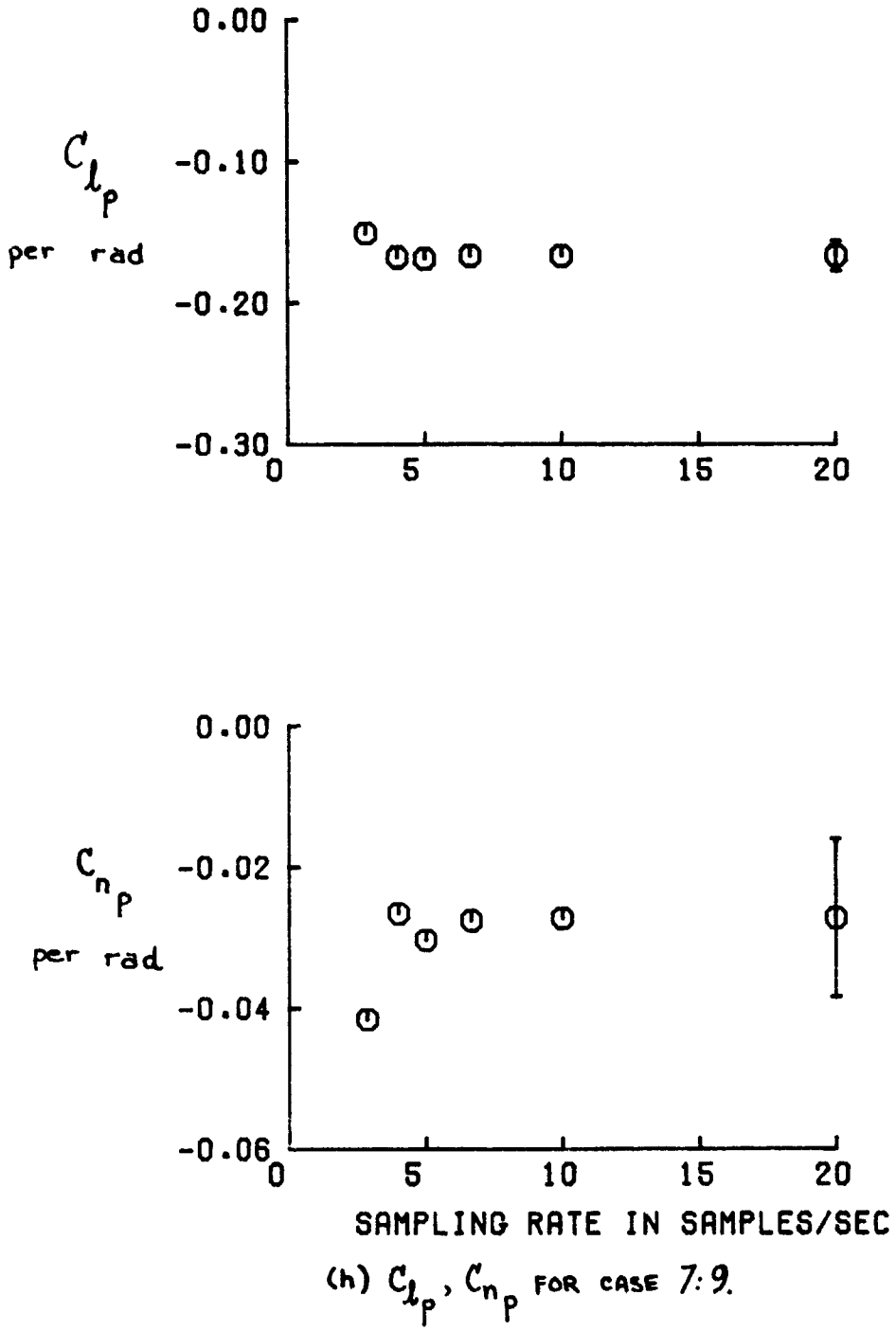

(h) C_{l_p}, C_{n_p} FOR CASE 7:9.

Figure 12. Continued.

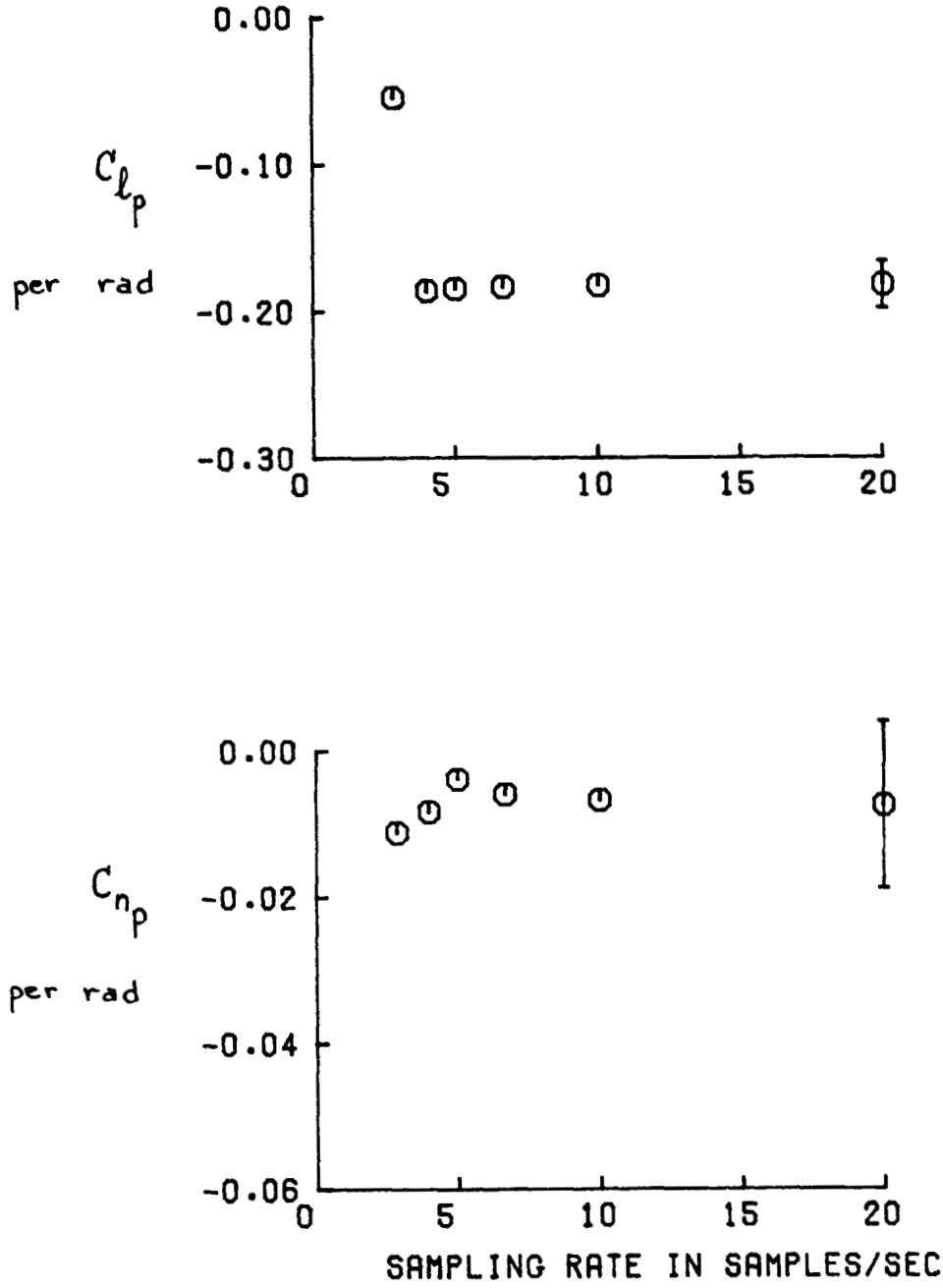

(i) C_{l_p}, C_{n_p} FOR CASE 7:17

Figure 12. Continued.

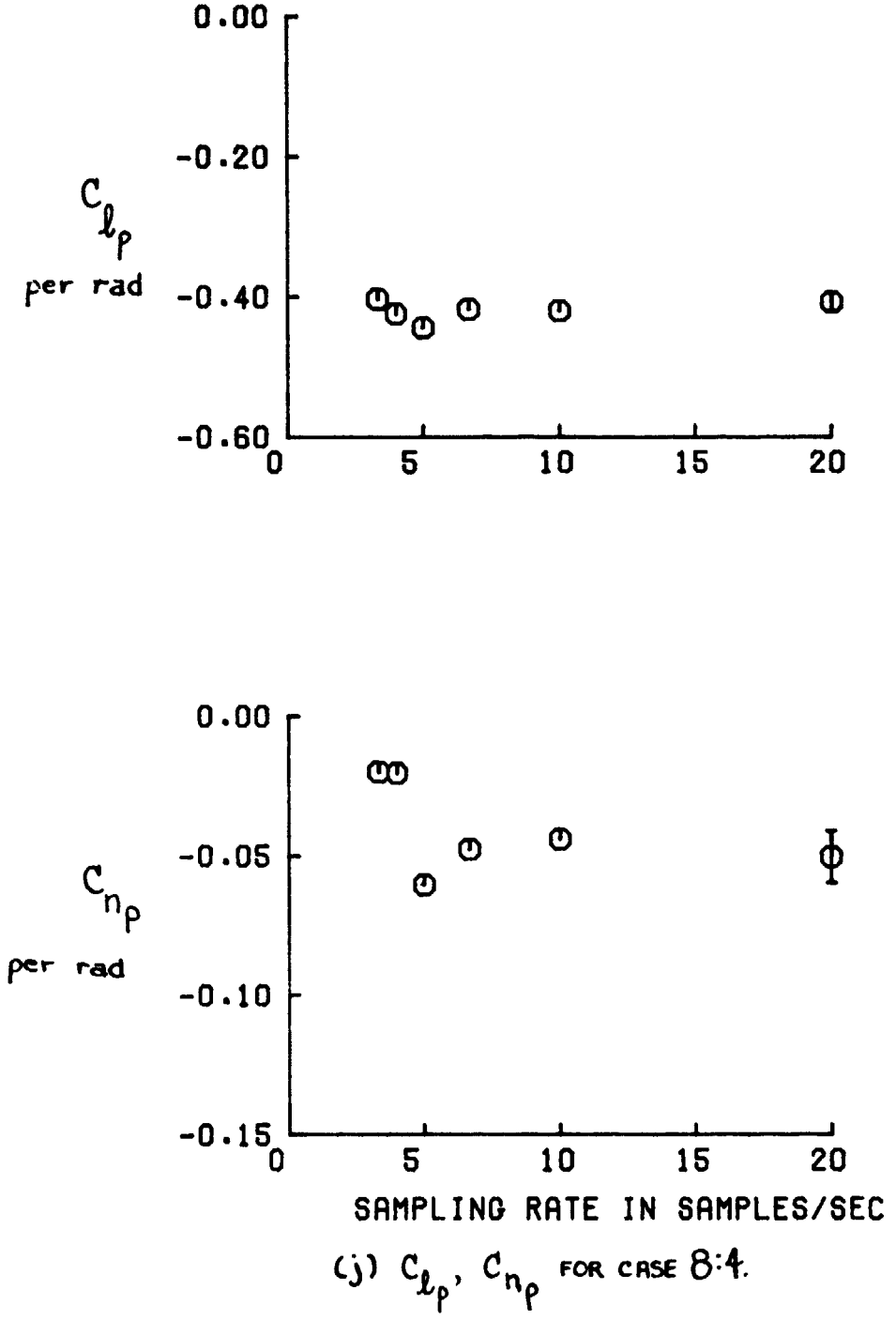

(j) C_{l_p}, C_{n_p} FOR CASE 8:4.

Figure 12. Continued.

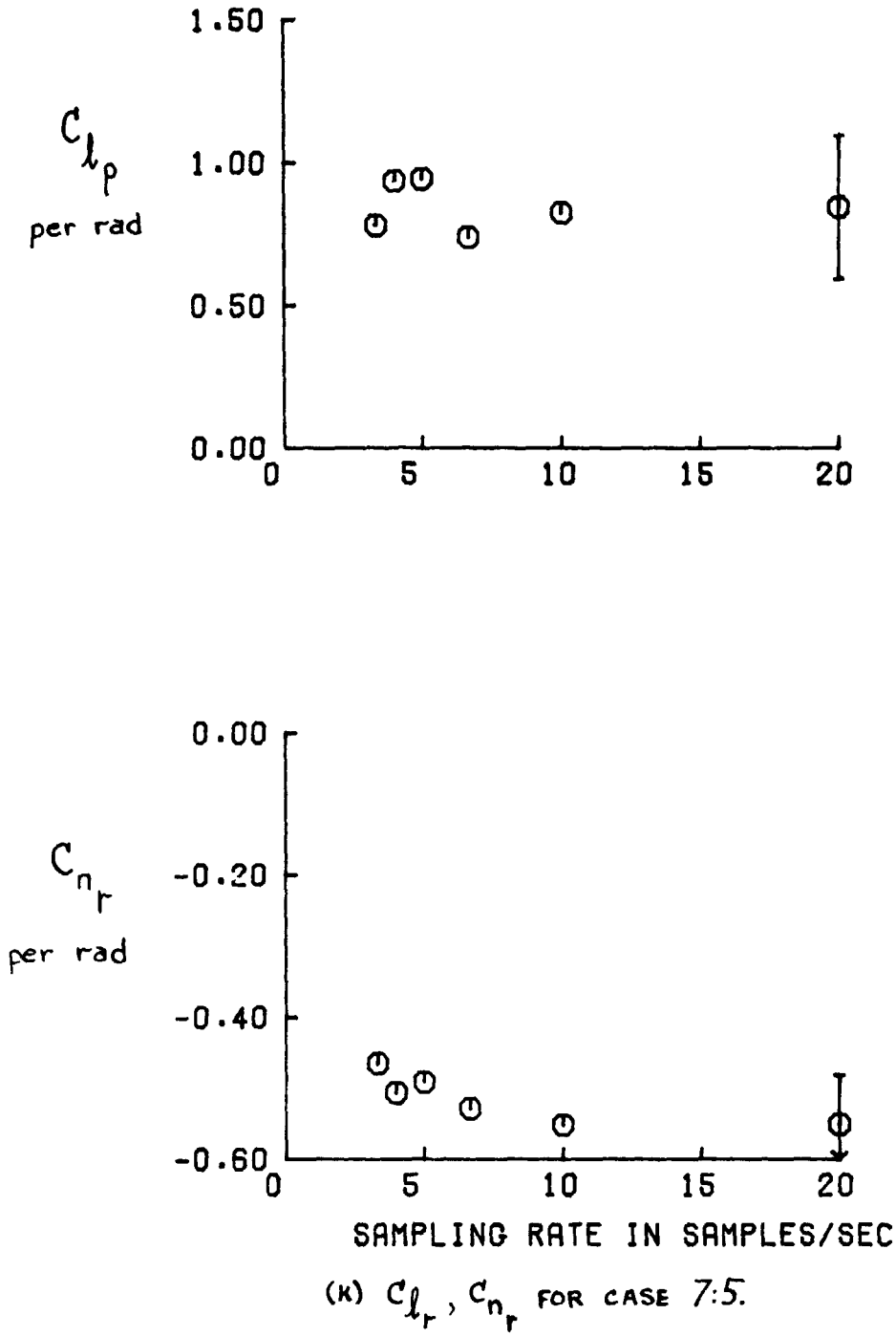

(K) C_{l_r}, C_{n_r} FOR CASE 7:5.

Figure 12. Continued.

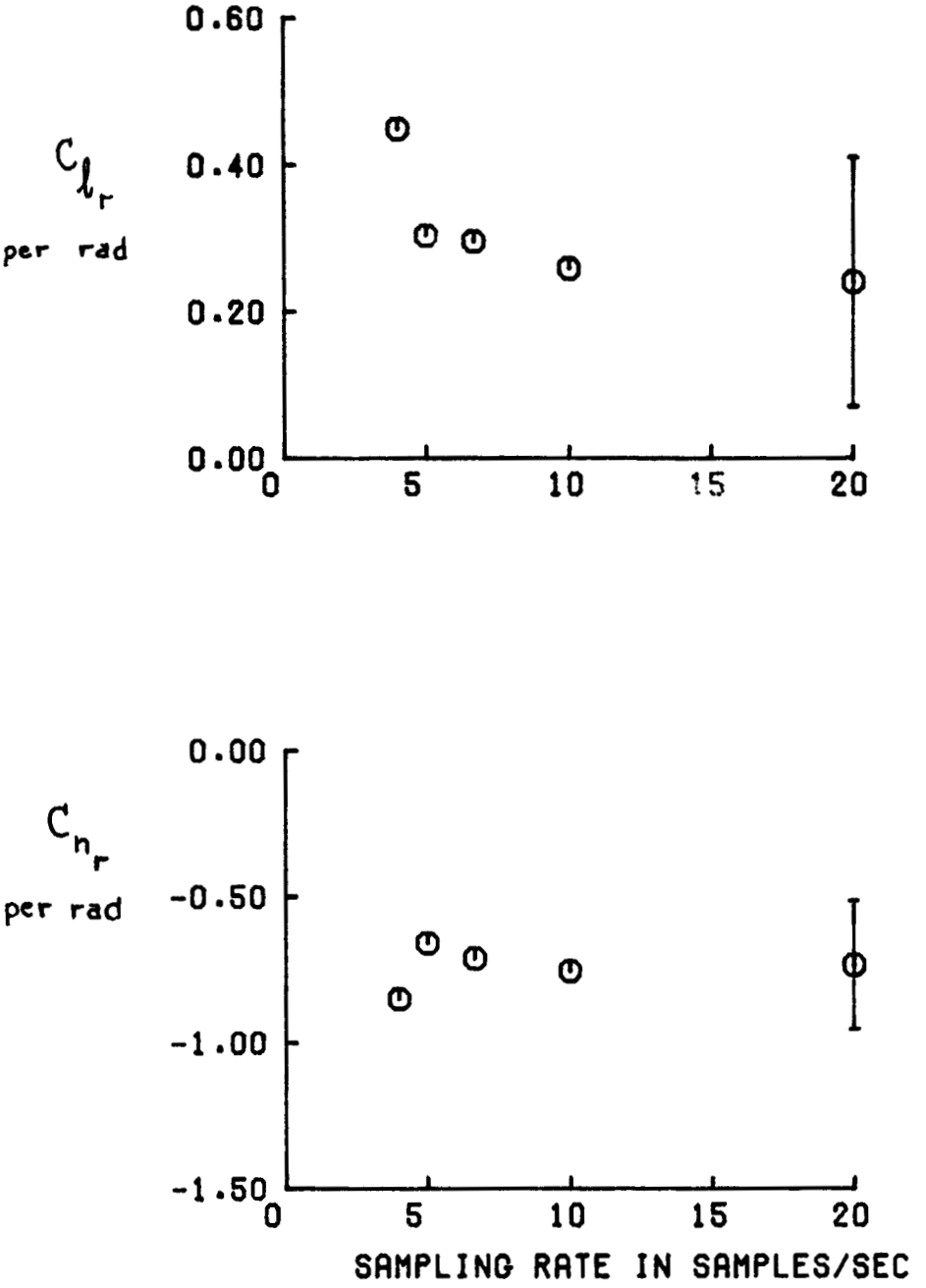

(l.) C_{l_r}, C_{n_r} FOR CASE 7.6.

Figure 12. Continued.

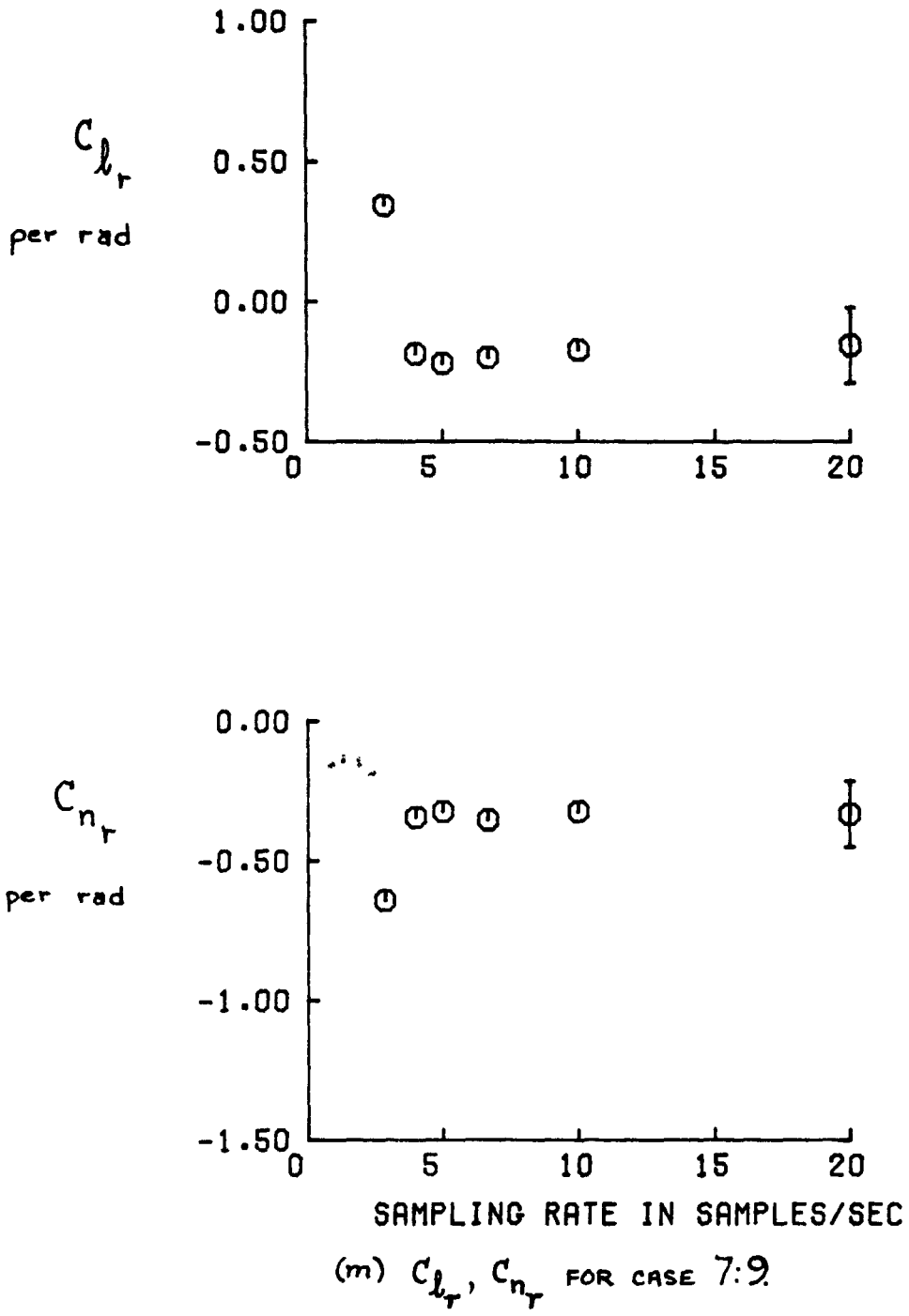

(m) C_{l_r}, C_{n_r} FOR CASE 7:9

Figure 12. Continued.

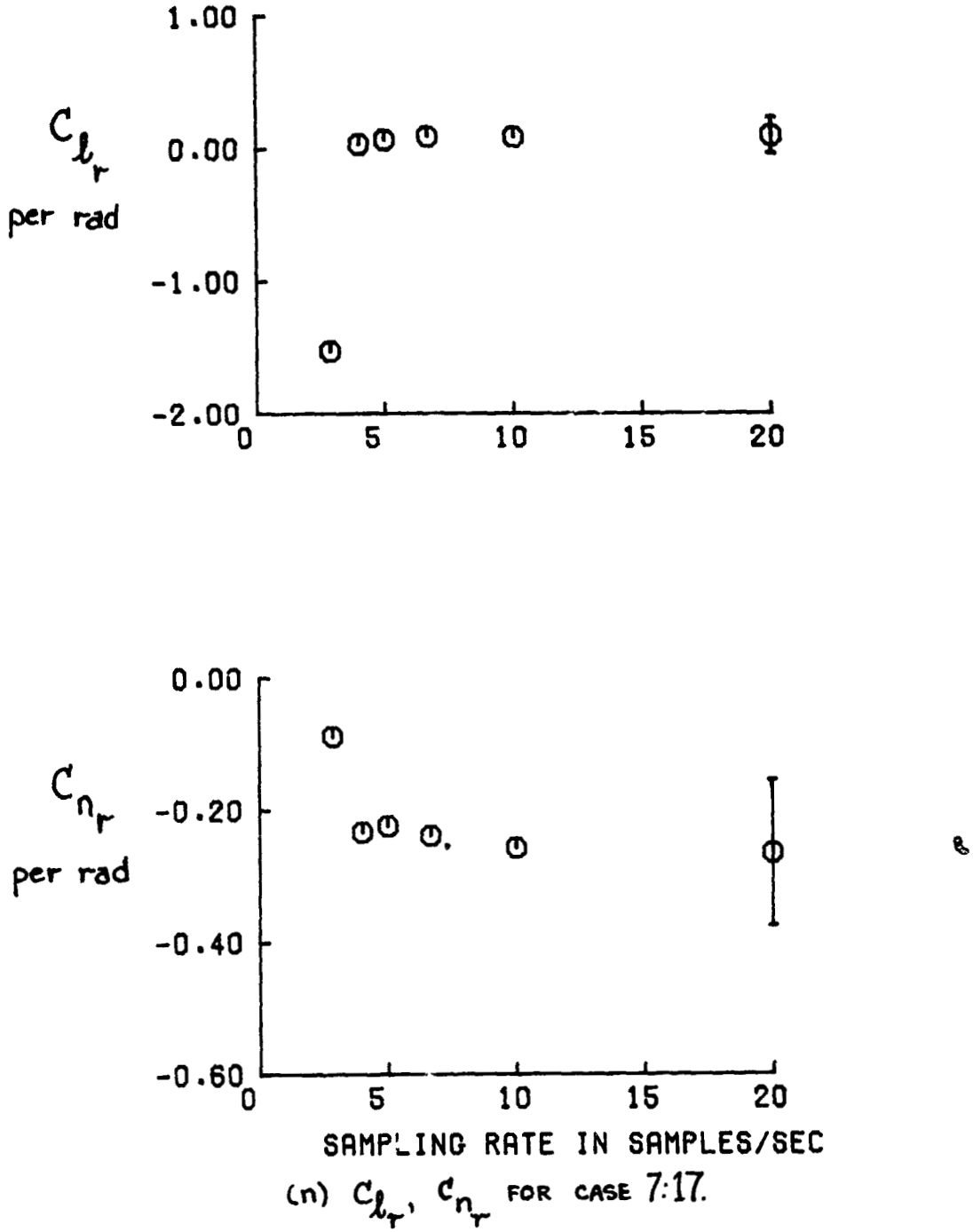

(n) C_{l_r}, C_{n_r} FOR CASE 7:17.

Figure 12. Continued.

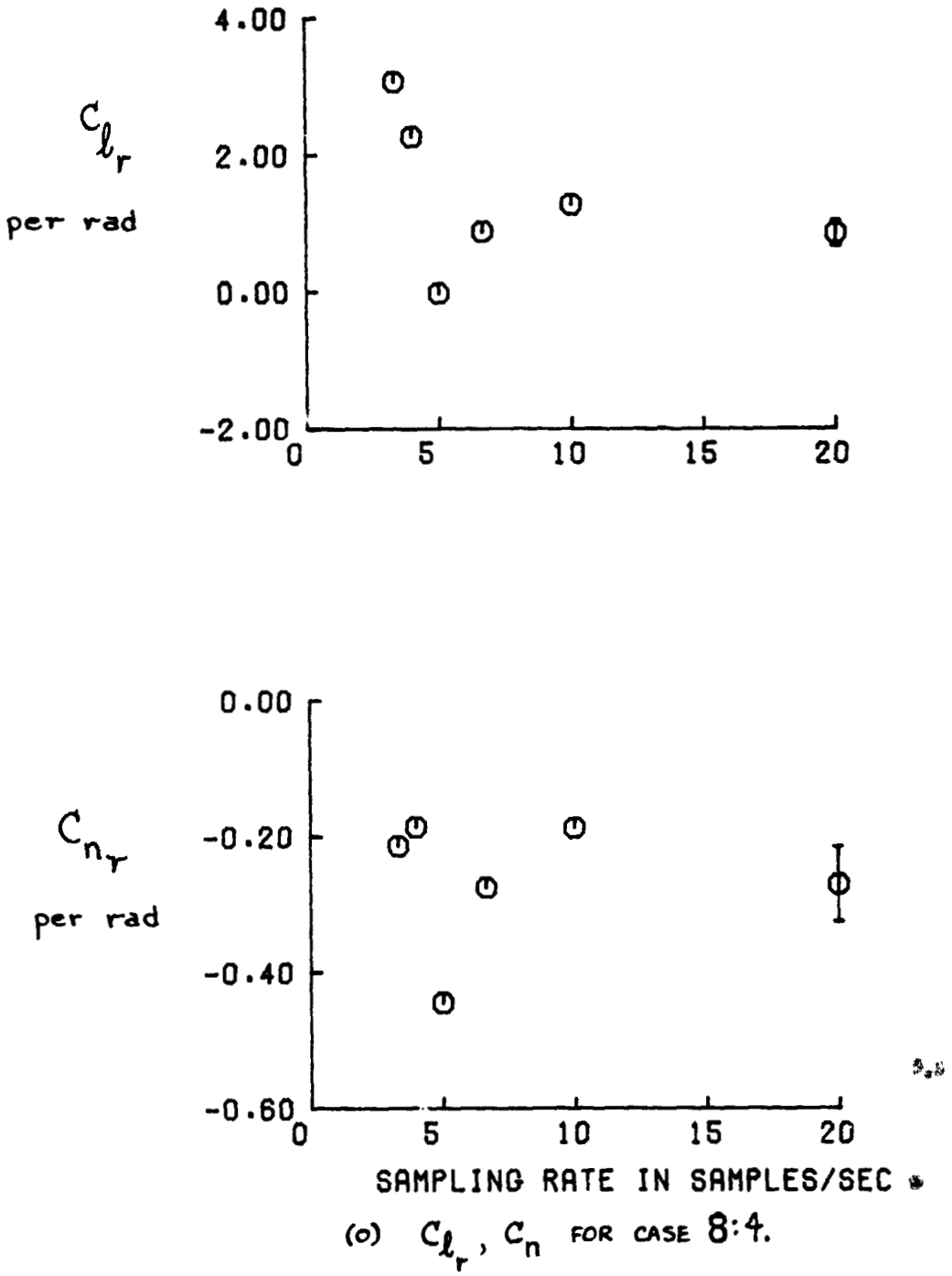

(o) C_{l_r}, C_n FOR CASE 8:4.

Figure 12. Continued.

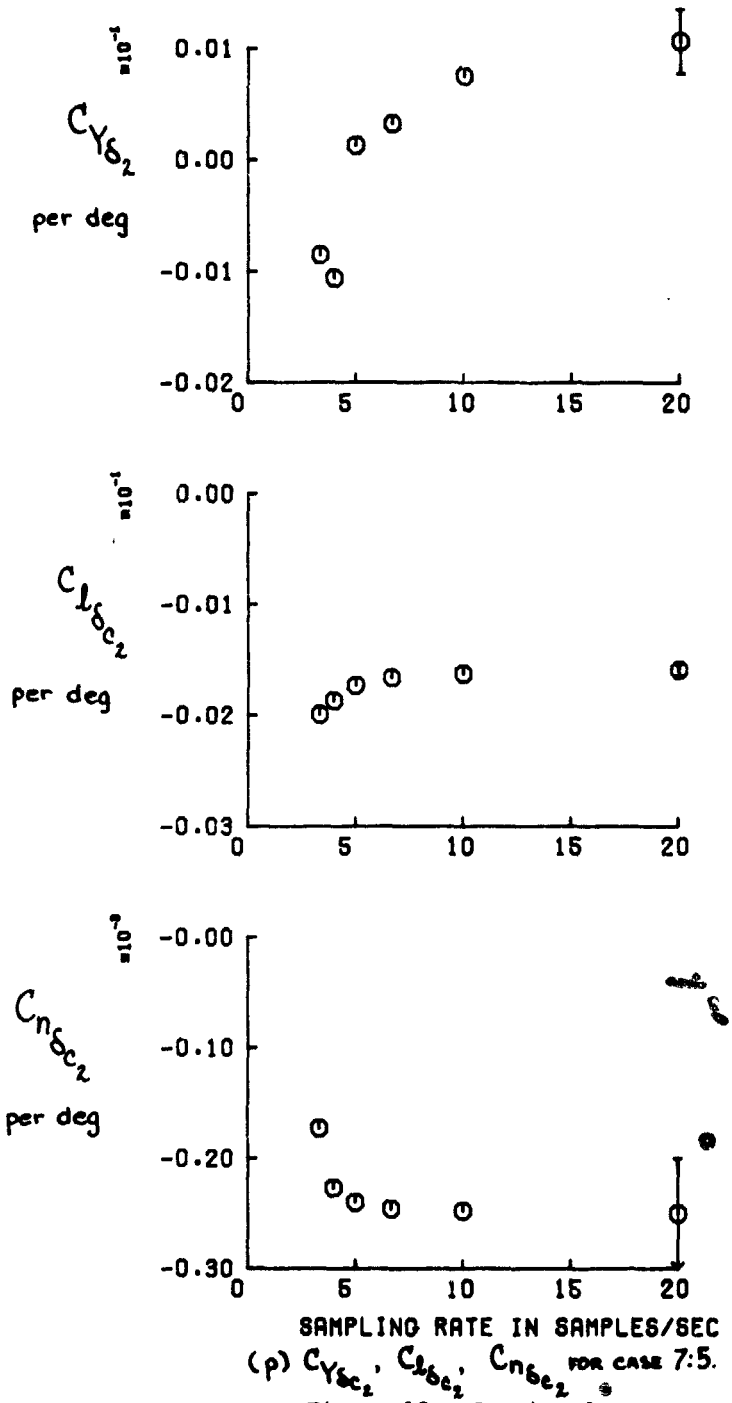

(ρ) $C_{Y_{\delta_{c_2}}}$, $C_{l_{\delta_{c_2}}}$, $C_{n_{\delta_{c_2}}}$ FOR CASE 7:5.

Figure 12. Continued.

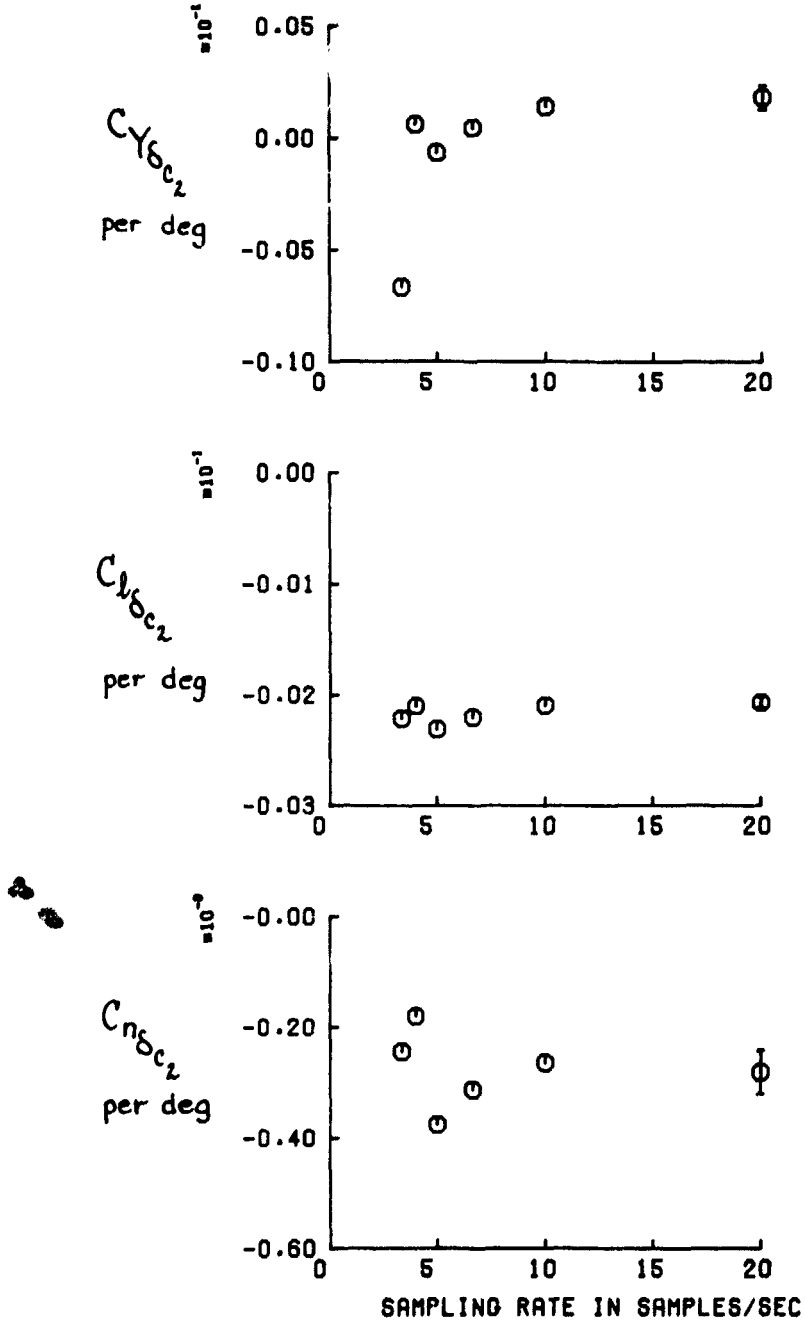

(q) $C_{Y_{\delta_{c_2}}}$, $C_{l_{\delta_{c_2}}}$, $C_{n_{\delta_{c_2}}}$ FOR CASE 7:6.

Figure 12. Continued.

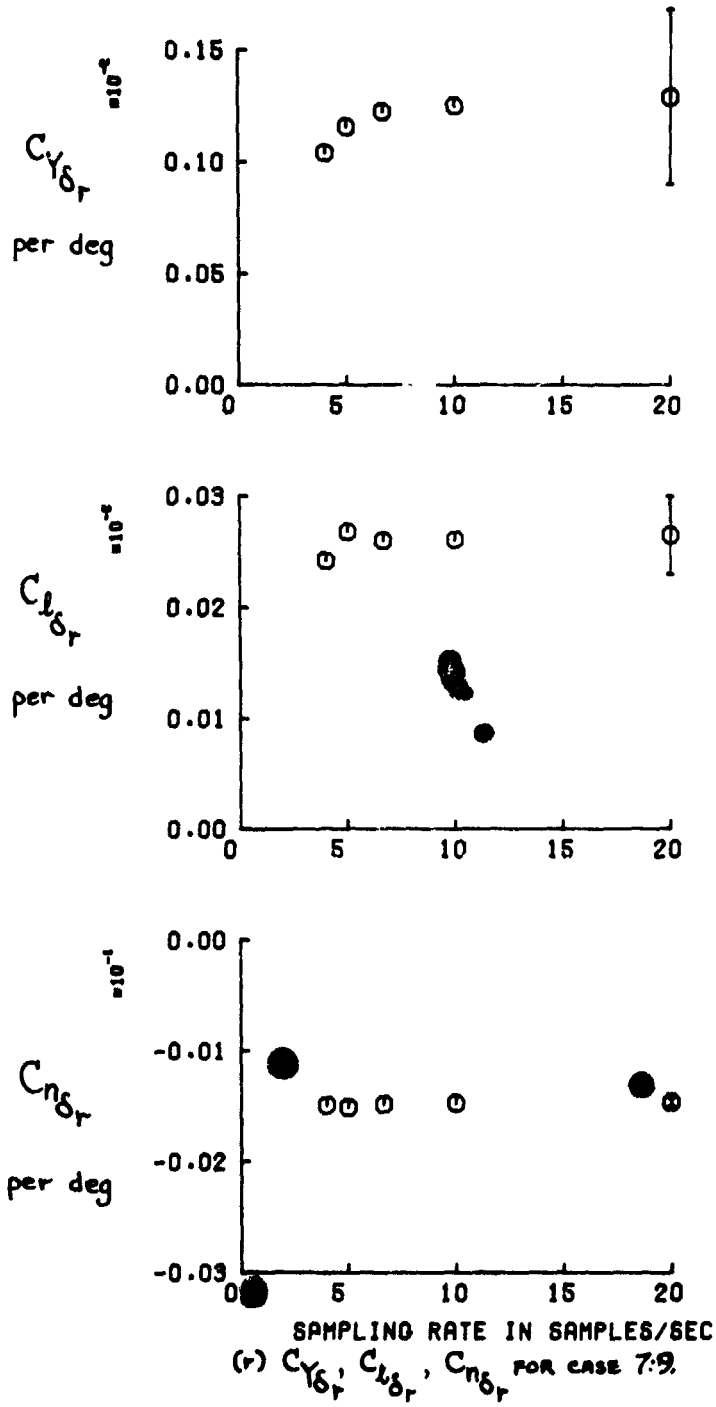

(r) $C_{Y_{\delta_r}}$, $C_{l_{\delta_r}}$, $C_{n_{\delta_r}}$ FOR CASE 7:9

Figure 12. Continued.

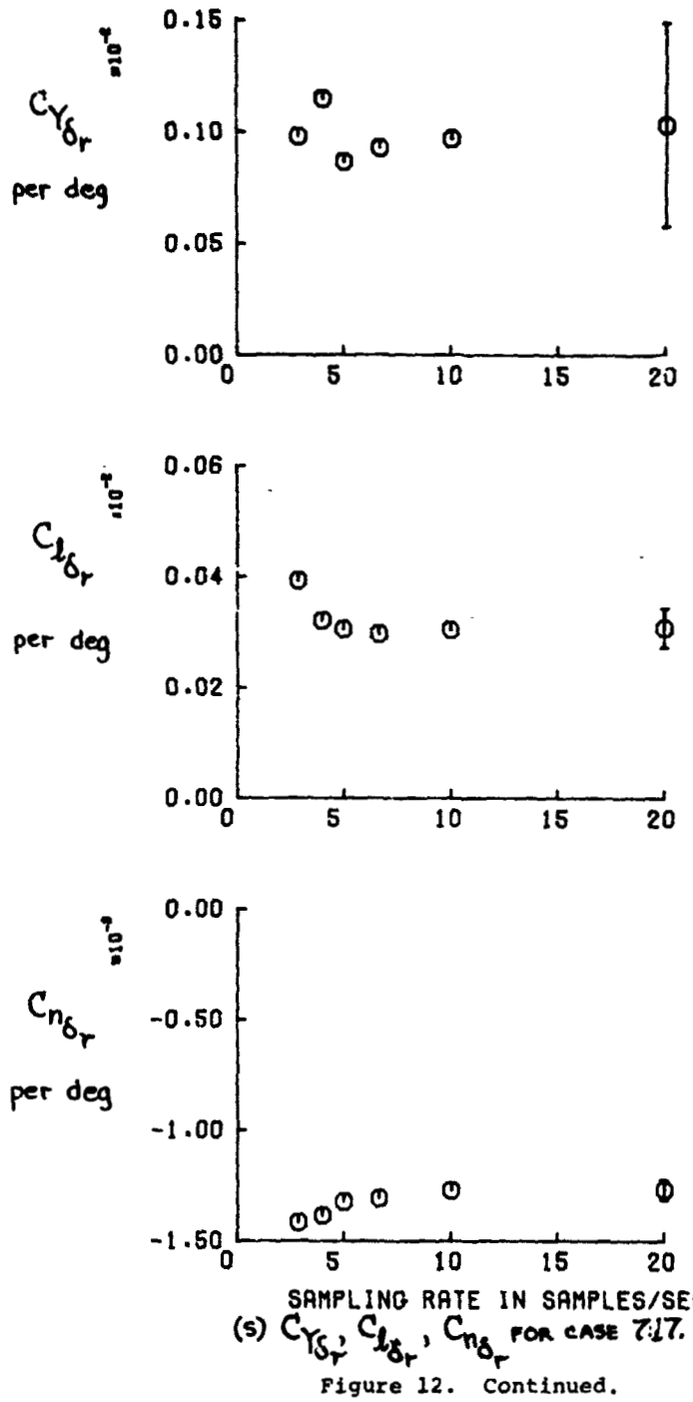

(s) $C_{Y_{\delta_r}}$, $C_{l_{\delta_r}}$, $C_{n_{\delta_r}}$ FOR CASE 7:17.

Figure 12. Continued.

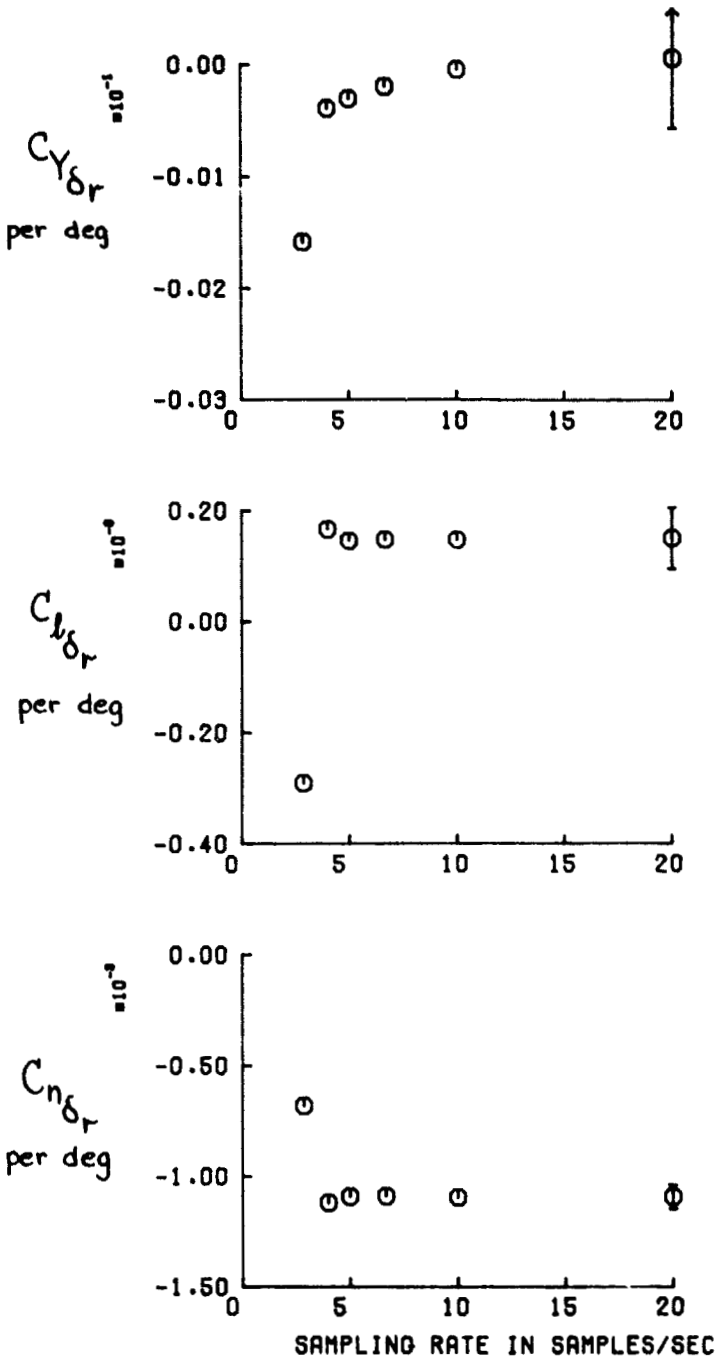

(t) $C_{Y_{\delta_r}}$, $C_{l_{\delta_r}}$, $C_{n_{\delta_r}}$ FOR CASE 8:4.

Figure 12. Concluded

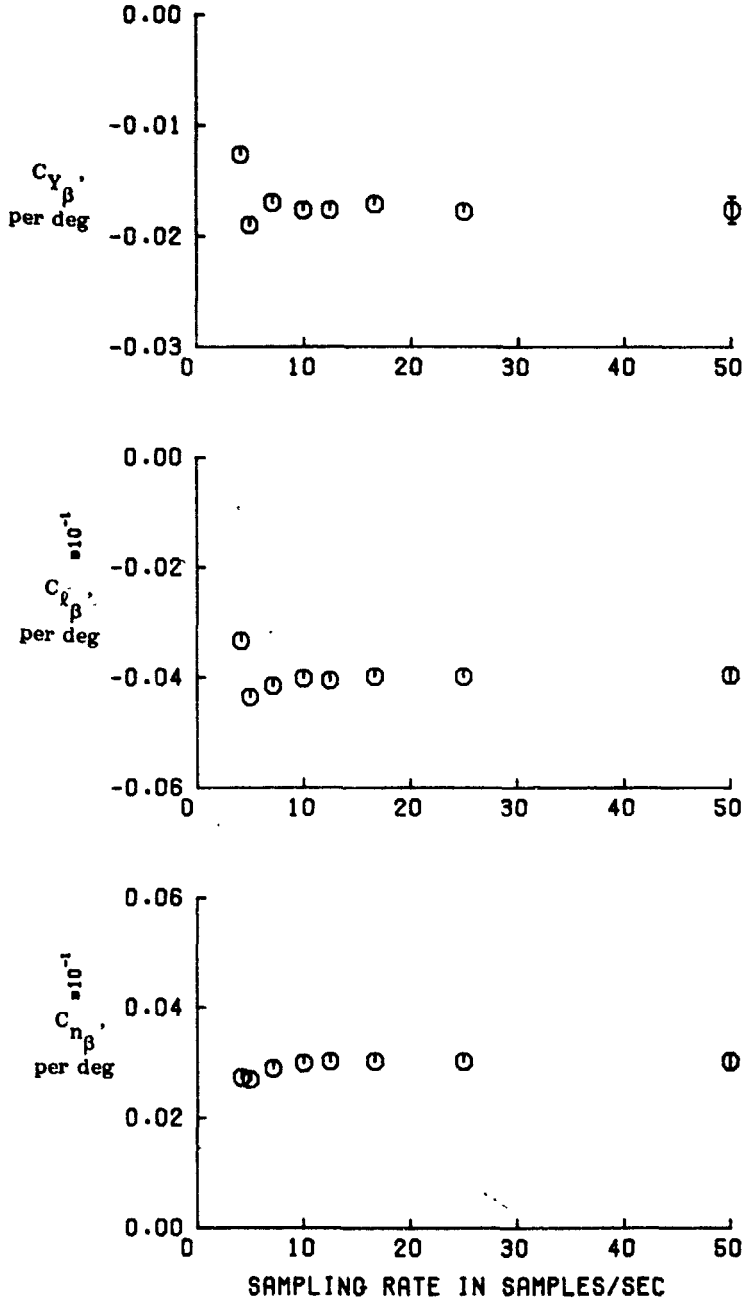

(a) C_{Y_β}, C_{ℓ_β}, C_{n_β}.

Figure 13. Estimated lateral-directional derivatives as a function of sampling rate. Aircraft E.

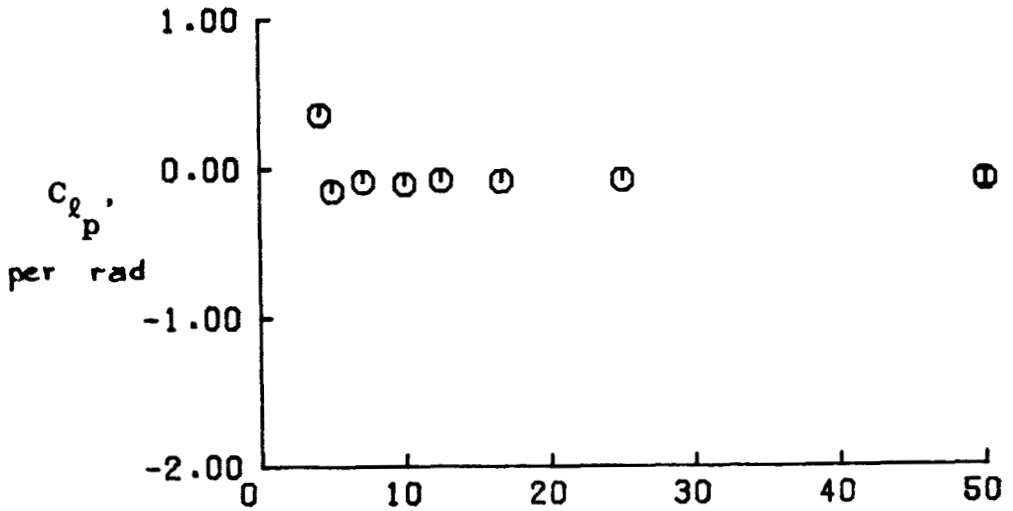

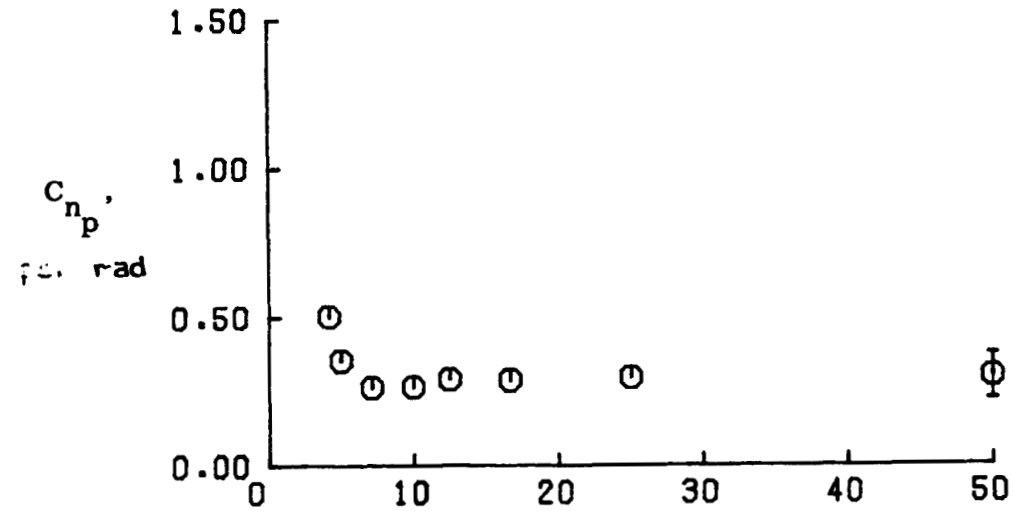

(b) C_{ℓ_p}, C_{n_p}.

Figure 13. Continued

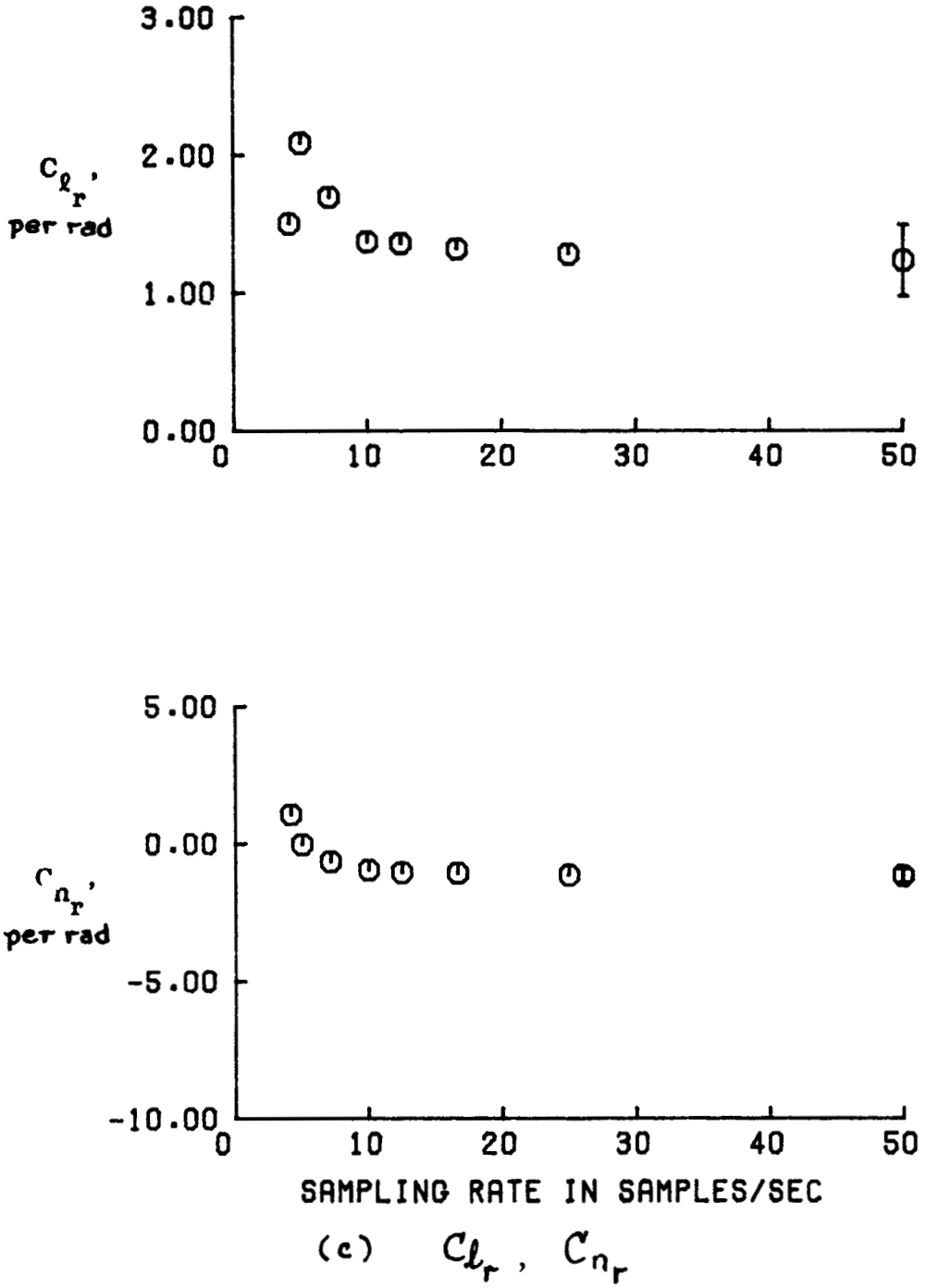

(c) $C\ell_r$, C_{n_r}

Figure 13. Continued.

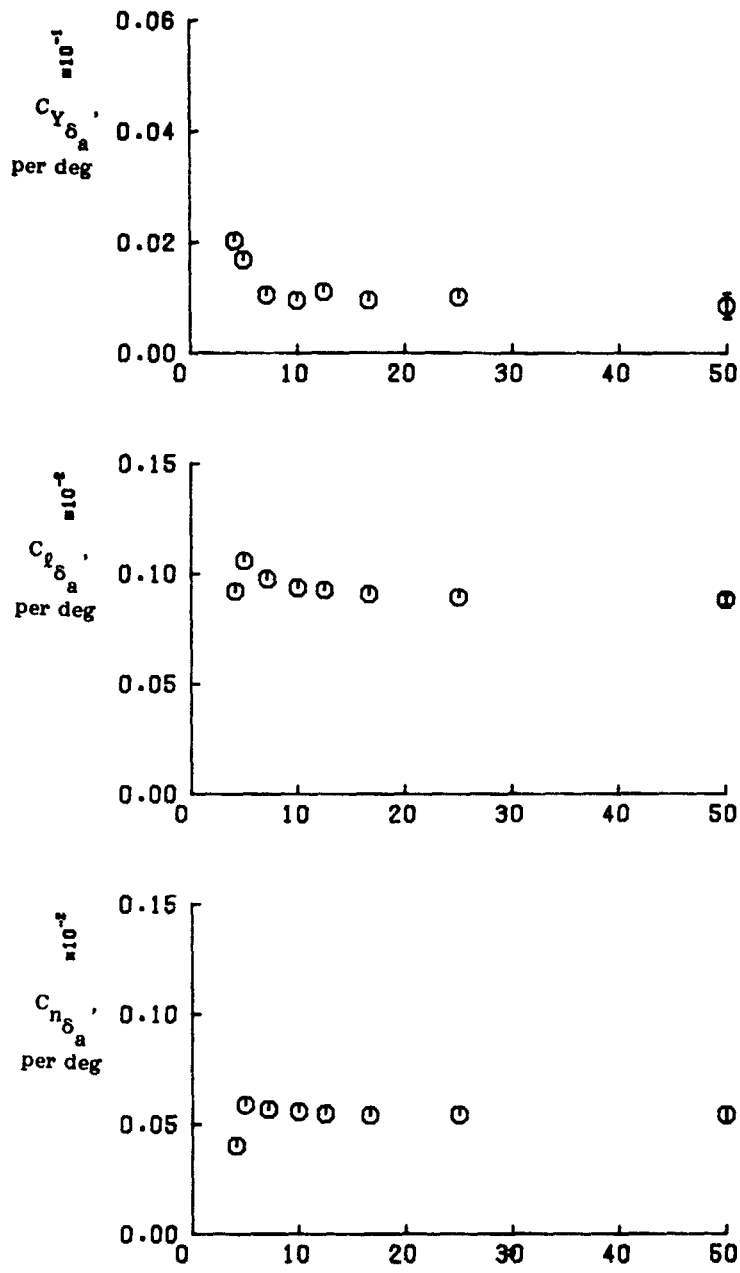

(d) $C_{Y_{\delta_a}}$, $C_{\ell_{\delta_a}}$, $C_{n_{\delta_a}}$.

Figure 13. Continued.

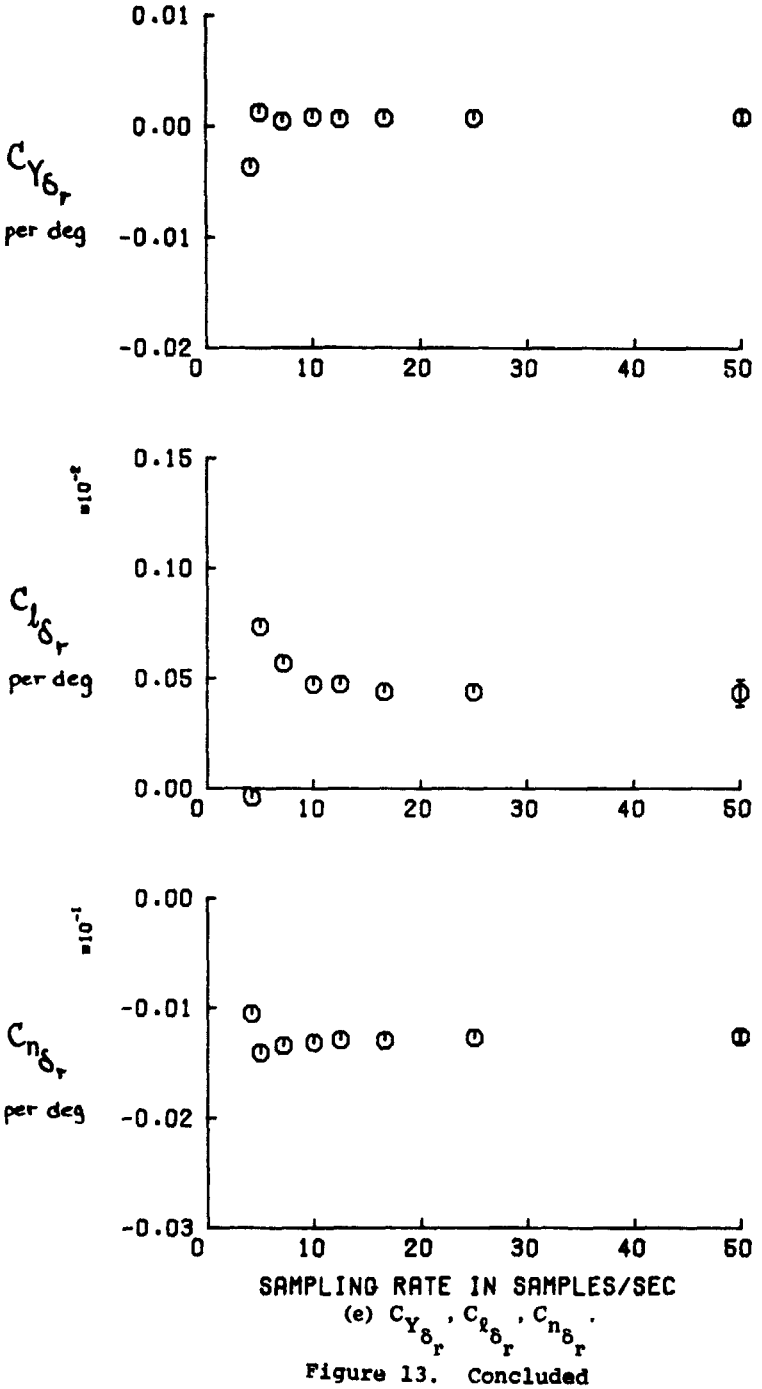

(e) $C_{Y_{\delta_r}}$, $C_{\ell_{\delta_r}}$, $C_{n_{\delta_r}}$.

Figure 13. Concluded

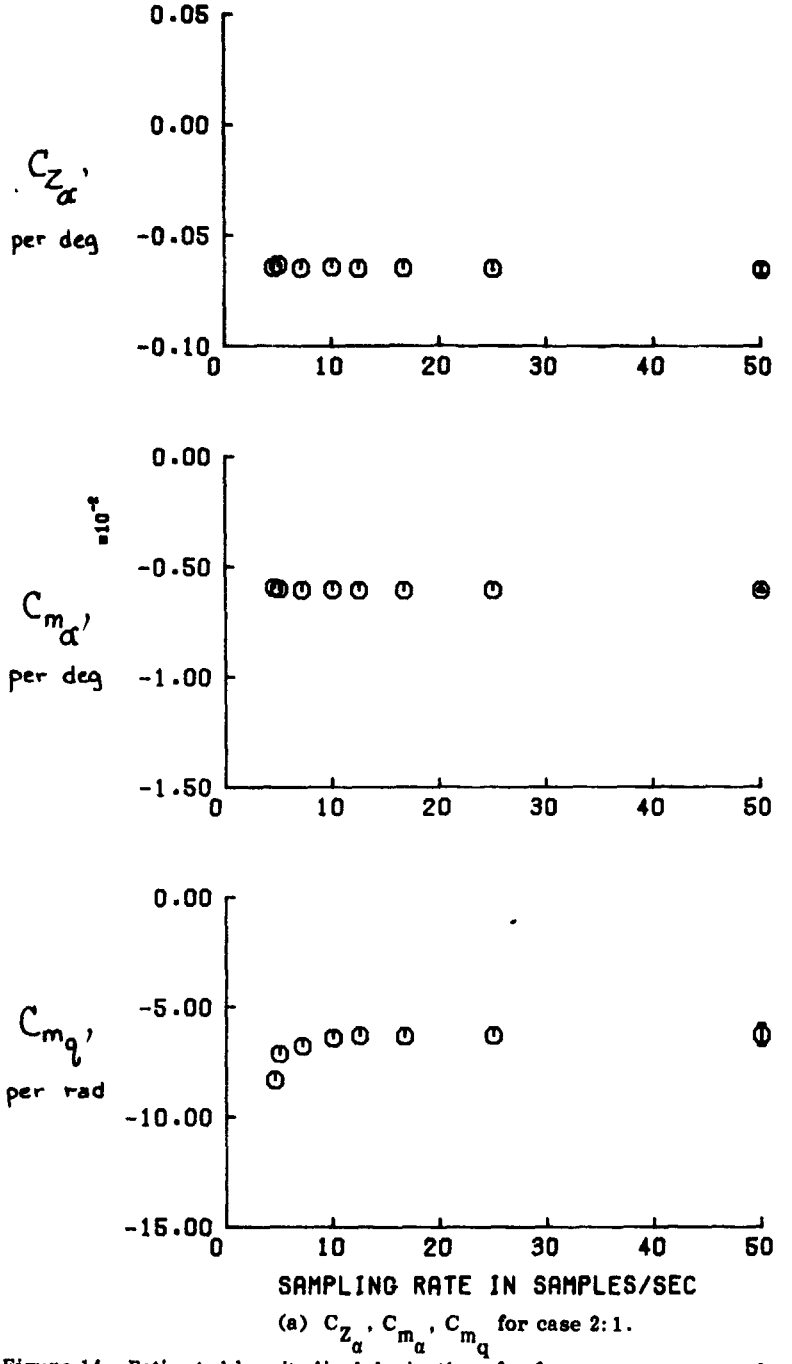

(a) C_{Z_α}, C_{m_α}, C_{m_q} for case 2:1.

Figure 14. Estimated longitudinal derivatives for four maneuvers as a function of sampling rate. Aircraft B.

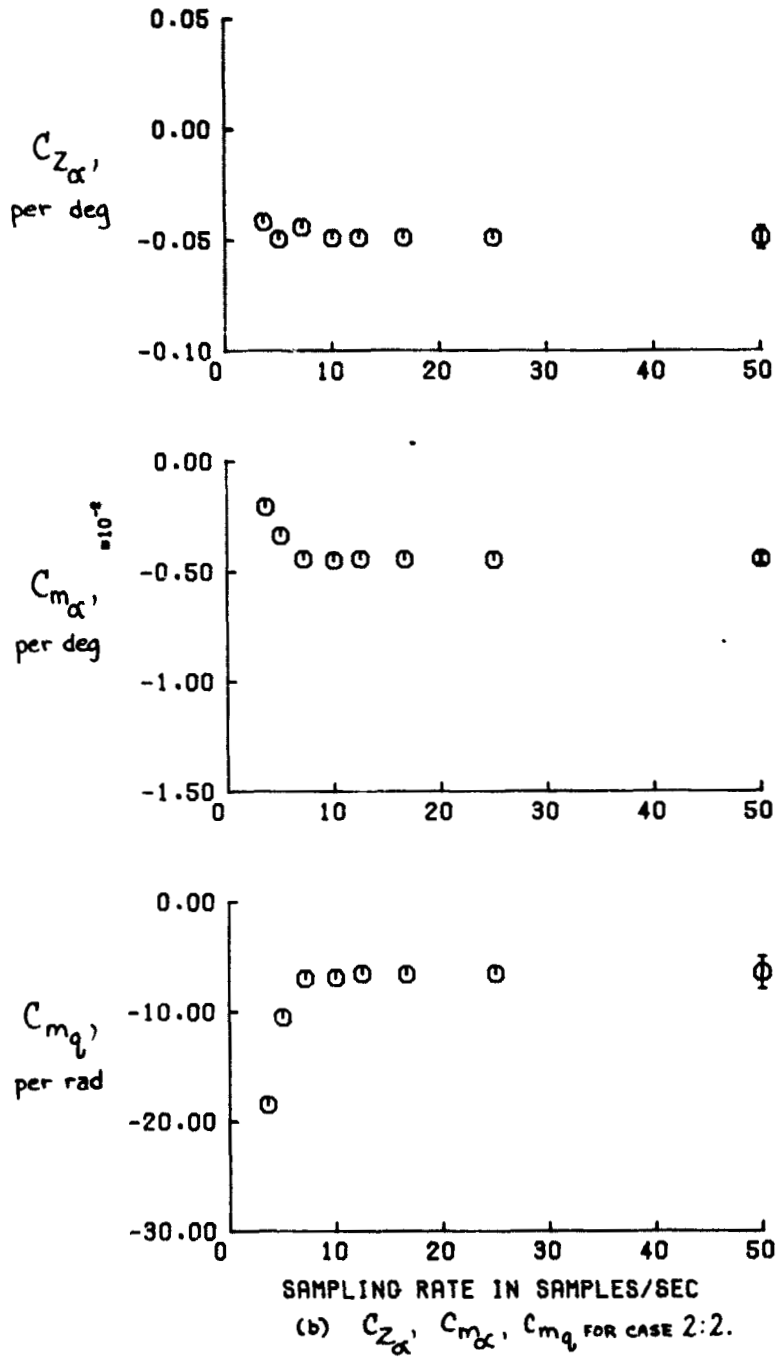

(b) C_{Z_α}, C_{m_α}, C_{m_q} FOR CASE 2:2.

Figure 14. Continued

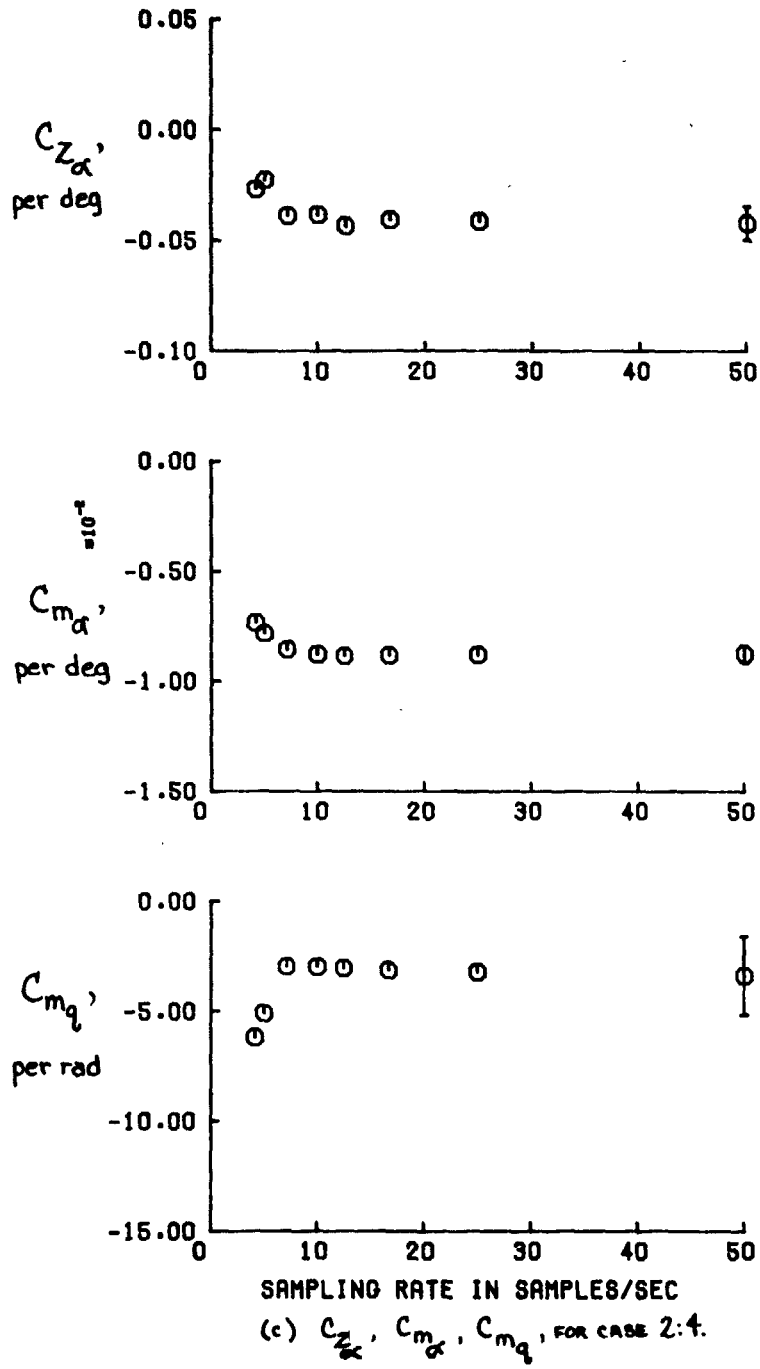

(c) $C_{Z_{\delta_e}}$, C_{m_α}, C_{m_q}, FOR CASE 2:4.

Figure 14. Continued.

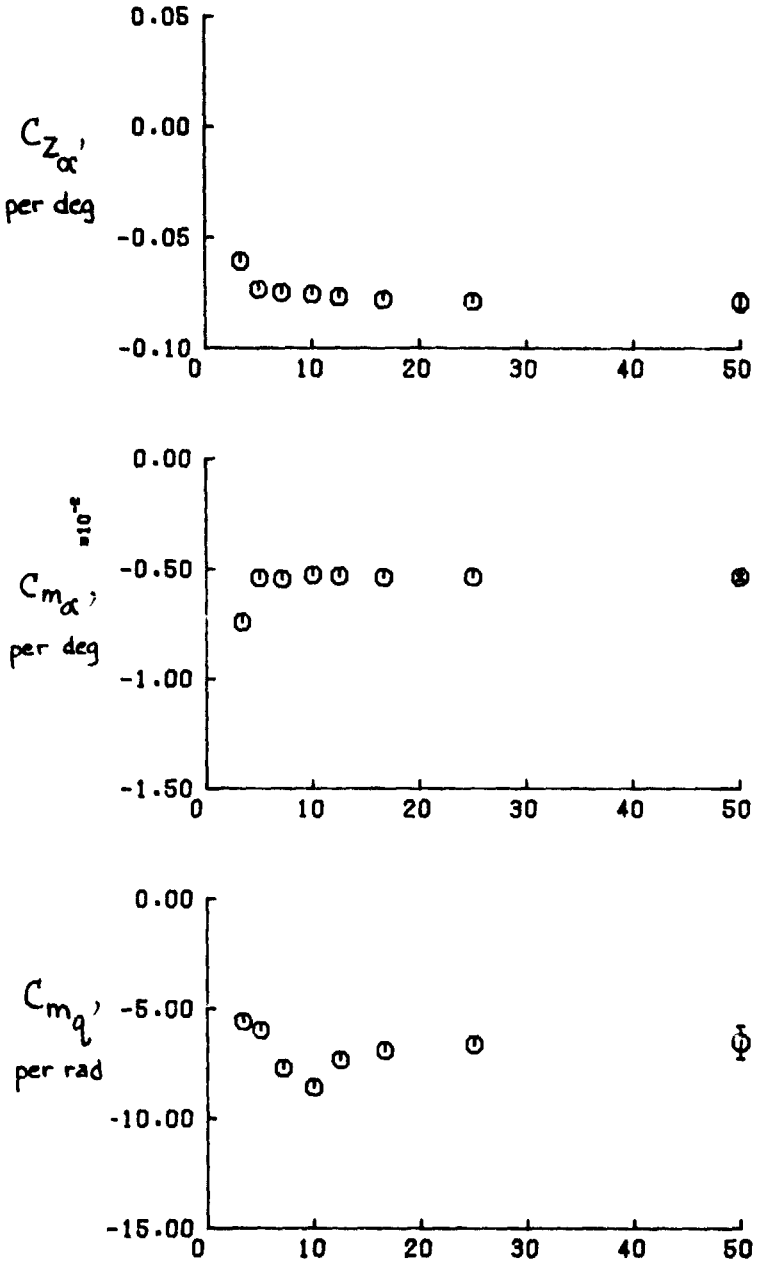

(d) C_{Z_α}, C_{m_α}, C_{m_q} FOR CASE 5:1A.

Figure 14. Continued.

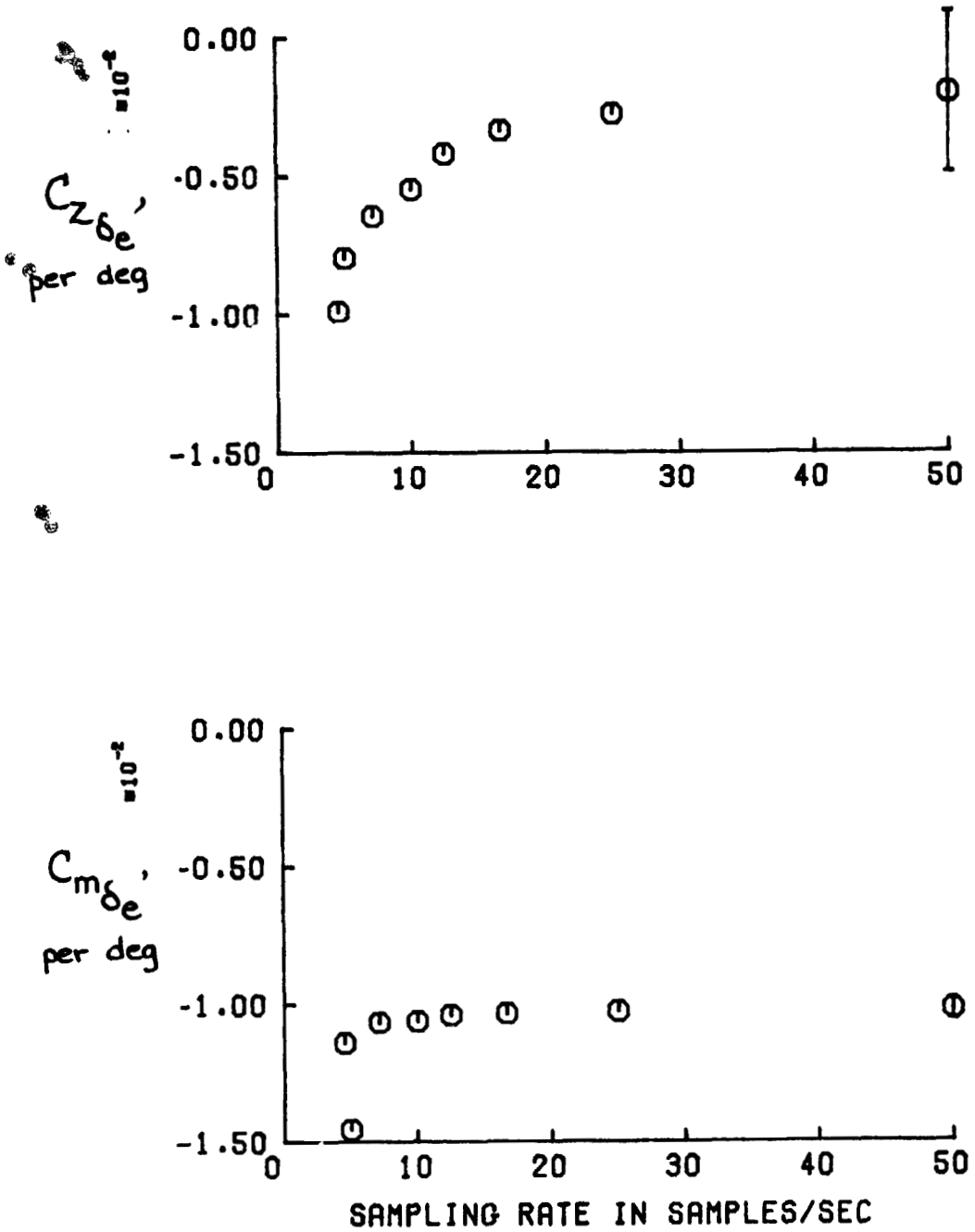

(e) $C_{Z_{\delta_e}}$, $C_{m_{\delta_e}}$ for case 2:1.

Figure 14. Continued.

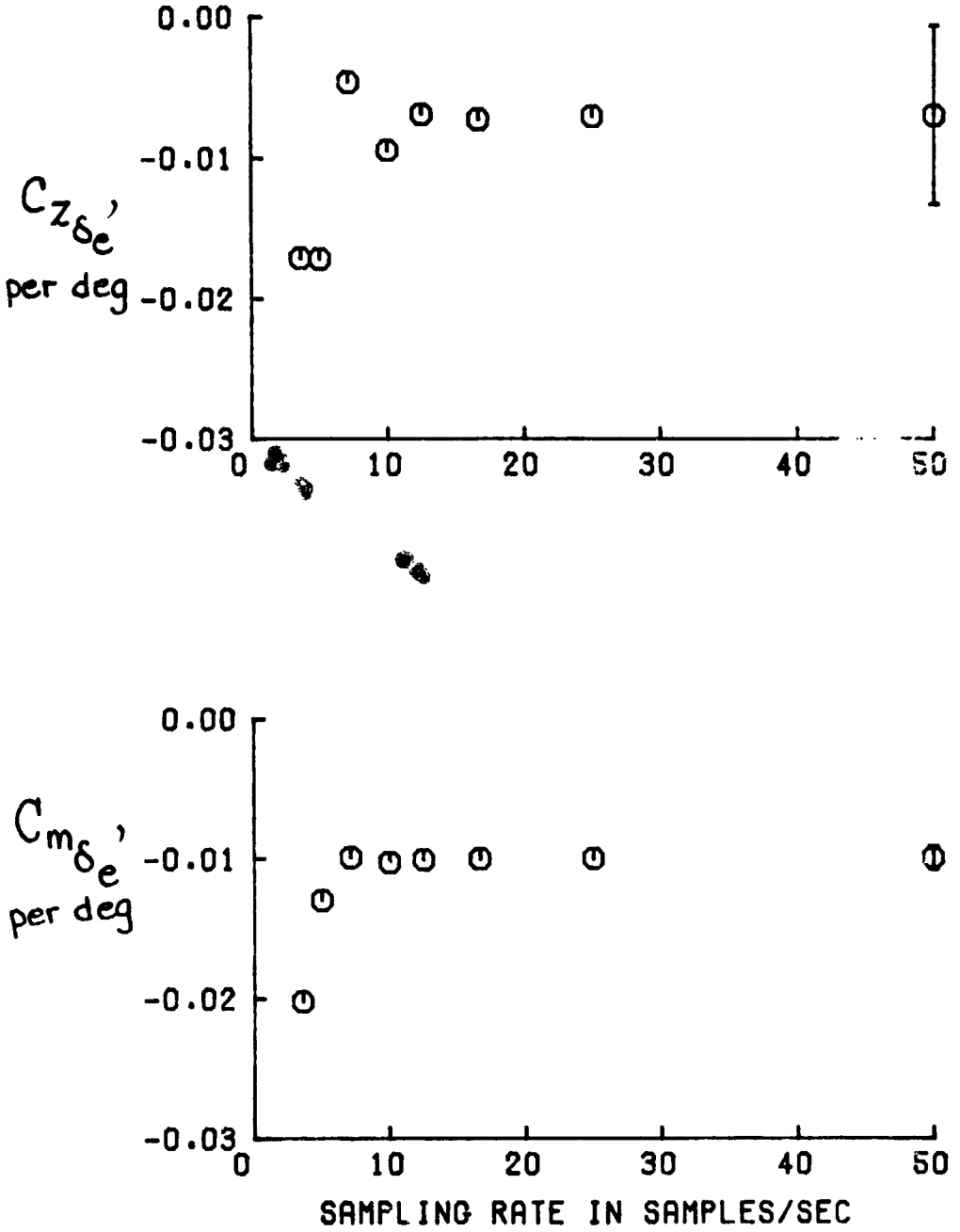

(f) $C_{Z_{\delta_e}}$, $C_{m_{\delta_e}}$ for case 2:2.

Figure 14. Continued.

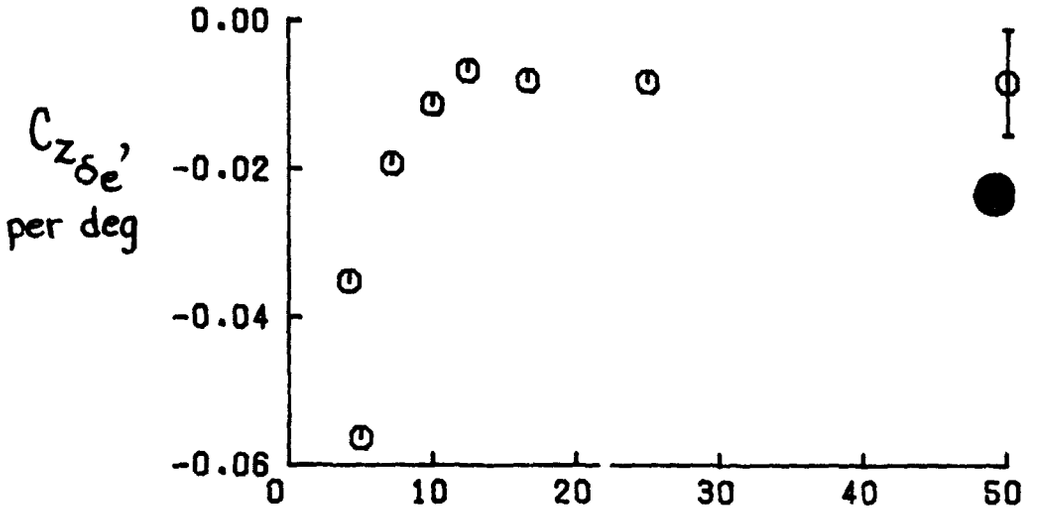

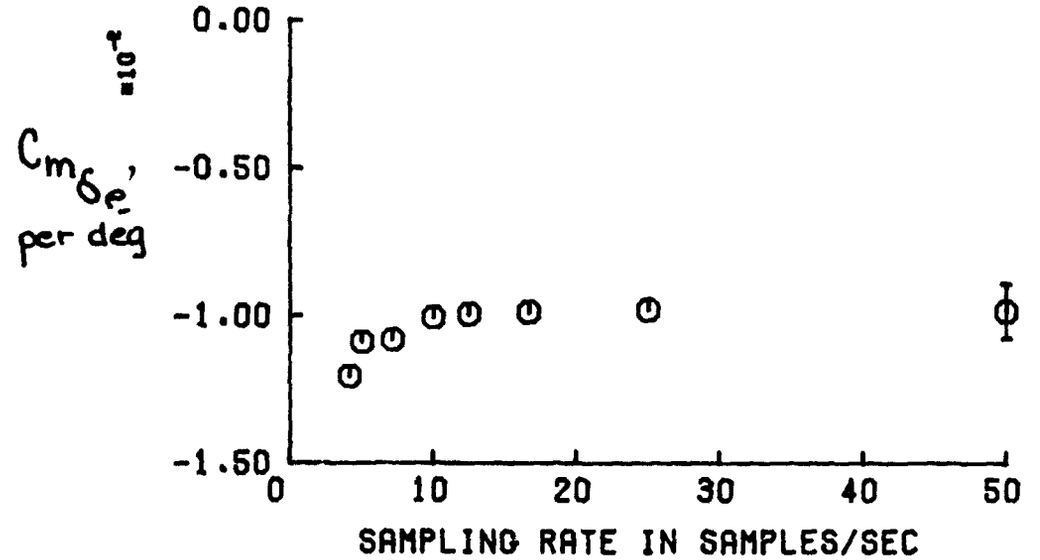

(g) $C_{Z_{\delta_e}}$, $C_{m_{\delta_e}}$ for case 2:4.

Figure 14. Continued.

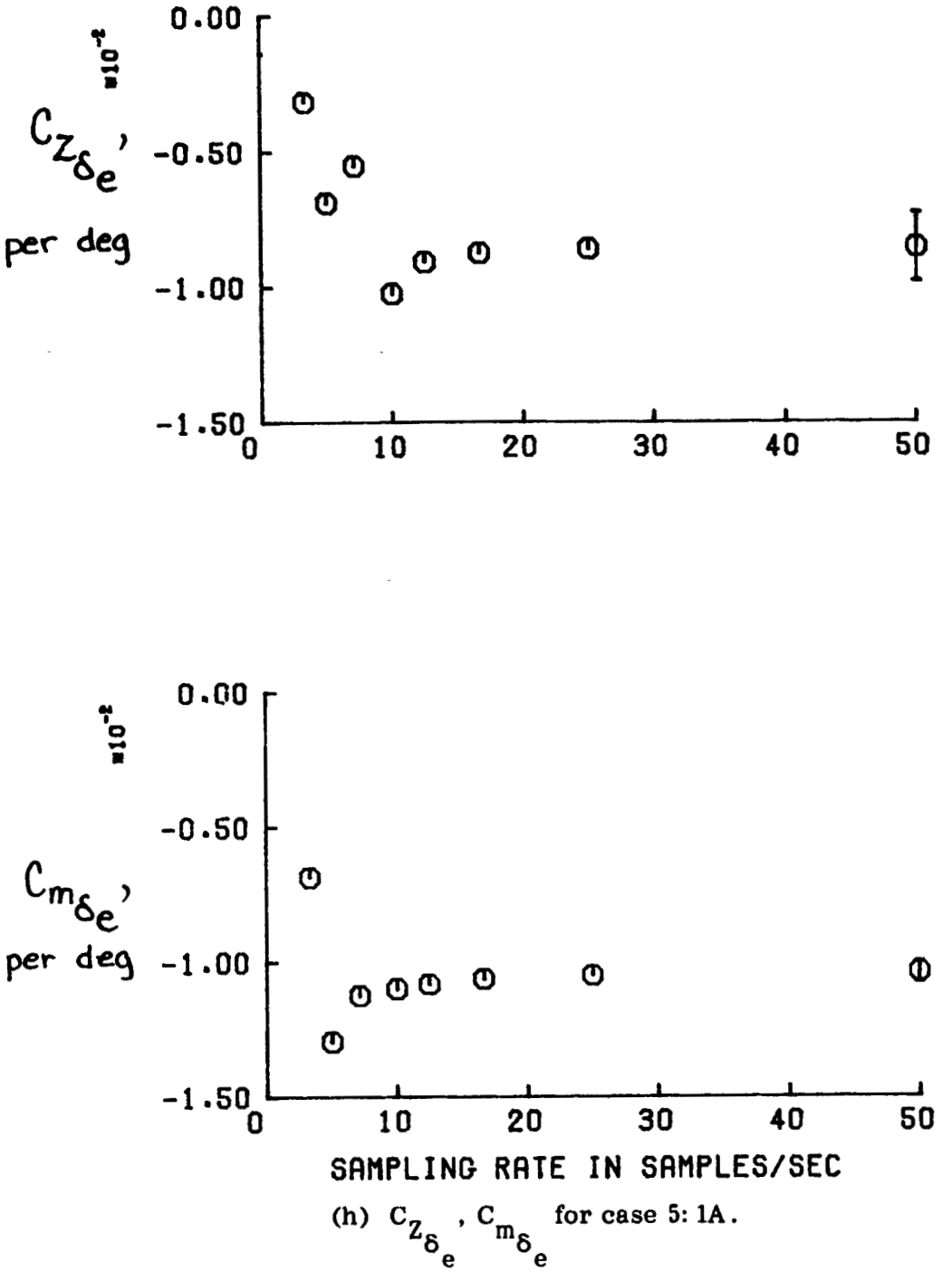

(h) $C_{Z_{\delta_e}}$, $C_{m_{\delta_e}}$ for case 5: 1A.

Figure 14. Concluded.

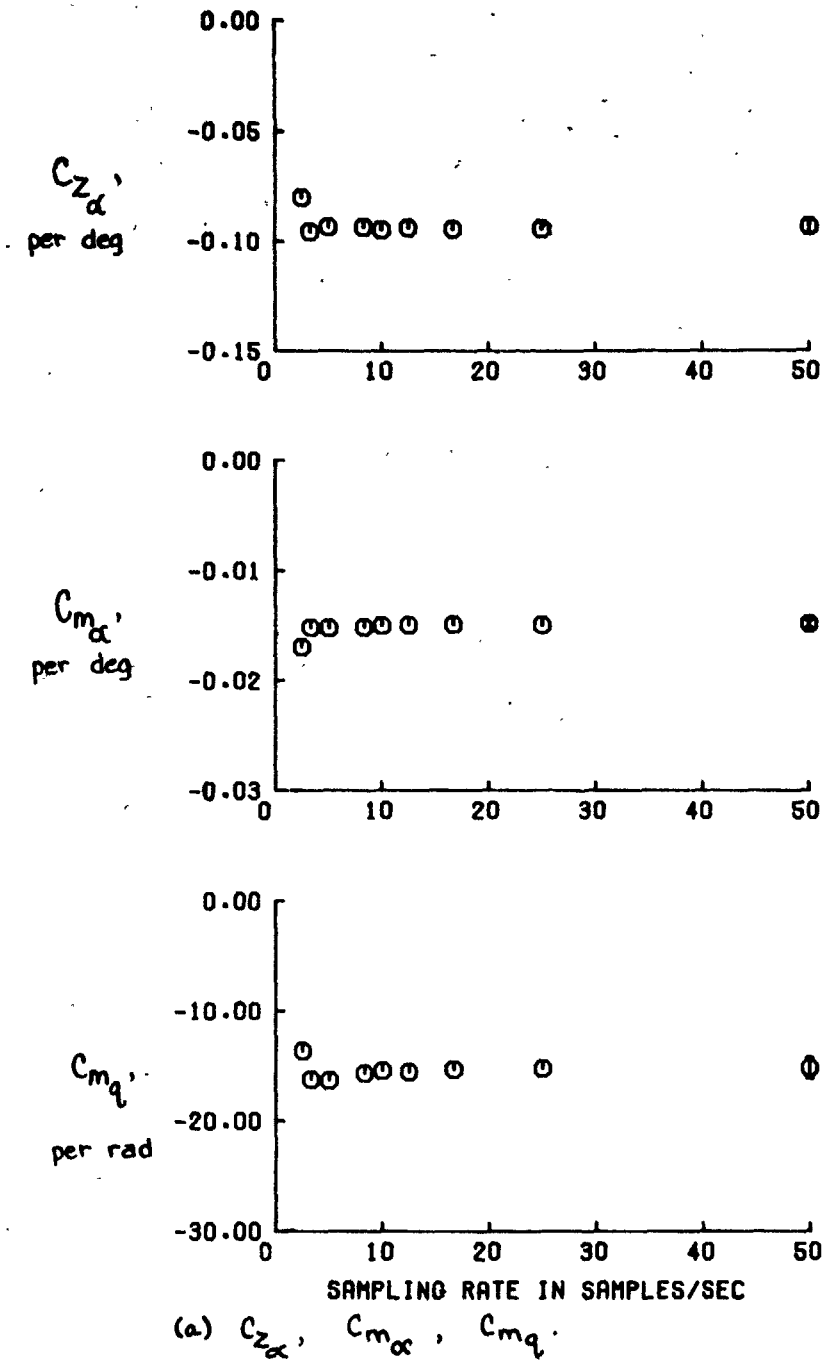

(a) C_{Z_α}, C_{m_α}, C_{m_q}.

Figure 15. Estimated longitudinal derivatives as a function of sampling rate. Aircraft C.

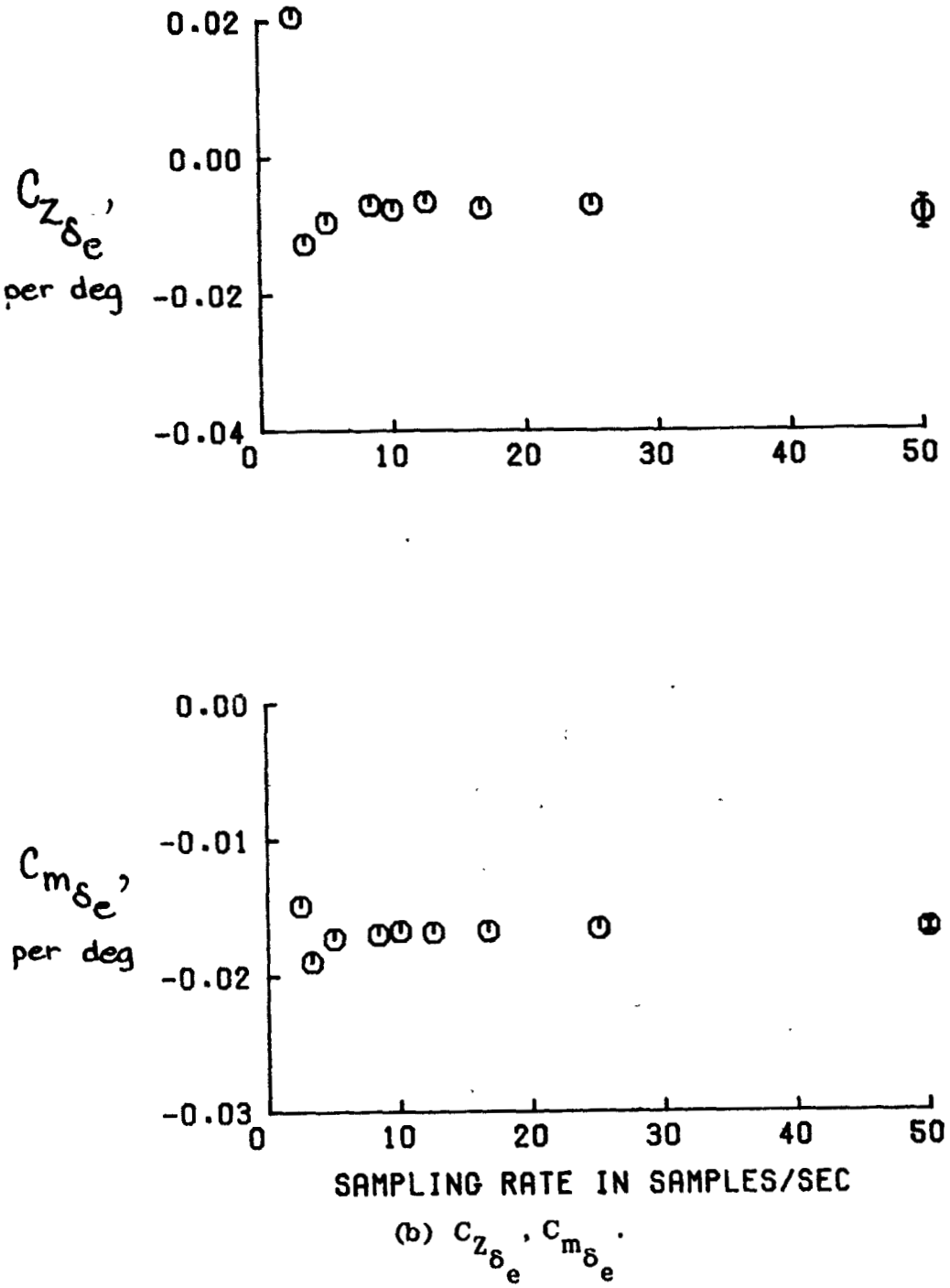

(b) $C_{Z_{\delta_e}}$, $C_{m_{\delta_e}}$.

Figure 15. Concluded

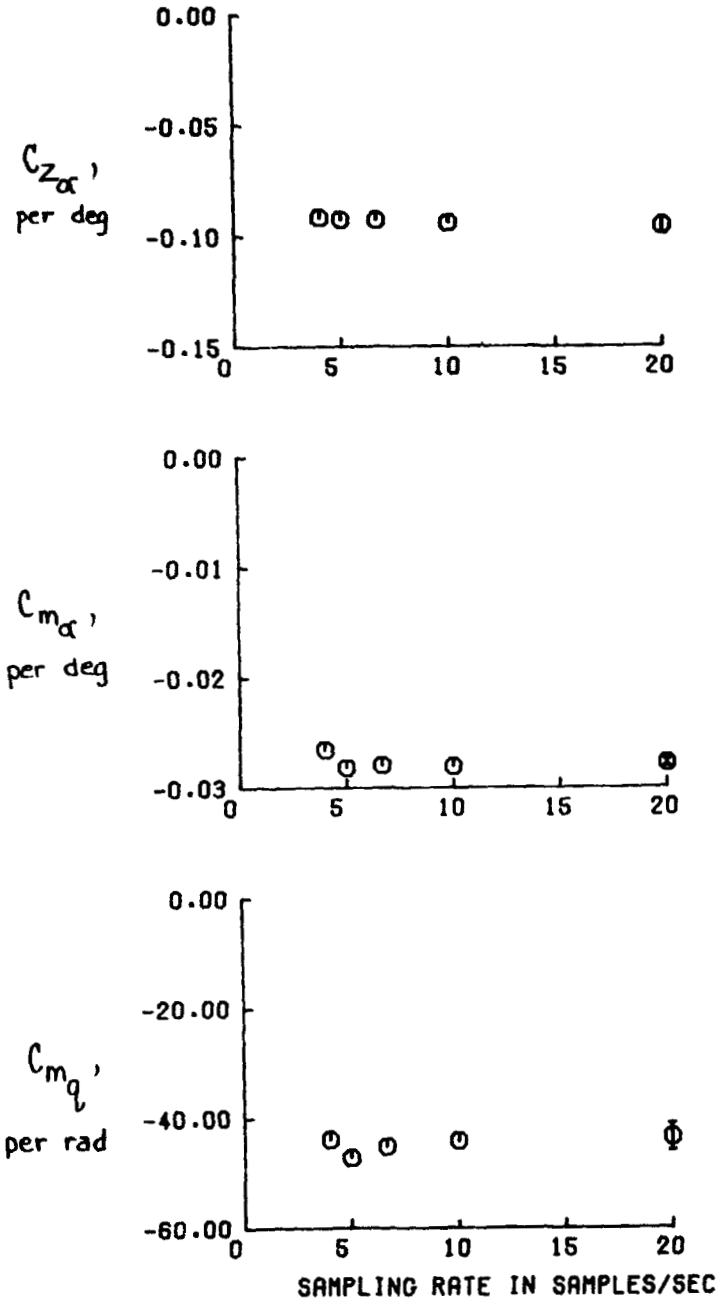

(a) C_{Z_α}, C_{m_α}, C_{m_q} FOR CASE 5:4.

Figure 16. Estimated longitudinal derivatives for four maneuvers as a function of sampling rate. Aircraft D.

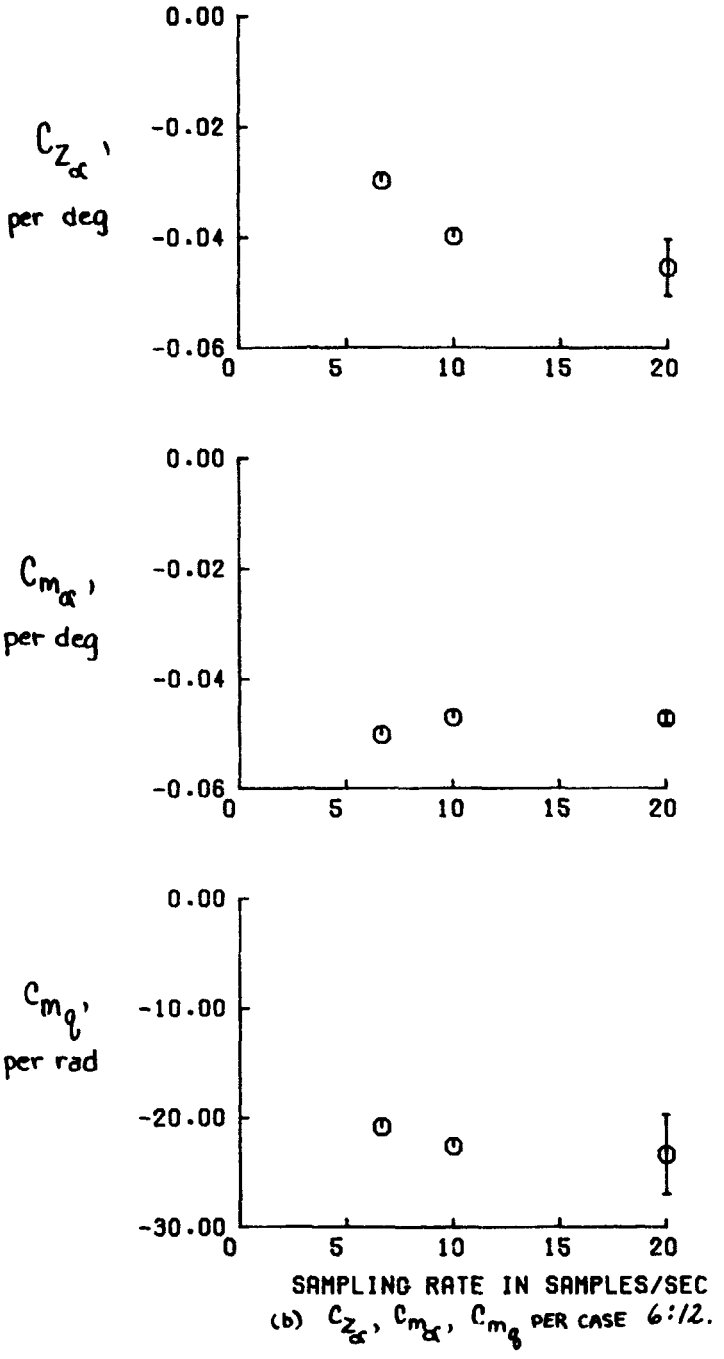

Figure 16. Continued

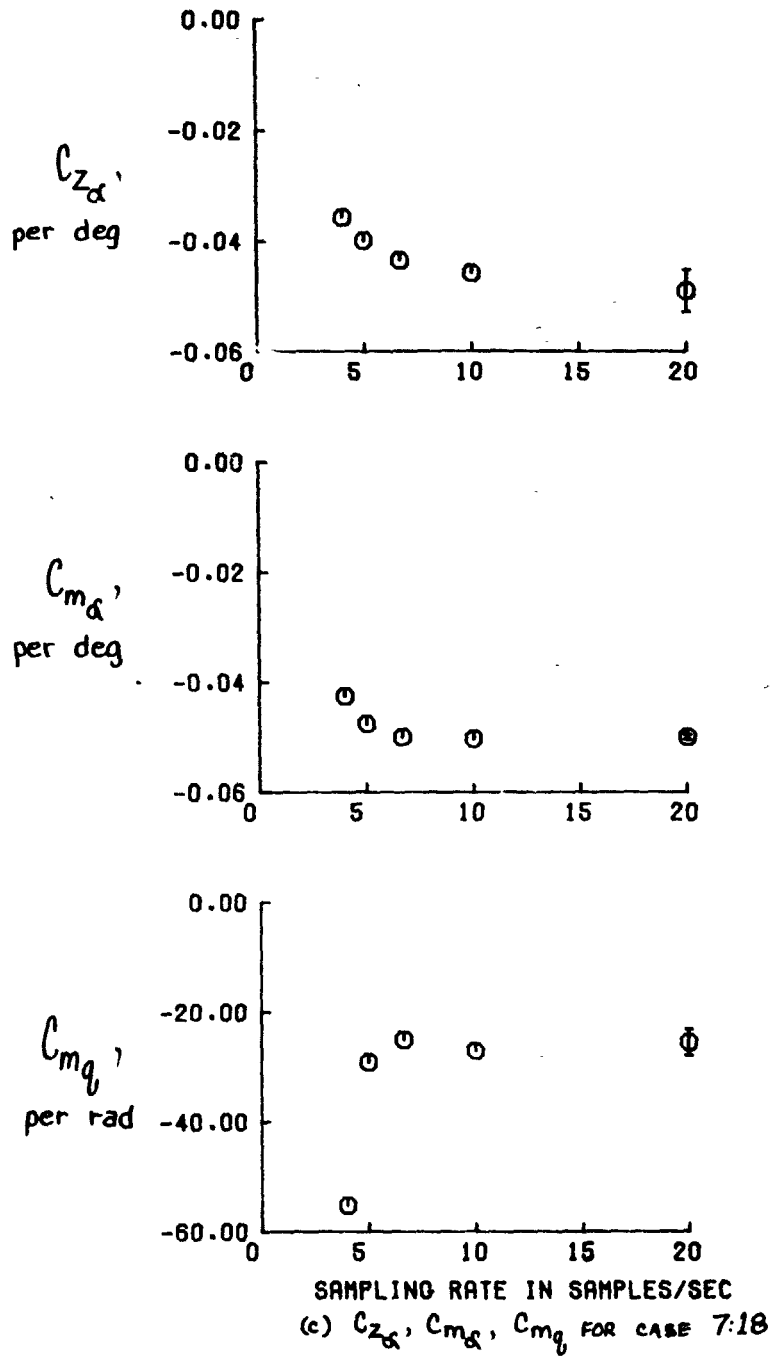

(c) C_{Z_α}, C_{m_α}, C_{m_q} FOR CASE 7:18

Figure 16. Continued.

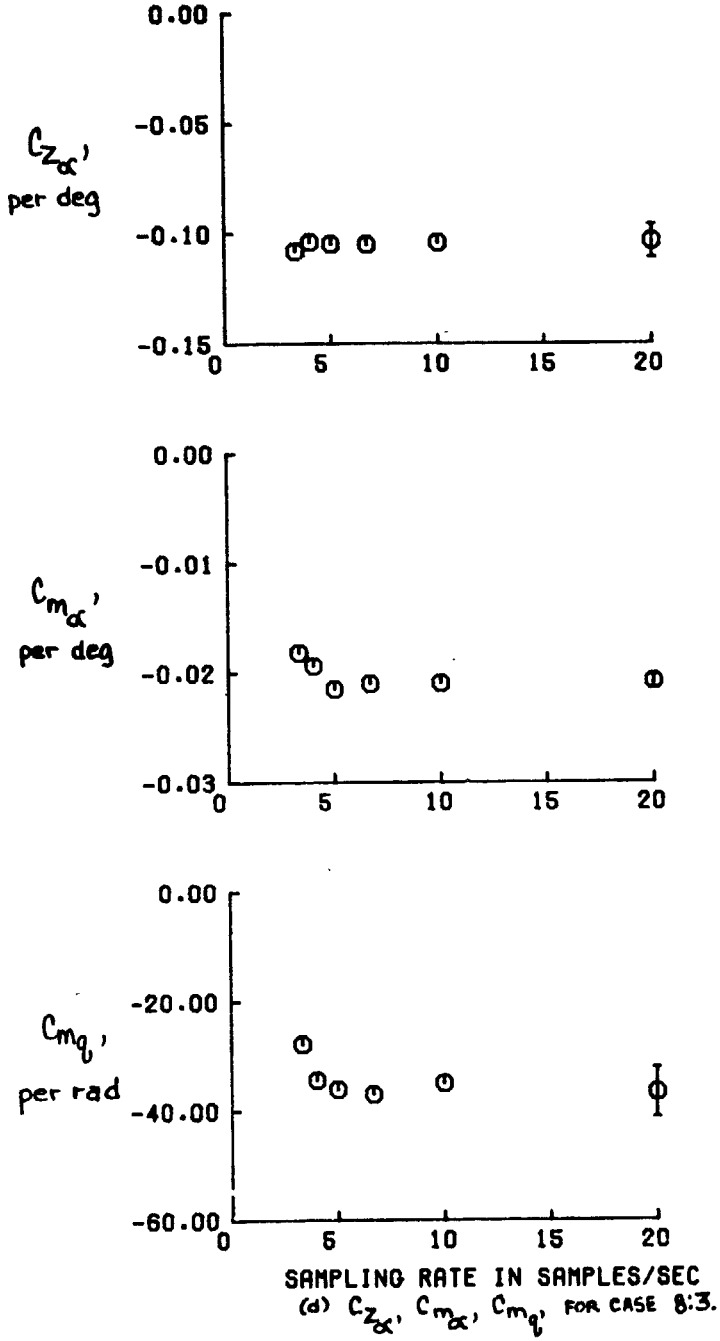

(d) C_{Z_α}, C_{m_α}, C_{m_q}, FOR CASE 8:3.

Figure 16. Continued.

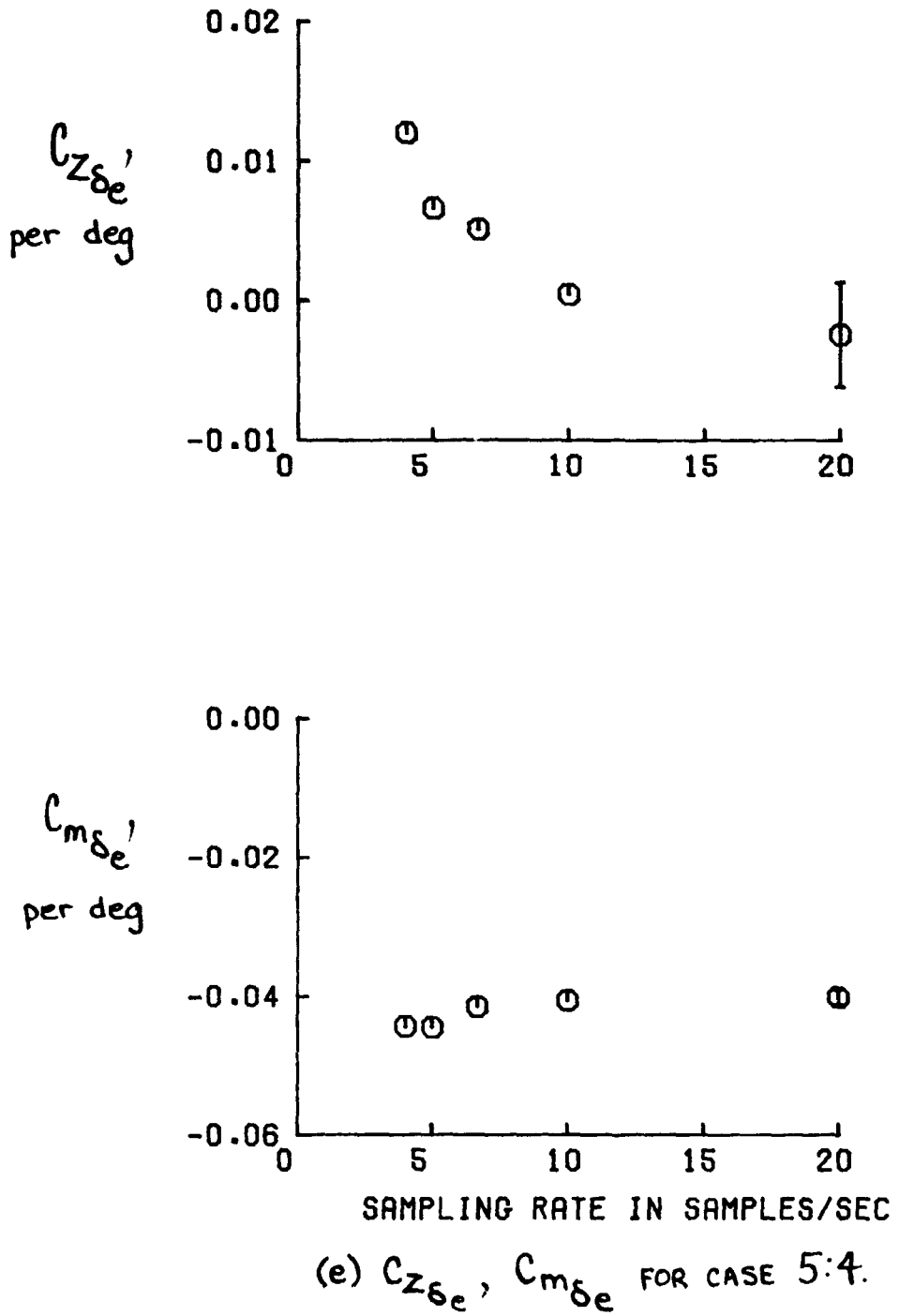

(e) $C_{Z_{\delta_e}}$, $C_{m_{\delta_e}}$ FOR CASE 5:4.

Figure 16. Continued.

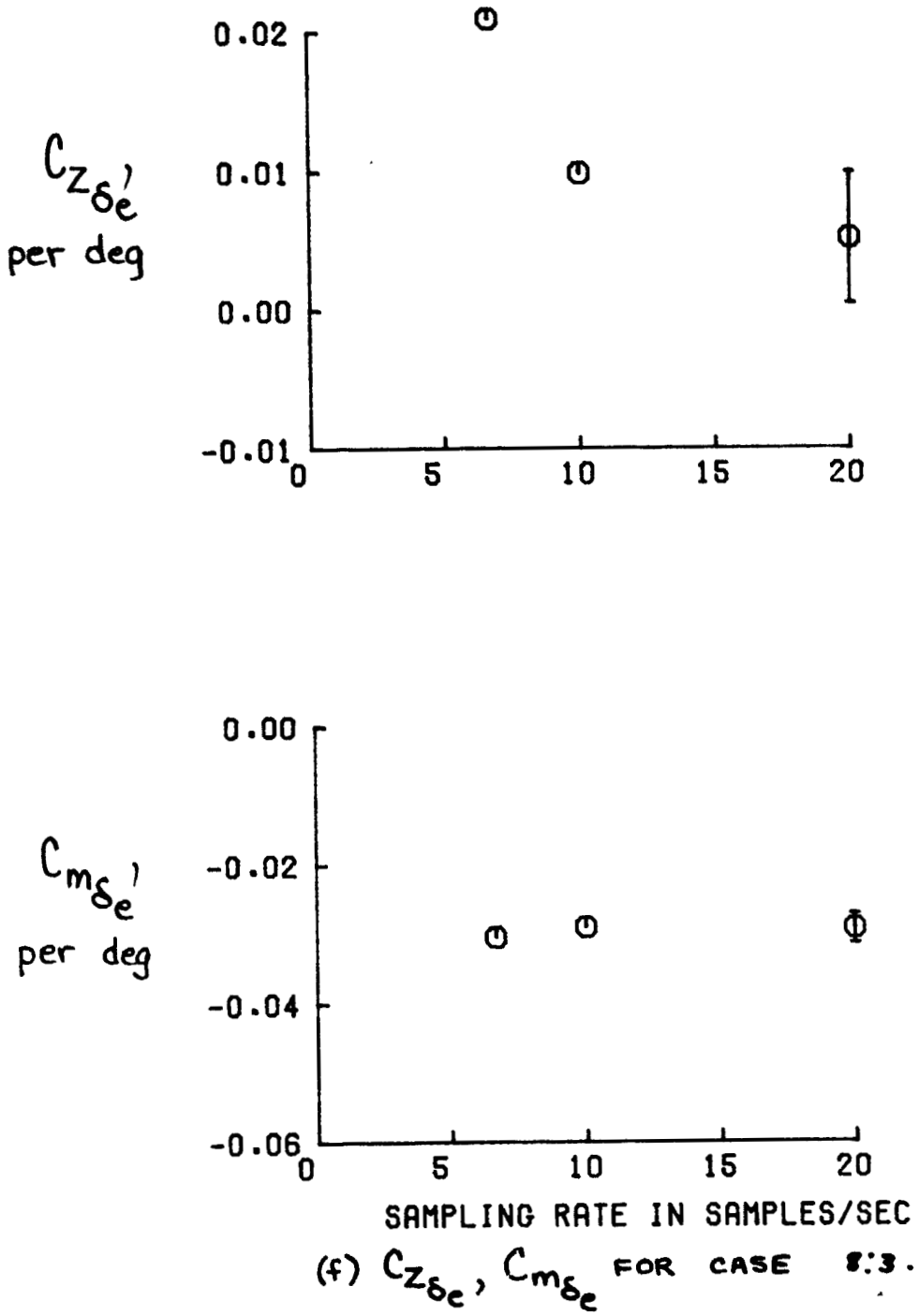

(f) $C_{Z_{\delta_e}}$, $C_{m_{\delta_e}}$ FOR CASE 8.3.

Figure 16. Continued.

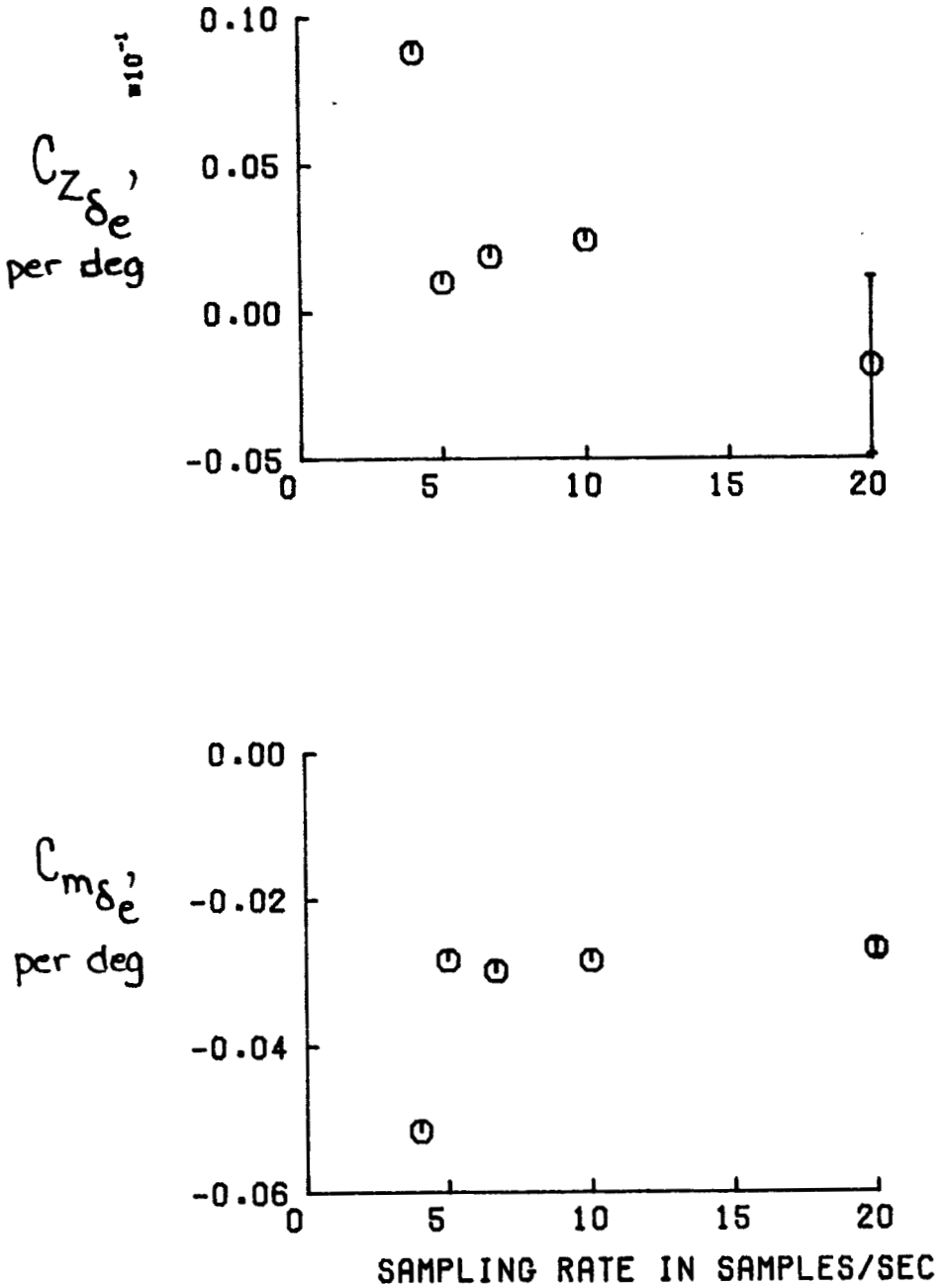

(g) $C_{Z_{\delta_e}}$, $C_{m_{\delta_e}}$ FOR CASE 7:18.

Figure 16. Continued.

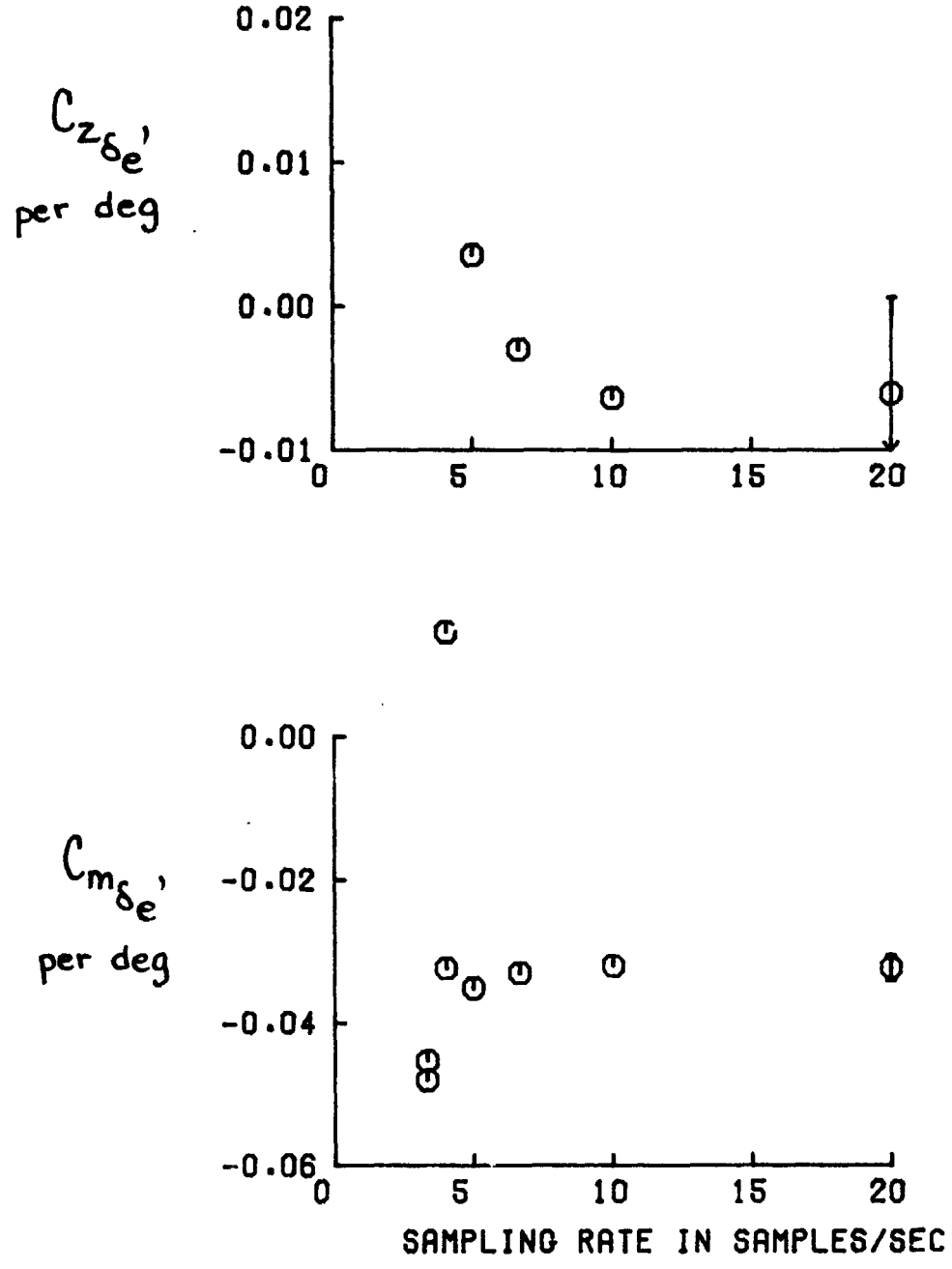

(h) $C_{z_{\delta_e}}$, $C_{m_{\delta_e}}$ FOR CASE 6:12.

Figure 16. Concluded.

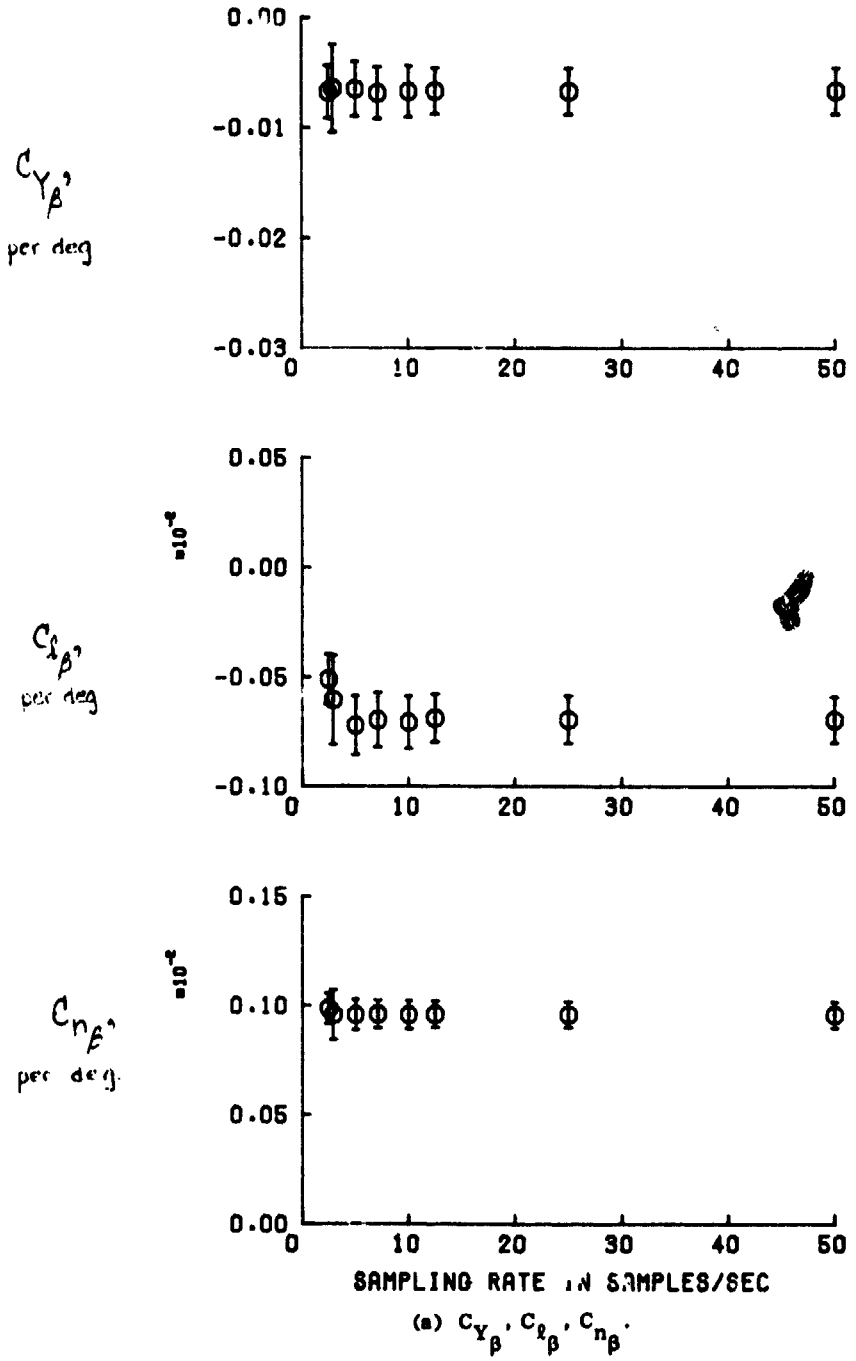

(a) C_{Y_β}, C_{ℓ_β}, C_{n_β}.

Figure 17. Estimated lateral-directional derivatives and uncertainty levels for Aircraft A maneuver as function of sampling rate.

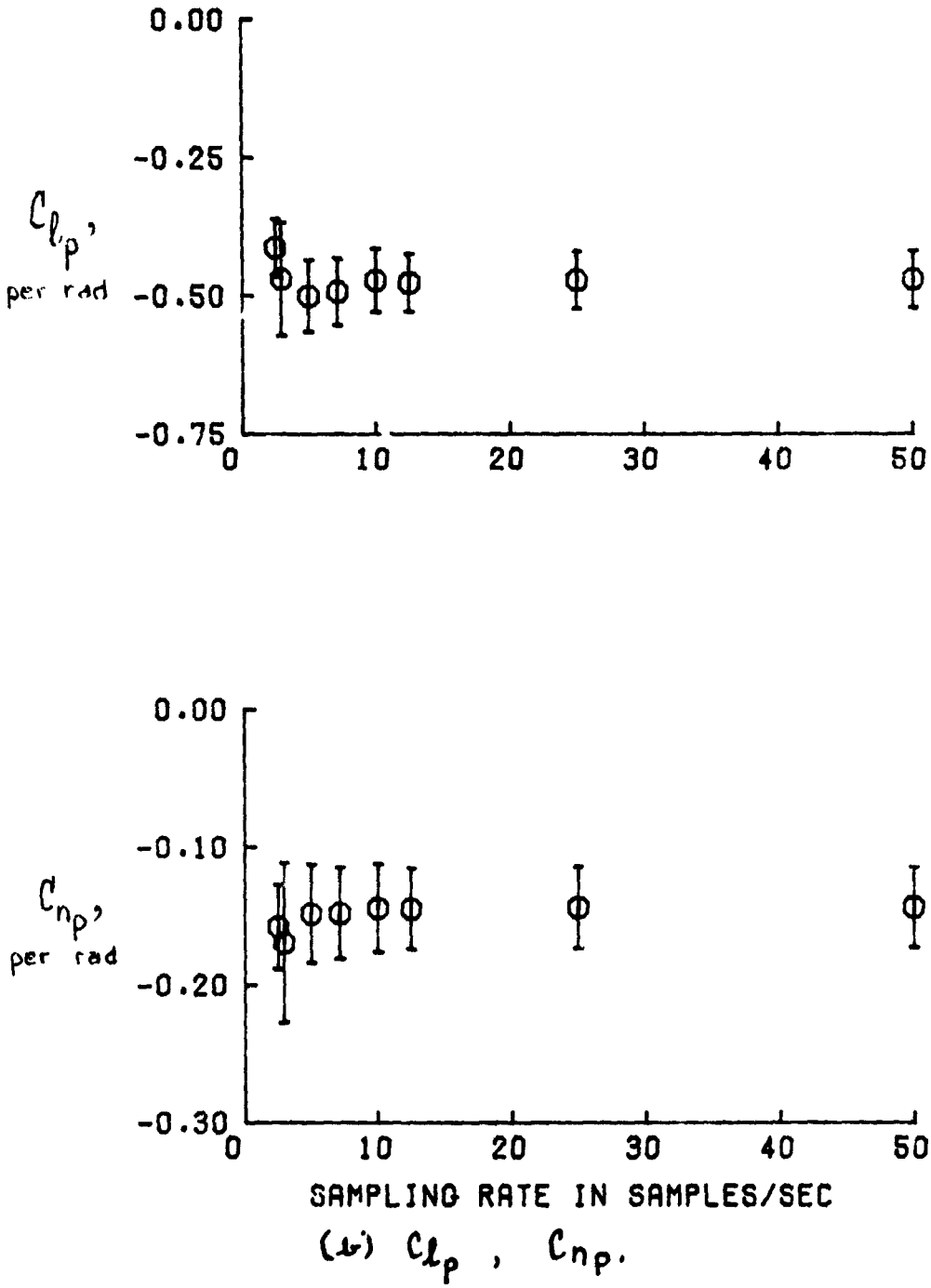

(b) C_{l_p} , C_{n_p}.

Figure 17. Continued

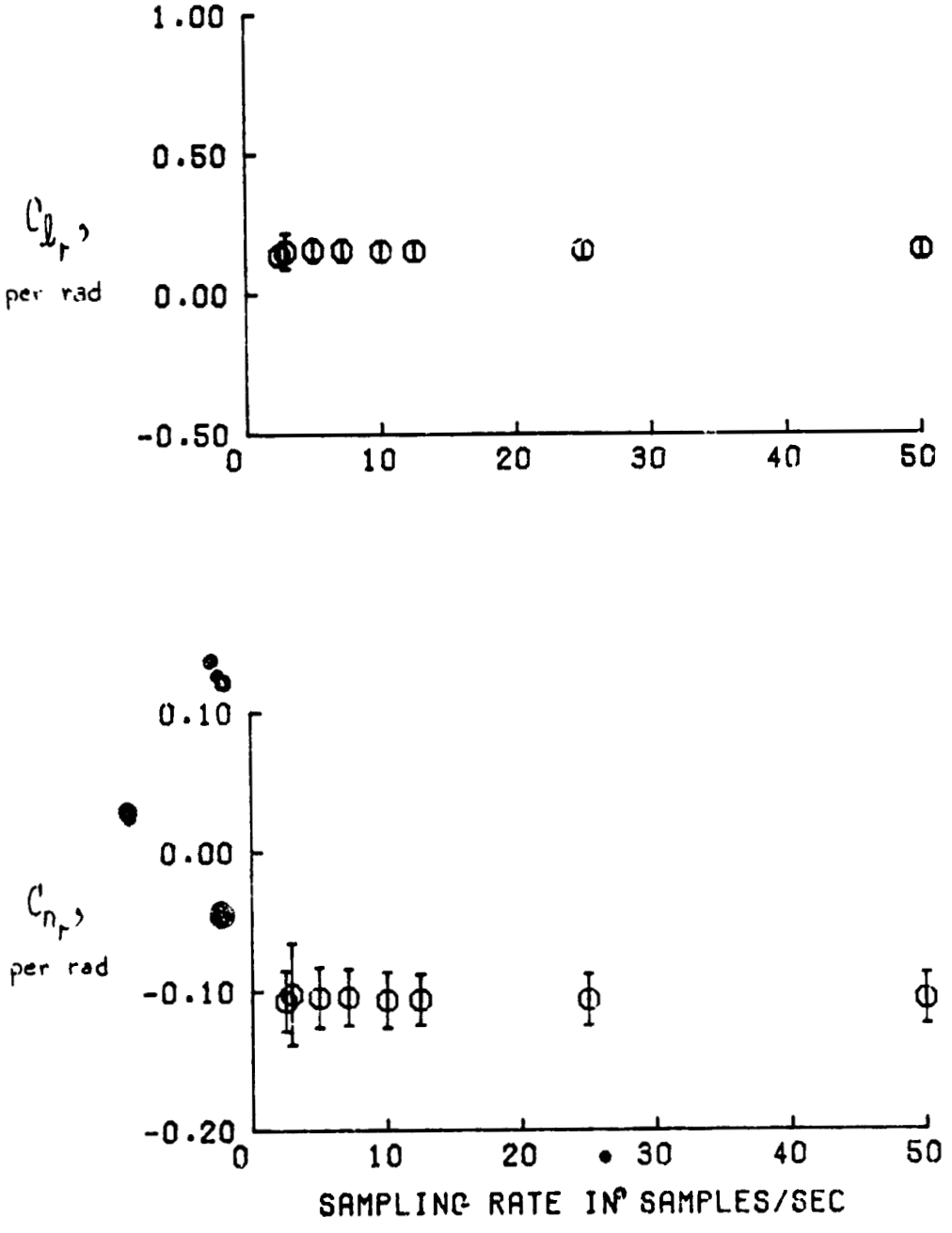

(c) C_{ℓ_r}, C_{n_r}.

Figure 17. Continued.

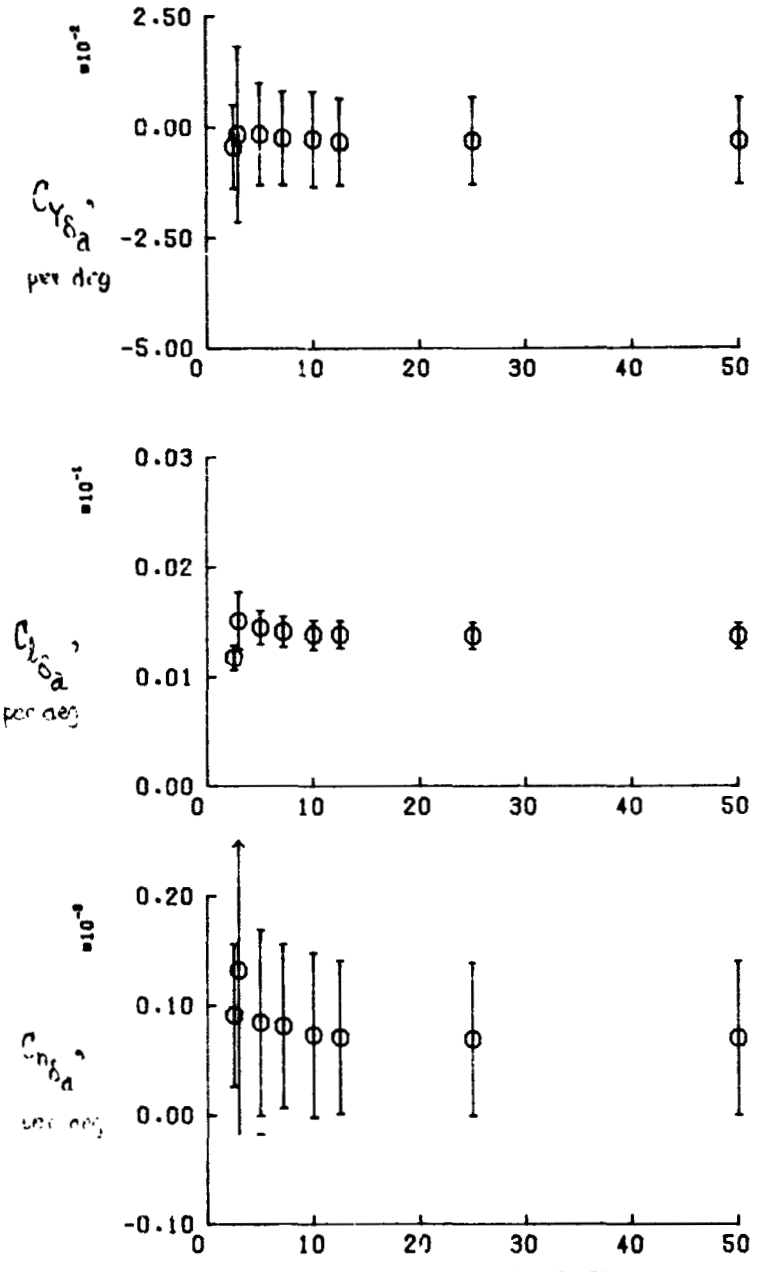

(d) $C_{Y_{\delta_a}}$, $C_{\ell_{\delta_a}}$, $C_{n_{\delta_a}}$.

Figure 17. Concluded